Twisted fracton models in three dimensions

Hao Song,[1,*] Abhinav Prem,[2,†] Sheng-Jie Huang,[2] and M. A. Martin-Delgado[1]
[1]*Departamento de Física Teórica, Universidad Complutense, 28040 Madrid, Spain*
[2]*Department of Physics and Center for Theory of Quantum Matter, University of Colorado, Boulder, Colorado 80309, USA*

(Received 28 July 2018; revised manuscript received 8 February 2019; published 9 April 2019)

We study novel three-dimensional gapped quantum phases of matter which support quasiparticles with restricted mobility, including immobile "fracton" excitations. So far, most existing fracton models may be instructively viewed as generalized Abelian lattice gauge theories. Here, by analogy with Dijkgraaf-Witten topological gauge theories, we discover a natural generalization of fracton models, obtained by twisting the gauge symmetries. Introducing generalized gauge transformation operators carrying an extra phase factor depending on local configurations, we construct a plethora of exactly solvable three-dimensional models, which we dub "twisted fracton models." A key result of our approach is to demonstrate the existence of rich non-Abelian fracton phases of distinct varieties in a three-dimensional system with finite-range interactions. For an accurate characterization of these novel phases, the notion of being *inextricably non-Abelian* is introduced for fractons and quasiparticles with one-dimensional mobility, referring to their new behavior of displaying braiding statistics that is, and remains, non-Abelian regardless of which quasiparticles with higher mobility are added to or removed from them. We also analyze these models by embedding them on a 3-torus and computing their ground-state degeneracies, which exhibit a surprising and novel dependence on the system size in the non-Abelian fracton phases. Moreover, as an important advance in the study of fracton order, we develop a general mathematical framework which systematically captures the fusion and braiding properties of fractons and other quasiparticles with restricted mobility.

DOI: 10.1103/PhysRevB.99.155118

I. INTRODUCTION

The study of topological quantum phases of matter has led to remarkable new discoveries, both theoretically and experimentally, and has profoundly influenced our understanding of quantum many-body physics. Starting with the discovery of the fractional quantum Hall effect [1,2], it was realized that there exist quantum phases of matter which lie outside Landau's symmetry breaking paradigm. One such class of phases are those with intrinsic topological order, which are gapped quantum phases of matter distinguished by patterns of long-range entanglement in their ground states [3–5]. Nontrivial topological orders, examples of which include quantum Hall states and gapped spin liquids, may exhibit striking phenomena such as excitations with fractionalized statistics, locally indistinguishable degenerate ground states, and robust gapless edge states [2,6–14]. The potential application of topological states for fault-tolerant quantum computation [15–18] has provided another main motivation for current intensive study on topological orders.

The landscape of topological quantum phases becomes much richer in the presence of global symmetries. Even in the absence of intrinsic topological order, distinct phases protected by some unbroken symmetry are possible, leading to the modern notion of symmetry protected topological (SPT) phases [19,20], of which the 1D Haldane phase for spin-1 chain [21–25] and topological insulators [26–34] are paradigmatic examples. Further considering the interplay between nontrivial topological order and global symmetries leads to the concept of symmetry enriched topological (SET) phases, which have been of much recent interest [35–42].

The topological nature of these phases is reflected in the fact that their low-energy behavior is governed by a topological quantum field theory (TQFT), which in turn allows one to develop general mathematical frameworks for understanding their physics. In particular, the language of tensor category theory has proven hugely successful in analyzing intrinsic topological orders in $d = 2$ spatial dimensions. It is now well-understood that the fusion and braiding properties of quasiparticles—anyons—in a topologically ordered spin system are described by a unitary modular tensor category (UMTC) [14,43]. For instance, the UMTC describing the anyons in Kitaev's quantum double model (i.e., a lattice realization of gauge theory for $d = 2$) based on a finite group G is given by the representation theory of the quantum double algebra $\mathcal{D}(G)$ [15,44–46]. Rich topological orders also exist in $d = 3$ spatial dimensions [47–50] and they may provide fault-tolerant quantum computing schemes with advantages over their $d = 2$ cousins as exemplified by the color codes [16,17,51]. Since challenges vary with dimensions as seen in classifying manifolds [52–55], the theory of topological orders for $d = 3$ is less developed compared to $d = 2$ and remains an active research topic [56,57].

Recently, a new class of models have brought to light novel gapped quantum phases of matter which lie beyond the conventional framework of topological order. These phases, which are said to possess "fracton order," were originally

*haosong@ucm.es
†Present address: Princeton Center for Theoretical Science, Princeton University, NJ 08544, USA.

discovered in exactly solvable $d = 3$ lattice models and exhibit a rich phenomenology, including a locally stable ground-state degeneracy on the 3-torus which depends subextensively (hence nontopologically) on the system size and quasiparticles with restricted mobility [58–61]. In particular, these models strikingly host quasiparticles—fractons—which are intrinsically immobile (i.e., cannot be moved by string operators). This peculiar and striking feature serves as a defining characteristic of fracton phases and has recently led to a flurry of theoretical interest in understanding these phases from a variety of perspectives [58–93]. A recent review on current progress in this field can be found in Ref. [94].

The gapped fracton models discovered and studied thus far can be be broadly separated into type-I and type-II fracton phases, in the taxonomy of Ref. [61]. In type-I (respectively, type-II) phases, fractons appear at the corners of membrane-like (fractal-like) operators. A further distinguishing feature of type-I phases is the presence of topologically nontrivial excitations which are mobile along sub-dimensional manifolds (lines or planes) of the three-dimensional system, while all topologically nontrivial excitations in type-II phases are strictly immobile. Well-known examples of type-I phases are Chamon's model [58,62], the X-cube model [61], and the checkerboard model [61], while Haah's code [59] remains the paradigmatic model for type-II fracton phases. In this paper, we will restrict our attention to type-I fracton phases.

A natural question to pose is whether existing models exhaust the possible kinds of quasiparticles which a fracton phase may harbor. In particular, is it possible for fractons or excitations with restricted mobility to have a multichannel fusion rule, i.e., be non-Abelian? In type-I fracton phases, certain topological excitations can move only along subdimensional manifolds and may thus braid nontrivially with each other, allowing some notion of nontrivial statistics to survive even though the system is three-dimensional. Thus, while in principle there appears to be no obstruction to realizing non-Abelian statistics in type-I fracton phases, a new framework is clearly needed to capture this more general class of systems, which is a primary motivation for this work.

Constructing and studying exactly solvable models has proven a fruitful approach in exploring the landscape of gapped quantum phases of matter [14–17,45–48,95–107]. For conventional topological orders, a key insight for constructing new exactly solvable models was provided by a gauging procedure relating (short-range entangled) SPT states to (long-range entangled) topological orders described by twisted gauge theories [98]. Specifically, this gauging procedure relates lattice nonlinear σ-models for SPT phases [20] to (lattice realizations of) Dijkgraaf-Witten topological gauge theories [108] describing topological orders which host quasiparticle (respectively, loop) excitations in $d = 2$ (respectively, $d = 3$) spatial dimensions with rich statistical properties [49,50,109–112]. Dijkgraaf-Witten topological gauge theory (also referred to as twisted gauge theory) generalizes standard lattice gauge theory by "twisting" its gauge transformations, i.e., by allowing them to carry an extra phase factor specified by a $(d + 1)$-cocycle $\omega \in Z^{d+1}(G, \mathrm{U}(1))$ and local field configurations, where G is the gauge group.

Similarly to the duality between SPT states and topological orders, it has been realized that certain (Abelian) type-I fracton models, such as the X-cube, can be related through a generalized gauging procedure to short-range entangled states with subsystem symmetries [61,91,113]. Based on this observation, most exactly solvable fracton models can be naturally interpreted as generalized lattice gauge theories [61]. Motivated by this interpretation of fracton models, and by the twisting procedure for obtaining Dijkgraaf-Witten theories from standard gauge theories, here we consider twisting certain type-I fracton models along planes by 3-cocycles. This allows us to systematically generate a rich family of type-I fracton models—dubbed "twisted fracton models"—which realize non-Abelian excitations with restricted mobility, such as non-Abelian fractons. In this paper, we extensively explore the properties of twisted fracton models, which form a natural platform for realizing a wide variety of novel quasiparticles, and elucidate the related notion of braiding excitations with restricted mobility.

Given the length of this paper, we now highlight our procedure and main results.

A. Summary of main results

In this paper, we develop a general procedure for systematically constructing exactly solvable models, which we dub *twisted fracton models*, thereby greatly expanding the set of type-I fracton phases and establishing a general mathematical framework within which to study non-Abelian fracton orders. We start by observing that the X-cube and checkerboard models [61], as originally defined, can both be viewed as generalized Abelian lattice gauge theories. Then, in analogy with Dijkgraaf-Witten topological gauge theory, we observe that the generalized gauge transformations can be twisted as well. This leads us to a plethora of exactly solvable three-dimensional models exhibiting a landscape of rich and hitherto undiscovered behaviors, of which we present the twisted X-cube and twisted checkerboard models as paradigmatic examples.

Importantly, these exactly solvable models establish the existence of novel type-I fracton phases hosting *inextricably non-Abelian* fractons, which we will define shortly in this section before providing examples based on concrete models in later sections. Moreover, in contrast to other approaches for generalizing type-I fracton orders [74,92], which are based on coupling stacks of $d = 2$ topological phases, our construction here has a cleaner connection to TQFTs (explicitly, Dijkgraaf-Witten topological gauge theories) realizing similar braiding properties, which enables us to thoroughly analyze the resulting fracton models. For instance, we compute their ground-state degeneracy (GSD) on a 3-torus T^3 explicitly, revealing the novel dependence of this GSD on system size in non-Abelian fracton phases for the first time.

In our analysis of the spectrum of twisted fracton models, there emerges a systematic route for describing the braiding and fusion properties of quasiparticles, including those with restricted mobility. Some key definitions, which intuitively reveal the structure of these phases, are as follows. A 0d (respectively, 1d, 2d) mobile quasiparticle is an excited finite region which can move as a whole in 0 (respectively, 1, 2) dimensions. We further call it *intrinsically* 0d (respectively, 1d, 2d) mobile if it is not a fusion result of quasiparticles

with higher mobility. For instance, a quasiparticle mobile only along the x axis can be obtained by fusing two anyons from two decoupled 2d topologically ordered systems lying along the xy and zx planes, respectively, but we do not call it intrinsically 1d mobile. In our terminology, a *fracton* is then simply defined as an intrinsically 0d mobile (i.e., intrinsically immobile) quasiparticle.

To classify particle types in type-I fracton phases, we introduce the x (respectively, y, z) *topological charges* of a quasiparticle, which are detected by braiding 2d mobile quasiparticles around it in the yz (respectively, zx, xy) planes. Assuming no nontrivial 3d mobile quasiparticles,[1] the particle type of an excitation is then specified by its x, y, z topological charges, which may be subject to some constraints. In addition, the *quantum dimension* of a quasiparticle equals the product of quantum dimensions associated with its topological charges in the three directions.

We now define what it means for quasiparticles with restricted mobility to be *inextricably non-Abelian*. A quasiparticle is *Abelian* (respectively, *non-Abelian*) if its quantum dimension is 1 (respectively, greater than 1). An *inextricably* non-Abelian fracton is one which is *not* a fusion result of an Abelian fracton with some mobile quasiparticles. Similarly, an *inextricably* non-Abelian 1d mobile quasiparticle is one that cannot be obtained by fusing an Abelian 1d mobile quasiparticle with some 2d mobile quasiparticles. Significantly, this implies that a fracton model hosting either an inextricably non-Abelian fracton or an inextricably non-Abelian 1d mobile quasiparticle *cannot* be understood as some Abelian fracton order weakly coupled to layers of conventional two-dimensional topological states. This is one of the central results of our work, as it demonstrates the existence of a fundamentally new class of fracton orders.

Studying the excitations of twisted fracton models, we show that both inextricably non-Abelian fractons and inextricably non-Abelian 1d mobile quasiparticles may be realized within twisted checkerboard models. On the other hand, twisted X-cube models host only inextricably non-Abelian 1d mobile quasiparticles. Thus we find two basic types of non-Abelian fracton orders: one which allows fractons (and 1d mobile quasiparticles simultaneously) inextricably non-Abelian and one which only hosts inextricably non-Abelian 1d mobile quasiparticles. Actually, in our twisted fracton models, quasiparticles may have inextricably non-Abelian topological charges in one, two or three directions, which reveals a further distinction between varieties of fracton phases.

As a further technical contribution, we provide a detailed derivation of the categorical description for anyons in twisted discrete gauge theories directly from their lattice models in two spatial dimensions, which is absent in the literature. Necessary mathematical details are included in appendices to make our derivation and discussion self-contained. This treatment applies straightforwardly to studying twisted fracton models as well.

[1]This holds for all the fracton models in this paper. Otherwise, if nontrivial 3d mobile quasiparticles (e.g., charges in 3+1D gauge theory and fermions) exist, extra particle type characterizations like particle-loop braiding and fermion parity may be needed.

B. Outline

We now outline the remainder of this paper. In Sec. II, we treat lattice models of twisted gauge theories in two spatial dimensions. While the results contained in the section may be familiar to readers, we emphasize that our treatment differs from previous approaches and is directly applicable to the twisted fracton models introduced later. We characterize conventional topological orders by deriving properties such as their ground-state degeneracy on a torus and the braiding and fusion properties of anyons. The braiding of anyons is especially transparent in our treatment, wherein anyons are represented as punctures on a disk.

In Sec. III, we introduce new families of exactly solvable twisted fracton models. In particular, we introduce twisted versions of two paradigmatic examples of three-dimensional fracton order: twisted X-cube models and twisted checkerboard models. Rather than reviewing the untwisted $\mathbb{Z}_2$ X-cube and checkerboard models, for which the reader is referred to Refs. [60,61], we first define these models based on arbitrary finite Abelian groups G. We then twist the gauge symmetry by nontrivial 3-cocycles [i.e., elements of $Z^3(G, \mathrm{U}(1))$ defined in Appendix A 1][2] to arrive at the twisted fracton models.

Sections IV and V are devoted to calculating the nontrivial ground-state degeneracies (GSD) of twisted fracton models with the system defined on a 3-torus. The explicit calculations for both the twisted X-cube (Sec. IV) and checkerboard (Sec. V) models serve three purposes. Firstly, the subextensive system size dependence of the GSD in all cases demonstrates clearly that the models under consideration are gapped phases. In fact, it becomes clear from our later analysis of quasiparticles that this GSD is stable against arbitrary local perturbations and hence reveals that the system is nontrivially long-range entangled. Secondly, the dependence of the GSD on the system size in all models under consideration establishes the geometric nature of fracton phases: they are sensitive not only to the global topology but also to geometry. This provides a clear distinction between conventional topological order and fracton order. Thirdly, the new exotic dependence of GSD on system size [e.g. Eqs. (199), (209), (210), and (262)] strongly hints at the existence of novel non-Abelian fracton phases.

In Secs. VI and VII, the quasiparticle spectra of the twisted X-cube and checkerboard models are analyzed respectively; here, we classify all particle types and study their braiding and fusion properties. Importantly, our analysis uncovers a systematic route for describing quasiparticles in type-I fracton phases. First, we explain how the particle type of an excited spot is labeled by its x, y, z *topological charges*, which can be detected by braiding 2d mobile quasiparticles around it in the yz, zx, xy planes, respectively. Further, we elucidate the notions of *mobility* and *quantum dimension* for quasiparticles and determine them through the topological charge data. We also discuss certain fusion and braiding processes in general.

[2]Since all nontrivial quasiparticles in the fracton models under study have mobility within 2 or lower spatial dimensions, we only need 3-cocyles (instead of 4-cocycles) to modify their braiding statistics by analogy to Dijkgraaf-Witten topological gauge theories in (2+1)-dimensional space-time.

In order to illustrate the variety of novel fracton phases which may be accessed through our construction, we examine certain examples explicitly. We find that semionic or inextricably non-Abelian 1d mobile quasiparticles are allowed in some twisted X-cube models (Sec. VI). On the other hand, the twisted checkerboard models (Sec. VII) are shown to realize a broader variety of excitations. Specifically, we show the existence of inextricably non-Abelian fractons in a twisted checkerboard model based on the group $G = \mathbb{Z}_2 \times \mathbb{Z}_2 \times \mathbb{Z}_2$.

The paper concludes in Sec. VIII with a discussion of avenues for future investigation and of open questions raised by the present results. To keep this paper self-contained, necessary mathematical materials are provided in the appendices. Specifically, Appendix A contains the definitions of group cohomology, triangulated manifolds, and the associated Dijkgraaf-Witten weight and partition function. Appendix B reviews the quasitriangular quasi-Hopf algebra structure of a twisted quantum double $\mathcal{D}^{\omega}(G)$ and the tensor category of its representations.

II. 2D LATTICE MODELS OF TWISTED GAUGE THEORIES

In this section, we will present a self-contained treatment of exactly solvable lattice models motivated by the gauge theory in two spatial dimensions based on a finite group G, which are often called *quantum double models*, and their twisted versions. Here G may be non-Abelian and its identity element is denoted as e. Our treatment generalizes to fracton models directly in later sections.

A. Description of lattice models

1. Untwisted models

As a warm-up, let us first recall the standard lattice model of a gauge theory in two spatial dimensions [15], based on a finite group G with identity element denoted by e. To be concrete, we work on a square lattice (i.e., a two-dimensional manifold composed of square plaquettes) Σ. The discussion in this section actually applies to any other planar lattice.

Let $E(\Sigma)$ be the set of its edges with a chosen orientation each as shown by the black arrows in Fig. 1(a). In addition, the sets of vertices and plaquettes of Σ are denoted by $V(\Sigma)$ and $F(\Sigma)$, respectively. Technically, all the edges and plaquettes are thought to be closed, i.e., they include their boundaries. In particular, each plaquette contains all its edges. Moreover, for any region (i.e., subspace) Γ of Σ, let $V(\Gamma)$, $E(\Gamma)$, and $F(\Gamma)$ denote the subsets of $V(\Sigma)$, $E(\Sigma)$, and $F(\Sigma)$ that collect all the vertices, edges and plaquettes inside Γ, respectively.

A local Hilbert space (also called a *spin* for short) with an orthonormal basis $\{|\ell, \sigma\rangle\}_{\sigma\in G}$ is assigned to each edge $\ell \in E(\Sigma)$. Thus the Hilbert space $\mathcal{H}(E(\Gamma), G)$ associated with any region Γ of Σ is spanned by the vectors

$$|\zeta\rangle := \bigotimes_{\ell\in E(\Gamma)} |\ell, \zeta(\ell)\rangle \tag{1}$$

labeled by $\zeta \in G^{E(\Gamma)}$, where $G^{E(\Gamma)} := \mathrm{Fun}(E(\Gamma), G)$ is the set of functions from $E(\Gamma)$ to G. Each element of $G^{E(\Gamma)}$ specifies a *spin configuration* on Γ. On the whole lattice Σ, the total Hilbert space is $\mathcal{H}(E(\Sigma), G)$.

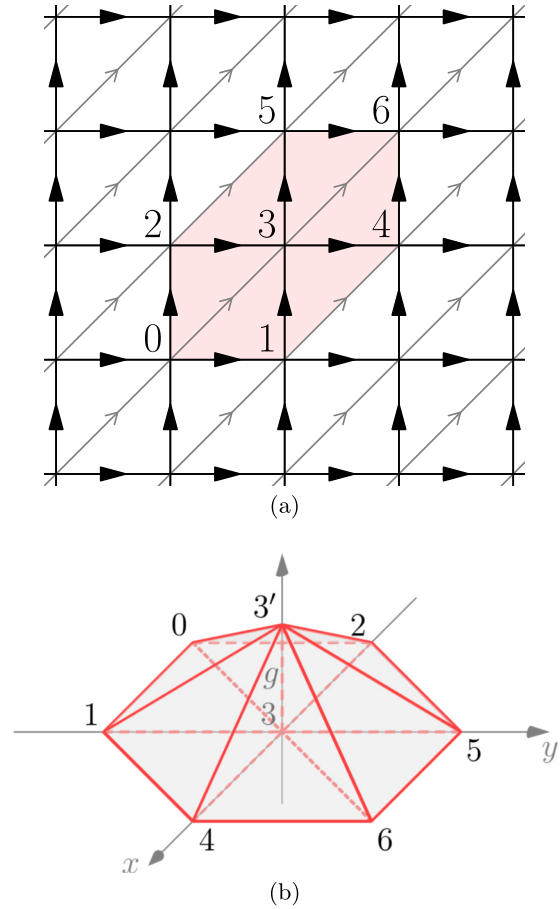

FIG. 1. Lattice model of gauge theory in 2+1 dimensions. (a) The physical degrees of freedom are on the black oriented edges of the square lattice. Auxiliary grey edges are added to give a complete triangulation. (b) P_v^g for $v = 3$ is presented by a triangulated pyramid P_v^g with edges oriented according to the local ordering of vertices $0 < 1 < 2 < 3 < 3' < 4 < 5 < 6$ and $[33']$ colored by $g \in G$. For each tetrahedron, $\mathrm{sgn}([v_0v_1v_2v_3])$ equals the sign of the triple product $\overrightarrow{v_0v_1} \cdot (\overrightarrow{v_0v_2} \times \overrightarrow{v_0v_3})$. For example, $\mathrm{sgn}([0133']) = +1$ and $\mathrm{sgn}([233'5]) = -1$.

Suppose that $\mathcal{O}$ is an operator acting on $\mathcal{H}(E(\Sigma), G)$. We say that $\mathcal{O}$ is supported on a region $\Gamma \subseteq \Sigma$ if it can be expressed as $\mathcal{O} = \mathcal{O}_\Gamma \otimes 1_{\Sigma\setminus\Gamma}$, where $\mathcal{O}_\Gamma$ is an operator acting on $\mathcal{H}(E(\Gamma), G)$ and $1_{\Sigma\setminus\Gamma}$ denotes the identity operator acting on the rest of the spins. Usually, $1_{\Sigma\setminus\Gamma}$ is omitted in notations and the operators acting on $\mathcal{H}(E(\Gamma), G)$ are automatically viewed as operators acting on $\mathcal{H}(E(\Sigma), G)$ as well.

On each vertex v, we have a *gauge transformation operator*

$$A_v^g := \bigotimes_{\ell\ni v} L_v^g(\ell) \tag{2}$$

for each $g \in G$, where $\ell \ni v$ means that ℓ connects to v. In addition, for $\ell = [v_0v_1]$,

$$L_v^g(\ell) := \begin{cases} \sum_{\sigma\in G} |\ell, g\sigma\rangle\langle\ell, \sigma|, & v_0 = v, v_1 \neq v, \\ \sum_{\sigma\in G} |\ell, \sigma\rangle\langle\ell, \sigma g|, & v_0 \neq v, v_1 = v, \\ \sum_{\sigma\in G} |\ell, g\sigma g^{-1}\rangle\langle\ell, \sigma|, & v_0 = v, v_1 = v, \\ 1, & v \notin \ell. \end{cases} \tag{3}$$

The third line in this definition of L_v^g takes care of the possibility ℓ being a loop, which happens when the size of the square lattice with periodic boundary condition reduces to 1 in one direction.

It is straightforward to check that

$$\left(A_v^g\right)^\dagger = A_v^{g^{-1}}, \quad A_v^g A_v^h = A_v^{gh}, \tag{4}$$

$$\left[A_{v_0}^g, A_{v_1}^h\right] = 0, \quad \text{if } v_0 \neq v_1. \tag{5}$$

$\forall v, v_0, v_1 \in V(\Sigma), \forall g, h \in G$. Thus we have a set of mutually commuting Hermitian local projectors, also known as *stabilizers* in the quantum computation literature,

$$A_v := \frac{1}{|G|}\sum_{g\in G} A_v^g \tag{6}$$

labeled by vertices.

On each plaquette p, we have a projector which requires the triviality of flux

$$B_p := \sum_{\zeta\in G^{E(p)}} \delta_{\zeta([v_0v_1])\zeta([v_1v_2])\zeta([v_2v_3])\zeta([v_3v_0]),e} |\zeta\rangle\langle\zeta|, \tag{7}$$

where e is the identity element of G and $v_0v_1v_2v_3$ is a sequence of vertices around the boundary of p. If the orientation of an edge $\ell = [v_0v_1]$ is inverse to what is picked in Fig. 1(a) (i.e., $[v_1v_0] \in E(\Sigma)$), then $\zeta(\ell) := (\zeta([v_1v_0]))^{-1}$.

It can be checked that all the projectors A_v and B_p labeled by vertices and plaquettes commute with each other. They form a set of stabilizers that completely fix local degrees of freedom. In other words,

$$H = -\sum_v A_v - \sum_p B_p \tag{8}$$

is a gapped Hamiltonian. In particular, it has a finite ground-state degeneracy when embedded in a torus (i.e., with periodic boundary conditions), which is independent of system size and robust to any local perturbations.

2. *Twisted models*

Motivated by Dijkgraaf-Witten topological gauge theories [108], the above lattice model based on a finite group G can be twisted by a 3-cocycle $\omega \in Z^3(G, \mathrm{U}(1))$, i.e., a function $\omega : G\times G\times G \to \mathrm{U}(1)$ satisfying the so-called *cocycle condition*

$$\frac{\omega(g_2,g_3,g_4)\omega(g_1,g_2g_3,g_4)\omega(g_1,g_2,g_3)}{\omega(g_1g_2,g_3,g_4)\omega(g_1,g_2,g_3g_4)} = 1. \tag{9}$$

The resulting twisted models are classified by the corresponding group cohomology $[\omega] \in H^3(G, \mathrm{U}(1))$. Details of Dijkgraaf-Witten topological gauge theories and group cohomology are summarized in Appendix A. Without loss of generality, we will always require ω to be *normalized*, i.e., $\omega(g_1, g_2, g_3) = 1$ whenever any one of g_1, g_2, g_3 equals the identity $e \in G$ in this paper.

In the twisted model, we will keep B_p unchanged. For any region Γ of Σ, let

$$G_B^{E(\Gamma)} := \{\zeta \in G^{E(\Sigma)} \mid B_p|\zeta\rangle = |\zeta\rangle, \forall p \in F(\Gamma)\}, \tag{10}$$

whose element are called *locally flat* spin configurations on Γ. Let $\mathcal{H}_B(E(\Gamma), G)$ denote the Hilbert subspace spanned by $|\zeta\rangle$ with $\zeta \in G_B^{E(\Gamma)}$.

In order to define twisted versions of gauge transformation operators, we pick a complete triangulation of Σ by adding the grey oriented edges shown in Fig. 1(a). The orientations of edges are picked such that there is no triangle whose three edges form a closed walk; such a choice is called a *branching structure* [20]. Then every triangle τ is ordered and should be labeled as $[\tau_0\tau_1\tau_2]$ with vertices ordered such that the orientations of the edges $[\tau_0\tau_1]$, $[\tau_1\tau_2]$, and $[\tau_0\tau_2]$ coincide with the branching structure.

Technically, the branched triangulation makes Σ into a Δ-complex. The definition of a Δ-complex is given in Ref. [114]. For a general Δ-complex $\mathtt{X}$, we denote the set of n-simplices (i.e., vertices for $n = 0$, edges for $n = 1$, triangles for $n = 2$, tetrahedrons for $n = 3$ and so on) in $\mathtt{X}$ by $\Delta^n(\mathtt{X})$.

A function $\xi \in G^{\Delta^1(\mathtt{X})}$ is called a *G-coloring* (or simply *coloring* [36]) of $\mathtt{X}$, if $\xi([\tau_0\tau_1])\xi([\tau_1\tau_2]) = \xi([\tau_0\tau_2])$ on any triangle $[\tau_0\tau_1\tau_2] \in \Delta^2(\mathtt{X})$. The set of G-colorings of $\mathtt{X}$ is denoted $\mathrm{Col}(\mathtt{X}; G)$ or simply $\mathrm{Col}(\mathtt{X})$ when G does not need to be specified explicitly.

For each $v \in V(\Sigma)$, let $\Sigma[v]$ be the region inside Σ made of all plaquettes adjacent to v. Take the vertex $v = 3$ shown in Fig. 1(a) for instance: $\Sigma[v]$ contains four plaquettes (around v) including their edges (twelve in total). Then $\Sigma[v]$ is a Δ-subcomplex of Σ as well and each $\zeta \in G_B^{E(\Sigma[v])}$ determines a coloring of $\Sigma[v]$. In particular, the group element assigned to the edge [03] is $\zeta([01])\zeta([13]) = \zeta([02])\zeta([23])$.

Further, we construct a pyramid $\mathtt{P}_v$ over v like the one in Fig. 1(b), whose bottom is the union of all triangles adjacent to v. Let v' denote the apex of $\mathtt{P}_v$. With $[vv'] = g$ (i.e., $[vv']$ colored by $g \in G$), the pyramid is denoted $\mathtt{P}_v^g$ and presents an operator (supported on $\Sigma[v]$)

$$P_v^g := \sum_{\zeta\in G_B^{E(\Sigma[v])}} |\zeta\rangle\omega\left[\zeta, \mathtt{P}_v^g\right]\langle\zeta|A_v^g, \tag{11}$$

where $\omega[\zeta, \mathtt{P}_v^g]$ is the Dijkgraaf-Witten weight, defined by Eq. (A7), on $\mathtt{P}_v$ with the coloring specified by $[vv'] = g$ and ζ on the bottom. Explicitly, for $v = 3$ in Fig. 1,

$$\omega\left[\zeta, \mathtt{P}_v^g\right] = \frac{[0133'][133'4][33'46]}{[0233'][233'5][33'56]}, \tag{12}$$

where each tetrahedron $[v_0v_1v_2v_3]$ stands for the phase factor $\omega([v_0v_1], [v_1v_2], [v_2v_3])$ with edges short for their associated group elements. With the *bottom* of $\mathtt{P}_v^g$ colored by ζ, its top has to be colored by $\zeta A_v^g \in G_B^{E(\Sigma[v])}$ specified by $\langle\zeta A_v^g| := \langle\zeta|A_v^g$ and we have

$$[0133'] = \omega(\zeta([01]), \zeta([13]), g), \tag{13}$$

$$[133'4] = \omega(\zeta([13]), g, g^{-1}\zeta([34])), \tag{14}$$

$$[33'46] = \omega(g, g^{-1}\zeta([34]), \zeta([46])), \tag{15}$$

$$[0233'] = \omega(\zeta([02]), \zeta([23]), g), \tag{16}$$

$$[233'5] = \omega(\zeta([23]), g, g^{-1}\zeta([35])), \tag{17}$$

$$[33'56] = \omega(g, g^{-1}\zeta([35]), \zeta([56])). \tag{18}$$

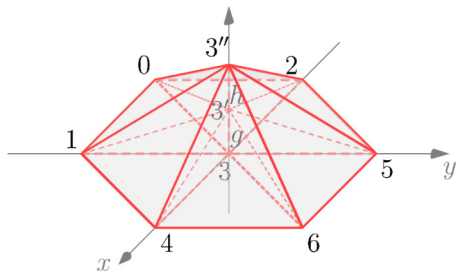

FIG. 2. Stacking two pyramids over a vertex as a graphic representation of $P_v^g P_v^h$.

Since ω is assumed to be normalized, $g = e$ (the identity of G) implies $\omega[\zeta, \mathrm{P}_v^g] = 1$ for any locally flat spin configuration $\zeta \in G_B^{E(\Sigma[v])}$. Hence P_v^e just requires the local flatness near the vertex v. In other words, $P_v^e = \prod_{p \ni v} B_p$ with $p \ni v$ denoting that plaquette p is adjacent to v.

With this graphic representation of P_v^g in Fig. 1(b), we can demonstrate some crucial properties of these operators. First, on a single vertex, $\omega[\zeta, \mathrm{P}_v^g]\omega[\zeta A_v^g, \mathrm{P}_v^h]$ can be presented as a stack of pyramids colored by ζ on the bottom and $[33'] = g$, $[3'3''] = h$ as shown in Fig. 2. Thus it is the Dijkgraaf-Witten weight on this particular coloring of the stack, which is a pyramid over v with a different bulk triangulation. Topologically, the pyramid is just a ball with a particular surface triangulation. The cocycle condition of ω implies that the Dijkgraaf-Witten weight assigned to a ball only depends on its surface triangulation and coloring, which is discussed in Appendix A 3 in a general setting. Therefore $\omega[\zeta, \mathrm{P}_v^g]\omega[\zeta A_v^g, \mathrm{P}_v^h] = \omega[\zeta, \mathrm{P}_v^{gh}]$ and hence

$$P_v^g P_v^h = P_v^{gh}. \tag{19}$$

Setting $h = g^{-1}$, we get $\omega[\zeta, \mathrm{P}_v^g]\omega[\zeta A_v^g, \mathrm{P}_v^{g^{-1}}] = 1$ and hence $\omega[\zeta A_v^g, \mathrm{P}_v^{g^{-1}}] = (\omega[\zeta, \mathrm{P}_v^g])^*$. Thus

$$\left(P_v^g\right)^\dagger = P_v^{g^{-1}}. \tag{20}$$

Together, Eqs. (19) and (20) imply that

$$P_v := \frac{1}{|G|} \sum_{g \in G} P_v^g \tag{21}$$

is a Hermitian projector.

Besides, $P_{v_0}^g$ and $P_{v_1}^h$ commute for two vertices $v_0 \neq v_1$. This is clear if v_0 and v_1 are nonadjacent [i.e., not connected by an edge in $\Delta^1(\Sigma)$]. For adjacent v_0 and v_1, still $P_{v_0}^g P_{v_1}^h = P_{v_1}^h P_{v_0}^g$; their nonzero matrix elements $\langle\zeta|P_{v_0}^g P_{v_1}^h|\zeta'\rangle$ and $\langle\zeta|P_{v_1}^h P_{v_0}^g|\zeta'\rangle$ equal the Dijkgraaf-Witten weight on the topological balls (obtained by stacking pyramids in two orders as in Fig. 3) with identical triangulation and G-coloring in surface. In short,

$$\left[P_{v_0}^g, P_{v_1}^h\right] = 0 \text{ if } v_0 \neq v_1, \tag{22}$$

$\forall g, h \in G$. As a result, the set of Hermitian projectors $\{P_v\}_{v \in V(\Sigma)}$ labeled by vertices commute with each other.

When the 3-cocycle is completely trivial (i.e., $\omega \equiv 1$), the operator P_v^g reduces to $A_v^g \prod_{p \ni v} B_p$. So P_v^g is the twisted version of A_v^g with the projector $\prod_{p \ni v} B_p$ included. The Hamiltonian can be simply expressed as

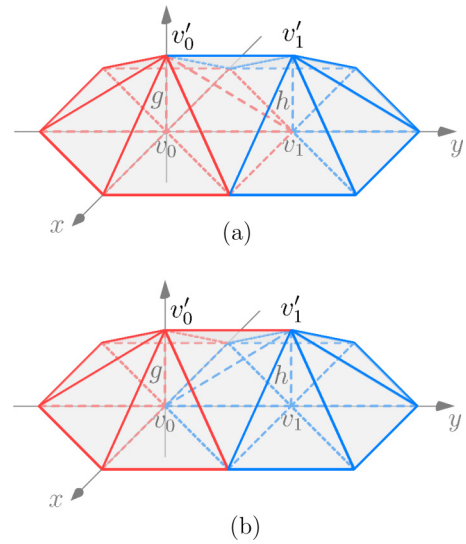

FIG. 3. Two orders of stacking two pyramids over two adjacent vertices, with (a) and (b) presenting $P_{v_0}^g P_{v_1}^h$ and $P_{v_1}^h P_{v_0}^g$, respectively.

$$H = -\sum_v P_v, \tag{23}$$

whose ground states are specified by $P_v = 1$. When $\omega \equiv 1$, the ground states are the same as those specified by $A_v = B_p = 1$.

In order to familiarize readers with our notations, let us express P_v^g more concretely in the example based on the twisted $\mathbb{Z}_2$ gauge theory. For $G = \mathbb{Z}_2 = \{0, 1\}$, there is only one nontrivial normalized 3-cocycle

$$\omega(f, g, h) = \begin{cases} -1, & f = g = h = 1, \\ 1, & \text{otherwise.} \end{cases} \tag{24}$$

On each edge lies a qubit. In terms of Pauli operators,

$$B_p = \frac{1}{2}\left(1 + \prod_{\ell \in E(p)} \sigma_\ell^z\right), \tag{25}$$

$$P_v^{(g=0)} = \prod_{p \ni v} B_p, \tag{26}$$

$$P_v^{(g=1)} = \prod_{p \ni v} B_p \sum_\zeta |\zeta\rangle\omega\left[\zeta, \mathrm{P}_v^1\right]\langle\zeta| \prod_{\ell \ni v} \sigma_\ell^x, \tag{27}$$

where $p \ni v$ (respectively, $\ell \ni v$) means that p (respectively, ℓ) connects to v. The phase factor $\omega[\zeta, \mathrm{P}_v^1] = \pm 1$ is given by Eq. (12) for $v = 3$ in Fig. 1. The tetrahedron over each triangle inside the hexagon $\hexagon_v$ centered at v contributes -1 to $\omega[\zeta, \mathrm{P}_v^1]$, if ζ colors the edges of the triangle in the same way as ζ_a in Fig. 4(a); otherwise, its contribution is $+1$. It is straightforward to check that $\omega[\zeta, \mathrm{P}_v^1] = -1$ if and only if ζ colors two edges next nearest to each other, such as [25] and [46] in Figs. 4(b) and 4(d), differently from the rest four edges on $\partial\hexagon_v$ (i.e., the boundary of $\hexagon_v$).

We will see soon that this model gives rise to anyons with topological spins $\pm i$ and hence describes the double semion topological phase [95,115]. Yet it does not look like the well-known double semion string-net model [95], even

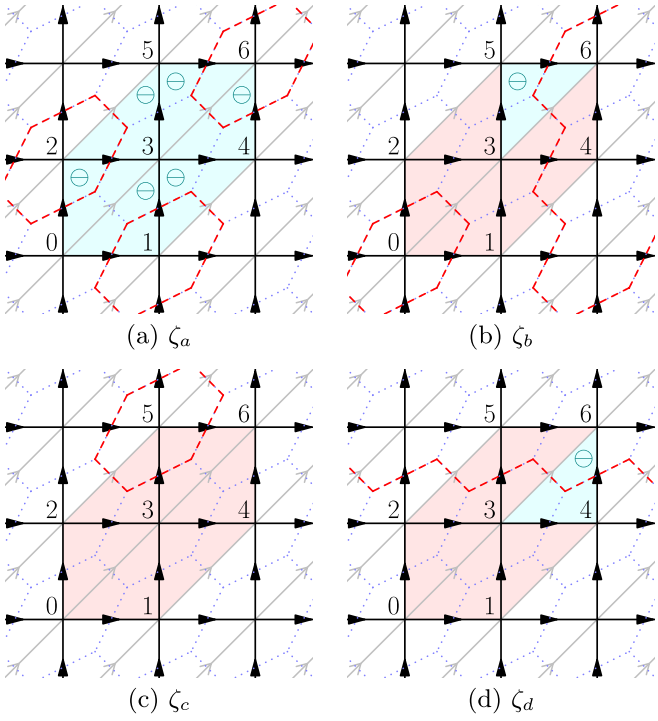

(a) ζ_a (b) ζ_b (c) ζ_c (d) ζ_d

FIG. 4. Locally flat spin configurations $\zeta = \zeta_a,\ \zeta_b,\ \zeta_c,\ \zeta_d$ for $G = \mathbb{Z}_2 = \{0, 1\}$ are presented by dashed strings (red online) without termination on the dual lattice of the triangulation: a spin is in state $|1\rangle$ if and only if its corresponding edge goes cross a string. Inside the hexagon $\hexagon_v = [014652]$ centered at $v = 3$, each triangle marked $\ominus$ (cyan online) is associated with a tetrahedron contributing -1 to $\omega[\mathsf{P}_v^1, \zeta]$, while other triangles contribute trivially.

after the degrees of freedom are matched by the duality shown in Fig. 4. The phase factor contained by the term corresponding to $P_v^{(g=1)}$ in the double semion string-net model is $-(-1)^{N_v/2} = -i^{N_v}$ with N_v the number of times that strings intersect with $\partial\hexagon_v$ (equivalently, the number of edges colored by 1 along $\partial\hexagon_v$). However, $\omega[\zeta_c, \mathsf{P}_v^1] = -\omega[\zeta_d, \mathsf{P}_v^1] = 1$ for $v = 3$, although $N_v = 2$ in both Figs. 4(c) and 4(d). This discrepancy can be cured by a basis transformation

$$\mathcal{U} = \bigotimes_{\ell\in\Delta^1(\Sigma)} i^{\zeta(\ell)}|\zeta\rangle\langle\zeta|, \tag{28}$$

which is a tensor product of local unitary quantum gates. For it to be well-defined, $\zeta([03])$ is set to $\zeta([01])\zeta([13])$ for auxiliary diagonal edges like [03] in Fig. 4 even when ζ is not locally flat. In particular, it adds an extra -1 to $P_v^{(g=1)}$ acting on ζ_d, since $P_v^{(g=1)}$ changes the number of edges colored 1 in the triangulation by 2. By $\mathcal{U}$, the Hamiltonian in Eq. (23) is transformed into the well-known form of double semion string-net model [95]. Explicitly, $\mathcal{U}P_v^{(g=1)}\mathcal{U}^\dagger = -i^{N_v}\cdot\prod_{p\ni v} B_p\cdot\prod_{\ell\ni v}\sigma_\ell^x$ with

$$N_v = \frac{1-\sigma^z_{[01]}}{2} + \frac{1-\sigma^z_{[13]}\sigma^z_{[34]}}{2} + \frac{1-\sigma^z_{[46]}}{2} + \frac{1-\sigma^z_{[02]}}{2} + \frac{1-\sigma^z_{[23]}\sigma^z_{[35]}}{2} + \frac{1-\sigma^z_{[56]}}{2} \tag{29}$$

counting how many of the edges [01], [14], [46], [02], [25] and [56] (i.e., those along $\partial\hexagon_v$) for $v = 3$ in Fig. 4 are colored by 1. Then $\mathcal{U}P_v\mathcal{U}^\dagger = P_v^{(g=0)} + \mathcal{U}P_v^{(g=1)}\mathcal{U}^\dagger$ and $\prod_v \mathcal{U}P_v\mathcal{U}^\dagger$ acting on $\bigotimes_\ell |0\rangle_\ell$ gives a ground state of the form $\sum_X (-1)^{\mathrm{loop}(X)}|X\rangle$, where $\mathrm{loop}(X)$ is the total number of loops (i.e., strings without termination) on the dual lattice of locally flat spin configuration X.

Another important example of twisted gauge theory is based on $G = \mathbb{Z}_2\times\mathbb{Z}_2\times\mathbb{Z}_2$ with the 3-cocycle

$$\omega(f, g, h) = e^{i\pi(f^{(1)}g^{(2)}h^{(3)})}, \tag{30}$$

where $f = (f^{(1)}, f^{(2)}, f^{(3)}), g = (g^{(1)}, g^{(2)}, g^{(3)}), h = (h^{(1)}, h^{(2)}, h^{(3)}) \in G$. It describes a non-Abelian topological phase [116], albeit G is Abelian. The corresponding lattice model contains three qubits, manipulated by Pauli operators $\sigma_\ell^{(j)\mu}$ with $j = 1, 2, 3$ and $\mu = x, y, z$, on each edge ℓ. Thus Eq. (25) defines a $B_p^{(j)}$ for each j. Their product $B_p = \prod_{j=1}^3 B_p^{(j)}$ requires the flux triviality and further defines $P_v^{000} = \prod_{p\ni v} B_p$. Elements of G are also denoted 000, 100, ... for short. A generic P_v^g is generated by P_v^{100}, P_v^{010}, and P_v^{001}, which can be simply expressed in terms of Pauli operators as well. For example, only the tetrahedrons in Eqs. (15) and (18) contribute a nontrivial factor to P_v^{100} at $v = 3$ in Fig. 1. Explicitly,

$$P_v^{100} = (-1)^{\frac{1}{2}(1-\sigma^{(2),z}_{[34]})\cdot\frac{1}{2}(1-\sigma^{(3),z}_{[46]})} \cdot(-1)^{\frac{1}{2}(1-\sigma^{(2),z}_{[35]})\cdot\frac{1}{2}(1-\sigma^{(3),z}_{[56]})}\cdot\prod_{p\ni v} B_p\cdot\prod_{\ell\ni v}\sigma_\ell^{(1)x}. \tag{31}$$

Then $P_v = \frac{1}{8}(P_v^{000}+P_v^{100})(P_v^{000}+P_v^{010})(P_v^{000}+P_v^{001})$. Besides $H = -\sum_v P_v$, the model may be defined by alternate Hamiltonians like $H = -\sum_v(P_v^{100}+P_v^{010}+P_v^{001})$; they have the same ground states. The general theory in Sec. II C tells us that this model hosts anyons described by the representation theory of the twisted quantum algebra $\mathcal{D}^\omega(G)$ with details in Appendix B. For the current situation, there are 14 two-dimensional irreducible representations shown in Table I and the corresponding anyons would present non-Abelian braiding statistics.

To conclude this section, we would like to generalize the above definition of P_v^g to take care of singular triangulations, where vertices of a triangle may coincide. This is done by replacing $\omega[\zeta, \mathsf{P}_v^g]$ in Eq. (11) with

$$\omega[\Sigma, v; \zeta, g] := \prod_{\tau\in\Delta^2(v,\Sigma)}\left(\frac{[\tau_0\tau_1\tau_2\tau_2'][\tau_0\tau_0'\tau_1'\tau_2']}{[\tau_0\tau_1\tau_1'\tau_2']}\right)^{\mathrm{sgn}(\tau)}, \tag{32}$$

where Σ is a surface whose triangulation may be singular and $\Delta^2(v,\Sigma)$ denotes the set of triangles adjacent to the vertex v in Σ. For each triangle $\tau = [\tau_0\tau_1\tau_2]$, the sign $\mathrm{sgn}(\tau)$ is $+1$ (respectively, -1) if the branching structure orders its vertices in the counterclockwise (respectively, clockwise) way. To define and compute $[\tau_0\tau_1\tau_2\tau_2'][\tau_0\tau_0'\tau_1'\tau_2']/[\tau_0\tau_1\tau_1'\tau_2'] \in \mathrm{U}(1)$, we present it graphically as a prism in Fig. 5 with bottom $[\tau_0\tau_1\tau_2]$ colored by ζ. Moreover, for $i = 0, 1, 2$, we color $[\tau_i\tau_i']$ by g if $\tau_i = v$ and e otherwise. Then the coloring of the rest of the edges is completely determined and each tetrahedron stands for the phase factor assigned by ω. For example,

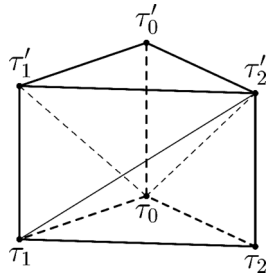

FIG. 5. Default triangulation of a prism over $\tau \times \mathtt{I}$, where $\tau = [\tau_0\tau_1\tau_2]$ and $\mathtt{I} = [0, 1]$. The Dijkgraaf-Witten weight on this prism is $[\tau_0\tau_1\tau_2\tau_2'][\tau_0\tau_0'\tau_1'\tau_2']/[\tau_0\tau_1\tau_1'\tau_2']$, where each tetrahedron $[v_0v_1v_2v_3]$ stands for $\omega([v_0v_1], [v_1v_2], [v_2v_3])$ with edges short for the group elements assigned by the coloring.

by $[\tau_0\tau_1\tau_2\tau_2']$ we mean $\omega([\tau_0\tau_1], [\tau_1\tau_2], [\tau_2\tau_2'])$ with edges $[\tau_0\tau_1], [\tau_1\tau_2], [\tau_2\tau_2']$ short for the group elements assigned to them by this coloring. It is easy to see that $\omega[\Sigma, v; \zeta, g]$ reduces back to $\omega[\zeta, \mathrm{P}_v^g]$ if the triangulation is regular.

B. Ground-state degeneracy on torus

Suppose that the lattice model of a twisted gauge theory is defined with periodic boundary conditions in both directions. In other words, the lattice Σ is embedded in a topological torus T^2.

Let us compute its ground-state degeneracy. Technically, it equals $\mathrm{tr}P$, the trace of

$$P := \prod_{v\in V(\Sigma)} P_v \tag{33}$$

over the physical Hilbert space $\mathcal{H}(E(\Sigma), G)$, or equivalently over $\mathcal{H}_B(E(\Sigma), G)$. Hence,

$$\mathrm{tr}P = \frac{1}{|G^{V(\Sigma)}|} \sum_{\zeta\in G_B^{E(\Sigma)}} \sum_{\eta\in G^{V(\Sigma)}} \langle\zeta| \prod_v P_v^{\eta(v)} |\zeta\rangle, \tag{34}$$

where $V(\Sigma)$ is the set of vertices of Σ and $G^{V(\Sigma)}$ is the set of functions from $V(\Sigma)$ to G.

Pick a vertex $u \in V(\Sigma)$ and two noncontractible loops q_x, q_y based at u along the two spatial directions. For any $\zeta \in \mathrm{Col}(\Sigma, G)$, let h_1 and h_2 be the group elements assigned by ζ to q_x and q_y respectively. The choices of η such that $\langle\zeta| \prod_v A_v^{\eta(v)} |\zeta\rangle \neq 0$ are labeled by $h_3 := \eta(u) \in Z_G(h_1, h_2)$, where $Z_G(h_1, h_2)$ is the centralizer of $\{h_1, h_2\}$ in G. Actually, $\langle\zeta| \prod_v A_v^{\eta(v)} |\zeta\rangle$ can be thought of as the Dijkgraaf-Witten weight $\omega[\mathrm{T}^2 \times \mathtt{I}; \zeta, \zeta, h_3]$ on a triangulated space $\mathrm{T}^2 \times \mathtt{I}$ with its bottom $\mathrm{T}^2 \times \{0\}$ and top $\mathrm{T}^2 \times \{1\}$ both colored by ζ and an edge $[uu']$ colored by h_3. Here $\mathtt{I} = [0, 1]$ and u, u' stand for $u \times \{0\}$, $u \times \{1\}$ respectively. Further, since the bottom and top of $\mathrm{T}^2 \times \mathtt{I}$ are identically triangulated and colored, we can simply glue them together and view $\langle\zeta| \prod_v A_v^{\eta(v)} |\zeta\rangle$ as the Dijkgraaf-Witten weight on the three dimensional torus T^3, which only depends on the group elements associated with the three noncontractible loops based at a vertex. Thus

$$\langle\zeta| \prod_v A_v^{\eta(v)} |\zeta\rangle = \omega[\mathrm{T}^3; h_1, h_2, h_3], \tag{35}$$

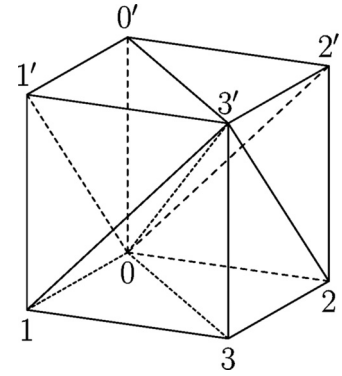

FIG. 6. A triangulation of a cube. The eight vertices are ordered as $0 < 0' < 1 < 1' < 2 < 2' < 3 < 3'$; their ordering assigns orientations to edges, triangles and tetrahedrons. Gluing the three pairs of opposite faces of the cube gives a triangulated three-dimensional torus T^3.

when it is nonzero. Further, Eq. (34) reduces to

$$\mathrm{tr}P = \mathcal{Z}_\omega(\mathrm{T}^3). \tag{36}$$

In other words, the ground-state degeneracy on T^2 equals the Dijkgraaf-Witten partition function on T^3.

For the purpose of calculation, we can use the simplest triangulation of T^3 shown in Fig. 6 and get

$$\begin{aligned}\omega[\mathrm{T}^3; h_1, h_2, h_3] &= \frac{[0133'][00'1'3']}{[011'3']} \cdot \frac{[022'3']}{[0233'][00'2'3']} \\ &= \frac{\omega_{h_3}(h_1, h_2)}{\omega_{h_3}(h_2, h_1)},\end{aligned} \tag{37}$$

where $[01] = h_1$, $[02] = h_2$, $[00'] = h_3$ and for $g, s, t \in G$,

$$\omega_g(s, t) := \frac{\omega(g, s, t)\omega(s, t, (st)^{-1}gst)}{\omega(s, s^{-1}gs, t)}. \tag{38}$$

Thus we can compute the ground-state degeneracy $\mathrm{tr}P$ on T^2 explicitly by

$$\begin{aligned}\mathrm{tr}P = \mathcal{Z}_\omega(\mathrm{T}^3) = \frac{1}{|G|} \sum_{h_1,h_2,h_3\in G} &\delta_{h_1h_2,h_2h_1} \\ \cdot \delta_{h_1h_3,h_3h_1} \cdot \delta_{h_2h_3,h_3h_2} &\cdot \frac{\omega_{h_3}(h_1, h_2)}{\omega_{h_3}(h_2, h_1)}.\end{aligned} \tag{39}$$

In particular, if G is Abelian and $\omega \equiv 1$, then $\mathrm{tr}P = |G|^2$.

1. Example: $G = \mathbb{Z}_2$ twisted

As an example of a twisted model, we consider $G = \mathbb{Z}_2 = \{0, 1\}$ with a nontrivial 3-cocyle given by Eq. (24). We will see soon that this model gives rise to anyons with topological spins $\pm i$ and hence describes the double semion topological phase [95,115]. Although $[\omega]$ is nontrivial in $H^3(G, \mathrm{U}(1))$, we still have $\frac{\omega_{h_3}(h_1,h_2)}{\omega_{h_3}(h_2,h_1)} \equiv 1$ and hence $\mathrm{tr}P = |G|^2$, the same ground-state degeneracy on T^2 as in the untwisted model.

2. Example: $G = \mathbb{Z}_m^3$ with $\omega(f, g, h) = e^{i\frac{2\pi}{m} f^{(1)} g^{(2)} h^{(3)}}$

Another interesting model can be constructed with $G = \mathbb{Z}_m \times \mathbb{Z}_m \times \mathbb{Z}_m \equiv \mathbb{Z}_m^3$ with a 3-cocyle

$$\omega(f, g, h) = e^{i\frac{2\pi}{m} f^{(1)} g^{(2)} h^{(3)}}, \tag{40}$$

for $f = (f^{(1)}, f^{(2)}, f^{(3)})$, $g = (g^{(1)}, g^{(2)}, g^{(3)})$, $h = (h^{(1)}, h^{(2)}, h^{(3)}) \in G$, where the product $f^{(1)} g^{(2)} h^{(3)}$ is well-defined from the ring structure of $\mathbb{Z}_m$. Now

$$\frac{\omega_{h_3}(h_1, h_2)}{\omega_{h_3}(h_2, h_1)} = \exp\left(i\frac{2\pi}{m} \begin{vmatrix} h_1^{(1)} & h_2^{(1)} & h_3^{(1)} \\ h_1^{(2)} & h_2^{(2)} & h_3^{(2)} \\ h_1^{(3)} & h_2^{(3)} & h_3^{(3)} \end{vmatrix} \right) \tag{41}$$

$$= \exp\left\{ i\frac{2\pi}{m} (h_1 \times h_2) \cdot h_3 \right\} \tag{42}$$

is nontrivial, where we write

$$f \times g := (f^{(2)} g^{(3)} - f^{(3)} g^{(2)}, f^{(3)} g^{(1)} - f^{(1)} g^{(3)}, f^{(1)} g^{(2)} - f^{(2)} g^{(1)}), \tag{43}$$

$$f \cdot g := f^{(1)} g^{(1)} + f^{(2)} g^{(2)} + f^{(3)} g^{(3)}, \tag{44}$$

for any $g, h \in G$.

By noticing the identity

$$\frac{1}{|G|} \sum_{h_3 \in G} \exp\left\{ i\frac{2\pi}{m} (h_1 \times h_2) \cdot h_3 \right\} = \delta_{h_1 \times h_2, 0}, \tag{45}$$

we get an explicit formula for the ground-state degeneracy on T^2

$$\mathrm{tr} P = \mathcal{Z}_\omega(\mathrm{T}^3) = \sum_{h_1, h_2 \in G} \delta_{h_1 \times h_2, 0}. \tag{46}$$

In particular, for $m = 2$, we have

$$\mathrm{tr} P = \mathcal{Z}_\omega(\mathrm{T}^3) = 22, \tag{47}$$

which is quite different from the untwisted case whose ground-state degeneracy on T^2 is $|G|^2 = 64$.

C. Anyons and twisted quantum double algebra

It is well-known that the quasiparticles in these two-dimensional models are anyons and that the total number of particle types equals the ground-state degeneracy on a torus T^2. Explicitly, the particle types of anyons can be labeled by irreducible representations (up to isomorphism) of the twisted quantum double algebra $\mathcal{D}^\omega(G)$. Actually, $\mathcal{D}^\omega(G)$ can be enhanced into a quasitriangular quasi-Hopf algebra equipped with a coproduct $\Delta : \mathcal{D}^\omega(G) \otimes \mathcal{D}^\omega(G) \to \mathcal{D}^\omega(G)$ and a universal R matrix $R \in \mathcal{D}^\omega(G) \otimes \mathcal{D}^\omega(G)$; the extra structures encode the fusion and braiding properties of anyons. If $\omega \equiv 1$, then $\mathcal{D}^\omega(G)$ reduces to the normal quantum double $\mathcal{D}(G)$, which is a quasitriangular Hopf algebra and used in studying the standard gauge theories in two spatial dimensions [15,44–46]. The lattices models of (twisted) gauge theories in two spatial dimensions are thus also called (twisted) quantum double models. The mathematical details of $\mathcal{D}^\omega(G)$ and its representations are summarized in Appendix B. Below, we will elucidate the notion of anyon and its connection to the representation theory of $\mathcal{D}^\omega(G)$ in the concrete lattice models.

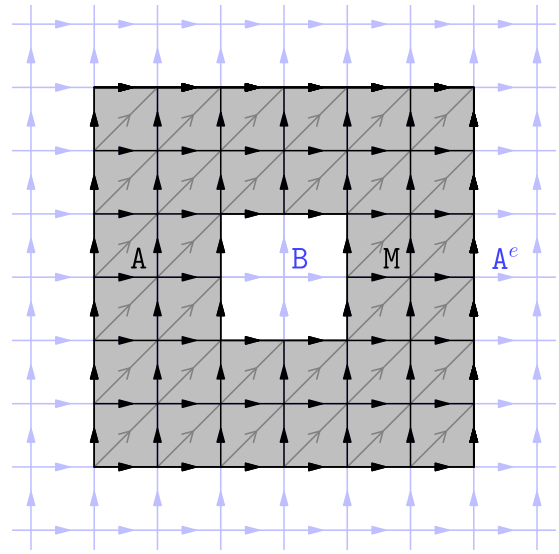

(a)

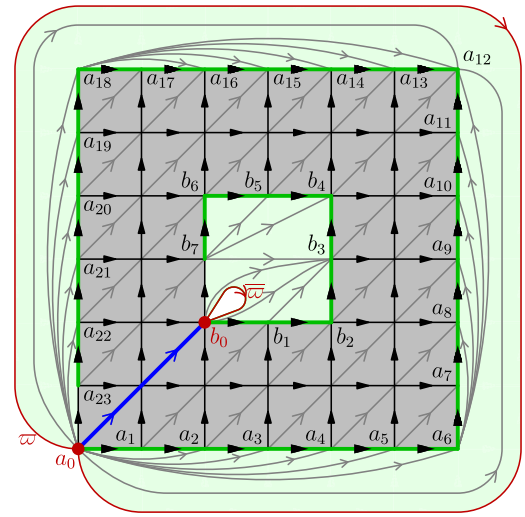

(b)

FIG. 7. Hilbert space used for classifying excitations within a finite region B. (a) There is no excitation in the grey region $\mathtt{M} = \mathtt{A} - \mathtt{B}^\circ$, where A is a larger region containing B and $\mathtt{B}^\circ$ is the interior of B. (b) Extra P_v^g operators for $v \in V(\partial\mathtt{M})$ and $g \in G$ can be defined by embedding M into a topological annulus $\overline{\mathtt{M}}$. The boundary of $\overline{\mathtt{M}}$ is the disjoint union of two loops; $\partial\overline{\mathtt{M}} = (-\varpi) \cup \overline{\varpi}$, where the minus sign means that the orientation of ϖ is opposite to the one induced from $\overline{\mathtt{M}}$.

1. Topological charge and representation

First, let us classify the *particle types* of an excited finite region (i.e., a localized quasiparticle), such as the small white square region B at the center of Fig. 7(a). For topologically ordered systems in two spatial dimensions, we also use the terminology *topological charge* as an synonym of particle type. To make it well-defined, we suppose that B is an isolated excitation inside a much larger region A. Then there is an excitation-free topological annulus $\mathtt{M} := \mathtt{A} - \mathtt{B}^\circ$, such as the shaded region in Fig. 7(a), separating B from the other

excitations in $\mathtt{A}^e$. Here, $\mathtt{X}^e$ (respectively, $\mathtt{X}^\circ$) denotes the exterior (respectively, interior) of any topological space $\mathtt{X}$. Such states lie in the Hilbert subspace $\mathcal{H}(E(\mathtt{A}^e), G) \otimes \mathcal{H}_0(\mathtt{M}) \otimes \mathcal{H}(E(\mathtt{B}^\circ), G)$, where $\mathcal{H}_0(\mathtt{M})$ is the Hilbert subspace selected out of the locally flat states $\mathcal{H}_B(E(\mathtt{M}), G)$ by the projector

$$P(\mathtt{M}) := \prod_{v \in V(\mathtt{M}^\circ)} P_v. \tag{48}$$

Since hopping between states of $\mathcal{H}(\mathtt{A}^e)$ [respectively, $\mathcal{H}(\mathtt{B}^\circ)$] can be made by operators supported on $\mathtt{A}^e$ (respectively, $\mathtt{B}^\circ$), they are irrelevant to the discussion of particle types. Below, we only need to focus on $\mathcal{H}_0(\mathtt{M})$.

It is easy to see that the dimension of $\mathcal{H}_0(\mathtt{M})$ grows with the number of spins along the boundary of $\mathtt{M}$. To facilitate the analysis of $\mathcal{H}_0(\mathtt{M})$, we embed $\mathtt{M}$ in a larger topological annulus $\overline{\mathtt{M}}$ which covers all shaded regions (grey and green online) and add edges to finish a triangulation of $\overline{\mathtt{M}}$ as shown in Fig. 7(b). Obviously, each coloring of $\mathtt{M}$ extends to $\overline{\mathtt{M}}$ uniquely. We label the outer (respectively, inner) boundary of $\overline{\mathtt{M}}$ by ϖ (respectively, $\overline{\varpi}$), which is a loop with base point a_0 (respectively, b_0). Let $\langle a_0 b_0 \rangle$ be the thick path (blue online) from a_0 to b_0 in Fig. 7(b). Let T_g, $\overline{T}_h$, and $T_s^{\langle a_0 b_0 \rangle}$ be the Hermitian projectors requiring the group elements associated with paths $[a_0 a_1 a_2 \cdots a_{23} a_0]$, $[b_0 b_1 b_2 \cdots b_7 b_0]$ and $\langle a_0 b_0 \rangle$ to be $g, h, s \in G$ respectively.

As shown in Fig. 7(b), the vertices along the outer and inner boundaries of $\mathtt{M}$ (i.e., $\partial\mathtt{A}$ and $\partial\mathtt{B}$) are labeled as $a_0, a_1, \ldots, a_{23}$ and $b_0, b_1, \ldots, b_7$, respectively. Pick any two functions

$$\chi : \{[a_i a_{i+1}]\}_{i=0,1,\ldots,22} \to G, \tag{49}$$

$$\overline{\chi} : \{[b_i b_{i+1}]\}_{i=0,1,\ldots,6} \to G. \tag{50}$$

Let $T[\chi]$ (respectively, $T[\overline{\chi}]$) be the Hermitian projector requiring $\zeta([a_i a_{i+1}]) = \chi([a_i a_{i+1}])$ for $i = 0, 1, \ldots, 22$ (respectively, $\zeta([a_i a_{i+1}]) = \overline{\chi}([b_i b_{i+1}])$ for $i = 0, 1, \ldots, 6$). Obviously, $T[\chi]$ (respectively, $T[\overline{\chi}]$) is supported on the thick edges (green online) along the outer (respectively, inner) boundary of $\mathtt{M}$.

The Hermitian projectors T_g, $T_s^{\langle a_0 b_0 \rangle}$, $T[\chi]$, and $T[\overline{\chi}]$ commute with each other. It is a straightforward computation to show that, on $\mathcal{H}(E(\mathtt{M}), G)$,

$$\mathrm{tr}\left(T_g T_s^{\langle a_0 b_0 \rangle} T[\chi] T[\overline{\chi}] P(\mathtt{M})\right) = 1. \tag{51}$$

Therefore we can label a basis of $\mathcal{H}_0(\mathtt{M})$ by g, s, χ, and $\overline{\chi}$.

To give a graphic representation of the basis vectors, let $\mathtt{D}_g^s$ be an annulus with *colored triangulation* (i.e., triangulation in which some edges carry fixed group elements) as shown in Fig. 8(a). Gluing $\overline{\mathtt{M}}$ with $\mathtt{D}_g^s$ along the outer and inner boundaries (i.e., loops ϖ and $\overline{\varpi}$) respectively, we get a triangulated torus, denoted $(-\overline{\mathtt{M}}) \cup_{\varpi\overline{\varpi}} \mathtt{D}_g^s$. Let $G^{E(\mathtt{M})}(\chi, \overline{\chi})$ be the set of spin configurations coinciding with $\chi, \overline{\chi}$ on the corresponding edges [green online in Fig. 7(b)]. Further, let $Z_\omega(\zeta; \mathtt{D}_g^s)$ be the Dijkgraaf-Witten partition function on a solid torus whose surface is $(-\overline{\mathtt{M}}) \cup_{\varpi\overline{\varpi}} \mathtt{D}_g^s$, like the one in Fig. 8(b), with $E(\mathtt{M})$ fixed to $\zeta \in G^{E(\mathtt{M})}(\chi, \overline{\chi})$. Explicitly, $Z_\omega(\zeta; \mathtt{D}_g^s)$ is the sum of Dijkgraaf-Witten weight over colorings of the solid torus coinciding with g, s and ζ on the corresponding edges. Details of Dijkgraaf-Witten partition function are included in Appendix A. Here, if ζ is locally flat (i.e., $\zeta \in G_B^{E(\mathtt{M})}$) and assigns g, s to paths $[a_0 a_1 a_2 \cdots a_{23} a_0]$, $\langle a_0 b_0 \rangle$, respectively, then $\mathcal{Z}_\omega(\zeta; \mathtt{D}_g^s) \in U(1)$; otherwise, there is no valid coloring on the solid torus and hence $\mathcal{Z}_\omega(\zeta; \mathtt{D}_g^s) = 0$. Then, the vectors

$$\left|\chi, \overline{\chi}; \mathtt{D}_g^s\right\rangle := \sum_{\zeta \in G_B^{E(\mathtt{M})}(\chi, \overline{\chi})} \frac{\mathcal{Z}_\omega\left(\zeta; \mathtt{D}_g^s\right)}{|G|^{\frac{|V(\mathtt{M}^\circ)|}{2}}} |\zeta\rangle \tag{52}$$

labeled by χ, $\overline{\chi}$, g, s form an orthonormal basis of $\mathcal{H}_0(\mathtt{M})$, where $G_B^{E(\mathtt{M})}(\chi, \overline{\chi}) := G^{E(\mathtt{M})}(\chi, \overline{\chi}) \cap G_B^{E(\mathtt{M})}$. For $v \in \mathtt{M}^\circ$, it is

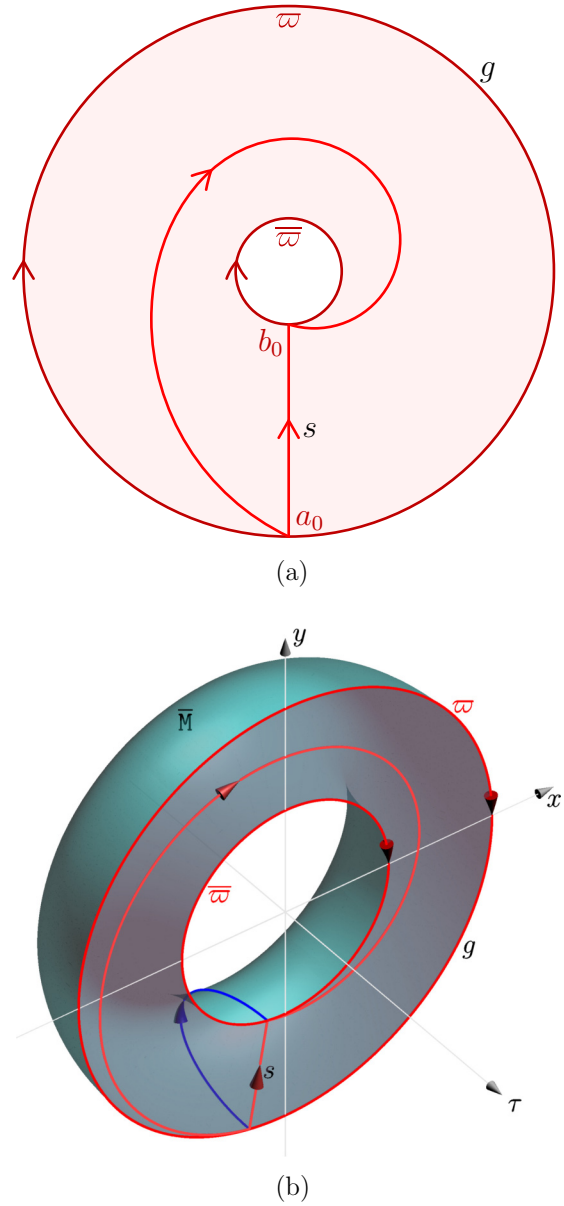

FIG. 8. Graphic representation of $|\chi, \overline{\chi}; \mathtt{D}_g^s\rangle$. (a) An annulus (i.e., one-hole disk) with colored triangulation $\mathtt{D}_g^s$. (b) A solid torus whose surface is $(-\overline{\mathtt{M}}) \cup_{\varpi\overline{\varpi}} \mathtt{D}_g^s$. The minus sign emphasizes that the orientation of $\overline{\mathtt{M}}$ points towards the inside of the solid torus according to the right-hand rule. The two annuli $\overline{\mathtt{M}}$ and $\mathtt{D}_g^s$ are drawn curved and flat, respectively; their shared boundary is the disjoint union of the two loops ϖ and $\overline{\varpi}$. The state $|\chi, \overline{\chi}; \mathtt{D}_g^s\rangle$ is specified by $\langle\zeta|\chi, \overline{\chi}; \mathtt{D}_g^s\rangle = \mathcal{N}\mathcal{Z}_\omega(\zeta; \mathtt{D}_g^s)$ for $\zeta \in G^{E(\mathtt{M})}(\chi, \overline{\chi})$, where $\mathcal{Z}_\omega(\zeta; \mathtt{D}_g^s)$ is the Dijkgraaf-Witten partition function on this solid torus and $\mathcal{N}$ is a normalization factor.

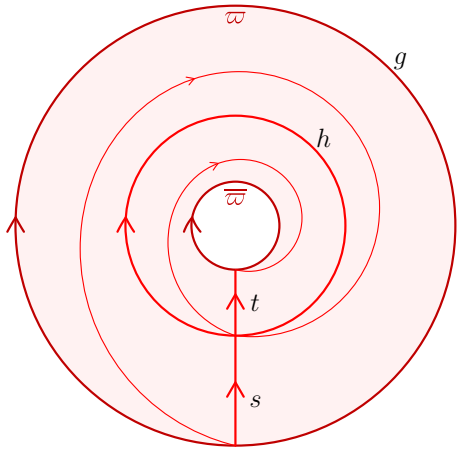

FIG. 9. An annulus (i.e., one-hole disk) with colored triangulation $\mathtt{D}_g^s\mathtt{D}_h^t$. It determines a legitimate coloring and corresponds to a nonzero state $|\mathtt{D}_g^s\mathtt{D}_h^t\rangle$ if and only if $g = shs^{-1}$.

obvious $P_v = 1$ (and hence $P_v^g = 1, \forall g \in G$) on these states by noticing

$$\langle\zeta|P_v\big|\chi, \overline{\chi}; \mathtt{D}_g^s\big\rangle = \mathcal{Z}_\omega\big(\zeta; \mathtt{D}_g^s\big) = \big\langle\zeta\big|\chi, \overline{\chi}; \mathtt{D}_g^s\big\rangle \tag{53}$$

using the graphic representation of P_v^g given by Eq. (11) and Fig. 1(b).

In general, we can consider states presented by other triangulations of the annulus. Let $\mathtt{D}_g^s\mathtt{D}_h^t$ denote an triangulated annulus carrying fixed group elements $g,\ h,\ s,\ t \in G$ on its four edges as shown in Fig. 9; it is obtained by connecting $\mathtt{D}_g^s$ and $\mathtt{D}_h^t$. Similarly, gluing $\overline{\mathtt{M}}$ and $\mathtt{D}_g^s\mathtt{D}_h^t$ along loops ϖ and $\overline{\varpi}$ gives a torus $(-\overline{\mathtt{M}}) \cup_{\varpi\overline{\varpi}} \mathtt{D}_g^s\mathtt{D}_h^t$. Analogous to Eq. (52), we can define

$$\big|\chi, \overline{\chi}; \mathtt{D}_g^s\mathtt{D}_h^t\big\rangle := \sum_{\zeta\in G_B^{E(\mathtt{M}^\circ)}(\chi,\overline{\chi})} \frac{\mathcal{Z}_\omega\big(\zeta; \mathtt{D}_g^s\mathtt{D}_h^t\big)}{|G|^{\frac{|V(\mathtt{M}^\circ)|}{2}}}|\zeta\rangle, \tag{54}$$

where $\mathcal{Z}_\omega(\zeta; \mathtt{D}_g^s\mathtt{D}_h^t)$ is the Dijkgraaf-Witten partition function on a solid torus whose surface is $(-\overline{\mathtt{M}}) \cup_{\varpi\overline{\varpi}} \mathtt{D}_g^s\mathtt{D}_h^t$.

We notice

$$\mathcal{Z}_\omega\big(\zeta; \mathtt{D}_g^s\mathtt{D}_h^t\big) = \mathcal{Z}_\omega\big(\zeta; \mathtt{D}_g^{st}\big)\mathcal{Z}_\omega\big(\mathtt{D}_g^{st}; \mathtt{D}_g^s\mathtt{D}_h^t\big), \tag{55}$$

$$\mathcal{Z}_\omega\big(\mathtt{D}_g^{st}; \mathtt{D}_g^s\mathtt{D}_h^t\big) = \delta_{g,shs^{-1}}\omega_g(s,t), \tag{56}$$

where $\omega_g(s,t)$ is defined as

$$\omega_g(s,t) := \frac{\omega(g,s,t)\omega(s,t,(st)^{-1}g(st))}{\omega\big(s, s^{-1}gs, t\big)}. \tag{57}$$

Therefore $\forall g, h, s, t \in G$, we have

$$\big|\chi, \overline{\chi}; \mathtt{D}_g^s\mathtt{D}_h^t\big\rangle = \delta_{g,shs^{-1}}\omega_g(s,t)\big|\chi, \overline{\chi}; \mathtt{D}_g^{st}\big\rangle, \tag{58}$$

which motivates the definition of an algebra $\mathcal{D}^\omega(G)$, called a *twisted quantum double* of G. Formally, $\mathcal{D}^\omega(G)$ is spanned by $\{D_g^s\}_{g,s\in G}$ with multiplication rule

$$D_g^sD_h^t := \delta_{g,shs^{-1}}\omega_g(s,t)D_g^{st}, \quad \forall g, h, s, t \in G. \tag{59}$$

More details about $\mathcal{D}^\omega(G)$ are included in Appendix B.

We have seen that $\mathcal{H}_0(\mathtt{M})$ factors into

$$\mathcal{H}_0(\mathtt{M}) = \mathcal{H}(\partial\mathtt{A}) \otimes \mathcal{H}(\partial\mathtt{B}) \otimes \mathcal{H}_*(\overline{\mathtt{M}}), \tag{60}$$

where $\mathcal{H}(\partial\mathtt{A})$, $\mathcal{H}(\partial\mathtt{B})$, and $\mathcal{H}_*(\overline{\mathtt{M}})$ are the Hilbert spaces spanned by orthonormal bases $\{|\chi\rangle\}$, $\{|\overline{\chi}\rangle\}$, and $\{|\mathtt{D}_g^s\rangle\}$ respectively. Using $\overline{\mathtt{M}}$ and Eq. (11) with $\omega[\zeta, \mathtt{P}_v^g]$ replaced by Eq. (32), we extend the definition of P_v^g to include vertices on $\partial\mathtt{M}$ as well. Explicitly,

$$P_v^g := \sum_{\zeta\in G_B^{E(\overline{\mathtt{M}[v]})}} |\zeta\rangle\omega[\overline{\mathtt{M}}, v; \zeta, g]\big\langle\zeta A_v^g\big|, \tag{61}$$

$\forall g \in G, \forall v \in V(\mathtt{M})$, where $\overline{\mathtt{M}[v]} = \mathtt{M}[v]$ for $v \in \mathtt{M}^\circ$ while $\overline{\mathtt{M}[v]} = \mathtt{M}[v] \cup \partial\mathtt{A}$ (respectively, $\overline{\mathtt{M}[v]} = \mathtt{M}[v] \cup \partial\mathtt{B}$) for $v \in \partial\mathtt{A}$ (respectively, $v \in \partial\mathtt{B}$) with $\mathtt{M}[v]$ the region made of all plaquettes adjacent to v inside $\mathtt{M}$. They still satisfy Eq. (22). Except for $v = a_0$ and b_0, Eqs. (19) and (20) also hold. Hence $\{P_v := \frac{1}{|G|}\sum_g P_v^g\}_{v\neq a_0,b_0}$ are mutual commuting Hermitian projectors. Let

$$P_{\partial\mathtt{A}} := \prod_{v\in V(\partial\mathtt{A})\setminus\{a_0\}} P_v, \tag{62}$$

$$P_{\partial\mathtt{B}} := \prod_{v\in V(\partial\mathtt{B})\setminus\{b_0\}} P_v. \tag{63}$$

Then $|G|^{|V(\partial\mathtt{A})|-1}T[\chi]P_{\partial\mathtt{A}}T[\chi']$ realizes a generic operator $|\chi\rangle\langle\chi'|$ on $\mathcal{H}(\partial\mathtt{A})$. Thus $\mathcal{H}(\partial\mathtt{A})$ describes only degrees of freedom near $\partial\mathtt{A}$ (i.e., the outer boundary of $\mathtt{M}$). Similarly, $\mathcal{H}(\partial\mathtt{B})$ describes only degrees of freedom near $\partial\mathtt{B}$. Both $\mathcal{H}(\partial\mathtt{A})$ and $\mathcal{H}(\partial\mathtt{B})$ are irrelevant to classification of particle types.

Moreover, the operators

$$\pi\big(D_g^s\big) := |G|^{|V(\partial\mathtt{A})|-1}\sum_\chi T[\chi]T_gP_{a_0}^sP_{\partial\mathtt{A}}T[\chi], \tag{64}$$

$$\overline{\pi}\big(D_h^t\big) := |G|^{|V(\partial\mathtt{B})|-1}\sum_{\overline{\chi}} T[\overline{\chi}]\big(\overline{T}_hP_{b_0}^t\big)^\dagger P_{\partial\mathtt{B}}T[\overline{\chi}], \tag{65}$$

labeled by $D_g^s,\ D_h^t \in \mathcal{D}^\omega(G)$ and supported near $\partial\mathtt{A}$, $\partial\mathtt{B}$, respectively, only act nontrivially on $\mathcal{H}_*(\overline{\mathtt{M}})$. Explicitly,

$$\pi\big(D_g^s\big)\big|\chi, \overline{\chi}; \mathtt{D}_h^t\big\rangle = \big|\chi, \overline{\chi}; \mathtt{D}_g^s\mathtt{D}_h^t\big\rangle, \tag{66}$$

$$\overline{\pi}\big(D_h^t\big)\big|\chi, \overline{\chi}; \mathtt{D}_g^s\big\rangle = \big|\chi, \overline{\chi}; \mathtt{D}_g^s\mathtt{D}_h^t\big\rangle. \tag{67}$$

Thus π and $\overline{\pi}$ turn $\mathcal{H}_*(\overline{\mathtt{M}})$ into a regular $\mathcal{D}^\omega(G)$-$\mathcal{D}^\omega(G)$-bimodule; i.e., the left and right actions of $\mathcal{D}^\omega(G)$ on $\mathcal{H}_*(\overline{\mathtt{M}})$ specified by π and $\overline{\pi}$, respectively, are the same as how $\mathcal{D}^\omega(G)$ acts on itself via algebra multiplication.

In addition, an $*$-algebra structure on $\mathcal{D}^\omega(G)$ can be specified by

$$\big(D_g^s\big)^\dagger := \omega_g^*(s, s^{-1})D_{s^{-1}gs}^{s^{-1}}, \quad \forall g, s \in G, \tag{68}$$

where $\omega_g^*(s, s^{-1})$ is the complex conjugate of $\omega_g(s, s^{-1})$. Then it is straightforward to check that

$$\pi\big(\big(D_g^s\big)^\dagger\big) = \big(\pi\big(D_g^s\big)\big)^\dagger, \tag{69}$$

$$\overline{\pi}\big(\big(D_h^t\big)^\dagger\big) = \big(\overline{\pi}\big(D_h^t\big)\big)^\dagger, \tag{70}$$

by using the identity [117]

$$\omega_g(s,t)\omega_g(st,u) = \omega_g(s,tu)\omega_{s^{-1}gs}(t,u), \tag{71}$$

$\forall g, s, t, u \in G$. We also notice that setting $t = s^{-1}$ and $u = s$ in Eq. (71) gives $\omega_g(s, s^{-1}) = \omega_{s^{-1}gs}(s^{-1}, s)$, which ensures $((D_g^s)^\dagger)^\dagger = D_g^s$.

Since π is a left regular representation of a unital algebra, it is faithful. So $\mathcal{D}^\omega(G)$ can be viewed as a subalgebra, closed under the Hermitian conjugate, of $\mathcal{L}(\mathcal{H}_*(\overline{\mathtt{M}}))$. Here $\mathcal{L}(V)$ denote the algebra of all linear operators on a vector space V. Thus $\mathcal{D}^\omega(G)$ is a finite dimensional C^*-algebra and hence semisimple. Therefore $\mathcal{D}^\omega(G)$ is isomorphic to a direct sum of matrix algebras

$$\mathcal{D}^\omega(G) \xrightarrow[*-\text{algebra}\cong]{\rho:=\bigoplus_{\mathfrak{a}\in\mathfrak{Q}}\rho_{\mathfrak{a}}} \bigoplus_{\mathfrak{a}\in\mathfrak{Q}} \mathcal{L}(\mathcal{V}_{\mathfrak{a}}), \tag{72}$$

where $\mathfrak{Q}$ labels the isomorphism classes of irreducible representations of $\mathcal{D}^\omega(G)$ and $\mathcal{V}_{\mathfrak{a}} = (\rho_{\mathfrak{a}}, V_{\mathfrak{a}})$ is a finite dimensional Hilbert space carrying an representation $\rho_{\mathfrak{a}}$ corresponding to $\mathfrak{a} \in \mathfrak{Q}$. Moreover, $\mathcal{L}(\mathcal{V}_{\mathfrak{a}})$ is the algebra of linear operators on $\mathcal{V}_{\mathfrak{a}}$; it is isomorphic to the algebra of $n_{\mathfrak{a}} \times n_{\mathfrak{a}}$ square matrices, where $n_{\mathfrak{a}} := \dim_{\mathbb{C}} \mathcal{V}_{\mathfrak{a}}$. More explanations about this isomorphism ρ are included in Appendix B 5. Let $\{|\mathfrak{a}; i\rangle\}_{i=1,\ldots,n_{\mathfrak{a}}}$ be an orthonormal basis of $\mathcal{V}_{\mathfrak{a}}$. Via ρ in Eq. (72), we can view $\{|\mathfrak{a}; i\rangle\langle\mathfrak{a}; j|\}_{i,j=1,2,\ldots,n_{\mathfrak{a}}}^{\mathfrak{a}\in\mathfrak{Q}}$ as a basis of $\mathcal{D}^\omega(G)$.

As a $\mathcal{D}^\omega(G)$-$\mathcal{D}^\omega(G)$-bimodule, $\mathcal{H}_*(\overline{\mathtt{M}})$ can be identified with $\mathcal{D}^\omega(G)$ and further get decomposed

$$\begin{aligned}\mathcal{H}_*(\overline{\mathtt{M}}) &\xrightarrow[\sim]{|\mathtt{D}_g^s\rangle\mapsto D_g^s} \mathcal{D}^\omega(G)\\ &\xrightarrow[\sim]{\tilde\rho:=\bigoplus_{\mathfrak{a}\in\mathfrak{Q}}\sqrt{\frac{n_{\mathfrak{a}}}{|G|}}\rho_{\mathfrak{a}}} \bigoplus_{\mathfrak{a}\in\mathfrak{Q}} \mathcal{L}(\mathcal{V}_{\mathfrak{a}}) = \bigoplus_{\mathfrak{a}\in\mathfrak{Q}} \mathcal{V}_{\mathfrak{a}}\otimes\mathcal{V}_{\mathfrak{a}}^*,\end{aligned} \tag{73}$$

where $\mathcal{V}_{\mathfrak{a}}^*$ is the dual space (spanned by $\{\langle\mathfrak{a}; i|\}_{i=1,\ldots,n_{\mathfrak{a}}}$) of $\mathcal{V}_{\mathfrak{a}}$. The normalizations for $\tilde\rho$ on each sector are picked different from ρ such that inner product is also respected. As a Hilbert space, it is convenient to write the basis vectors of $\mathcal{L}(\mathcal{V}_{\mathfrak{a}})$ (respectively, $\mathcal{V}_{\mathfrak{a}}^*$) as $|\mathfrak{a}; i, \overline{j}\rangle := |\mathfrak{a}; i\rangle\langle\mathfrak{a}; j|$ (respectively, $|\mathfrak{a}; \overline{j}\rangle := \langle\mathfrak{a}; j|$). The default inner product on $\mathcal{V}_{\mathfrak{a}}^*$ is given by $\langle\mathfrak{a}; \overline{j'}|\mathfrak{a}; \overline{j}\rangle := \langle\mathfrak{a}; j|\mathfrak{a}; j'\rangle$. The tensor product specifies the inner product on $\mathcal{L}(\mathcal{V}_{\mathfrak{a}})$; equivalently, $\langle\mathcal{O}_1|\mathcal{O}_2\rangle = \mathrm{tr}(\mathcal{O}_1^\dagger\mathcal{O}_2), \forall\mathcal{O}_1, \mathcal{O}_2 \in \mathcal{L}(\mathcal{V}_{\mathfrak{a}})$.

By construction, $|\mathfrak{q}; k'\rangle\langle\mathfrak{q}; k| \in \mathcal{D}^\omega(G)$ acts as

$$\pi(|\mathfrak{q}; k'\rangle\langle\mathfrak{q}; k|)|\mathfrak{a}; i, \overline{j}\rangle = \delta_{(\mathfrak{q},k),(\mathfrak{a},i)}|\mathfrak{a}; k', \overline{j}\rangle, \tag{74}$$

$$\overline{\pi}(|\mathfrak{q}; k'\rangle\langle\mathfrak{q}; k|)|\mathfrak{a}; i, \overline{j}\rangle = \delta_{(\mathfrak{a},j),(\mathfrak{q},k')}|\mathfrak{a}; i, \overline{k}\rangle. \tag{75}$$

Clearly, each $\mathfrak{a} \in \mathfrak{Q}$ labels a topological charge; it can be detected but cannot be changed by operators supported near either $\partial\mathtt{A}$ or $\partial\mathtt{B}$. Moreover, i and $\overline{j}$ in $|\mathfrak{a}; i, \overline{j}\rangle$, i.e., the two factors of $\mathcal{V}_{\mathfrak{a}} \otimes \mathcal{V}_{\mathfrak{a}}^*$ in Eq. (73), describe the remaining degrees of freedom near $\partial\mathtt{A}$ and $\partial\mathtt{B}$ respectively.

Applying the above analysis of topological charges to the reduced situation with $\mathtt{B} = \emptyset$ and $\mathtt{M} = \mathtt{A} - \mathtt{B}^\circ = \mathtt{A}$, we can prove that the ground states on any closed manifold are locally indistinguishable. Now $\mathcal{H}_0(\mathtt{M})$ has only the degrees of freedom labeled by χ along $\partial\mathtt{A}$. Further, suppose that $\mathcal{O}$ is any local operator inside $\mathtt{A}$ (away from $\partial\mathtt{A}$). Then $P(\mathtt{M})\mathcal{O}P(\mathtt{M})$ (equal to the action of $\mathcal{O}$ on the ground-state subspace) must be a scalar, because it commutes with $T[\chi]$ and hence cannot flip χ. Therefore no local operator can distinguish ground states.

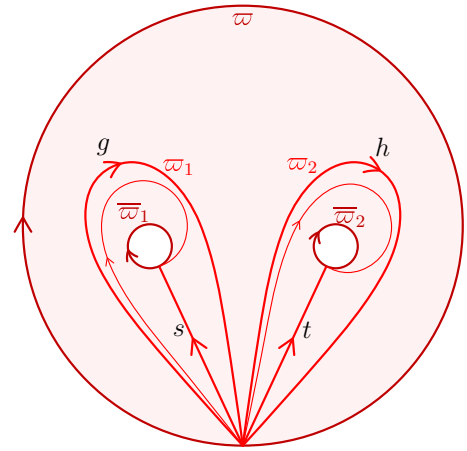

FIG. 10. A two-hole disk with colored triangulation $\mathtt{D}_g^s \otimes \mathtt{D}_h^t$.

To facilitate later discussions, let us describe $\mathcal{H}_0(\mathtt{M})$ in more detail when $\mathtt{B} = \emptyset$. The Δ-complex $\overline{\mathtt{M}}$ used for defining P_v^g for $v \in \partial\mathtt{M}$ now reduces to a disk whose boundary is a loop ϖ. With no hole in $\overline{\mathtt{M}}$, the group element assigned to ϖ must be trivial. Thus we may also view $\overline{\mathtt{M}}$ as a sphere by identifying all points of ϖ without affecting the definition of P_v^g. Then, analogous to Eq. (52), a basis of $\mathcal{H}_0(\mathtt{M})$ can be specified by the Dijkgraaf-Witten partition function on a ball with surface $\overline{\mathtt{M}}$.

2. Fusion and coproduct

The setup is similar to Fig. 7(a), but now $\mathtt{A}$ contains two spatially separated excited spots $\mathtt{B}_1$ and $\mathtt{B}_2$, and we are going to analyze the Hilbert space on the region $\mathtt{M} := \mathtt{A} - \mathtt{B}_1^\circ - \mathtt{B}_2^\circ$. We embed $\mathtt{M}$ into a slightly bigger triangulated two-hole disk $\overline{\mathtt{M}}$ with extra edges added along $\partial\mathtt{B}_1$, $\partial\mathtt{B}_2$ and $\partial\mathtt{A}$, as we did for $\mathtt{A} - \mathtt{B}^\circ$. The boundary of $\overline{\mathtt{M}}$ is three disjoint loops, i.e., $\partial\mathtt{M} = (-\varpi) \cup \varpi_1 \cup \varpi_2$, where the minus sign means that the orientation of ϖ is opposite to the one induced from $\overline{\mathtt{M}}$ as shown in Fig. 10.

Let $\mathtt{D}_g^s \otimes \mathtt{D}_h^t$ denote a two-hole disk with the colored triangulation shown in Fig. 10. Analogous to the case of one-hole disk (i.e., annulus), the Hilbert space $\mathcal{H}_*(\overline{\mathtt{M}})$ relevant to topological charge analysis is spanned by spanned by $\{|\mathtt{D}_g^s \otimes \mathtt{D}_h^t\rangle\}_{g,h,s,t\in G}$. It describes the states selected out of $\mathcal{H}(E(\mathtt{M}), G)$ by $P_v = 1, \forall v \in V(\mathtt{M}^\circ)$ up to some compatible colorings χ, $\overline{\chi}_1$ and $\overline{\chi}_2$ of $\partial\mathtt{A}$, $\partial\mathtt{B}_1$ and $\partial\mathtt{B}_2$, via the analog of Eq. (52) on a three-dimensional manifold with surface $(-\overline{\mathtt{M}}) \cup_{\varpi\overline{\varpi}_1\overline{\varpi}_2} \mathtt{D}_g^s \otimes \mathtt{D}_h^t$ (i.e., the genus-two surface obtained by gluing $\overline{\mathtt{M}}$ with $\mathtt{D}_g^s \otimes \mathtt{D}_h^t$ along loops ϖ, $\overline{\varpi}_1$ and $\overline{\varpi}_2$). The minus sign emphasizes that the orientation of $\overline{\mathtt{M}}$ points towards the inside of the three-dimensional manifold. In general, other colored triangulations of a two-hole disk with boundary $(-\varpi) \cup \overline{\varpi}_1 \cup \overline{\varpi}_2$ can be used to present states in $\mathcal{H}_*(\overline{\mathtt{M}})$ as well.

Using the isomorphism $\tilde\rho$ in Eq. (73), we have

$$\begin{aligned}\mathcal{H}_*(\overline{\mathtt{M}}) &\xrightarrow[\sim]{|\mathtt{D}_g^s\otimes\mathtt{D}_h^t\rangle\mapsto D_g^s\otimes D_h^t} \mathcal{D}^\omega(G)^{\otimes 2}\\ &\xrightarrow[\sim]{\tilde\rho\otimes\tilde\rho} \bigotimes_{\mathfrak{a}_1,\mathfrak{a}_2\in\mathfrak{Q}} \mathcal{V}_{\mathfrak{a}_1}^{(1)} \otimes \mathcal{V}_{\mathfrak{a}_1}^{(1)*} \otimes \mathcal{V}_{\mathfrak{a}_2}^{(2)} \otimes \mathcal{V}_{\mathfrak{a}_2}^{(2)*},\end{aligned} \tag{76}$$

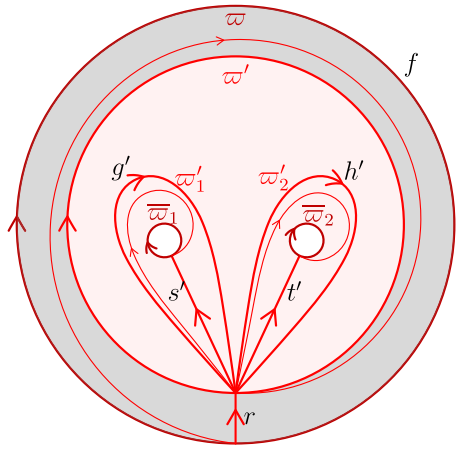

(a)

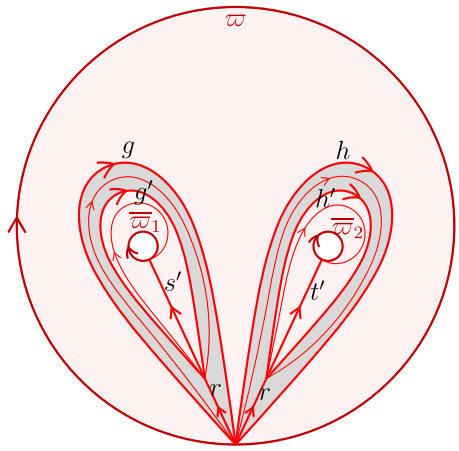

(b)

FIG. 11. Graphic representations of (a) $\pi(D_f^r)|\mathtt{D}_{g'}^{s'}\otimes\mathtt{D}_{h'}^{t'}\rangle$ and (b) $|\mathtt{D}_g^r\mathtt{D}_{g'}^{s'}\otimes\mathtt{D}_h^r\mathtt{D}_{h'}^{t'}\rangle$.

where $\mathcal{V}_{\mathfrak{a}_1}^{(1)}$ and $\mathcal{V}_{\mathfrak{a}_2}^{(2)}$ are Hilbert spaces carrying irreducible representations corresponding to $\mathfrak{a}_1,\mathfrak{a}_2\in\mathfrak{Q}$. The degrees of freedom $\mathcal{V}_{\mathfrak{a}_1}^{(1)*}$ and $\mathcal{V}_{\mathfrak{a}_2}^{(2)*}$ (in particular, topological charges $\mathfrak{a}_1$ and $\mathfrak{a}_2$) can be pinned by operators supported near near $\partial\mathtt{B}_1$ and $\partial\mathtt{B}_2$ respectively. The operators $\pi(\mathtt{D}_f^r)$ for $f,r\in G$ defined by Eq. (64) specifies the total topological charge inside $\mathtt{A}$. The action of $\pi(\mathtt{D}_f^r)$ is presented in Fig. 11(a). Explicitly,

$$\pi\left(D_f^r\right)\left|\mathtt{D}_{g'}^{s'}\otimes\mathtt{D}_{h'}^{t'}\right\rangle=\sum_{gh=f}\omega^r(g,h)\left|\mathtt{D}_g^r\mathtt{D}_{g'}^{s'}\otimes\mathtt{D}_h^r\mathtt{D}_{h'}^{t'}\right\rangle,\tag{77}$$

for $f,\ g',\ h',\ r,\ s',\ t'\in G$, where

$$\omega^r(g,h):=\frac{\omega(g,h,r)\omega(r,r^{-1}gr,r^{-1}hr)}{\omega(g,r,r^{-1}hr)}\tag{78}$$

and $|\mathtt{D}_g^r\mathtt{D}_{g'}^{s'}\otimes\mathtt{D}_h^r\mathtt{D}_{h'}^{t'}\rangle$ is presented by the colored triangulation in Fig. 11(b). A quick way to check Eq. (77) is to notice that $\langle\mathtt{D}_g^s\otimes\mathtt{D}_h^t|\pi(D_f^r)|\mathtt{D}_{g'}^{s'}\otimes\mathtt{D}_{h'}^{t'}\rangle$ corresponds to a solid torus whose surface is the gluing result of the two-hole disks in Figs. 10 and 11(a) along ϖ, $\overline{\varpi}_1$ and $\overline{\varpi}_2$. The solid torus can be partitioned into two solid tori relating $\mathtt{D}_g^{rs'}\sim\mathtt{D}_g^r\mathtt{D}_{g'}^{s'}$, $\mathtt{D}_h^{rt'}\sim\mathtt{D}_h^r\mathtt{D}_{h'}^{t'}$ and a prism over the triangle with

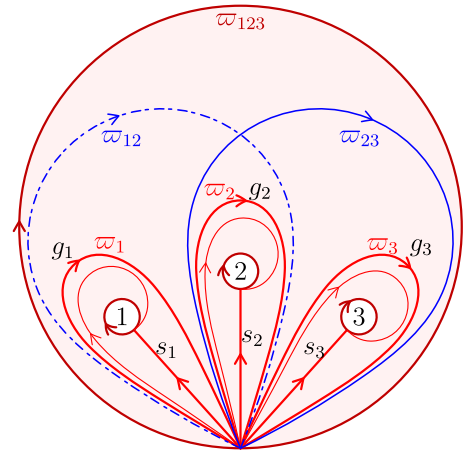

FIG. 12. A retriangulation of a three-hole disk is made by replacing loop ϖ_{12} with loop ϖ_{23}.

edges ϖ,ϖ_1,ϖ_2. The prism gives the factor $\omega^r(g,h)$. Thus $\pi(D_f^r)$ is specified by the coproduct

$$\Delta:\mathcal{D}^\omega(G)\to\mathcal{D}^\omega(G)\otimes\mathcal{D}^\omega(G);$$
$$D_f^r\mapsto\Delta\left(D_f^r\right)=\sum_{gh=f}\omega^r(g,h)D_g^r\otimes D_h^r.\tag{79}$$

On $\mathcal{V}_{\mathfrak{a}_1}^{(1)}\otimes\mathcal{V}_{\mathfrak{a}_2}^{(2)}$ [i.e., a sector of $\mathcal{H}_*(\overline{\mathtt{M}})$ with local degrees of freedom at $\partial\mathtt{B}_1$ and $\partial\mathtt{B}_2$ pinned], the operator $\pi(D_f^r)$ acts as $(\rho_{\mathfrak{a}_1}^{(1)}\otimes\rho_{\mathfrak{a}_2}^{(2)})\circ\Delta$, making $\mathcal{V}_{\mathfrak{a}_1}^{(1)}\otimes\mathcal{V}_{\mathfrak{a}_2}^{(2)}$ a representation of $\mathcal{D}^\omega(G)$. In general, $\mathcal{V}_{\mathfrak{a}_1}^{(1)}\otimes\mathcal{V}_{\mathfrak{a}_2}^{(2)}$ is reducible

$$\mathcal{V}_{\mathfrak{a}_1}^{(1)}\otimes\mathcal{V}_{\mathfrak{a}_2}^{(2)}=\bigoplus_{\mathfrak{a}}V_{\mathfrak{a}}^{\mathfrak{a}_1\mathfrak{a}_2}\otimes\mathcal{V}_{\mathfrak{a}}\tag{80}$$

with spaces of intertwiners $V_{\mathfrak{a}}^{\mathfrak{a}_1\mathfrak{a}_2}:=\mathrm{Hom}(\mathcal{V}_{\mathfrak{a}},\mathcal{V}_{\mathfrak{a}_1}^{(1)}\otimes\mathcal{V}_{\mathfrak{a}_2}^{(2)})$, where $\mathcal{V}_{\mathfrak{a}}$ is a Hilbert space carrying an irreducible representation of $\mathcal{D}^\omega(G)$ corresponding to the total topological charge $\mathfrak{a}\in\mathfrak{Q}$. The dimension $N_{\mathfrak{a}_1\mathfrak{a}_2}^{\mathfrak{a}}=\dim_{\mathbb{C}}V_{\mathfrak{a}}^{\mathfrak{a}_1\mathfrak{a}_2}$ counts the number of ways to fuse $\mathfrak{a}_1,\mathfrak{a}_2$ into $\mathfrak{a}$ and is called a *fusion rule*.

To describe more than two quasiparticles, we need to understand the associative property of any three topological charges. As before, the topological degrees of freedom are encoded in the Hilbert space $\mathcal{H}_*(\overline{\mathtt{M}})$ with a basis presented by colorings of a triangulated three-hole disk. However, there are two natural triangulations as shown in Fig. 12; we can either group holes 1,2 together by loop ϖ_{12} or group holes 2,3 together by loop ϖ_{23}. The two triangulations lead to two different bases $\{|(\mathtt{D}_{g_1}^{s_1}\otimes\mathtt{D}_{g_2}^{s_2})\otimes\mathtt{D}_{g_3}^{s_3}\rangle\}$ and $\{|\mathtt{D}_{g_1}^{s_1}\otimes(\mathtt{D}_{g_2}^{s_2}\otimes\mathtt{D}_{g_3}^{s_3})\rangle\}$. Noticing that changing from the triangulation with ϖ_{12} to the one with ϖ_{23} corresponds to a tetrahedron whose edges are loops ϖ_1, ϖ_2, ϖ_3, ϖ_{12}, ϖ_{23}, and ϖ_{123}, we get the basis transformation

$$\left|\left(\mathtt{D}_{g_1}^{s_1}\otimes\mathtt{D}_{g_2}^{s_2}\right)\otimes\mathtt{D}_{g_3}^{s_3}\right\rangle=\frac{\left|\mathtt{D}_{g_1}^{s_1}\otimes\left(\mathtt{D}_{g_2}^{s_2}\otimes\mathtt{D}_{g_3}^{s_3}\right)\right\rangle}{\omega(g_1,g_2,g_3)}.\tag{81}$$

In other words, $\mathcal{H}_*(\overline{\mathtt{M}})$ can be identified with $(\mathcal{D}^\omega(G))^{\otimes3}$ in two ways

$$\varphi_{(12)3}:\mathcal{H}_*(\overline{\mathtt{M}})\xrightarrow{\sim}(\mathcal{D}^\omega(G))^{\otimes3},$$
$$\left|\left(\mathtt{D}_{g_1}^{s_1}\otimes\mathtt{D}_{g_2}^{s_2}\right)\otimes\mathtt{D}_{g_3}^{s_3}\right\rangle\mapsto D_{g_1}^{s_1}\otimes D_{g_2}^{s_2}\otimes D_{g_3}^{s_3},\tag{82}$$

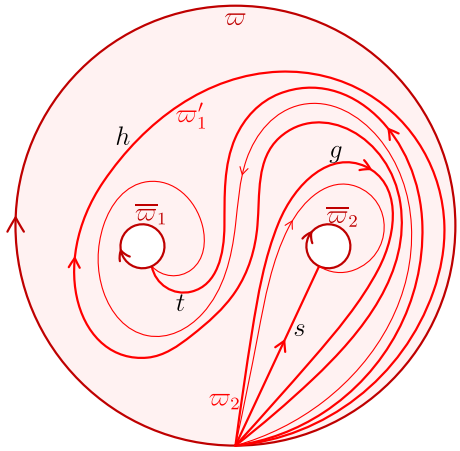

FIG. 13. Graphic representation of $\mathcal{R}|\mathtt{D}_g^s \otimes \mathtt{D}_h^t\rangle$.

$$\begin{aligned}&\varphi_{1(23)} : \mathcal{H}_*(\overline{\mathtt{M}}) \xrightarrow{\sim} (\mathcal{D}^\omega(G))^{\otimes 3},\\ &\left|\mathtt{D}_{g_1}^{s_1} \otimes \left(\mathtt{D}_{g_2}^{s_2} \otimes \mathtt{D}_{g_3}^{s_3}\right)\right\rangle \mapsto D_{g_1}^{s_1} \otimes D_{g_2}^{s_2} \otimes D_{g_3}^{s_3},\end{aligned} \tag{83}$$

with the basis transformation encoded by the Drinfeld associator $\phi := \sum_{f,g,h} \omega(f,g,h)^{-1} D_f^e \otimes D_g^e \otimes D_h^e$ [i.e., $\phi A = \varphi_{1(23)} \circ \varphi_{(12)3}^{-1}(A), \forall A \in \mathcal{D}^\omega(G)^{\otimes 3}$].

Three copies of Eq. (73) give

$$(\mathcal{D}^\omega(G))^{\otimes 3} \xrightarrow[\sim]{\tilde{\rho}^{\otimes 3}} \bigoplus_{\mathfrak{a}_1,\mathfrak{a}_2,\mathfrak{a}_3 \in \mathfrak{Q}} \bigotimes_{n=1}^{3} \left(\mathcal{V}_{\mathfrak{a}_n}^{(n)} \otimes \mathcal{V}_{\mathfrak{a}_n}^{(n)*}\right), \tag{84}$$

where $\mathcal{V}_{\mathfrak{a}_n}^{(n)} = (\rho_{\mathfrak{a}_n}^{(n)}, V_{\mathfrak{a}_n}^{(n)})$ is an irreducible representation of $\mathcal{D}^\omega(G)$ on a Hilbert space $V_{\mathfrak{a}_n}^{(n)}$. Since ϕ does not act on local degrees of freedom $\mathcal{V}_{\mathfrak{a}_n}^{(n)*}$, we can safely fixed a state of $\mathcal{V}_{\mathfrak{a}_n}^{(n)*}$ and just consider $\bigotimes_{n=1}^3 \mathcal{V}_{\mathfrak{a}_n}^{(n)}$ for describing fusion and braiding processes. However, to interpret the states, we need to specify whether we are using $\varphi_{(12)3}$ or $\varphi_{1(23)}$ by writing $\bigotimes_{n=1}^3 \mathcal{V}_{\mathfrak{a}_n}^{(n)}$ as either $(\mathcal{V}_{\mathfrak{a}_1}^{(1)} \otimes \mathcal{V}_{\mathfrak{a}_2}^{(2)}) \otimes \mathcal{V}_{\mathfrak{a}_3}^{(3)}$ or $\mathcal{V}_{\mathfrak{a}_1}^{(1)} \otimes (\mathcal{V}_{\mathfrak{a}_2}^{(2)} \otimes \mathcal{V}_{\mathfrak{a}_3}^{(3)})$. Under $\varphi_{(12)3}$ (respectively, $\varphi_{1(23)}$), the action of $\mathcal{D}^\omega(G)$ defined by Eq. (64) is given by $(\Delta \otimes \mathrm{id}) \circ \Delta$ [respectively, $(\mathrm{id} \otimes \Delta) \circ \Delta$]. Moreover, the basis transformation is presented by the action of ϕ on $\bigotimes_{n=1}^3 \mathcal{V}_{\mathfrak{a}_n}^{(n)}$.

The above discussion can be generalized to any finite number of excitations. For example, the topological degrees of freedom associated with four topological charges $\mathfrak{a}_1$, $\mathfrak{a}_2$, $\mathfrak{a}_3$ and $\mathfrak{a}_4$ can be expressed in any one of the forms $((\mathcal{V}_{\mathfrak{a}_1}^{(1)} \otimes \mathcal{V}_{\mathfrak{a}_2}^{(2)}) \otimes \mathcal{V}_{\mathfrak{a}_3}^{(3)}) \otimes \mathcal{V}_{\mathfrak{a}_4}^{(4)}$, $(\mathcal{V}_{\mathfrak{a}_1}^{(1)} \otimes \mathcal{V}_{\mathfrak{a}_2}^{(2)}) \otimes (\mathcal{V}_{\mathfrak{a}_3}^{(3)} \otimes \mathcal{V}_{\mathfrak{a}_4}^{(4)})$, and $\mathcal{V}_{\mathfrak{a}_1}^{(1)} \otimes (\mathcal{V}_{\mathfrak{a}_2}^{(2)} \otimes (\mathcal{V}_{\mathfrak{a}_3}^{(3)} \otimes \mathcal{V}_{\mathfrak{a}_4}^{(4)}))$.

3. Braiding and universal R matrix

Let us define an operator $\mathcal{R}$ to decribe the braiding of any two anyons. Graphically, $\mathcal{R}|\mathtt{D}_g^s \otimes \mathtt{D}_h^t\rangle$ is presented by Fig. 13. Explicitly, in the original basis $\{|\mathtt{D}_g^s \otimes \mathtt{D}_h^t\rangle\}_{g,h,s,t\in G}$ labeled by the colorings of the triangulated two-hole disk shown in Fig. 10, we have

$$\mathcal{R}\left|\mathtt{D}_g^s \otimes \mathtt{D}_h^t\right\rangle = \left|D^g \mathtt{D}_h^t \otimes \mathtt{D}_g^s\right\rangle, \tag{85}$$

where $D^g := \sum_{f\in G} D_f^g$ acts on $\mathtt{D}_h^t$ as $D^g \mathtt{D}_h^t = \mathtt{D}_{ghg^{-1}}^g \mathtt{D}_h^t$, describing the change of $\mathtt{D}_h^t$ as it moves along loop ϖ_2.

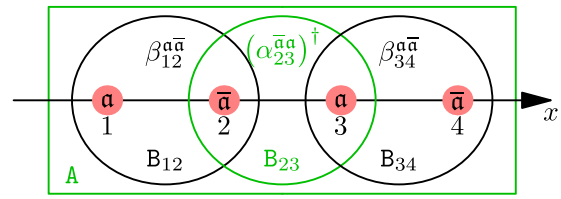

FIG. 14. Creating four quasiparticles of topological charges $\mathfrak{a}$, $\bar{\mathfrak{a}}$, $\mathfrak{a}$, $\bar{\mathfrak{a}}$ at spots 1,2,3,4 (red online) respectively in two different ways $\beta_{12}^{\mathfrak{a}\bar{\mathfrak{a}}}\beta_{34}^{\mathfrak{a}\bar{\mathfrak{a}}}$ and $(\alpha_{23}^{\bar{\mathfrak{a}}\mathfrak{a}})^\dagger \beta_{14}^{\mathfrak{a}\bar{\mathfrak{a}}}$. The operator $\beta_{12}^{\mathfrak{a}\bar{\mathfrak{a}}}$ (respectively, $\beta_{34}^{\mathfrak{a}\bar{\mathfrak{a}}}$, $(\alpha_{23}^{\bar{\mathfrak{a}}\mathfrak{a}})^\dagger$, $\beta_{14}^{\mathfrak{a}\bar{\mathfrak{a}}}$) supported within oval $\mathtt{B}_{12}$ (respectively, oval $\mathtt{B}_{34}$, oval $\mathtt{B}_{23}$, rectangle $\mathtt{A}$) creates a pair of quasiparticles at spots 1,2 (respectively, spots 3,4, spots 2,3, spots 1,4) carrying the labeled topological charges.

The universal R matrix of $\mathcal{D}^\omega(G)$ is

$$R = \sum_{g\in G} D_g^e \otimes D^g. \tag{86}$$

In terms of R, the braiding operator can be express as

$$\mathcal{R} = \wp R, \tag{87}$$

where $\wp$ permutes the two factors of each basis vector $|\mathtt{D}_g^s \otimes \mathtt{D}_h^t\rangle$ (i.e., $\wp|\mathtt{D}_g^s \otimes \mathtt{D}_h^t\rangle = |\mathtt{D}_h^t \otimes \mathtt{D}_g^s\rangle$). Under the action of local operators near $\overline{\varpi}_1$ and $\overline{\varpi}_2$, the Hilbert space reduces into sectors labeled by particles types of the two anyons.

To summarize, the quantum double algebra $\mathcal{D}^\omega(G)$ is a quasi-Hopf algebra and its representations form a unitary modular tensor category—a special type of braided tensor category—describing the behaviors of anyons that appear in the lattice models of twisted gauge theories. Explicit examples can be found in Appendix B 7.

D. Measuring invariants associated with topological charges

To conclude the discussion of the lattice models based on twisted gauge theories, we now explain how to define and detect some key properties of topological charges by simple and universal measurements.

1. Quantum dimension

To define and measure the quantum dimension associated with a topological charge $\mathfrak{a}$, we consider two different processes creating four quasiparticles of topological charges $\mathfrak{a}$, $\bar{\mathfrak{a}}$, $\mathfrak{a}$, $\bar{\mathfrak{a}}$ at spots 1,2,3,4 as shown in Fig. 14. Let $\mathtt{B}_{12}$, $\mathtt{B}_{23}$ and $\mathtt{B}_{34}$ be the three oval regions containing spots 1,2, spots 2,3 and spots 3,4 respectively. Pick an operator $\beta_{12}^{\mathfrak{a}\bar{\mathfrak{a}}}$ (respectively, $\beta_{34}^{\mathfrak{a}\bar{\mathfrak{a}}}$, $\beta_{14}^{\mathfrak{a}\bar{\mathfrak{a}}}$) supported in oval $\mathtt{B}_{12}$ (respectively, oval $\mathtt{B}_{34}$, rectangle $\mathtt{A}$) that creates a pair of quasiparticles with topological charges $\mathfrak{a}$, $\bar{\mathfrak{a}}$ at spots 1,2 (respectively, spots 3,4, spots 1,4). Moreover, pick an operator $\alpha_{23}^{\bar{\mathfrak{a}}\mathfrak{a}}$ supported in oval $\mathtt{B}_{23}$ to annihilate a pair of anyons with topological charges $\bar{\mathfrak{a}}$, $\mathfrak{a}$ at spots 2, 3. The choice of these operators can be fixed up to some phase factors by the normalization

$$\alpha_{23}^{\bar{\mathfrak{a}}\mathfrak{a}}\left(\alpha_{23}^{\bar{\mathfrak{a}}\mathfrak{a}}\right)^\dagger = \beta^\dagger \beta = 1, \quad \forall \beta = \beta_{12}^{\mathfrak{a}\bar{\mathfrak{a}}}, \beta_{34}^{\mathfrak{a}\bar{\mathfrak{a}}}, \beta_{14}^{\mathfrak{a}\bar{\mathfrak{a}}} \tag{88}$$

on the vacuum $|\Omega\rangle$. Then $\alpha_{23}^{\bar{\mathfrak{a}}\mathfrak{a}}\beta_{12}^{\mathfrak{a}\bar{\mathfrak{a}}}\beta_{34}^{\mathfrak{a}\bar{\mathfrak{a}}}|\Omega\rangle$ and $\beta_{14}^{\mathfrak{a}\bar{\mathfrak{a}}}|\Omega\rangle$ are the same state and hence there is $u_{\mathfrak{a}} \in \mathbb{C}$ such that

$$\alpha_{23}^{\bar{\mathfrak{a}}\mathfrak{a}}\beta_{12}^{\mathfrak{a}\bar{\mathfrak{a}}}\beta_{34}^{\mathfrak{a}\bar{\mathfrak{a}}}|\Omega\rangle = u_{\mathfrak{a}}\beta_{14}^{\mathfrak{a}\bar{\mathfrak{a}}}|\Omega\rangle. \tag{89}$$

Let $d_{\mathfrak{a}} := \frac{1}{|u_{\mathfrak{a}}|}$; it is called the *quantum dimension* associated with the topological charge $\mathfrak{a}$.

In other words, the overlap between $(\alpha_{23}^{\bar{\mathfrak{a}}\mathfrak{a}})^{\dagger}\beta_{14}^{\mathfrak{a}\bar{\mathfrak{a}}}|\Omega\rangle$ and $\beta_{12}^{\mathfrak{a}\bar{\mathfrak{a}}}\beta_{34}^{\mathfrak{a}\bar{\mathfrak{a}}}|\Omega\rangle$ is $u_{\mathfrak{a}}$. Let $\mathfrak{q}_{23}$ be the total topological charge of quasiparticles at spots 2,3. Then in a basis labeled by $\mathfrak{q}_{23}$, the only component of $\beta_{12}^{\mathfrak{a}\bar{\mathfrak{a}}}\beta_{34}^{\mathfrak{a}\bar{\mathfrak{a}}}|\Omega\rangle$ with $\mathfrak{q}_{23}$ trivial is $u_{\mathfrak{a}}(\alpha_{23}^{\bar{\mathfrak{a}}\mathfrak{a}})^{\dagger}\beta_{14}^{\mathfrak{a}\bar{\mathfrak{a}}}|\Omega\rangle$. Therefore the quantum dimension $d_{\mathfrak{a}}$ can be defined and measured by topological charge projectors. Since topological charges can be detected by braiding, there exists a projector $P_{\mathfrak{q}}^{\mathtt{R}}$ supported near $\partial\mathtt{R}$ and commuting with the Hamiltonian requires that the total topological charge inside a finite region $\mathtt{R}$ is $\mathfrak{q}$. If $|\Psi\rangle$ is a state with four excited spots as in Fig. 14 satisfying $P_{\mathfrak{o}}^{\mathtt{A}} = P_{\mathfrak{a}}^{\mathtt{B}_1} = P_{\bar{\mathfrak{a}}}^{\mathtt{B}_2} = P_{\mathfrak{a}}^{\mathtt{B}_3} = P_{\bar{\mathfrak{a}}}^{\mathtt{B}_4} = P_{\mathfrak{o}}^{\mathtt{B}_{12}} = P_{\mathfrak{o}}^{\mathtt{B}_{34}} = 1$, then $d_{\mathfrak{a}}$ can also be defined and measured by

$$\frac{1}{d_{\mathfrak{a}}} := \frac{\langle\Psi|P_{\mathfrak{o}}^{\mathtt{B}_{23}}|\Psi\rangle}{\langle\Psi|\Psi\rangle}, \tag{90}$$

where $\mathfrak{o}$ denotes the trivial topological charge and $\mathtt{B}_j$ is any oval region containing only spot j, for $j = 1, 2, 3, 4$.

Now let us compute $d_{\mathfrak{a}}$ for $\mathfrak{a} \in \mathfrak{Q}$ in a model of twisted gauge theory. Pick a representation $\mathcal{V}_{\mathfrak{a}} = (\rho_{\mathfrak{a}}, V_{\mathfrak{a}})$ for $\mathfrak{a}$. Let $\alpha_{\mathfrak{a}} : \mathcal{V}_{\mathfrak{a}}^* \otimes \mathcal{V}_{\mathfrak{a}} \to \mathbb{C}$ and $\beta_{\mathfrak{a}} : \mathbb{C} \to \mathcal{V}_{\mathfrak{a}} \otimes \mathcal{V}_{\mathfrak{a}}^*$ be the two intertwiners defined by Eqs. (B19) and (B20). Using the antipode (S, α, β) given in Eqs. (B31)–(B33), we have $\alpha_{\mathfrak{a}}\alpha_{\mathfrak{a}}^{\dagger} = \beta_{\mathfrak{a}}^{\dagger}\beta_{\mathfrak{a}} = \dim \mathcal{V}_{\mathfrak{a}}$. Thus up to a phase factor, $\alpha_{23}^{\bar{\mathfrak{a}}\mathfrak{a}}\beta_{12}^{\mathfrak{a}\bar{\mathfrak{a}}}\beta_{34}^{\mathfrak{a}\bar{\mathfrak{a}}}$ acts on the vacuum as

$$\begin{aligned}
&\mathbb{C} \xrightarrow{\frac{\beta_{\mathfrak{a}}}{\sqrt{\dim \mathcal{V}_{\mathfrak{a}}}} \otimes \frac{\beta_{\mathfrak{a}}}{\sqrt{\dim \mathcal{V}_{\mathfrak{a}}}}} (\mathcal{V}_{\mathfrak{a}} \otimes \mathcal{V}_{\mathfrak{a}}^*) \otimes (\mathcal{V}_{\mathfrak{a}} \otimes \mathcal{V}_{\mathfrak{a}}^*) \\
&= ((\mathcal{V}_{\mathfrak{a}} \otimes \mathcal{V}_{\mathfrak{a}}^*) \otimes \mathcal{V}_{\mathfrak{a}}) \otimes \mathcal{V}_{\mathfrak{a}}^* \\
&\xrightarrow{\phi \otimes \mathrm{id}_{\mathfrak{a}}} (\mathcal{V}_{\mathfrak{a}} \otimes (\mathcal{V}_{\mathfrak{a}}^* \otimes \mathcal{V}_{\mathfrak{a}})) \otimes \mathcal{V}_{\mathfrak{a}}^* \\
&\xrightarrow{\mathrm{id}_{\mathfrak{a}} \otimes \frac{\beta_{\mathfrak{a}}}{\sqrt{\dim \mathcal{V}_{\mathfrak{a}}}} \otimes \mathrm{id}_{\mathfrak{a}}} \mathcal{V}_{\mathfrak{a}} \otimes \mathcal{V}_{\mathfrak{a}}^*,
\end{aligned} \tag{91}$$

where the equality in the first line is obtained by noticing that the state in $\mathcal{V}_{\mathfrak{a}} \otimes \mathcal{V}_{\mathfrak{a}}^*$ created from vacuum has trivial total topological charge. It gets simplified to

$$\mathbb{C} \xrightarrow{(\dim \mathcal{V}_{\mathfrak{a}})^{-\frac{3}{2}}\beta_{\mathfrak{a}}} \mathcal{V}_{\mathfrak{a}} \otimes \mathcal{V}_{\mathfrak{a}}^*, \tag{92}$$

by the fact that the composition in Eq. (B21) equals identity. Therefore $\alpha_{23}^{\bar{\mathfrak{a}}\mathfrak{a}}\beta_{12}^{\mathfrak{a}\bar{\mathfrak{a}}}\beta_{34}^{\mathfrak{a}\bar{\mathfrak{a}}}|\Omega\rangle = (\dim \mathcal{V}_{\mathfrak{a}})^{-1}\beta_{14}^{\mathfrak{a}\bar{\mathfrak{a}}}|\Omega\rangle$ up to a phase factor and hence

$$d_{\mathfrak{a}} = \dim \mathcal{V}_{\mathfrak{a}}. \tag{93}$$

Roughly, the quantum dimension $d_{\mathfrak{a}}$ tells how strongly $\mathfrak{a}$ and $\bar{\mathfrak{a}}$ are entangled when they are restricted to a trivial total topological charge.

The diagrammatic presentation used in tensor categories provides a useful tool in describing the splitting, fusion, and braiding processes of anyons [14,38]. Let

(94)

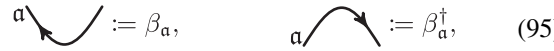

(95)

The pair of linear maps $\alpha_{\mathfrak{a}}$ and $\beta_{\mathfrak{a}}$ are picked such that the compositions in Eq. (B21) and (B22) equal identities, which are graphically presented as

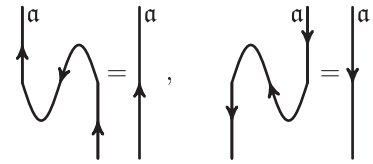

(96)

Here a vertical line with label $\mathfrak{a}$ and an upward (respectively, downward) arrow is interpreted as the identity operator on the topological charge $\mathfrak{a}$ (respectively, $\bar{\mathfrak{a}}$). Convenient normalizations compatible with Eq. (96) can be picked as

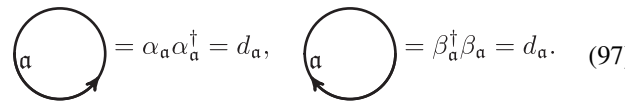

(97)

Notice that $\alpha_{\bar{\mathfrak{a}}}^{\dagger}, \beta_{\mathfrak{a}} \in V_{\mathfrak{o}}^{\mathfrak{a}\bar{\mathfrak{a}}}$ and hence they just differ by a phase factor (i.e., $\beta_{\mathfrak{a}} = \varkappa_{\mathfrak{a}}\alpha_{\bar{\mathfrak{a}}}^{\dagger}$), where $\mathfrak{o}$ denotes the trivial topological charge. Further, if $\bar{\mathfrak{a}} = \mathfrak{a}$, then $\alpha_{\bar{\mathfrak{a}}} = \alpha_{\mathfrak{a}}$ is already fixed by the choice of $\beta_{\mathfrak{a}}$ via Eq. (96). In this case, $\varkappa_{\mathfrak{a}}$ is well-defined. It takes values ± 1 and is called the *Frobenius-Schur indicator* [14].

For $\bar{\mathfrak{a}} = \mathfrak{a}$, we can measure $\varkappa_{\mathfrak{a}}$ by

$$\left(\beta_{23}^{\mathfrak{a}\mathfrak{a}}\right)^{\dagger}\beta_{12}^{\mathfrak{a}\mathfrak{a}}\beta_{34}^{\mathfrak{a}\mathfrak{a}}|\Omega\rangle = \frac{\varkappa_{\mathfrak{a}}}{d_{\mathfrak{a}}}\beta_{14}^{\mathfrak{a}\mathfrak{a}}|\Omega\rangle. \tag{98}$$

in the setting of Fig. 14, where $(\beta_{23}^{\mathfrak{a}\mathfrak{a}})^{\dagger}$ is supported in oval $\mathtt{B}_{23}$ and annihilates a pair of anyons both of topological charge $\mathfrak{a}$ at spots 2,3. The operators $\beta_{12}^{\mathfrak{a}\mathfrak{a}}, \beta_{23}^{\mathfrak{a}\mathfrak{a}}, \beta_{34}^{\mathfrak{a}\mathfrak{a}}$ can be compared with $\beta_{14}^{\mathfrak{a}\mathfrak{a}}$ by hopping operators. For $i = 1, 2, 3$, let $\mathcal{O}_i^{\mathfrak{a}}$ be an operators supported on the oval $\mathtt{B}_{i(i+1)}$ that moves a quasiparticle of topological charge $\mathfrak{a}$ from spot i to spot $i + 1$. We can require $\beta_{12}^{\mathfrak{a}\mathfrak{a}} = (\mathcal{O}_3^{\mathfrak{a}}\mathcal{O}_2^{\mathfrak{a}})^{\dagger}\beta_{14}^{\mathfrak{a}\mathfrak{a}}$, $\beta_{34}^{\mathfrak{a}\mathfrak{a}} = \mathcal{O}_2^{\mathfrak{a}}\mathcal{O}_1^{\mathfrak{a}}\beta_{14}^{\mathfrak{a}\mathfrak{a}}$ and $\beta_{23}^{\mathfrak{a}\mathfrak{a}} = \mathcal{O}_1^{\mathfrak{a}}(\mathcal{O}_3^{\mathfrak{a}})^{\dagger}\beta_{14}^{\mathfrak{a}\mathfrak{a}}$ on $|\Omega\rangle$. Then it is easy to see that the measurement of $\varkappa_a$ via Eq. (98) is well-defined, i.e., independent of the remaining freedom of adding phase factors to $\mathcal{O}_1^{\mathfrak{a}}$, $\mathcal{O}_2^{\mathfrak{a}}$, $\mathcal{O}_3^{\mathfrak{a}}$, and $\beta_{14}^{\mathfrak{a}\mathfrak{a}}$.

2. Braiding statistics

In Fig. 15, the hopping processes of a single quasiparticle of topological charge $\mathfrak{q} \in \mathfrak{Q}$ between the three spots (red, blue, and grey online) can be made by operators $\mathcal{U}_1^{\mathfrak{q}}$, $\mathcal{O}_2^{\mathfrak{q}}$, $\mathcal{U}_3^{\mathfrak{q}}$ supported near the corresponding arrows. To resolve the phase factor ambiguity, we require $\mathcal{U}_3^{\mathfrak{q}}\mathcal{U}_1^{\mathfrak{q}}\mathcal{O}_2^{\mathfrak{q}} = 1$ in moving a single quasiparticle starting at spot 2. Then

$$\mathcal{U}_3^{\mathfrak{b}}\mathcal{O}_2^{\mathfrak{a}}\mathcal{U}_1^{\mathfrak{b}} : \mathcal{V}_{\mathfrak{a}}^{(2)} \otimes \mathcal{V}_{\mathfrak{b}}^{(3)} \xrightarrow{\mathcal{R}} \mathcal{V}_{\mathfrak{b}}^{(3)} \otimes \mathcal{V}_{\mathfrak{a}}^{(2)}, \tag{99}$$

$$\mathcal{U}_3^{\mathfrak{a}}\mathcal{O}_2^{\mathfrak{b}}\mathcal{U}_1^{\mathfrak{a}}\mathcal{U}_3^{\mathfrak{b}}\mathcal{O}_2^{\mathfrak{a}}\mathcal{U}_1^{\mathfrak{b}} : \mathcal{V}_{\mathfrak{a}}^{(2)} \otimes \mathcal{V}_{\mathfrak{b}}^{(3)} \xrightarrow{\mathcal{R}^2} \mathcal{V}_{\mathfrak{a}}^{(2)} \otimes \mathcal{V}_{\mathfrak{b}}^{(3)} \tag{100}$$

braid topological charges $\mathfrak{a}, \mathfrak{b} \in \mathfrak{Q}$ initially at spots 2 and 3, where $\mathcal{V}_{\mathfrak{a}}^{(2)}$ and $\mathcal{V}_{\mathfrak{b}}^{(3)}$ are the corresponding representations. When $\mathfrak{a} = \mathfrak{b}$, the action of $\mathcal{R}$, denoted $\mathcal{R}^{\mathfrak{a}\mathfrak{a}}$, is precisely captured by Eq. (99). When $\mathfrak{a} \neq \mathfrak{b}$, we cannot fixed the phase

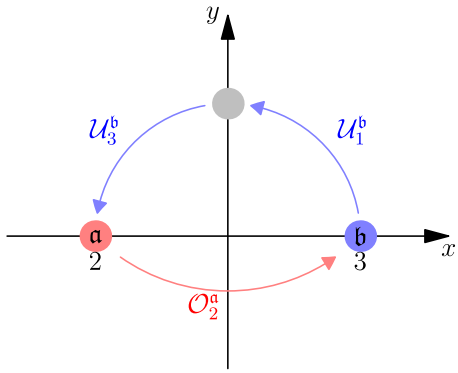

FIG. 15. Two anyons of topological charge $\mathfrak{a}$ and $\mathfrak{b}$ at spots 2 and 3 are braided by $\mathcal{U}_3^{\mathfrak{b}}\mathcal{O}_2^{\mathfrak{a}}\mathcal{U}_1^{\mathfrak{b}}$, where $\mathcal{U}_1^{\mathfrak{q}}$, $\mathcal{O}_2^{\mathfrak{q}}$ and $\mathcal{U}_3^{\mathfrak{q}}$ are the hopping operators (for topological charge $\mathfrak{q}$) indicated by and supported near the three arrows, respectively.

factor of $\mathcal{U}_1^{\mathfrak{b}}\mathcal{O}_2^{\mathfrak{a}}\mathcal{U}_3^{\mathfrak{b}}$. Only $\mathcal{R}^2$, called the *monodromy operator*, is well-defined via Eq. (100).

Graphically, $\mathcal{R}^{\mathfrak{ba}}:\mathcal{V}_{\mathfrak{a}}\otimes\mathcal{W}_{\mathfrak{b}}\to\mathcal{W}_{\mathfrak{b}}\otimes\mathcal{V}_{\mathfrak{a}}$ is presented as

$$:=\mathcal{R}^{\mathfrak{ba}}, \tag{101}$$

where $\mathcal{V}_{\mathfrak{a}}$ and $\mathcal{W}_{\mathfrak{b}}$ are irreducible representations for $\mathfrak{a},\mathfrak{b}\in\mathfrak{Q}$, respectively.

In general, $\mathcal{R}^{\mathfrak{aa}}$ is a matrix even when restricted to a definite total topological charge $\mathfrak{c}$, because $N_{\mathfrak{aa}}^{\mathfrak{c}}$ may be greater than 1. To get a simple scalar out of $\mathcal{R}^{\mathfrak{aa}}$, let us consider a process beginning and ending with the vacuum as follows. First, we create four anyons at the spots positioned as in Fig. 14; a pair of anyons with topological charges $\bar{\mathfrak{a}}$, $\mathfrak{a}$ (respectively, $\mathfrak{a}$, $\bar{\mathfrak{a}}$) are created at spots 1,2 (respectively, 3,4) with an operator $(\alpha_{12}^{\bar{\mathfrak{a}}\mathfrak{a}})^\dagger$ (respectively, $\beta_{34}^{\mathfrak{a}\bar{\mathfrak{a}}}$) supported in oval $\mathtt{B}_{12}$ (respectively, $\mathtt{B}_{34}$). We normalize these operators by

$$\alpha_{12}^{\bar{\mathfrak{a}}\mathfrak{a}}\left(\alpha_{12}^{\bar{\mathfrak{a}}\mathfrak{a}}\right)^\dagger=\left(\beta_{34}^{\mathfrak{a}\bar{\mathfrak{a}}}\right)^\dagger\beta_{34}^{\mathfrak{a}\bar{\mathfrak{a}}}=1 \tag{102}$$

on the vacuum. Second, the anyons both with topological charge $\mathfrak{a}$ at spots 2,3 are braided by $\mathcal{U}_3^{\mathfrak{a}}\mathcal{O}_2^{\mathfrak{a}}\mathcal{U}_1^{\mathfrak{a}}$ as in Fig. 15. Finally, $\alpha_{12}^{\bar{\mathfrak{a}}\mathfrak{a}}(\beta_{34}^{\mathfrak{a}\bar{\mathfrak{a}}})^\dagger$ annihilates the four anyons. Then the *topological spin* $\theta_{\mathfrak{a}}$ associated with $\mathfrak{a}\in\mathfrak{Q}$ is the phase factor of

$$\frac{\theta_{\mathfrak{a}}}{d_{\mathfrak{a}}}:=\langle\Omega|\alpha_{12}^{\bar{\mathfrak{a}}\mathfrak{a}}\left(\beta_{34}^{\mathfrak{a}\bar{\mathfrak{a}}}\right)^\dagger\mathcal{U}_1^{\mathfrak{a}}\mathcal{O}_2^{\mathfrak{a}}\mathcal{U}_3^{\mathfrak{a}}\left(\alpha_{12}^{\bar{\mathfrak{a}}\mathfrak{a}}\right)^\dagger\beta_{34}^{\mathfrak{a}\bar{\mathfrak{a}}}|\Omega\rangle, \tag{103}$$

whose amplitude specifies the quantum dimension $d_{\mathfrak{a}}$ as well.[3] Graphically, this equation is presented as

$$\frac{\theta_{\mathfrak{a}}}{d_{\mathfrak{a}}}=\frac{1}{d_{\mathfrak{a}}^2}$$

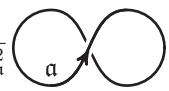

, (104)

[3]If $d_{\mathfrak{a}}>1$, the total topological charge of spots 1 and 2 becomes unfixed after the braiding of the two $\mathfrak{a}$ anyons (at spots 2 and 3). Hence it is also clear that this braiding does not commute with any braiding process of an additional anyon around spots 1 and 2 together distinguishing their fusion channels. Thus $d_{\mathfrak{a}}>1$ is a criterion for $\mathfrak{a}$ to be non-Abelian; an anyon with quantum dimension greater than one must be involved in some noncommutative braiding processes.

where $\frac{1}{d_{\mathfrak{a}}^2}$ on the right-hand side comes from the different normalization conventions set by Eqs. (97) and (102). For the models of twisted gauge theories,

$$\theta_{\mathfrak{a}}=\frac{1}{d_{\mathfrak{a}}}\mathrm{tr}(\wp R,\mathcal{V}_{\mathfrak{a}}\otimes\mathcal{V}_{\mathfrak{a}}), \tag{105}$$

where $\wp:\mathcal{V}_{\mathfrak{a}}\otimes\mathcal{V}_{\mathfrak{a}}\to\mathcal{V}_{\mathfrak{a}}\otimes\mathcal{V}_{\mathfrak{a}};\ v^{(1)}\otimes v^{(2)}\mapsto v^{(2)}\otimes v^{(1)}$, and $\mathrm{tr}(\wp R,\mathcal{V}_{\mathfrak{a}}\otimes\mathcal{V}_{\mathfrak{a}})$ is the trace of $\wp R$ over $\mathcal{V}_{\mathfrak{a}}\otimes\mathcal{V}_{\mathfrak{a}}$.

For $\mathfrak{a}\neq\mathfrak{b}$, the monodromy operator $\mathcal{R}^2=\mathcal{R}^{\mathfrak{ab}}\mathcal{R}^{\mathfrak{ba}}$ is diagonalized in the basis with definite total topological charge. Explicitly,

$$\mathcal{R}^2=\mathcal{R}_{\mathfrak{c}}^{\mathfrak{ab}}\mathcal{R}_{\mathfrak{c}}^{\mathfrak{ba}}=\frac{\theta_{\mathfrak{c}}}{\theta_{\mathfrak{a}}\theta_{\mathfrak{b}}}\mathrm{id}_{V_{\mathfrak{c}}^{\mathfrak{ab}}}, \tag{106}$$

on the sector with definite total topological charge $\mathfrak{c}$ [14].

Analogously to the discussion of topological spin, we are interested in the following process. First, four anyons with topological charges $\mathfrak{a}$, $\bar{\mathfrak{a}}$, $\mathfrak{b}$, $\bar{\mathfrak{b}}$ are created at spots 1,2,3,4 positioned as in Fig. 14 by operators $\beta_{12}^{\mathfrak{a}\bar{\mathfrak{a}}}\beta_{34}^{\mathfrak{b}\bar{\mathfrak{b}}}$, where $\beta_{12}^{\mathfrak{a}\bar{\mathfrak{a}}}$, $\beta_{34}^{\mathfrak{b}\bar{\mathfrak{b}}}$ are supported on ovals $\mathtt{B}_{12}$, $\mathtt{B}_{34}$, respectively, and normalized in a similar way as in Eq. (102). Second, a monodromy operator braiding $\bar{\mathfrak{a}}$ and $\mathfrak{b}$ is realized as in Eq. (100). Finally, the four anyons are annihilated by $(\beta_{12}^{\mathfrak{a}\bar{\mathfrak{a}}}\beta_{34}^{\mathfrak{b}\bar{\mathfrak{b}}})^\dagger$. The expectation value of the whole process on the vacuum $|\Omega\rangle$ is

$$\mathsf{S}_{\mathfrak{ab}}:=\frac{1}{d_{\mathfrak{a}}d_{\mathfrak{b}}}$$

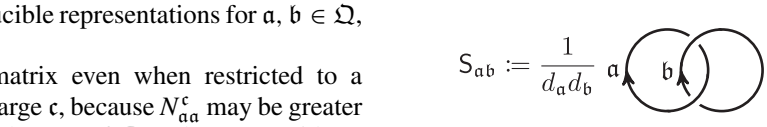

$$=\sum_{\mathfrak{c}\in\mathfrak{Q}}N_{\bar{\mathfrak{a}}\mathfrak{b}}^{\mathfrak{c}}\frac{\theta_{\mathfrak{c}}}{\theta_{\mathfrak{a}}\theta_{\mathfrak{b}}}\frac{d_{\mathfrak{c}}}{d_{\mathfrak{a}}d_{\mathfrak{b}}}, \tag{107}$$

where the factor $\frac{1}{d_{\mathfrak{a}}d_{\mathfrak{b}}}$ is from the normalization difference between $(\beta_{12}^{\mathfrak{a}\bar{\mathfrak{a}}})^\dagger\beta_{12}^{\mathfrak{a}\bar{\mathfrak{a}}}=(\beta_{34}^{\mathfrak{b}\bar{\mathfrak{b}}})^\dagger\beta_{34}^{\mathfrak{b}\bar{\mathfrak{b}}}=1$ on $|\Omega\rangle$ and Eq. (97). In the literature [14,38], $\mathsf{S}_{\mathfrak{ab}}$ are often rescaled to $\mathcal{S}_{\mathfrak{ab}}=\frac{d_{\mathfrak{a}}d_{\mathfrak{b}}}{\mathcal{D}}\mathsf{S}_{\mathfrak{ab}}$ and put into a matrix form $\mathcal{S}=(\mathcal{S}_{\mathfrak{ab}})_{\mathfrak{a},\mathfrak{b}\in\mathfrak{Q}}$, called the *topological S matrix*, which is closely related to a modular transformation of torus [108,109]. Here

$$\mathcal{D}:=\sqrt{\sum_{\mathfrak{a}\in\mathfrak{Q}}d_{\mathfrak{a}}^2} \tag{108}$$

is called the total quantum dimension. For the models of twisted gauge theories,

$$\mathsf{S}_{\mathfrak{ab}}^*=\mathsf{S}_{\bar{\mathfrak{a}}\mathfrak{b}}=\frac{1}{d_{\mathfrak{a}}d_{\mathfrak{b}}}\mathrm{tr}((\wp R)^2,\mathcal{V}_{\mathfrak{a}}\otimes\mathcal{V}_{\mathfrak{b}}), \tag{109}$$

where $\wp:\mathcal{V}\otimes\mathcal{W}\to\mathcal{W}\otimes\mathcal{V};\ v\otimes w\mapsto w\otimes v$ is the permutation operator acting on the tensor product of any two vectors spaces and $\mathrm{tr}((\wp R)^2,\mathcal{V}_{\mathfrak{a}}\otimes\mathcal{V}_{\mathfrak{b}})$ is the trace of $(\wp R)^2$ over $\mathcal{V}_{\mathfrak{a}}\otimes\mathcal{V}_{\mathfrak{b}}$.

III. TWISTED FRACTON MODELS

We now introduce generalizations of two paradigmatic three-dimensional gapped fracton phases: the X-cube model [61] and the checkerboard model [60,61]. Instead of reviewing the $\mathbb{Z}_2$ variants of these models, which have been intensely studied recently, we will introduce general versions of these models based on a finite Abelian group G (with identity element denoted 0) and get them generalized further by twisting. We note that in contrast with the original formulation of the

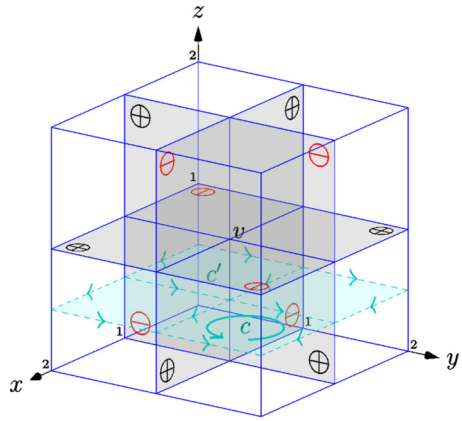

FIG. 16. The cubic lattice Λ for X-cube models. Spins labeled by an Abelian group G lie on faces. The generalized gauge transformation A_v^g flips spins by g (respectively, $-g$) on the faces marked $\oplus$ (respectively, $\ominus$). The cross section Σ_1^z is the intersection of Λ with the plane $z = \frac{1}{2}$ (cyan). The arrowed arc (cyan) indicates the z flux of the associated cube.

X-cube model, where spins were defined to live on links of a cubic lattice, here we formulate this model on the dual lattice, where spins live on faces of the cubic lattice.

A. Twisted X-cube models

Given a simple cubic lattice Λ, we pick the coordinates such that its vertices are in $\mathbb{Z}^3$ as shown in Fig. 16. Each edge (respectively, face, cube) is labeled by the coordinates of its center. Let Λ^0 (respectively, Λ^1, Λ^2, Λ^3) be the label set for vertices (respectively, edges, faces, cubes), whose elements are usually denoted as v (respectively, ℓ, p, c). Then

$$\Lambda^1 = \Lambda^1_x \cup \Lambda^1_y \cup \Lambda^1_z, \tag{110}$$

where $\Lambda^1_x = \Lambda^0 + (\frac{1}{2}, 0, 0)$, $\Lambda^1_y = \Lambda^0 + (0, \frac{1}{2}, 0)$, and $\Lambda^1_z = \Lambda^0 + (0, 0, \frac{1}{2})$ are the sets of x, y, and z edges (i.e., edges lying in the x, y, and z directions) respectively. Similarly,

$$\Lambda^2 = \Lambda^2_{xy} \cup \Lambda^2_{yz} \cup \Lambda^2_{zx}, \tag{111}$$

where $\Lambda^2_{xy} = \Lambda^0 + (\frac{1}{2}, \frac{1}{2}, 0)$, $\Lambda^1_{yz} = \Lambda^0 + (0, \frac{1}{2}, \frac{1}{2})$ and $\Lambda^1_{zx} = \Lambda^0 + (\frac{1}{2}, 0, \frac{1}{2})$ are the sets of xy, yz, and zx faces (i.e., faces perpendicular to the z, x, and y directions), respectively. In addition,

$$\Lambda^3 = \Lambda^0 + \tfrac{1}{2}(1, 1, 1). \tag{112}$$

In the following, we would like to consider a cubic lattice on a three-dimensional torus T^3, obtained by identifying $(x, y, z) \sim (x + L_x, y, z) \sim (x, y + L_y, z) \sim (x, y, z + L_z)$ with L_x, L_y, $L_z \in \mathbb{Z}$ describing the system size. Such a lattice has vertices $\Lambda^0 = \mathbb{Z}_{L_x} \times \mathbb{Z}_{L_y} \times \mathbb{Z}_{L_z}$ and the infinite case can be viewed as its thermodynamic limit.

Given any region Γ of Λ, let $\Lambda^n(\Gamma)$ for $n = 0,\ 1,\ 2,\ 3$ be the label sets of the vertices, edges, faces, cubes contained in Γ, respectively. Similarly, we may define sets $\Lambda^1_x(\Gamma)$, $\Lambda^2_{xy}(\Gamma)$ and etc. For instance, $c \in \Lambda^3(\Gamma)$ means $c \subseteq \Gamma$ with $c \in \Lambda^3$ viewed as the region occupied by the cube c (boundary included). In particular, $c \in \Lambda^3(\Gamma)$ implies $\Lambda^n(c) \subseteq \Lambda^n(\Gamma)$, $\forall n = 0,\ 1,\ 2,\ 3$. For any cube c, $\Lambda^3(c) = \{c\}$ and $\Lambda^2(c)$ [respectively, $\Lambda^1(c)$, $\Lambda^0(c)$] is the set of the six faces (respectively, 12 edges, 8 vertices) of c.

1. X-cube model based on a finite Abelian group

Let G be a finite Abelian group,[4] with 0 denoting its identity element. A local Hilbert space (also called a *spin* for short) spanned by an orthonoraml basis $\{|p, g\rangle\}_{g\in G}$ is assigned to each face $p \in \Lambda^2$. Then the Hilbert space associated with any region Γ of Λ, denoted $\mathcal{H}(\Lambda^2(\Gamma), G)$, is spanned by

$$|\vartheta\rangle := \bigotimes_{p\in\Lambda^2(\Gamma)} |p, \vartheta(p)\rangle, \tag{113}$$

with $\vartheta \in G^{\Lambda^2(\Gamma)}$, where $G^{\Lambda^2(\Gamma)} := \mathrm{Fun}(\Lambda^2(\Gamma), G)$ is the set of functions from $\Lambda^2(\Gamma)$ to G. Each element of $G^{\Lambda^2(\Gamma)}$ specifies a *spin configuration* on Γ. On the whole lattice, the total Hilbert space is $\mathcal{H}(\Lambda^2, G)$.

For each vertex v, we define a function κ_v from Λ^2 to $\mathbb{Z}$, which maps $p = (p^x, p^y, p^z) \in \Lambda^2$ to

$$\kappa_v(p) := \sum_{s\in\Lambda^0(p)} (-1)^{s^x+s^y+s^z-p^x-p^y-p^z} \delta_{s,v}. \tag{114}$$

Graphically, κ_v is presented in Fig. 16; its value is $+1$ (respectively, -1) on faces marked $\oplus$ (respectively, $\ominus$) and zero on all faces not adjacent to v.

In an untwisted X-cube model, $\forall g \in G$, a *(generalized) gauge transformation operator* A_v^g associated with each vertex v can be defined as

$$A_v^g := \sum_{\vartheta\in G^{\Lambda^2}} |\vartheta + \kappa_v g\rangle\langle\vartheta|. \tag{115}$$

Clearly, it is supported on the twelve faces adjacent to v.

If $G = \mathbb{Z}_2 = \{0, 1\}$, then A_v^1 is the product of the Pauli operators σ^x on the twelve faces. As v labels a cube of the dual lattice and the twelve faces corresponds to the edges of this cube, A_v^1 is an X-cube operator in the dual lattice. Thus the original X-cube model [61] is a special case of the family of models we are constructing here.

In addition, supported on each cube $c \in \Lambda^3$, we have *(generalized) flux projectors*

$$B_c^x := \sum_{\vartheta\in G^{\Lambda^2(c)}} \delta_{\partial_y\vartheta(c)-\partial_z\vartheta(c),0} |\vartheta\rangle\langle\vartheta|, \tag{116}$$

$$B_c^y := \sum_{\vartheta\in G^{\Lambda^2(c)}} \delta_{\partial_z\vartheta(c)-\partial_x\vartheta(c),0} |\vartheta\rangle\langle\vartheta|, \tag{117}$$

$$B_c^z := \sum_{\vartheta\in G^{\Lambda^2(c)}} \delta_{\partial_x\vartheta(c)-\partial_y\vartheta(c),0} |\vartheta\rangle\langle\vartheta|, \tag{118}$$

$$B_c := B_c^x B_c^y B_c^z, \tag{119}$$

[4] In order for generalized gauge transformation operators defined by Eq. (115) to commute with each other on different vertices, G has to be Abelian. This is quite different from conventional lattice gauge theories and this is why realizing non-Abelian fracton phases is a nontrivial problem.

where $\partial_x\vartheta(c) := \vartheta(c+(\frac{1}{2},0,0)) - \vartheta(c-(\frac{1}{2},0,0))$ and $\partial_y\vartheta$, $\partial_z\vartheta$ are defined analogously. As in Fig. 16, the zx and yz faces of cube c can be thought as edges of the square with an arrowed arc; thus, B_c^z can be understood as a projector requiring the z flux of cube c to be trivial.

It is straightforward to check that $\forall v, v_0, v_1 \in \Lambda^0(\Lambda)$, $\forall c, c_0, c_1 \in \Lambda^3(\Lambda)$, $\forall g, h \in G$, $\forall \mu, \nu \in \{x, y, z\}$,

$$A_v^g A_v^h = A_v^{g+h},\ (A_v^g)^\dagger = A_v^{-g},\ \left(B_c^\mu\right)^\dagger = B_c^\mu, \tag{120}$$

$$\left[A_{v_0}^g, A_{v_1}^h\right] = \left[A_v^g, B_c^\mu\right] = \left[B_{c_0}^\mu, B_{c_1}^\nu\right] = 0. \tag{121}$$

Thus we have mutually commuting Hermitian operators

$$A_v := \frac{1}{|G|}\sum_{g\in G} A_v^g, \tag{122}$$

associated with vertices, which also commute with flux projectors. Finally, we arrive at the Hamiltonian of the X-cube model, which is

$$H = -\sum_{v\in\Lambda^0} A_v - \sum_{c\in\Lambda^3} B_c, \tag{123}$$

with ground states specified by $A_v = B_c^x = B_c^y = B_c^z = 1$. As we will compute, the ground-state degeneracy of the untwisted X-cube model on a lattice Λ with underlying manifold T^3 and vertices $\Lambda^0 = \mathbb{Z}_{L_x}\times\mathbb{Z}_{L_y}\times\mathbb{Z}_{L_z}$ is

$$GSD(\Lambda) = |G|^{2(L_x+L_y+L_z)-3}. \tag{124}$$

As $\log_{|G|} GSD(\Lambda)$ is negligible compared to $L_xL_yL_z$ in the thermodynamic limit, the model is gapped.

2. X-cube models twisted by 3-cocycles

The X-cube model based on an Abelian group G can be twisted by 3-cocycles slice by slice. Let Σ_i^x, Σ_j^y and Σ_k^z denote the intersection of Λ with the plane

$$x = i - \tfrac{1}{2}, \quad \forall i \in \mathbb{Z}_{L_x}, \tag{125}$$

$$y = j - \tfrac{1}{2}, \quad \forall j \in \mathbb{Z}_{L_y}, \tag{126}$$

$$z = k - \tfrac{1}{2}, \quad \forall k \in \mathbb{Z}_{L_z}, \tag{127}$$

respectively. For example, the cross section Σ_1^z is shown in Fig. 16.

Each cross section is a square lattice, whose vertices (respectively, edges, plaquettes) correspond to the edges (respectively, faces, cubes) of Λ intersected by the plane. Let $E(\Sigma_i^x)$, $E(\Sigma_j^y)$ and $E(\Sigma_k^z)$ be the set of edges with orientation chosen as in Fig. 1. By restriction, each $\vartheta \in G^{\Lambda^2}$ gives $\vartheta_i^x \in G^{E(\Sigma_i^x)}$, $\vartheta_j^y \in G^{E(\Sigma_j^y)}$ and $\vartheta_k^z \in G^{E(\Sigma_k^z)}$. We notice that B_c^x, B_c^y and B_c^z are then the flux projectors for these square lattices. A complete triangulation of each cross section is made as in Fig. 1.

Let ω be an assignment that assigns 3-cocycles ω_i^x, ω_j^y, $\omega_k^z \in Z^3(G, \mathrm{U}(1))$ to the slices Σ_i^x, Σ_j^y, Σ_k^z respectively. For any region Γ of Λ, let

$$G_B^{\Lambda^2(\Gamma)} := \left\{\vartheta \in G^{\Lambda^2(\Gamma)} \mid B_c|\vartheta\rangle = |\vartheta\rangle, \forall c \in \Lambda^3(\Gamma)\right\}, \tag{128}$$

whose elements are called *locally flat* spin configurations on Γ. For each vertex v and $g \in G$, we define an operator

$$P_v^g := \sum_{\vartheta\in G_B^{\Lambda^2(\Lambda[v])}} |\vartheta\rangle\omega[\Lambda, v; \vartheta, g]\langle\vartheta - \kappa_v g| \tag{129}$$

supported on $\Lambda[v]$ (i.e., the region made of cubes adjacent to v inside Λ), with

$$\omega[\Lambda, v; \vartheta, g] := \prod_{\mu=x,y,z} \frac{\omega\left[\Sigma_{v-}^\mu, t_\mu^- v; \vartheta, g\right]}{\omega\left[\Sigma_{v+}^\mu, t_\mu^+ v; \vartheta - \kappa_v g, g\right]}, \tag{130}$$

where $t_\mu^\pm v = v \pm (\frac{1}{2},0,0), v \pm (0,\frac{1}{2},0), v \pm (0,0,\frac{1}{2})$ for $\mu = x, y, z$ respectively. In addition, $\Sigma_{v\pm}^\mu$ is the cross section perpendicular to the μ direction and containing $t_\mu^\pm v$ as a vertex. As an example, $\Sigma_{v-}^z = \Sigma_1^z$ (cyan online) for $v = (1,1,1)$ in Fig. 16. A local coloring of $\Sigma_{v\pm}^\mu$ near $t_\mu^\pm v$ is made by both $\xi = \vartheta$ and $\vartheta - \kappa_v g \in G_B^{\Lambda^2(\Lambda[v])}$. Then $\omega[\Sigma_{v\pm}^\mu, t_\mu^\pm v; \xi, g]$ denotes the phase factor specified by Eq. (32) as in the quantum double model on $\Sigma_{v\pm}^\mu$ twisted by the 3-cocycle assigned to $\Sigma_{v\pm}^\mu$.

In a periodic lattice Λ with $L_x, L_y, L_z \geqslant 2$, each vertex is regular. Thus $\omega[\Sigma_{v\pm}^z, t_z^\pm v; \xi, g]$ can be represented as a pyramid P_v^g as in Fig. 1(b) with bottom colored by ξ and computed by Eq. (12) with the replacement

$$\begin{array}{lcccccccc} v=3 & [01] & [13] & [34] & [46] & [56] & [35] & [23] & [02] \\ t_z^\pm v+ & \frac{120}{-2} & \frac{010}{-2} & \frac{100}{2} & \frac{210}{2} & \frac{120}{2} & \frac{010}{2} & \frac{100}{-2} & \frac{210}{-2} \end{array}, \tag{131}$$

i.e., replacing [01], [13], ... by the vertical faces (colored by ξ) centered at $t_z^\pm v - \frac{1}{2}(1,2,0), t_z^\pm v - \frac{1}{2}(0,1,0), \ldots$ respectively. Here $\frac{ijk}{\pm 2}$ is short for $\pm\frac{1}{2}(i,j,k)$. For the vertex labeled v in Fig. 16, $t_z^- v + \{\frac{120}{-2}, \frac{010}{-2}, \ldots\}$ denote the eight vertical faces (of the cubes c, c') that intersect with $z = \frac{1}{2}$ (cyan online) and $t_z^+ v + \{\frac{120}{-2}, \frac{010}{-2}, \ldots\}$ their translation results by one unit in the z direction. Permuting the x, y, z coordinates in Eq. (131) gives the expressions of $\omega[\Sigma_{v\pm}^\mu, t_\mu^\pm v; \xi, g]$ for $\mu = x, y$.

Let $\overline{\mathrm{P}}_v^g$ denote the same pyramid over v as P_v^g in Fig. 1(b) but with the middle edge oriented as $[v'v]$ (i.e., pointing downwards) and colored as $[v'v] = g$. We notice that $\omega[\Sigma_{v+}^\mu, t_\mu^+ v; \vartheta - \kappa_v g, g]^{-1}$ equals the Dijkgraaf-Witten weight on $\overline{\mathrm{P}}_{t_\mu^+ v}^g$ (over $t_\mu^+ v$ on Σ_{v+}^μ) with top colored by $\vartheta - \kappa_v g$. By graphic arguments similar to those given in Figs. 2 and 3, we see that $\forall v, v_0, v_1 \in \Lambda^0$, $\forall g, h \in G$,

$$\left(P_v^g\right)^\dagger = P_v^{-g}, \quad P_v^g P_v^h = P_v^{g+h}, \quad \left[P_{v_0}^g, P_{v_1}^h\right] = 0. \tag{132}$$

They actually hold with P_v^g well-defined by Eqs. (129) and (130) even if the periodic lattice Λ has $L_\mu = 1$ for some $\mu = x, y, z$.

Therefore we have mutually commuting Hermitian local projectors

$$P_v := \frac{1}{|G|}\sum_{g\in G} P_v^g \tag{133}$$

labeled by vertives. If all 3-cocycles are trivial, then P_v reduces to $A_v\prod_{c\ni v} B_c$, where $c \ni v$ means that c connects to v.

The Hamiltonian of the twisted X-cube model on a periodic lattice Λ is

$$H = -\sum_{v\in\Lambda^0} P_v, \tag{134}$$

with ground states specified by $P_v = 1$ for all vertices.

To help the reader get acquainted with our notations, let us use Pauli operators to express two simple examples. First, in an X-cube model based on $G = \mathbb{Z}_2 = \{0, 1\}$, there is a qubit on each face and a projector

$$B_c^z = \tfrac{1}{2}\big(1 + \sigma^z_{c+\frac{100}{2}}\sigma^z_{c-\frac{100}{2}}\sigma^z_{c+\frac{010}{2}}\sigma^z_{c-\frac{010}{2}}\big), \tag{135}$$

on each cube c, where $c + \frac{100}{2}$ (respectively, $c - \frac{100}{2}$, $c + \frac{010}{2}$, $c - \frac{010}{2}$) denotes the front (respectively, back, left and right) face of the cube c. Physically, B_c^z requires the z flux of c to be trivial, as illustrated by the arrowed arc in Fig. 16. Moreover, the projectors B_c^x and B_c^y are expressed analogously, $B_c = B_c^x B_c^y B_c^z$, and $P_v^{(g=0)} = \prod_{c\ni v} B_c$ with $c \ni v$ denoting that c connects to the vertex v.

Suppose that cross sections Σ_k^z for all k are twisted by ω in Eq. (24) in the model based on $G = \mathbb{Z}_2$. Up to a basis transformation $\mathcal{U} = \prod_k \mathcal{U}_k^z$ with $\mathcal{U}_k^z$ a finite-depth quantum circuit defined analogously to Eq. (28) for Σ_k^z, we can express $P_v^{(g=1)}$ as

$$P_v^{(g=1)} = \big(-i^{N^z_{v-}}\big)\cdot\big(-i^{N^z_{v+}}\big)\cdot\prod_{c\ni v} B_c \cdot \prod_{p\ni v}\sigma_p^x, \tag{136}$$

where the factor $-i^{N^z_{v\pm}}$ comes from the twisting of $\Sigma^z_{v\pm}$ and $N^z_{v\pm}$ is given by Eq. (29) with [01], [13], ... replaced by $t_z^{\pm}v - \frac{1}{2}(1,2,0)$, $t_z^{\pm}v - \frac{1}{2}(0,1,0)$, ... as in Eq. (131).

As another example, an X-cube model based on $G = \mathbb{Z}_2 \times \mathbb{Z}_2 \times \mathbb{Z}_2$ (with elements shortly denoted as 000, 100, ...) contains three copies of Pauli operators $\{\sigma_p^{(j)\mu}\}_{j=1,2,3}^{\mu=x,y,z}$ on each face p, leading to $B_c^{(j)}$, respectively. Then $B_c = \prod_{j=1}^3 B_c^{(j)}$ requires the flux triviality, $P_v^{000} = \prod_{c\ni v} B_c$, and the untwisted $P_v^{100} = P_v^{000}\cdot\prod_{p\ni v}\sigma_p^{(1)x}$. Twisting each of $\Sigma^\mu_{v\pm}$ by ω in Eq. (30) adds to P_v^{100} two more controlled-Z operators analogous to those in Eq. (31). The other two generators P_v^{010}, P_v^{001}, of P_v^g are expressed similarly.

By analogy to quantum double models, we expect that quasiparticles violating $B_c = 1$ would show some features of semions or non-Abelian anyons in these two examples, which will be further studied in Sec. VI.

B. Twisted checkerboard models

A three-dimensional checkerboard Λ, as shown in Fig. 17(a), is obtained by coloring half of the cubes grey in a cubic lattice. Let $\Lambda^3_\bullet$ (respectively, $\Lambda^3_\circ$) be the set of grey (respectively, blank) cubes. Let Λ^0 be the set of vertices. We also divide Λ^0 into two groups $\Lambda^0_\bullet$ and $\Lambda^0_\circ$, marked $\bullet$ and $\circ$, respectively, in Fig. 17(a). In the chosen coordinates,

$$\Lambda^0_\bullet = \{(i,j,k)\in\Lambda^0 \mid i+j+k \text{ is even}\}, \tag{137}$$

$$\Lambda^0_\circ = \{(i,j,k)\in\Lambda^0 \mid i+j+k \text{ is odd}\}. \tag{138}$$

Notice that all the grey (respectively, uncolored) cubes are centered at $\Lambda^0_\bullet + \frac{1}{2}(1,1,1)$ ([respectively, $\Lambda^0_\circ + \frac{1}{2}(1,1,1)$]).

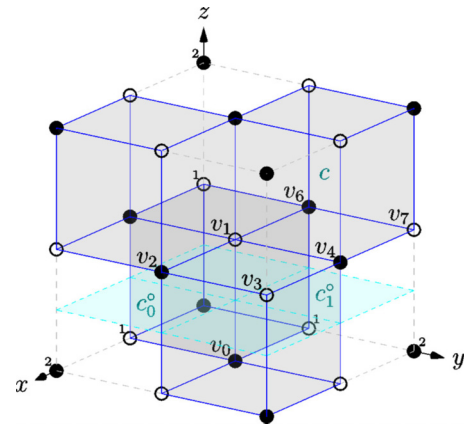

(a) Three-dimensional checkerboard Λ

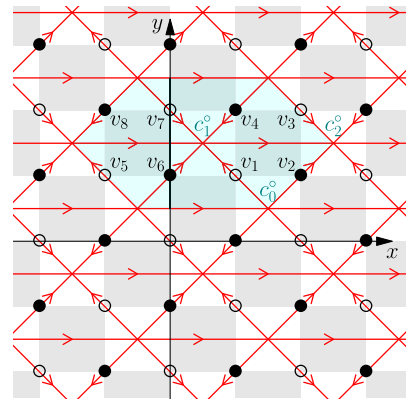

(b) Triangulation of Σ_k^z with k odd.

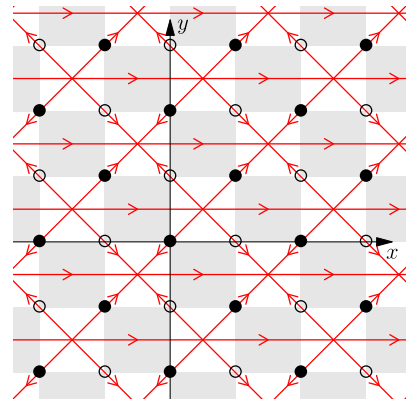

(c) Triangulation of Σ_k^z with k even.

FIG. 17. (a) The three-dimensional checkerboard Λ with vertices marked as either $\bullet$ or $\circ$. The cross section Σ_k^z is the intersection of Λ with the plane $z = k - \frac{1}{2}$, such as Σ_1^z (cyan). [(b) and (c)] A branched triangulation (red) of Σ_k^z with the positions of vertices of Λ on the plane $z = k$ included. Permuting x, y, z cyclically gives triangulations of Σ_i^x and Σ_j^y. Some vertices on $z = 1$ and some cubes intersecting with $z = \frac{1}{2}$ [cyan in (a)] are labeled in (b).

For an infinite system, $\Lambda^0 = \mathbb{Z}^3$. In the following discussion, however, we prefer to identify $(x, y, z) \sim (x + L_x, y, z) \sim (x, y + L_y, z) \sim (x, y, z + L_z)$ and consider the resulting checkerboard on T^3, where L_x, L_y and L_y need to be even integers in order to be compatible with the checker pattern. Such a lattice has vertices $\Lambda^0 = \mathbb{Z}_{L_x}\times\mathbb{Z}_{L_y}\times\mathbb{Z}_{L_z}$ and the infinite case can be viewed as its thermodynamic limit.

Since the checkerboard is just the cubic lattice with a checker pattern, we can use notations introduced for the cubic lattice with or without decoration. For instance, $\Lambda^3(\Gamma)$ stands for the set of cubes inside region Γ and its subset of grey cubes is denoted by $\Lambda^3_\bullet(\Gamma) := \Lambda^3_\bullet \cap \Lambda^3(\Gamma)$. In addition, Σ^x_i still denotes the intersection of Λ with the plane $x = i - \frac{1}{2}$, but now it is not only a square lattice but also a two-dimensional checkerboard.

1. Checkerboard model based on a finite Abelian group

Let G be a finite Abelian group, with 0 denoting its identity element. A local Hilbert space (also called a *spin* for short) spanned by an orthonormal basis $\{|v, g\rangle\}_{g\in G}$ is assigned to each vertex $v \in \Lambda^0$. Thus the Hilbert space associated to any region Γ of Λ, denoted $\mathcal{H}(\Lambda^0(\Gamma), G)$, is spanned by

$$|\vartheta\rangle := \bigotimes_{v\in\Lambda^0(\Gamma)} |v, \vartheta(v)\rangle \tag{139}$$

with $\vartheta \in G^{\Lambda^0(\Gamma)}$, where $G^{\Lambda^0(\Gamma)} := \mathrm{Fun}(\Lambda^0(\Gamma), G)$ is the set of functions from $\Lambda^0(\Gamma)$ (i.e., the vertices in Γ) to G. Each $\vartheta \in G^{\Lambda^0(\Gamma)}$ specifies a *spin configuration* on Γ. On the whole lattice, the total Hilbert space is $\mathcal{H}(\Lambda^0, G)$.

For each grey cube c, let $\mathbf{1}_c : \Lambda^0 \to \{0, 1\}$ be the indicator function of $\Lambda^0(c)$, which has the value 1 on each vertex of c and 0 on any vertex not in c. For $g \in G$, we define a *(generalized) gauge transformation operator*

$$A^g_c := \sum_{\vartheta\in G^{\Lambda^0}} |\vartheta + \mathbf{1}_c g\rangle\langle\vartheta| \tag{140}$$

to flip spins on all the vertices of c. Clearly, it is supported on c. In addition, let $(-1)^v : \Lambda^0 \to \{1, -1\}$ be the function which has the value 1 on each $v \in \Lambda^0_\circ$ and -1 on each $v \in \Lambda^0_\bullet$. For each grey cube $c \in \Lambda^3_\bullet$, we define a *(generalized) flux projector* (supported on c) as

$$B_c := \sum_{\vartheta\in G^{\Lambda^0}} \delta_{\sum_{v\in\Lambda^0(c)}(-1)^v\vartheta(v),0}|\vartheta\rangle\langle\vartheta|. \tag{141}$$

It is straightforward to check that

$$\left(A^g_c\right)^\dagger = A^{-g}_c, \quad A^g_c A^h_c = A^{g+h}_c, \quad (B_c)^\dagger = B_c, \tag{142}$$

$$\left[A^g_{c_0}, A^h_{c_1}\right] = \left[A^g_{c_0}, B_{c_1}\right] = \left[B_{c_0}, B_{c_1}\right] = 0, \tag{143}$$

$\forall c, c_0, c_1 \in \Lambda^3_\bullet$, $\forall g, h \in G$. Thus we have mutually commuting Hermitian operators

$$A_c := \frac{1}{|G|}\sum_{g\in G} A^g_c, \tag{144}$$

associated with grey cubes, which also commute with flux projectors on grey cubes. The Hamiltonian of the checkerboard model is then given by

$$H = -\sum_{c\in\Lambda^3_\bullet}(A_c + B_c), \tag{145}$$

whose ground states are specified by $A_c = B_c = 1$. As we will compute later, the ground-state degeneracy of this model on a checkerboard Λ with underlying manifold T^3 and vertices $\Lambda^0 = \mathbb{Z}_{L_x} \times \mathbb{Z}_{L_y} \times \mathbb{Z}_{L_z}$ is

$$GSD(\Lambda) = |G|^{2(L_x+L_y+L_z)-6}, \tag{146}$$

As $\log_{|G|} GSD(\Lambda)$ is negligible compared to $L_xL_yL_z$ in the thermodynamic limit, the model is gapped.

For $G = \mathbb{Z}_2$, the model reduces to the original checkerboard model defined by Vijay, Haah, and Fu [61].

2. Checkerboard models twisted by 3-cocycles

To relate the checkerboard with a lattice model of gauge theory, let us look at one cross section Σ^z_k first and triangulate it as in Figs. 17(b) or 17(c). Let $\Delta^n(\Sigma^z_k)$ be the set of n-simplices in this triangulation. In addition, we denote the set of edges with $\bullet$ or $\circ$ mark by $E(\Sigma^z_k)$, which gives a new square lattice structure of the two-dimensional checkerboard. Let $\Lambda^3_\bullet[\Sigma^z_k]$ (respectively, $\Lambda^3_\circ[\Sigma^z_k]$) be the set of grey (respectively, blank) cubes intersecting with Σ^z_k, which obviously labels the plaquettes (respectively, vertices) of the new square lattice structure of Σ^z_k. Similarly, let $\Lambda^1[\Sigma^z_k]$ be the set of edges in Λ that intersect with Σ^z_k; each $\ell \in \Lambda^1[\Sigma^z_k]$ is assumed oriented toward the positive direction of z. Then there is a one-to-one correspondence between $E(\Sigma^z_k)$ and $\Lambda^1[\Sigma^z_k]$; for example, the edge $[c^\circ_0 c^\circ_1]$ in Σ^z_1 shown by Fig. 17(b) corresponds to $[v_0v_1]$ in Fig. 17(a). Hence we will simply write $E(\Sigma^z_k) = \Lambda^1[\Sigma^z_k]$ and use them interchangeably.

Given $\vartheta \in G^{\Lambda^0}$, if we color $\ell = [vv'] \in \Lambda^1[\Sigma^z_k]$ by

$$\partial\vartheta(\ell) := \vartheta(v') - \vartheta(v). \tag{147}$$

Then, for Σ^z_k, we notice that B_c at $c \in \Lambda^3_\bullet[\Sigma^z_k]$ works as a flux operator and that $A^g_{t^\pm_z c}$ with $c \in \Lambda^3_\circ[\Sigma^z_k]$ works as a gauge transformation operator, where $t^+_z c$ (respectively, $t^-_z c$) is the grey cube above (respectively, below) $c \in \Lambda^3_\circ[\Sigma^z_k]$. Based on this observation, we construct a twisted version of A^g_c, denoted P^g_c, below.

To prepare for the definition, for any region Γ of Λ, let

$$G_B^{\Lambda^0(\Gamma)} := \left\{\vartheta \in G^{\Lambda^0(\Gamma)} \mid B_c|\vartheta\rangle = |\vartheta\rangle, \forall c \in \Lambda^3_\bullet(\Gamma)\right\}, \tag{148}$$

whose elements are called *locally flat* spin configurations on Γ. Moreover, for each cube $c \in \Lambda^3$, let $\Lambda[c]$ be the region made of the cubes whose intersection with c is not empty. Since $\partial\Lambda = \emptyset$ here, $\Lambda[c]$ is a cuboid region of size $3 \times 3 \times 3$ centered at c. Translating c by a unit in the positive (respectively, negative) μ direction gives a cube denoted $t^+_\mu c$ (respectively, $t^-_\mu c$) of color different from c, for $\mu = x, y, z$.

For grey cube c centered at $(c^x, c^y, c^z) + \frac{1}{2}(1, 1, 1)$, let

$$P^g_c := \sum_{\vartheta\in G_B^{\Lambda^0(\Lambda[c])}} |\vartheta\rangle\omega[\Lambda, c; \vartheta, g]\langle\vartheta - \mathbf{1}_c g|, \tag{149}$$

$\forall g \in G$, supported on $\Lambda[c]$, with

$$\begin{aligned}\omega[\Lambda, c; \vartheta, g] := &\frac{\omega\left[\Sigma^x_{c-}, t^-_x c; \partial\vartheta, (-1)^{c^z} g\right]}{\omega\left[\Sigma^x_{c+}, t^+_x c; \partial(\vartheta - \mathbf{1}_c g), (-1)^{c^z} g\right]}\\ &\cdot\frac{\omega\left[\Sigma^y_{c-}, t^-_y c; \partial\vartheta, (-1)^{c^x} g\right]}{\omega\left[\Sigma^y_{c+}, t^+_y c; \partial(\vartheta - \mathbf{1}_c g), (-1)^{c^x} g\right]}\\ &\cdot\frac{\omega\left[\Sigma^z_{c-}, t^-_z c; \partial\vartheta, (-1)^{c^y} g\right]}{\omega\left[\Sigma^z_{c+}, t^+_z c; \partial(\vartheta - \mathbf{1}_c g), (-1)^{c^y} g\right]},\end{aligned} \tag{150}$$

where Σ^{μ}_{c+} (respectively, Σ^{μ}_{c-}) is the cross section of Λ passing the center of $t^{+}_{\mu}c$ (respectively, $t^{-}_{\mu}c$) and perpendicular to the μ direction. The phase factors $\omega[\Sigma^{\mu}_{c-}, t^{-}_{\mu}c; \partial\vartheta, (-1)^{c^{\nu}}g]$ and $\omega[\Sigma^{\mu}_{c+}, t^{+}_{\mu}c; \partial(\vartheta - \mathbf{1}_c g), (-1)^{c^{\nu}}g]$ are defined by Eq. (32); they are the phase factors appearing in the gauge transformation $(-1)^{c^{\nu}}g$ on $\Sigma^{\mu}_{c\pm}$ twisted by the 3-cocycle assigned to $\Sigma^{\mu}_{c\pm}$.

Analogous to Eqs. (132), these operators satisfy

$$\left(P^{g}_{c}\right)^{\dagger} = P^{-g}_{c}, \quad P^{g}_{c}P^{h}_{c} = P^{g+h}_{c}, \quad \left[P^{g}_{c_0}, P^{h}_{c_1}\right] = 0, \tag{151}$$

$\forall g, h \in G$, $\forall c, c_0, c_1 \in \Lambda^{3}_{\bullet}$. Thus we have mutually commuting Hermitian local projectors labeled by grey cubes

$$P_c := \frac{1}{|G|}\sum_{g\in G} P^{g}_{c} \tag{152}$$

and the Hamiltonian of twisted checkerboard model

$$H = -\sum_{c\in\Lambda^{3}_{\bullet}} P_c, \tag{153}$$

with ground states specified by $P_c = 1$ for all grey cubes.

In order to clarify our notations, let us express some simple examples explicitly in terms of Pauli operators. First, a checkerboard model based on $G = \mathbb{Z}_2 = \{0, 1\}$ contains a qubit at each vertex. For each grey cube $c \in \Lambda^{\bullet}_{3}$, $B_c = \frac{1}{2}(1 + \prod_{v\in c}\sigma^{z}_{v})$ and $P^{(g=0)}_{c} = \prod_{c'\in\Lambda^{\bullet}_{3}: c'\cap c\neq\emptyset} B_{c'}$. If the model is twisted by ω in Eq. (24) along Σ^{z}_{k}, $\forall k$ but untwisted along any Σ^{x}_{i} and Σ^{y}_{j}, then [up to a finite-depth quantum circuit analogous to Eq. (28) for each Σ^{z}_{k}]

$$P^{(g=1)}_{c} = P^{(g=0)}_{c}\cdot\left(-i^{N^{z}_{c-}}\right)\cdot\left(-i^{N^{z}_{c+}}\right)\cdot\prod_{v\in c}\sigma^{x}_{v}, \tag{154}$$

where $N^{z}_{c-} = \frac{1}{2}\sum_{j=2,3,5,8}(1 - \sigma^{z}_{v_j}\sigma^{z}_{v_j-z}) + \frac{1}{2}(1 - \sigma^{z}_{v_1}\sigma^{z}_{v_1-z}\sigma^{z}_{v_6}\sigma^{z}_{v_6-z}) + \frac{1}{2}(1 - \sigma^{z}_{v_4}\sigma^{z}_{v_4-z}\sigma^{z}_{v_7}\sigma^{z}_{v_7-z})$ and N^{z}_{c+} is expressed similarly with v replaced by $v + 2\boldsymbol{z}$. We write $\boldsymbol{z}$ for short (0,0,1) and the positions of vertices $\{v_j\}_{j=1,2,\ldots,8}$ are shown in Figs. 17(a) and 17(b).

In addition, a checkerboard model based on $G = \mathbb{Z}_2\times\mathbb{Z}_2\times\mathbb{Z}_2$ (with elements often shortly denoted as 000, 100, $\cdots$) contains three qubits on each vertex v, manipulated by Pauli operators $\{\sigma^{(j)\mu}_{v}\}^{\mu=x,y,z}_{j=1,2,3}$. We thus have $B^{(j)}_{c}$ for $j = 1, 2, 3$ on each grey cube c. Together, $B_c = \prod^{3}_{j=1}B^{(j)}_{c}$ requires the flux triviality, $P^{000}_{c} = \prod_{c'\in\Lambda^{\bullet}_{3}: c'\cap c\neq\emptyset} B_{c'}$, and $P_c = \frac{1}{8}(P^{000}_{c} + P^{100}_{c})(P^{000}_{c} + P^{010}_{c})(P^{000}_{c} + P^{001}_{c})$. Because c°_{0} and c°_{1} are inequivalent in Fig. 17(b), the branching structure there is inconvenient in defining P^{g}_{c}, although it gives a simple gauge field interpretation of A_c and B_c. As change of branching structure only alters the definition of P^{g}_{c} by an unimportant finite-depth quantum circuit, we can use an alternate one that orders vertices of Σ^{z}_{k} (respectively, Σ^{x}_{i}, Σ^{y}_{j}) by their x (respectively, y, z) coordinate to get P^{g}_{c} expressed uniformly. Now, for instance, $c^{\circ}_{1} < c^{\circ}_{0} < c^{\circ}_{2}$ in Fig. 17(b). Suppose only Σ^{z}_{c-} (cyan online) is twisted by ω in Eq. (30) for the cube c in Fig. 17(a). Then

$$P^{100}_{c} = P^{000}_{c}\cdot(-1)^{\frac{1}{2}(1-\sigma^{(2),z}_{v_1}\sigma^{(2),z}_{v_1-z})\cdot\frac{1}{2}(1-\sigma^{(3),z}_{v_2}\sigma^{(3),z}_{v_2-z})} \cdot(-1)^{\frac{1}{2}(1-\sigma^{(2),z}_{v_4}\sigma^{(2),z}_{v_4-z})\cdot\frac{1}{2}(1-\sigma^{(3),z}_{v_3}\sigma^{(3),z}_{v_3-z})}\cdot\prod_{v\in c}\sigma^{(1)x}_{v}. \tag{155}$$

Analogously, twisting each of $\Sigma^{\mu}_{c\pm}$ by this ω adds two similar $(-1)^{\cdots}$ factors to P^{100}_{c}, P^{010}_{c}, and P^{001}_{c}. For simplicity, we may use $H = -\sum_{c\in\Lambda^{\bullet}}(P^{100}_{c} + P^{010}_{c} + P^{001}_{c})$ instead to get the same ground states as $H = -\sum_{c\in\Lambda^{3}_{\bullet}}P_c$.

Unlike X-cube models, a violation of $B_c = 1$ cannot always be removed by string operators in checkerboard models [61], which are thus expected to realize richer family of immobile quasiparticles (i.e., fractons) by twisting. Details of their quasiparticles will be studied in Sec. VII.

IV. GROUND-STATE DEGENERACY ON T^3: TWISTED X-CUBE MODELS

In this section, we consider a cubic lattice Λ embedded on a 3-torus (i.e., three-dimensional torus) T^3, whose vertex set is $\Lambda^0 = \mathbb{Z}_{L_x}\times\mathbb{Z}_{L_y}\times\mathbb{Z}_{L_z}$ with L_x, L_y, $L_z \in \mathbb{Z}$. A general method is developed here to compute the ground-state degeneracy, denoted $GSD(\Lambda)$, of a twisted X-cube model on Λ. In other words, we are going to determine $GSD(\Lambda)$ of a twisted X-cube model of system size $L_x\times L_y\times L_z$ with the periodic boundary condition identifying $(x + L_x, y, z) \sim (x, y + L_y, z) \sim (x, y, z + L_z) \sim (x, y, z)$. In particular, explicit computations will be given for examples based on groups $\mathbb{Z}_2$ and $\mathbb{Z}^3_2 \equiv \mathbb{Z}_2\times\mathbb{Z}_2\times\mathbb{Z}_2$.

A. Generic setting

The ground states are selected by the projector

$$P(\Lambda) := \prod_{v\in\Lambda^0} P_v. \tag{156}$$

Hence the ground-state degeneracy $GSD(\Lambda)$ equals the trace of $P(\Lambda)$. Explicitly,

$$\mathrm{tr}P(\Lambda) = \frac{1}{\left|G^{\Lambda^0}\right|}\sum_{\vartheta\in G^{\Lambda^2}_{B}}\sum_{\eta\in G^{\Lambda^0}}\langle\vartheta|\prod_{v}P^{\eta(v)}_{v}|\vartheta\rangle, \tag{157}$$

where $\langle\vartheta|\prod_v P^{\eta(v)}_{v}|\vartheta\rangle$ is nonzero if and only if $\vartheta \in G^{\Lambda^2}_{B}$ and $\prod_v A^{\eta(v)}_{v}|\vartheta\rangle = |\vartheta\rangle$. Let

$$G^{\Lambda^0}_{A} := \left\{\eta\in G^{\Lambda^0} \mid \prod_{v\in\Lambda^0}A^{\eta(v)}_{v}|\vartheta\rangle = |\vartheta\rangle\right\}. \tag{158}$$

We notice that $G^{\Lambda^0}_{A}$ is independent of ϑ and that each $\eta \in G^{\Lambda^0}_{A}$ can be specified by the following data:

$$\eta_o := \eta(0, 0, 0), \tag{159}$$

$$\partial\eta^{x}_{i} := \eta(i, 0, 0) - \eta(i - 1, 0, 0), \quad \forall i \in \mathbb{Z}_{L_x}, \tag{160}$$

$$\partial\eta^{y}_{j} := \eta(0, j, 0) - \eta(0, j - 1, 0), \quad \forall j \in \mathbb{Z}_{L_y}, \tag{161}$$

$$\partial\eta^{z}_{k} := \eta(0, 0, k) - \eta(0, 0, k - 1), \quad \forall k \in \mathbb{Z}_{L_z}, \tag{162}$$

subject to $\sum_n \partial\eta^{\lambda}_{n} = 0$, $\forall\lambda = x, y, z$ due to the periodic boundary condition. Therefore

$$\left|G^{\Lambda^0}_{A}\right| = |G|^{L_x+L_y+L_z-2}. \tag{163}$$

Any $\vartheta \in G_B^{\Lambda^2}$ assigns group elements to the two noncontractible loops of Σ_k^z in the x and y directions, respectively, as

$$\vartheta_k^z\langle x\rangle := \sum_{i\in\mathbb{Z}_{L_x}} \vartheta\left(i-\frac{1}{2},0,k-\frac{1}{2}\right), \tag{164}$$

$$\vartheta_k^z\langle y\rangle := \sum_{j\in\mathbb{Z}_{L_y}} \vartheta\left(0,j-\frac{1}{2},k-\frac{1}{2}\right), \tag{165}$$

$\forall k \in \mathbb{Z}_{L_z}$. Similarly, for Σ_i^x and Σ_j^y, we have

$$\vartheta_i^x\langle y\rangle := \sum_{j\in\mathbb{Z}_{L_y}} \vartheta\left(i-\frac{1}{2},j-\frac{1}{2},0\right), \tag{166}$$

$$\vartheta_i^x\langle z\rangle := \sum_{k\in\mathbb{Z}_{L_z}} \vartheta\left(i-\frac{1}{2},0,k-\frac{1}{2}\right), \tag{167}$$

$$\vartheta_j^y\langle z\rangle := \sum_{k\in\mathbb{Z}_{L_z}} \vartheta\left(0,j-\frac{1}{2},k-\frac{1}{2}\right), \tag{168}$$

$$\vartheta_j^y\langle x\rangle := \sum_{i\in\mathbb{Z}_{L_x}} \vartheta\left(i-\frac{1}{2},j-\frac{1}{2},0\right), \tag{169}$$

$\forall i \in \mathbb{Z}_{L_x}, \forall j \in \mathbb{Z}_{L_y}$. Clearly, they are subject to

$$\vartheta^{xy} = \sum_{i\in\mathbb{Z}_{L_x}} \vartheta_i^x\langle y\rangle = \sum_{j\in\mathbb{Z}_{L_y}} \vartheta_j^y\langle x\rangle, \tag{170}$$

$$\vartheta^{yz} = \sum_{j\in\mathbb{Z}_{L_y}} \vartheta_j^y\langle z\rangle = \sum_{k\in\mathbb{Z}_{L_z}} \vartheta_k^z\langle y\rangle, \tag{171}$$

$$\vartheta^{zx} = \sum_{k\in\mathbb{Z}_{L_z}} \vartheta_k^z\langle x\rangle = \sum_{i\in\mathbb{Z}_{L_x}} \vartheta_i^x\langle z\rangle, \tag{172}$$

where ϑ^{xy} (respectively, ϑ^{yz}, ϑ^{zx}) denotes the sum of $\vartheta(p)$ over faces lying in the plane $z=0$ (respectively, $x=0$, $y=0$).

Thus there are $|G|^{2(L_x+L_y+L_z)-3}$ choices of $\{\vartheta_n^\lambda\langle\mu\rangle\}$ (i.e., the group elements assigned to noncontractible loops of Σ_n^λ for all possible λ, n). With $\{\vartheta_n^\lambda\langle\mu\rangle\}$ fixed, we can pick: (1) $\vartheta(i-\frac{1}{2}, j-\frac{1}{2}, k)$ for $1\leqslant i<L_x$, $1\leqslant j<L_y$, $\forall k\in\mathbb{Z}_{L_z}$; (2) $\vartheta(i-\frac{1}{2}, 0, k-\frac{1}{2})$ for $1\leqslant i<L_x$, $1\leqslant k<L_z$; and (3) $\vartheta(0, j-\frac{1}{2}, k-\frac{1}{2})$ for $1\leqslant j<L_y$, $1\leqslant k<L_z$. In total, there are

$$\begin{aligned}&|G|^{(L_x-1)(L_y-1)L_z+(L_x-1)(L_z-1)+(L_y-1)(L_z-1)}\\&\quad=|G|^{L_xL_yL_z-L_x-L_y-L_z+2}\end{aligned} \tag{173}$$

different choices of $\vartheta\in G_B^{\Lambda^2}$ corresponding to the same $\{\vartheta_n^\lambda\langle\mu\rangle\}$. Therefore

$$\begin{aligned}\left|G_B^{\Lambda^2}\right| &= |G|^{2(L_x+L_y+L_z)-3}\times|G|^{L_xL_yL_z-L_x-L_y-L_z+2}\\&=|G|^{L_xL_yL_z+L_x+L_y+L_z-1}.\end{aligned} \tag{174}$$

1. Untwisted X-cube models

If the model is untwisted (i.e., $\omega\equiv 1$), then Eq. (157) reduces to

$$\begin{aligned}GSD(\Lambda)=\mathrm{tr}P(\Lambda)&=\frac{\left|G_A^{\Lambda^0}\right|\left|G_B^{\Lambda^2}\right|}{\left|G^{\Lambda^0}\right|}\\&=|G|^{2(L_x+L_y+L_z)-3}.\end{aligned} \tag{175}$$

This ground-state degeneracy was already mentioned in Eq. (124) as we introduced the model.

2. Twisted X-cube models

In a twisted X-cube model, each $\eta\in G_A^{\Lambda^0}$ makes a gauge transformation labeled by $\partial\eta_n^\lambda$ uniformly to each vertex of Σ_n^λ for $\lambda=x,y,z$. Therefore

$$\begin{aligned}\langle\vartheta|\prod_v P_v^{\eta(v)}|\vartheta\rangle=&\prod_{i\in\mathbb{Z}_{L_x}}\omega_i^x\left[\mathsf{T}^3;\vartheta_i^x\langle y\rangle,\vartheta_i^x\langle z\rangle,\partial\eta_i^x\right]\\&\cdot\prod_{i\in\mathbb{Z}_{L_y}}\omega_j^y\left[\mathsf{T}^3;\vartheta_j^y\langle z\rangle,\vartheta_j^y\langle x\rangle,\partial\eta_j^y\right]\\&\cdot\prod_{i\in\mathbb{Z}_{L_z}}\omega_k^z\left[\mathsf{T}^3;\vartheta_k^z\langle x\rangle,\vartheta_k^z\langle y\rangle,\partial\eta_k^z\right].\end{aligned} \tag{176}$$

We notice that $\langle\vartheta|\prod_v P_v^{\eta(v)}|\vartheta\rangle$ is a one-dimensional representation of $\eta\in G_A^{\Lambda^0}$. So $\sum_{\eta\in G_A^{\Lambda^0}}\langle\vartheta|\prod_v P_v^{\eta(v)}|\vartheta\rangle=0$ unless the representation is trivial.

Let Θ be the set of all possible choices of $\{\vartheta_n^\mu\langle\nu\rangle\}$ making $\langle\vartheta|\prod_v P_v^{\eta(v)}|\vartheta\rangle$ a trivial representation of $G_A^{\Lambda^0}$. Since there are $|G|^{L_xL_yL_z-L_x-L_y-L_z+2}$ choices of $\vartheta\in G_A^{\Lambda^0}$ for each selected $\{\vartheta_n^\mu\langle\nu\rangle\}$, explicit computation shows that the ground-state degeneracy on Λ embedded in T^3 is

$$\begin{aligned}GSD(\Lambda)&=\mathrm{tr}P(\Lambda)\\&=\frac{\left|G_A^{\Lambda^0}\right||G|^{L_xL_yL_z-L_x-L_y-L_z+2}|\Theta|}{|G^{\Lambda^0}|}=|\Theta|.\end{aligned} \tag{177}$$

So we can get $GSD(\Lambda)$ by counting the cardinality of Θ. By definition, $|\Theta|\leqslant 2(L_x+L_y+L_z)-3$. So the ground-state degeneracy of a twisted model is always less or equal to that of its untwisted version.

Technically, the triviality of $\langle\vartheta|\prod_v P_v^{\eta(v)}|\vartheta\rangle$ as a representation of $G_A^{\Lambda^0}$ is equivalent to

$$\prod_{n\in\mathbb{Z}_{L_\lambda}}\omega_n^\lambda\left[\mathsf{T}^3;\vartheta_n^\lambda\langle\mu\rangle,\vartheta_n^\lambda\langle\nu\rangle,\eta_n-\eta_{n-1}\right]=1, \tag{178}$$

$\forall(\lambda,\mu,\nu)=(x,y,z),(y,z,x),(z,x,y)$, $\forall\eta\in G^{L_\lambda}$. As

$$\begin{aligned}&\prod_{n\in\mathbb{Z}_{L_\lambda}}\omega_n^\lambda\left[\mathsf{T}^3;\vartheta_n^\lambda\langle\mu\rangle,\vartheta_n^\lambda\langle\nu\rangle,\eta_n-\eta_{n-1}\right]\\&\quad=\prod_{n\in\mathbb{Z}_{L_\lambda}}\frac{\omega_n^\lambda\left[\mathsf{T}^3;\vartheta_n^\lambda\langle\mu\rangle,\vartheta_n^\lambda\langle\nu\rangle,\eta_n\right]}{\omega_n^\lambda\left[\mathsf{T}^3;\vartheta_n^\lambda\langle\mu\rangle,\vartheta_n^\lambda\langle\nu\rangle,\eta_{n-1}\right]}\\&\quad=\prod_{n\in\mathbb{Z}_{L_\lambda}}\frac{\omega_n^\lambda\left[\mathsf{T}^3;\vartheta_n^\lambda\langle\mu\rangle,\vartheta_n^\lambda\langle\nu\rangle,\eta_n\right]}{\omega_{n+1}^\lambda\left[\mathsf{T}^3;\vartheta_{n+1}^\lambda\langle\mu\rangle,\vartheta_{n+1}^\lambda\langle\nu\rangle,\eta_n\right]},\end{aligned} \tag{179}$$

the condition is further equivalent to that $\exists\gamma^\lambda\in\widehat{G}$,

$$\omega_n^\lambda\left[\mathsf{T}^3;\vartheta_n^\lambda\langle\mu\rangle,\vartheta_n^\lambda\langle\nu\rangle,-\right]=\gamma^\lambda,\quad\forall n\in\mathbb{Z}_{L_\lambda}, \tag{180}$$

for $\lambda=x,\ y,\ z$ separately, where $\widehat{G}$ is the character group of G and $\omega_n^\lambda[\mathsf{T}^3;\vartheta_n^\lambda\langle\mu\rangle,\vartheta_n^\lambda\langle\nu\rangle,-]$ is viewed as a one-dimensional

representation of G with "$-$" denoting a place holder for a group element.

To take the constraints given by Eqs. (170)–(172) into consideration, let

$$\Theta^{\lambda}_{g,h,\gamma} := \Big\{(a,b)\in G^{L_\lambda}\times G^{L_\lambda}|\sum_n a_n = g, \sum_n b_n = h, \omega^{\lambda}_n[\mathrm{T}^3; a_n, b_n, -] = \gamma, \forall n\in\mathbb{Z}_{L_\lambda}\Big\}, \tag{181}$$

for $g,\ h\in G$, $\gamma\in\widehat{G}$ and $\lambda = x,\ y,\ z$. In addition, we write

$$\Theta^{\lambda}_{g,h} := \bigcup_{\gamma\in\widehat{G}}\Theta^{\lambda}_{g,h,\gamma}. \tag{182}$$

Then it is clear that

$$\Theta = \bigcup_{f,g,h\in G}\Theta^{x}_{f,g}\times\Theta^{y}_{g,h}\times\Theta^{z}_{h,f}. \tag{183}$$

Therefore the cardinalities of these sets satisfy

$$\big|\Theta^{\lambda}_{g,h}\big| = \sum_{\gamma\in\widehat{G}}\big|\Theta^{\lambda}_{g,h,\gamma}\big|, \tag{184}$$

$$|\Theta| = \sum_{f,g,h\in G}\big|\Theta^{x}_{f,g}\big|\big|\Theta^{y}_{g,h}\big|\big|\Theta^{z}_{h,f}\big|. \tag{185}$$

Below, we will explain how to use Eq. (185) to count $|\Theta|$ in the example based on $G=\mathbb{Z}_2^3$ with $\omega(f,g,h) = e^{i\pi f^{(1)}g^{(2)}h^{(3)}}$.

B. Example: $G = \mathbb{Z}_2$

As discussed in Sec. II B 1, we always have

$$\omega[\mathrm{T}^3; f, g, h] = \frac{\omega_h(f,g)}{\omega_h(g,f)} = 1, \tag{186}$$

$\forall f, g, h\in G$. Therefore the ground-state degeneracy remains unchanged from Eq. (175), i.e.,

$$GSD(\Lambda) = 2^{2(L_x+L_y+L_z)-3}, \tag{187}$$

no matter how we twist the model.

C. Example: $G = \mathbb{Z}_2^3$ with $\omega(f,g,h) = e^{i\pi f^{(1)}g^{(2)}h^{(3)}}$

As seen in Sec. II B 2, $\forall f, g, h\in G = \mathbb{Z}_2\times\mathbb{Z}_2\times\mathbb{Z}_2$,

$$\omega[\mathrm{T}^3; f, g, h] = e^{i\pi(f\times g)\cdot h}. \tag{188}$$

We identify $\widehat{G}\cong G$; in particular, $\omega[\mathrm{T}^3; f, g, -]\in\widehat{G}$ is identified with $f\times g\in G$.

To express $GSD(\Lambda) = |\Theta|$ in the form of Eq. (185), let us illustrate the calculation of $|\Theta^{\lambda}_{g,h,\gamma}|$, $\forall g, h, \gamma\in G$, $\forall\lambda = x, y, z$. To be concrete, we would like to take $\lambda = z$ as an example. There are many ways to twist the model with ω. Let us discuss case by case.

1. Some simple cases

Case 1. none of Σ^z_k are twisted.

Clearly, $\Theta^{z}_{g,h,\gamma} = \emptyset$ unless $\gamma = 0\equiv(0,0,0)$. For $\gamma = 0$, there are $|G|^{L_z-1}$ ways to pick $\{\vartheta^z_k\langle x\rangle\}_{k\in\mathbb{Z}_{L_z}}$ subject to $\sum_k\vartheta^z_k\langle x\rangle = g$ and similarly $|G|^{L_z-1}$ ways to pick $\{\vartheta^z_k\langle y\rangle\}_{k\in\mathbb{Z}_{L_z}}$ subject to $\sum_k\vartheta^z_k\langle x\rangle = h$. Thus in total

$$\big|\Theta^{z}_{g,h,\gamma}\big| = |G|^{2L_z-2}\delta_{\gamma,0} = 8^{2L_z-2}\delta_{\gamma,0}. \tag{189}$$

$$\big|\Theta^{z}_{g,h}\big| = \sum_{\gamma}\big|\Theta^{z}_{g,h,\gamma}\big| = 8^{2L_z-2}. \tag{190}$$

Case 2. Σ^z_k partially twisted by ω.

Suppose that Σ^z_k is twisted by ω for $k\in Z$ with Z some proper subset of $\mathbb{Z}_{L_z}$ (i.e., $Z\subsetneq\mathbb{Z}_{L_z}$). For convenience of later discussions, let $[\![g,h,\gamma]\!]_L$ be the cardinality of

$$[g,h,\gamma]_L := \Big\{(a,b)\in G^L\times G^L|\sum_n a_n = g, \sum_n b_n = h, a_n\times b_n = \gamma, \forall n\Big\}, \tag{191}$$

for $g,\ h,\gamma\in G$ and L a non-negative integer, where a_n and b_n are the components of a and b respectively. Then $[g,h,\gamma]_{|Z|}$ labels the choices of $\vartheta^z_k\langle x\rangle$ and $\vartheta^z_k\langle y\rangle$ for $k\in Z$, summed to g and h respectively. Each cross section Σ^z_k with $k\in\mathbb{Z}_{L_z}\backslash Z$ remains untwisted. Thus $\Theta^{z}_{g,h,\gamma} = \emptyset$ unless $\gamma = 0\equiv(0,0,0)$. In detail,

$$\big|\Theta^{z}_{g,h,\gamma}\big| = \delta_{\gamma,0}\sum_{g_1,h_1\in G}[\![g_1,h_1,0]\!]_{|Z|}|G|^{2(L_z-|Z|-1)}, \tag{192}$$

where $|G|^{2(L_z-|Z|-1)}$ is the number of ways to pick $\vartheta^z_k\langle x\rangle$ and $\vartheta^z_k\langle y\rangle$ for $k\in\mathbb{Z}_{L_z}\backslash Z$, summed to $g-g_1$ and $h-h_1$, respectively. Further, we notice that

$$\sum_{g,h\in G}[\![g,h,\gamma]\!]_L = \sum_{a,b\in G^L}\prod_{n=1}^{L}\delta_{a_n\times b_n,\gamma} = \Bigg(\sum_{a_1,b_1\in G}\delta_{a_1\times b_1,\gamma}\Bigg)^L = \begin{cases}22^L, & \gamma = (0,0,0),\\ 6^L, & \gamma\neq(0,0,0).\end{cases} \tag{193}$$

Therefore Eq. (192) gives

$$\big|\Theta^{z}_{g,h,\gamma}\big| = 22^{|Z|}\times 8^{2(L_z-|Z|-1)}\delta_{\gamma,0}, \tag{194}$$

$$\big|\Theta^{z}_{g,h}\big| = \sum_{\gamma}\big|\Theta^{z}_{g,h,\gamma}\big| = 22^{|Z|}\times 8^{2(L_z-|Z|-1)}. \tag{195}$$

We notice that Eq. (195) does not depend on g, h at all. We thus have a simple expression for the ground-state degeneracy if the model is twisted partially in all three directions. Explicitly, if Σ^x_i (respectively, Σ^y_j, Σ^z_k) is twisted for $i\in X\subsetneq\mathbb{Z}_{L_x}$ (respectively, $j\in Y\subsetneq\mathbb{Z}_{L_y}$, $k\in Z\subsetneq\mathbb{Z}_{L_z}$), the ground-state degeneracy for a system of size $L_x\times L_y\times L_z$ embedded on T^3, given by Eq. (185), gets simplified to

$$GSD(\Lambda) = |\Theta| = 22^{|X|+|Y|+|Z|}\cdot 8^{2(L_x+L_y+L_z-|X|-|Y|-|Z|)-3}, \tag{196}$$

where $|X|$, $|Y|$, and $|Z|$ are the numbers of cross sections Σ^{λ}_n twisted by ω in the three directions respectively.

Case 3. Σ_k^z twisted by ω for each $k \in \mathbb{Z}_{L_z}$.

By comparing definitions, we have

$$\left|\Theta^z_{g,h,\gamma}\right| = [\![g, h, \gamma]\!]_{L_z}. \tag{197}$$

Suppose that the model is partially twisted in the x and y directions. Then $|\Theta^x_{g,h}|$ and $|\Theta^y_{g,h}|$ are given by the analogues of Eq. (195). Together with Eqs. (184), (185), and (193), we get

$$GSD(\Lambda) = |\Theta| = 2^{2|X|+|Y|} 8^{2(L_x+L_y-|X|-|Y|)-3} \cdot (2^{2L_z} + 7 \times 6^{L_z}). \tag{198}$$

If both X and Y are empty, then the model is translation-invariant and its ground-state degeneracy is

$$GSD(\Lambda) = 8^{2(L_x+L_y)-3} \cdot (2^{2L_z} + 7 \times 6^{L_z}) \tag{199}$$

on a system of size $L_x \times L_y \times L_z$ embedded in T^3.

2. Computation of $[\![g, h, \gamma]\!]_L$

If the model is fully twisted in more than one direction, its ground-state degeneracy is much more complicated. To find an efficient algorithm to compute $[\![g, h, \gamma]\!]_L$, we first notice that

$$[\![g, h, \gamma]\!]_1 = \delta(g \times h, \gamma), \tag{200}$$

$$[\![g, h, \gamma]\!]_{L+L'} = \sum_{p,q\in G} [\![p, q, \gamma]\!]_L [\![g - p, h - q, \gamma]\!]_{L'}, \tag{201}$$

which follow from definitions.

To organize the data about $[\![g, h, \gamma]\!]_L$, let's consider the group ring $\mathbb{Z}G^2 := \mathbb{Z}[G \times G]$, which admits a polynomial representation

$$\mathbb{Z}G^2 \simeq \frac{\mathbb{Z}[s_1, s_2, s_3, t_1, t_2, t_3]}{\langle \{s_j^2 - 1, t_j^2 - 1\}_{j=1,2,3} \rangle}. \tag{202}$$

We write $s^a := s_1^{a^{(1)}} s_2^{a^{(2)}} s_3^{a^{(3)}}$, $t^a := t_1^{a^{(1)}} t_2^{a^{(2)}} t_3^{a^{(3)}}$ for short, $\forall a = (a^{(1)}, a^{(2)}, a^{(3)}) \in G = \mathbb{Z}_2^3$, and construct a polynomial

$$\rho_\gamma(s_1, s_2, s_3, t_1, t_2, t_3) := \sum_{g,h\in G} [\![g, h, \gamma]\!]_1 s^g t^h \tag{203}$$

for each $\gamma \in G$. Because of Eq. (201), ρ_γ^L as in $\mathbb{Z}G^2$ (i.e., the Lth power of ρ_θ modulo $\{s_j^2 - 1, t_j^2 - 1\}_{j=1,2,3}$) is

$$\rho_\gamma^L = \sum_{g,h\in G} [\![g, h, \gamma]\!]_L s^g t^h \mathrm{mod} \{s_j^2 - 1, t_j^2 - 1\}_{j=1,2,3}. \tag{204}$$

Thus $[\![g, h, \gamma]\!]_L$ can be expressed as a linear combination of $(\rho_\gamma(s, t))^L$ with $s, t \in Z_2^3$, where $Z_2 = \{1, -1\}$. Explicitly,

$$[\![g, h, \gamma]\!]_L = \frac{1}{2^6} \sum_{s,t\in Z_2^3} s^{-g} t^{-h} (\rho_\gamma(s, t))^L, \tag{205}$$

where $\rho_\gamma(s, t)$ stands for the value of ρ_γ at $s, t \in Z_2^3$.

For example, $\rho_0(1, 1, 1, 1, 1, 1) = \sum_{g,h\in G} [\![g, h, 0]\!]_1 = 22$ and $\rho_0(1, 1, 1, 1, 1, -1) = \sum_{g,h\in G} [\![g, h, 0]\!]_1 (-1)^{g^{(3)}} = 6$. Then Eq. (205) gives

$$[\![0, 0, 0]\!]_L = 2^{L-6}[42 \times (-1)^L + 21 \times 3^L + 11^L], \tag{206}$$

where each 0 is short for $(0, 0, 0) \in G = \mathbb{Z}_2^3$. For convenience of later discussions, we write

$$[\![g, h]\!]_L := \sum_{\gamma\in G} [\![g, h, \gamma]\!]_L. \tag{207}$$

By direct computation using Eq. (205), we get

$$[\![g, h]\!]_L = \begin{cases} 2^{L-6} \cdot \left(11^L + 49 \cdot 3^L + 294 \cdot (-1)^L + 168\right), & \text{if } g = h = 0, \\ 2^{L-6} \cdot \left(11^L + 17 \cdot 3^L + 6 \cdot (-1)^L - 24\right), & \text{if } g \times h = 0 \text{ but } (g, h) \neq (0, 0), \\ 2^{L-6} \cdot \left(11^L + 3^L - 10 \cdot (-1)^L + 8\right), & \text{if } g \times h \neq 0, \end{cases} \tag{208}$$

where 0 is short for the identity element $(0, 0, 0)$ of $G = \mathbb{Z}_2 \times \mathbb{Z}_2 \times \mathbb{Z}_2$.

3. Translation-invariant cases

The untwisted X-cube model has translation symmetries $(x, y, z) \to (x + 1, y, z)$, $(x, y, z) \to (x, y + 1, z)$ and $(x, y, z) \to (x, y, z + 1)$. To keep the translational symmetries of the X-cube model, for each direction $\lambda = x,\ y,\ z$, we either twist all Σ_n^λ by $\omega(f, g, h) = e^{i\pi f^{(1)} g^{(2)} h^{(3)}}$ or twist none of them. We have seen the ground-state degeneracy(199) if the model is fully twisted by ω in one direction. Now with Eqs. (184), (185), and (208), it is straightforward to compute the ground-state degeneracy $GSD(\Lambda)$ if the X-cube model is twisted by ω in two and three directions. Let us summarize the results below.

If we twist $\Sigma_i^x, \forall i \in \mathbb{Z}_{L_x}$ and $\Sigma_j^y, \forall j \in \mathbb{Z}_{L_y}$ but none of Σ_k^z, then the ground-state degeneracy is

$$GSD(\Lambda) = |G|^{2L_z-2} \sum_{f,g,h\in G} [\![f, g]\!]_{L_x} [\![g, h]\!]_{L_y} = 2^{L_x+L_y+6L_z-9}[252 \cdot (-1)^{L_x+L_y} + 77 \times 3^{L_x+L_y} + 11^{L_x+L_y} + 84 \cdot (-1)^{L_x} \cdot 3^{L_y} + 84 \cdot (-1)^{L_y} \cdot 3^{L_x} + 7 \times 3^{L_x} \times 11^{L_y} + 7 \times 3^{L_y} \times 11^{L_x}]. \tag{209}$$

The result for twisting any other two directions, like y and z, can be obtained by permuting $x,\ y,\ z$.

If the model is twisted in all three directions, then the expression for its ground-state degeneracy becomes

$$\begin{aligned} GSD(\Lambda) = |\Theta| &= \sum_{f,g,h\in G} [\![f,g]\!]_{L_x} [\![g,h]\!]_{L_y} [\![h,f]\!]_{L_z} \\ &= 2^{L_x+L_y+L_z-9} \cdot \{11^{L_x+L_y+L_z} + 1155 \times 3^{L_x+L_y+L_z} + 49728 \cdot (-1)^{L_x+L_y+L_z} + 9156[3^{L_x} \cdot (-1)^{L_y+L_z} \\ &+ 3^{L_y} \cdot (-1)^{L_z+L_x} + 3^{L_z} \cdot (-1)^{L_x+L_y}] + 2520[(-1)^{L_x} \cdot 3^{L_y+L_z} + (-1)^{L_y} \cdot 3^{L_z+L_x} + (-1)^{L_z} \cdot 3^{L_x+L_y}] \\ &+ 252[11^{L_x} \cdot (-1)^{L_y+L_z} + 11^{L_y} \cdot (-1)^{L_z+L_x} + 11^{L_z} \cdot (-1)^{L_x+L_y}] + 84[11^{L_x} \cdot 3^{L_y} \cdot (-1)^{L_z} + 11^{L_y} \cdot 3^{L_z} \cdot (-1)^{L_x} \\ &+ 11^{L_z} \cdot 3^{L_x} \cdot (-1)^{L_y} + 11^{L_y} \cdot 3^{L_x} \cdot (-1)^{L_z} + 11^{L_z} \cdot 3^{L_y} \cdot (-1)^{L_x} + 11^{L_x} \cdot 3^{L_z} \cdot (-1)^{L_y}] \\ &+ 77[11^{L_x} \cdot 3^{L_y+L_z} + 11^{L_y} \cdot 3^{L_z+L_x} + 11^{L_z} \cdot 3^{L_x+L_y}] + 7[11^{L_x+L_y} \cdot 3^{L_z} + 11^{L_y+L_z} \cdot 3^{L_x} + 11^{L_z+L_x} \cdot 3^{L_y}] \\ &+ 27552[(-1)^{L_x+L_y} + (-1)^{L_y+L_z} + (-1)^{L_z+L_x}] + 3360[3^{L_x} \cdot (-1)^{L_y} + 3^{L_y} \cdot (-1)^{L_z} + 3^{L_z} \cdot (-1)^{L_x} \\ &+ 3^{L_y} \cdot (-1)^{L_x} + 3^{L_z} \cdot (-1)^{L_y} + 3^{L_x} \cdot (-1)^{L_z}] + 672[3^{L_x+L_y} + 3^{L_y+L_z} + 3^{L_z+L_x}] \\ &+ 17472[(-1)^{L_x} + (-1)^{L_y} + (-1)^{L_z}] + 1344[3^{L_x} + 3^{L_y} + 3^{L_z}] + 13440\}. \end{aligned} \tag{210}$$

Both Eqs. (209) and (210) are much more complicated than we originally expected. In order to double check the validity of Eqs. (199), (209), and (210), we can plug in $L_x = L_y = L_z = 1$ and find that all of them give $GSD(\Lambda) = |G|^3$. This is what we would expect, as in this reduced case all operators A_v, B_c and P_v^g become the identity operator by definition. Thus $GSD(\Lambda)$ is just the dimension of the total Hilbert space for $L_x = L_y = L_z = 1$, which is $|G|^3$ as there are three faces in total. Despite the complexity of the GSD in the twisted case, it could be calculated straightforwardly within our framework. As in the second-to-last paragraph of Sec. II C 1, it can also be proved stable to local perturbations with using the results in Sec. VI A. The key point here is that the GSD for twisted fracton models depends explicitly on the system size, thus revealing the dependence of these phases on the geometry of the system. Moreover, we have noticed a dramatic change of GSD from partially twisted fracton models to fully twisted ones. As we will see in Sec. VI E 2, the qualitive difference are reflected on their excitations as well, for which we introduce the notion of inextricably non-Abelian 1d mobile quasiparticles.

V. GROUND-STATE DEGENERACY ON $\mathbb{T}^3$: TWISTED CHECKERBOARD MODELS

In this section, we consider a checkerboard Λ embedded on a 3-torus (i.e., three-dimensional torus) $\mathbb{T}^3$, whose vertex set is $\Lambda^0 = \mathbb{Z}_{L_x} \times \mathbb{Z}_{L_y} \times \mathbb{Z}_{L_z}$ with L_x, L_y, L_z even integers. A general method is developed here to compute the ground-state degeneracy, denoted $GSD(\Lambda)$, of a twisted checkerboard model on Λ. In other words, we are going to determine $GSD(\Lambda)$ of a twisted checkerboard model of system size $L_x \times L_y \times L_z$ with the periodic boundary condition identifying $(x + L_x, y, z) \sim (x, y + L_y, z) \sim (x, y, z + L_z) \sim (x, y, z)$. Below, let us first describe our calculation method in a generic setting and later illustrate it by explicit examples based on groups $\mathbb{Z}_2$ and $\mathbb{Z}_2^3 \equiv \mathbb{Z}_2 \times \mathbb{Z}_2 \times \mathbb{Z}_2$.

A. Generic setting

As a reminder, spins labeled by group elements of G are on vertices and the projectors P_c are associated with grey cubes $c \in \Lambda_\bullet^3$. In this section, we will use a triple of integers (c^x, c^y, c^z) to label the cube centered at $(c^x, c^y, c^z) + \frac{1}{2}(1, 1, 1)$.

The ground-state Hilbert subspace is the image of the projector

$$P(\Lambda) := \prod_{c\in\Lambda_\bullet^3} P_c. \tag{211}$$

So the ground-state degeneracy $GSD(\Lambda)$ equals the trace of $P(\Lambda)$. Explicitly,

$$\mathrm{tr}P(\Lambda) = \frac{1}{|G^{\Lambda^0}|} \sum_{\vartheta\in G_B^{\Lambda^0}} \sum_{\eta\in G^{\Lambda_\bullet^3}} \langle\vartheta| \prod_{c\in\Lambda_\bullet^3} P_c^{\eta(c)} |\vartheta\rangle, \tag{212}$$

where $\langle\vartheta| \prod_v P_v^{\eta(v)} |\vartheta\rangle$ is nonzero if and only if $\vartheta \in G_B^{\Lambda^0}$ and $\prod_{c\in\Lambda_\bullet^3} A_c^{\eta(c)} |\vartheta\rangle = |\vartheta\rangle$. Let

$$G_A^{\Lambda_\bullet^3} := \left\{ \eta \in G^{\Lambda_\bullet^3} \mid \prod_{c\in\Lambda_\bullet^3} A_c^{\eta(c)} |\vartheta\rangle = |\vartheta\rangle \right\}. \tag{213}$$

We notice that $G_A^{\Lambda_\bullet^3}$ is independent of ϑ and that each $\eta \in G_A^{\Lambda_\bullet^3}$ can be specified by

$$\eta_1 := \eta(0, 1, 1), \ \eta_2 := \eta(1, 0, 1), \ \eta_3 := \eta(1, 1, 0), \tag{214}$$

$$\partial\eta_i^x := \eta(i, 0, 0) - \eta(i - 2, 0, 0), \ \forall i \text{ even}, \tag{215}$$

$$\partial\eta_i^x := \eta(i, 1, 0) - \eta(i - 2, 1, 0), \ \forall i \text{ odd}, \tag{216}$$

$$\partial\eta_j^y := \eta(0, j, 0) - \eta(0, j - 2, 0), \ \forall j \text{ even}, \tag{217}$$

$$\partial\eta_j^y := \eta(0, j, 1) - \eta(0, j - 2, 1), \ \forall j \text{ odd}, \tag{218}$$

$$\partial\eta_k^z := \eta(0, 0, k) - \eta(0, 0, k - 2), \ \forall k \text{ even}, \tag{219}$$

$$\partial\eta_k^z := \eta(1, 0, k) - \eta(1, 0, k - 2), \ \forall k \text{ odd}, \tag{220}$$

subject to the constraints

$$\sum_{n \text{ odd}} \partial\eta_n^\mu = \sum_{n \text{ even}} \partial\eta_n^\mu = 0, \quad \forall \mu = x, y, z. \tag{221}$$

Therefore

$$\left|G_A^{\Lambda_\bullet^3}\right| = |G|^{L_x+L_y+L_z-3}. \tag{222}$$

Each $\vartheta \in G_B^{\Lambda^0}$ assigns group elements to the two noncontractible loops of Σ_k^z in the x and $(-1)^k y$ directions, respectively, as

$$\vartheta_k^z\langle x\rangle := (-1)^{k+1}\sum_{i\in\mathbb{Z}_{L_x}}(-1)^i\partial_z\vartheta(i,0,k), \tag{223}$$

$$\vartheta_k^z\langle y\rangle := (-1)^{k+1}\sum_{j\in\mathbb{Z}_{L_y}}(-1)^j\partial_z\vartheta(0,j,k), \tag{224}$$

$\forall k \in \mathbb{Z}_{L_z}$, where $\partial_z\vartheta(i,j,k) := \vartheta(i,j,k) - \vartheta(i,j,k-1)$. The branching structure is shown in Fig. 17. Similarly, the group elements along the noncontractible loops of Σ_i^x in the y and $(-1)^i z$ directions are

$$\vartheta_i^x\langle y\rangle := (-1)^{i+1}\sum_{j\in\mathbb{Z}_{L_y}}(-1)^j\partial_x\vartheta(i,j,0), \tag{225}$$

$$\vartheta_i^x\langle z\rangle := (-1)^{i+1}\sum_{k\in\mathbb{Z}_{L_z}}(-1)^k\partial_x\vartheta(i,0,k), \tag{226}$$

$\forall i \in \mathbb{Z}_{L_x}$, where $\partial_x\vartheta(i,j,k) := \vartheta(i,j,k) - \vartheta(i-1,j,k)$. The group elements along the noncontractible loops of Σ_j^y in the z and $(-1)^j x$ directions are

$$\vartheta_j^y\langle z\rangle := (-1)^{j+1}\sum_{k\in\mathbb{Z}_{L_z}}(-1)^k\partial_y\vartheta(0,j,k), \tag{227}$$

$$\vartheta_j^y\langle x\rangle := (-1)^{j+1}\sum_{i\in\mathbb{Z}_{L_x}}(-1)^i\partial_y\vartheta(i,0,k), \tag{228}$$

$\forall j \in \mathbb{Z}_{L_y}$, where $\partial_y\vartheta(i,j,k) := \vartheta(i,j,k) - \vartheta(i,j-1,k)$. Clearly, they are subject to

$$\begin{aligned}\vartheta^{xy} &= \sum_{i\ \text{even}}\vartheta_i^x\langle y\rangle = \sum_{j\ \text{even}}\vartheta_j^y\langle x\rangle,\\ &= \sum_{i\ \text{odd}}\vartheta_i^x\langle y\rangle = \sum_{j\ \text{odd}}\vartheta_j^y\langle x\rangle,\end{aligned} \tag{229}$$

$$\begin{aligned}\vartheta^{yz} &= \sum_{j\ \text{even}}\vartheta_j^y\langle z\rangle = \sum_{k\ \text{even}}\vartheta_k^z\langle y\rangle,\\ &= \sum_{j\ \text{odd}}\vartheta_j^y\langle z\rangle = \sum_{k\ \text{odd}}\vartheta_k^z\langle y\rangle,\end{aligned} \tag{230}$$

$$\begin{aligned}\vartheta^{zx} &= \sum_{k\ \text{even}}\vartheta_k^z\langle x\rangle = \sum_{i\ \text{even}}\vartheta_i^x\langle z\rangle,\\ &= \sum_{k\ \text{odd}}\vartheta_k^z\langle x\rangle = \sum_{i\ \text{odd}}\vartheta_i^x\langle z\rangle.\end{aligned} \tag{231}$$

where ϑ^{xy} (respectively, ϑ^{yz}, ϑ^{zx}) denotes the sum of $(-1)^v\vartheta(v)$ over vertices in the plane $z=0$ (respectively, $x=0$, $y=0$). So there are $|G|^{2(L_x+L_y+L_z)-9}$ choices of $\{\vartheta_n^\mu\langle\nu\rangle\}$ (i.e., the group elements assigned to noncontractible loops of Σ_n^μ for all possible μ, n).

There are $G^{L_xL_yL_z-(L_x-1)(L_y-1)(L_z-1)-2(L_x+L_y+L_z)+9}$ ways to color vertices on the planes $x=0$, $y=0$ and $z=0$ for each chosen $\{\vartheta_n^\mu\langle\nu\rangle\}$. Further, the number of choices of $\partial_z\vartheta$ to complete the coloring of Σ_k^z for each $k=1,2,\ldots,L_z-2$ equals $|G|^{\frac{1}{2}(L_x-2)(L_y-2)}$, where $\frac{1}{2}(L_x-2)(L_y-2)$ is the number of cubes in $\Lambda_\circ^3$ cut by Σ_k^z but not touching the planes $x=0$ and $y=0$. At this point, we have actually specified $\vartheta \in G_B^{\Lambda^0}$ already; in total,

$$\begin{aligned}\left|G_B^{\Lambda^0}\right| = |G|^{\frac{1}{2}(L_x-2)(L_y-2)(L_z-2)}\cdot|G|^{2(L_x+L_y+L_z)-9}\\ \cdot|G|^{L_xL_yL_z-(L_x-1)(L_y-1)(L_z-1)-2(L_x+L_y+L_z)+9},\end{aligned} \tag{232}$$

which simplifies to

$$\left|G_B^{\Lambda^0}\right| = |G|^{\frac{1}{2}L_xL_yL_z+L_x+L_y+L_z-3}. \tag{233}$$

1. Untwisted checkerboard models

If the model is untwisted (i.e., $\omega \equiv 1$), then Eq. (212) reduces to

$$\begin{aligned}GSD(\Lambda) = \mathrm{tr}P(\Lambda) &= \frac{\left|G_A^{\Lambda_\bullet^3}\right|\left|G_B^{\Lambda^0}\right|}{\left|G^{\Lambda_\bullet^3}\right|}\\ &= |G|^{2(L_x+L_y+L_z)-6}.\end{aligned} \tag{234}$$

This ground-state degeneracy was already mentioned in Eq. (146) as we introduced the model.

2. Twisted checkerboard models

In a twisted checkerboard model, each $\eta \in G_A^{\Lambda_\bullet^3}$ makes a gauge transformation labeled by $\partial\eta_n^\lambda$ uniformly to Σ_n^λ for $\lambda = x, y, z$. Therefore

$$\begin{aligned}\langle\vartheta|\prod_{c\in\Lambda_\bullet^3}P_c^{\eta(c)}|\vartheta\rangle = &\prod_{i\in\mathbb{Z}_{L_x}}\omega_i^x\left[\mathrm{T}^3;\vartheta_i^x\langle y\rangle,\vartheta_i^x\langle z\rangle,\partial\eta_i^x\right]\\ &\cdot\prod_{i\in\mathbb{Z}_{L_y}}\omega_j^y\left[\mathrm{T}^3;\vartheta_j^y\langle z\rangle,\vartheta_j^y\langle x\rangle,\partial\eta_j^y\right]\\ &\cdot\prod_{i\in\mathbb{Z}_{L_z}}\omega_k^z\left[\mathrm{T}^3;\vartheta_k^z\langle x\rangle,\vartheta_k^z\langle y\rangle,\partial\eta_k^z\right].\end{aligned} \tag{235}$$

We can view $\langle\vartheta|\prod_{c\in\Lambda_\bullet^3}P_c^{\eta(c)}|\vartheta\rangle$ as a one-dimensional representation of $\eta \in G_A^{\Lambda_\bullet^3}$. Therefore $\sum_{\eta\in G_A^{\Lambda_\bullet^3}}\langle\vartheta|\prod_{c\in\Lambda_\bullet^3}P_c^{\eta(c)}|\vartheta\rangle = 0$ unless the representation is trivial.

Let Θ collect all possible choices of $\{\vartheta_n^\lambda\langle\mu\rangle\}$ making $\langle\vartheta|\prod_{c\in\Lambda_\bullet^3}P_c^{\eta(c)}|\vartheta\rangle$ the trivial representation of $G_A^{\Lambda_\bullet^3}$. As there are $|G|^{L_xL_yL_z-(L_x-1)(L_y-1)(L_z-1)-2(L_x+L_y+L_z)+9}\cdot|G|^{\frac{1}{2}(L_x-2)(L_y-2)(L_z-2)}$ choices of $\vartheta \in G_A^{\Lambda_\bullet^3}$ for each chosen $\{\vartheta_n^\mu\langle\nu\rangle\}$, explicit computation shows that the ground-state degeneracy on Λ with underlying space T^3 is

$$\begin{aligned}GSD(\Lambda) &= \mathrm{tr}P(\Lambda)\\ &= |G|^{L_xL_yL_z-(L_x-1)(L_y-1)(L_z-1)-2(L_x+L_y+L_z)+9}\\ &\quad\cdot|G|^{\frac{1}{2}(L_x-2)(L_y-2)(L_z-2)}\cdot\frac{\left|G_A^{\Lambda_\bullet^3}\right|\left|\Theta\right|}{\left|G^{\Lambda_\bullet^3}\right|} = |G|^3|\Theta|.\end{aligned} \tag{236}$$

Therefore we can get $GSD(\Lambda)$ by counting the cardinality of Θ. By definition, $|\Theta| \leqslant 2(L_x+L_y+L_z)-9$. So the ground-state degeneracy of a twisted model is always less or equal to that of its untwisted version.

Technically, the triviality of $\langle\vartheta|\prod_{c\in\Lambda_\bullet^3}P_c^{\eta(c)}|\vartheta\rangle$ as a representation of $G_A^{\Lambda^0}$ is equivalent to requiring that

$$\prod_{n\in\mathbb{Z}_{L_\lambda}}\omega_n^\lambda\big[\mathrm{T}^3;\vartheta_n^\lambda\langle\mu\rangle,\vartheta_n^\lambda\langle\nu\rangle,\eta_n-\eta_{n-2}\big]=1, \tag{237}$$

$\forall(\lambda,\mu,\nu)=(x,y,z),(y,z,x),(z,x,y),\forall\eta\in G^{L_\lambda}$. Since

$$\begin{aligned}&\prod_{n\in\mathbb{Z}_{L_\lambda}}\omega_n^\lambda\big[\mathrm{T}^3;\vartheta_n^\lambda\langle\mu\rangle,\vartheta_n^\lambda\langle\nu\rangle,\eta_n-\eta_{n-2}\big]\\&=\prod_{n\in\mathbb{Z}_{L_\lambda}}\frac{\omega_n^\lambda\big[\mathrm{T}^3;\vartheta_n^\lambda\langle\mu\rangle,\vartheta_n^\lambda\langle\nu\rangle,\eta_n\big]}{\omega_n^\lambda\big[\mathrm{T}^3;\vartheta_n^\lambda\langle\mu\rangle,\vartheta_n^\lambda\langle\nu\rangle,\eta_{n-2}\big]}\\&=\prod_{n\in\mathbb{Z}_{L_\lambda}}\frac{\omega_n^\lambda\big[\mathrm{T}^3;\vartheta_n^\lambda\langle\mu\rangle,\vartheta_n^\lambda\langle\nu\rangle,\eta_n\big]}{\omega_{n+2}^\lambda\big[\mathrm{T}^3;\vartheta_{n+2}^\lambda\langle\mu\rangle,\vartheta_{n+2}^\lambda\langle\nu\rangle,\eta_n\big]},\end{aligned} \tag{238}$$

the condition is further equivalent to that $\exists\gamma_0^\lambda,\gamma_1^\lambda\in\widehat{G}$,

$$\omega_n^\lambda\big[\mathrm{T}^3;\vartheta_n^\lambda\langle\mu\rangle,\vartheta_n^\lambda\langle\nu\rangle,-\big]=\gamma^\lambda_{n\,(\mathrm{mod}\,2)},\forall n\in\mathbb{Z}_{L_\lambda}, \tag{239}$$

for $\lambda=x,y,z$ separately, where $\omega_n^\lambda[\mathrm{T}^3;\vartheta_n^\lambda\langle\mu\rangle,\vartheta_n^\lambda\langle\nu\rangle,-]$ is viewed as a one-dimensional representation of G with "$-$" denoting a place holder for a group element and $\widehat{G}$ stands for the character group of G.

To take the constraints given by Eqs. (229)–(231) into consideration, let

$$\begin{aligned}\Theta^{\lambda,\kappa}_{g,h,\gamma}:=\Big\{&(a,b)\in G^{\frac{L_\mu}{2}}\times G^{\frac{L_\mu}{2}}\big|\sum_n a_n=g,\sum_n b_n=h,\\&\omega_n^\lambda[\mathrm{T}^3;a_n,b_n,-]=\gamma,\forall n\in2\mathbb{Z}_{L_\lambda}+\kappa\Big\},\end{aligned} \tag{240}$$

for $g,\ h\in G$, $\gamma\in\widehat{G}$, $\lambda=x,\ y,\ z$, and $\kappa=0,1$. In addition, we write

$$\Theta^{\lambda,\kappa}_{g,h}:=\bigcup_{\gamma\in\widehat{G}}\Theta^{\lambda,\kappa}_{g,h,\gamma}, \tag{241}$$

It is straightforward to see that

$$\Theta=\bigcup_{f,g,h\in G}\Theta^{x,0}_{f,g}\times\Theta^{x,1}_{f,g}\times\Theta^{y,0}_{g,h}\times\Theta^{y,1}_{g,h}\times\Theta^{z,0}_{h,f}\times\Theta^{z,1}_{h,f}. \tag{242}$$

Therefore the cardinalities of these sets satisfy

$$\big|\Theta^{\lambda,\kappa}_{g,h}\big|=\sum_{\gamma\in\widehat{G}}\big|\Theta^{\lambda,\kappa}_{g,h,\gamma}\big|, \tag{243}$$

$$|\Theta|=\sum_{f,g,h\in G}\prod_{\kappa\in\mathbb{Z}_2}\big|\Theta^{x,\kappa}_{f,g}\big|\big|\Theta^{y,\kappa}_{g,h}\big|\big|\Theta^{z,\kappa}_{h,f}\big|. \tag{244}$$

Below, we will explain how to use Eq. (244) to count $|\Theta|$ in the example based on $G=\mathbb{Z}_2^3$ with $\omega(f,g,h)=e^{i\pi f^{(1)}g^{(2)}h^{(3)}}$.

B. Example: $G=\mathbb{Z}_2$

As discussed in Sec. II B 1, we always have

$$\omega[\mathrm{T}^3;f,g,h]=\frac{\omega_h(f,g)}{\omega_h(g,f)}=1, \tag{245}$$

$\forall f,\ g,\ h\in G$. Therefore Θ includes all possible choices of $\{\vartheta_n^\lambda(\mu)\}$ and hence $|\Theta|=|G|^{2(L_x+L_y+L_z)-9}$. Then

$$GSD(\Lambda)=|G|^3|\Theta|=2^{2(L_x+L_y+L_z)-6}, \tag{246}$$

which remains unchanged, no matter how we twist the model.

C. Example: $G=\mathbb{Z}_2^3$ with $\omega(f,g,h)=e^{i\pi f^{(1)}g^{(2)}h^{(3)}}$

As seen in Sec. II B 2, $\forall f,\ g,\ h\in G=\mathbb{Z}_2\times\mathbb{Z}_2\times\mathbb{Z}_2$,

$$\omega[\mathrm{T}^3;f,g,h]=e^{i\pi(f\times g)\cdot h}. \tag{247}$$

We identify $\widehat{G}\cong G$; in particular, $\omega[\mathrm{T}^3;f,g,-]\in\widehat{G}$ is identified with $f\times g\in G$.

First, let us illustrate the calculation of $|\Theta^{z,\kappa}_{g,h,\gamma}|$, $\forall g,h,\gamma\in G$, $\forall\kappa=0,1$ for some simple cases. The computation of $|\Theta^{\lambda,\kappa}_{g,h,\gamma}|$ for $\lambda=x,y$ is similar.

1. Some simple cases

Case 1. none of Σ_k^z are twisted.

Clearly, $\Theta^{z,\kappa}_{g,h,\gamma}=\emptyset$ unless $\gamma=0\equiv(0,0,0)$. For $\gamma=0$, there are $|G|^{\frac{1}{2}L_z-1}$ ways to pick $\{\vartheta_k^z\langle x\rangle\}_{k\in2\mathbb{Z}_{L_z}+\kappa}$ subject to $\sum_{k\in2\mathbb{Z}_{L_z}+\kappa}\vartheta_k^z\langle x\rangle=g$ and similarly $|G|^{\frac{1}{2}L_z-1}$ ways to pick $\{\vartheta_k^z\langle y\rangle\}_{k\in2\mathbb{Z}_{L_z}+\kappa}$ subject to $\sum_{k\in2\mathbb{Z}_{L_z}+\kappa}\vartheta_k^z\langle x\rangle=h$. In total, $\forall\kappa\in\{0,1\}$, $\forall g,\ h\in G$,

$$\big|\Theta^{z,\kappa}_{g,h,\gamma}\big|=|G|^{L_z-2}\delta_{\gamma,0}=8^{L_z-2}\delta_{\gamma,0}, \tag{248}$$

$$\big|\Theta^{z,\kappa}_{g,h}\big|=\sum_\gamma\big|\Theta^{z,\kappa}_{g,h,\gamma}\big|=8^{L_z-2}. \tag{249}$$

Case 2. Σ_k^z partially twisted by ω.

Suppose that Σ_k^z is twisted by ω for $k\in Z_\kappa\subsetneq2\mathbb{Z}_{L_z}+\kappa$, where $\kappa=0,1$. We would like to express $|\Theta^{z,\kappa}_{g,h,\gamma}|$ in terms of $[\![g,h,\gamma]\!]_L$, the cardinality of the set $[g,h,\gamma]_L$ defined by Eq. (191). We notice that $[g_1,h_1,\gamma]_{|Z_\kappa|}$ labels the choices of $\vartheta_k^z\langle x\rangle$ and $\vartheta_k^z\langle y\rangle$ for $k\in Z_\kappa$, satisfying $\vartheta_k^z\langle x\rangle\times\vartheta_k^z\langle y\rangle=\gamma$ and summed to g_1 and h_1, respectively. The remaining untwisted Σ_k^z with $k\in(2\mathbb{Z}_{L_z}+\kappa)\backslash Z_\kappa$ still requires $\gamma=0\equiv(0,0,0)$. Thus

$$\big|\Theta^{z,\kappa}_{g,h,\gamma}\big|=\delta_{\gamma,0}\sum_{g_1,h_1\in G}[\![g_1,h_1,0]\!]_{|Z_\kappa|}|G|^{L_z-2|Z_\kappa|-2}, \tag{250}$$

where $|G|^{L_z-2|Z_\kappa|-2}$ is the number of ways to pick $\vartheta_k^z\langle x\rangle$ and $\vartheta_k^z\langle y\rangle$ for $k\in(2\mathbb{Z}_{L_z}+\kappa)\backslash Z_\kappa$, summed to $g-g_1$ and $h-h_1$, respectively. With Eq. (193), it gets simplified to

$$\big|\Theta^{z,\kappa}_{g,h,\gamma}\big|=22^{|Z_\kappa|}\times8^{L_z-2|Z_\kappa|-2}\delta_{\gamma,0}, \tag{251}$$

$$\big|\Theta^{z,\kappa}_{g,h}\big|=\sum_\gamma\big|\Theta^{z,\kappa}_{g,h,\gamma}\big|=22^{|Z_\kappa|}\times8^{L_z-2|Z_\kappa|-2}. \tag{252}$$

We notice that Eq. (252) does not depend on g,h at all. Thus if Σ_i^x (respectively, Σ_j^y, Σ_k^z) is twisted for $i\in X_\kappa\subsetneq2\mathbb{Z}_{L_x}+\kappa$ (respectively, $j\in Y_\kappa\subsetneq2\mathbb{Z}_{L_y}+\kappa$, $k\in Z_\kappa\subsetneq\mathbb{Z}_{L_z}+\kappa$), then $GSD(\Lambda)$ for a system of size $L_x\times L_y\times L_z$ embedded on T^3, given by Eqs. (236) and (244), gets simplified to

$$\begin{aligned}GSD(\Lambda)&=|G|^3|\Theta|\\&=22^{|X|+|Y|+|Z|}\cdot8^{2(L_x+L_y+L_z-|X|-|Y|-|Z|)-6},\end{aligned} \tag{253}$$

where $X := X_0 \cup X_1, Y := Y_0 \cup Y_1, Z = Z_0 \cup Z_1$. In particular, it reduces to Eq. (234) as expected, if X, Y, Z are all empty.

Case 3. Σ_k^z twisted by ω for each $k \in 2\mathbb{Z}_{L_z}$.

By comparing definitions, we have

$$\left|\Theta^{z,0}_{g,h,\gamma}\right| = [\![g, h, \gamma]\!]_{\frac{1}{2}L_z}. \tag{254}$$

In addition, Σ_k^z (respectively, Σ_i^x, Σ_j^y) may be twisted by ω for $k \in Z_1 \subsetneq 2\mathbb{Z}_{L_z} + 1$ (respectively, $i \in X_\kappa \subsetneq 2\mathbb{Z}_{L_x} + \kappa$, $j \in Y_\kappa \subsetneq 2\mathbb{Z}_{L_y} + \kappa$ with $\kappa = 0, 1$) as well. Then $|\Theta^{z,1}_{g,h}|$ (respectively, $|\Theta^{x,\kappa}_{g,h}|$ and $|\Theta^{y,\kappa}_{g,h}|$) is given by Eq. (252) (respectively, its analog for the x and y direction). In total, Eqs. (193) and (244) give

$$\begin{aligned}|\Theta| = {} & 8^{2\left(L_x+L_y-|X|-|Y|-|Z_1|\right)+L_z-9} \cdot 22^{|X|+|Y|+|Z_1|} \\ & \cdot \left(22^{\frac{1}{2}L_z} + 7 \times 6^{\frac{1}{2}L_z}\right),\end{aligned} \tag{255}$$

where $X := X_0 \cup X_1$ and $Y = Y_0 \cup Y_1$. Therefore the ground-state degeneracy is

$$\begin{aligned}GSD(\Lambda) = |G|^3|\Theta| = {} & 8^{2\left(L_x+L_y-|X|-|Y|-|Z_1|\right)+L_z-6} \\ & \cdot 22^{|X|+|Y|+|Z_1|} \cdot \left(22^{\frac{1}{2}L_z} + 7 \times 6^{\frac{1}{2}L_z}\right).\end{aligned} \tag{256}$$

If $|X| = |Y| = |Z_1| = 0$, the model is translation-invariant and its ground-state degeneracy reduces to

$$GSD(\Lambda) = 8^{2(L_x+L_y)+L_z-6}\left(22^{\frac{1}{2}L_z} + 7 \times 6^{\frac{1}{2}L_z}\right) \tag{257}$$

with system size $L_x \times L_y \times L_z$ embedded on T^3.

2. Translation-invariant cases

The untwisted checkerboard model has the translation symmetries $(x, y, z) \to (x + 2, y, z)$, $(x, y, z) \to (x, y + 2, z)$ and $(x, y, z) \to (x, y, z + 2)$. To keep these translation symmetries, we either twist all Σ_n^λ for $n \in 2\mathbb{Z}_{L_\lambda} + \kappa$ together or twist none of them, where $\kappa = 0, 1$. With Eqs. (205), (208), (236), (243), and (244), we can compute the ground-state degeneracies $GSD(\Lambda)$ of each translation-invariant case. Let us list the results for some examples below.

Case 1. half of Σ_k^z's are twisted by ω (e.g., Σ_k^z is twisted by ω for $k \in 2\mathbb{Z}_{L_z}$).

The ground-state degeneracy is given by Eq. (257).

Case 2. half of Σ_n^λ's are twisted by ω in both the x and y directions (e.g., both Σ_i^x and Σ_j^y are twisted by ω for $i \in 2\mathbb{Z}_{L_x}$ and $j \in 2\mathbb{Z}_{L_y}$).

The ground-state degeneracy is

$$\begin{aligned}GSD(\Lambda) &= |G|^3|\Theta| \\ &= |G|^3 \sum_{f,g,h\in G} [\![f, g]\!]_{\frac{1}{2}L_x} [\![g, h]\!]_{\frac{1}{2}L_y} |G|^{L_x+L_y+2L_z-8} \\ &= 2^{\frac{7}{2}L_x+\frac{7}{2}L_y+6L_z-18}\Big[252 \cdot (-1)^{\frac{L_x+L_y}{2}} + 77 \times 3^{\frac{L_x+L_y}{2}} \\ &\quad + 11^{\frac{L_x+L_y}{2}} + 84 \cdot (-1)^{\frac{1}{2}L_x} \cdot 3^{\frac{1}{2}L_y} + 84 \cdot (-1)^{\frac{1}{2}L_y} \\ &\quad \cdot 3^{\frac{1}{2}L_x} + 7 \times 3^{\frac{1}{2}L_x} \times 11^{\frac{1}{2}L_y} + 7 \times 3^{\frac{1}{2}L_y} \times 11^{\frac{1}{2}L_x}\Big].\end{aligned} \tag{258}$$

The result for twisting by half any other two directions, like y and z, can be obtained by permuting x, y, z.

Case 3. half of Σ_n^λ's are twisted in all the three directions.

The ground-state degeneracy in this case is

$$\begin{aligned}GSD(\Lambda) &= |G|^3|\Theta| \\ &= |G|^3 \sum_{f,g,h\in G} [\![f, g]\!]_{\frac{L_x}{2}} [\![g, h]\!]_{\frac{L_y}{2}} [\![h, f]\!]_{\frac{L_z}{2}} |G|^{L_x+L_y+L_z-6} \\ &= 8^{L_x+L_y+L_z-3} \sum_{f,g,h\in G} [\![f, g]\!]_{\frac{L_x}{2}} [\![g, h]\!]_{\frac{L_y}{2}} [\![h, f]\!]_{\frac{L_z}{2}},\end{aligned} \tag{259}$$

where $\sum_{f,g,h\in G} [\![f, g]\!]_{\frac{1}{2}L_x} [\![g, h]\!]_{\frac{1}{2}L_y} [\![h, f]\!]_{\frac{1}{2}L_z}$ can either be calculated with Eq. (208) directly or be expressed by Eq. (210) with L_x, L_y, and L_z replaced by $\frac{1}{2}L_x$, $\frac{1}{2}L_y$, and $\frac{1}{2}L_z$, respectively.

Case 4. each Σ_k^z is twisted by ω for $k \in \mathbb{Z}_{L_z}$.

Here, the ground-state degeneracy is give by

$$\begin{aligned}GSD(\Lambda) &= |G|^3|\Theta| \\ &= |G|^3 \sum_{f,g,h\in G} [\![f, g]\!]^2_{\frac{L_z}{2}} |G|^{2L_x+2L_y-8} \\ &= 8^{2L_x+2L_y-6} \cdot 2^{L_z}\left(11^{L_z} + 14 \times 33^{\frac{L_z}{2}} + 133 \times 3^{L_z}\right. \\ &\quad \left. + 1344 \cdot (-1)^{\frac{L_z}{2}} + 504 \cdot (-1)^{\frac{L_z}{2}} \cdot 3^{\frac{L_z}{2}} + 2100\right),\end{aligned} \tag{260}$$

where $[\![f, g]\!]^2_{\frac{L_z}{2}}$ is the square of $[\![f, g]\!]_{\frac{L_z}{2}}$ specified by Eq. (208).

Case 5. both Σ_i^x and Σ_j^y twisted by ω for $i \in \mathbb{Z}_{L_x}$ and $j \in \mathbb{Z}_{L_y}$.

The ground-state degeneracy for this case is

$$\begin{aligned}GSD(\Lambda) &= |G|^3|\Theta| \\ &= |G|^3 \sum_{f,g,h\in G} [\![f, g]\!]^2_{\frac{L_x}{2}} [\![g, h]\!]^2_{\frac{L_y}{2}} |G|^{2L_z-4} \\ &= 8^{2L_z-1} \sum_{f,g,h\in G} [\![f, g]\!]^2_{\frac{L_x}{2}} [\![g, h]\!]^2_{\frac{L_y}{2}},\end{aligned} \tag{261}$$

where $[\![f, g]\!]_{\frac{L_x}{2}}$ and $[\![g, h]\!]_{\frac{L_y}{2}}$ are given by Eq. (208). Explicitly, $GSD(\Lambda)$ can be expressed as a long polynomial in terms of 2^{L_λ}, $(-1)^{\frac{1}{2}L_\lambda}$, $3^{\frac{1}{2}L_\lambda}$, $11^{\frac{1}{2}L_\lambda}$ with $\lambda = x, y$ and 2^{L_z}.

Case 6. all Σ_i^x, Σ_j^y and Σ_k^z twisted by ω for $i \in \mathbb{Z}_{L_x}$ $j \in \mathbb{Z}_{L_y}$, and $k \in \mathbb{Z}_{L_z}$.

The ground-state degeneracy is

$$\begin{aligned}GSD(\Lambda) &= |G|^3|\Theta| \\ &= |G|^3 \sum_{f,g,h\in G} [\![f, g]\!]^2_{\frac{L_x}{2}} [\![g, h]\!]^2_{\frac{L_y}{2}} [\![h, f]\!]^2_{\frac{L_z}{2}},\end{aligned} \tag{262}$$

where $[\![f, g]\!]_{\frac{L_x}{2}}$, $[\![g, h]\!]_{\frac{L_y}{2}}$, and $[\![h, f]\!]_{\frac{L_z}{2}}$ are given by Eq. (208). Explicitly, $GSD(\Lambda)$ can be expressed as a long polynomial in terms of 2^{L_λ}, $(-1)^{\frac{1}{2}L_\lambda}$, $3^{\frac{1}{2}L_\lambda}$, and $11^{\frac{1}{2}L_\lambda}$ with $\lambda = x,\ y,\ z$.

To conclude, we note that our formalism allows us to explicitly calculate the GSD of each twisted checkerboard model, which is also stable to local perturbations by the argument in the second-to-last paragraph of Sec. II C 1 using the results in Sec. VII A. Once again, we emphasize that the dependence of the GSD on the system size clearly reflect the geometric nature of gapped three-dimensional fracton

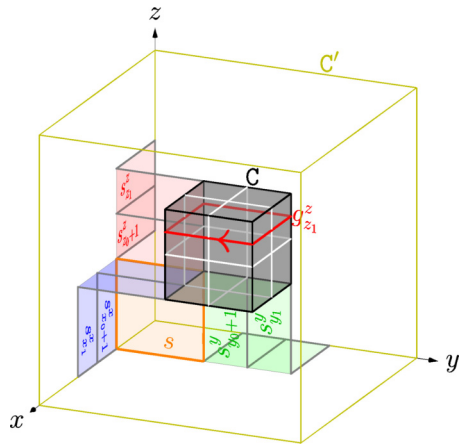

FIG. 18. An excited cuboid $\mathtt{C} = [x_0, x_1] \times [y_0, y_1] \times [z_0, z_1]$ isolated from other excitations outside $\mathtt{C}'$ in an X-cube model. The Hilbert space is spanned by the states $|\chi, \overline{\chi}; s, D_{\boldsymbol{g}}^{\boldsymbol{s}}\rangle$ with s and $\boldsymbol{s} = (s^x_{x_0+1}, \ldots, s^x_{x_1}, s^y_{y_0+1}, \ldots, s^y_{y_1}, s^z_{z_0+1}, \ldots, s^z_{z_1})$ specifying the sums of group elements on the faces in the corresponding membranes (colored orange, blue, green and red online), $\boldsymbol{g} = (g^x_{x_0+1}, \ldots, g^x_{x_1}, g^y_{y_0+1}, \ldots, g^y_{y_1}, g^z_{z_0+1}, \ldots, g^z_{z_1})$ describing fluxes around $\partial\mathtt{C}$, and χ (respectively, $\overline{\chi}$) being a spin configuration on $\partial\mathtt{C}'$ (respectively, $\partial\mathtt{C}$) compatible with $\boldsymbol{g}$.

orders. Also, a dramatic change from partially twisted model to fully twisted model is already observed in GSD. As we will see in Sec. VII E 5, this qualitative difference is reflected on excitations as well; in particular, fully twisted checkerboard model may host inextricably non-Abelian fractons.

VI. QUASIPARTICLES IN TWISTED X-CUBE MODELS

We have seen that there is a lot of freedom in twisting the X-cube model by 3-cocycles. Below, by an X-cube model based on an Abelian group G, we refer to any of these twisted versions, including the original untwisted one. We are going to develop a universal method for analyzing the properties of quasiparticles in these models. Technically, by a quasiparticle, we mean a finite excited region. Without loss of generality, we can simply study excited cuboids.

To study all possible excited states of a cuboid $\mathtt{C}$, such as the grey one of size $2 \times 2 \times 2$ in the center of Fig. 18, we remove all the requirements $P_v = 1$ for $v \in \mathtt{C}$. In addition, we would like that the other excitations are far away from $\mathtt{C}$. So we pick a much larger cuboid $\mathtt{C}'$ containing $\mathtt{C}$ deep inside, as shown in Fig. 18, and study the Hilbert subspace selected by $P_v = 1$ for $v \in \mathtt{C}' - \mathtt{C}^\circ$, where $\mathtt{C}^\circ$ is the interior of $\mathtt{C}$.

Such a Hilbert subspace describes an isolated excited cuboid $\mathtt{C}$ and it may be decomposed into more than one irreducible sector according to the actions of all local operators near $\mathtt{C}$, which leads to the notation of *particle type*. An excited spot (i.e., *quasiparticle*) is called *simple* if it is already projected into a definite particle type, which cannot be changed locally. In the following, we will work out the classification of particle types in the twisted fracton models. It turns out that each particle type can be labeled by the x, y and z *topological charges* subject to some constraints. Then the fusion of topological charges can be described by the coproduct of $\mathcal{D}^\omega(G)$.

Further, we notice that a quasiparticle is mobile in the x (respectively, y, z) direction if and only if its x (respectively, y, z) topological charge is trivial. A quasiparticle is called a *fracton* if it is not a fusion result of mobile quasiparticles. Necessarily, a fracton has to be immobile; it has nontrivial topological charges in all three directions. In addition, we will also describe some novel braiding processes of mobile quasiparticles with restricted mobilities in this section.

A. Particle type and topological charges

Let $\mathtt{C} = [x_0, x_1] \times [y_0, y_1] \times [z_0, z_1]$ be a generic cuboid and $\mathtt{C}' = [x'_0, x'_1] \times [y'_0, y'_1] \times [z'_0, z'_1]$ a much larger cube containing $\mathtt{C}$, as shown in Fig. 18. Further, let $\mathtt{M} = \mathtt{C}' - \mathtt{C}^\circ$, where $\mathtt{X}^\circ$ denotes the interior of any topological space $\mathtt{X}$. Then $\mathtt{M}$ is a three-dimensional manifold with boundary. We denote the set of cubes (respectively, faces, edges, vertices) inside $\mathtt{M}$ by $\Lambda^3(\mathtt{M})$ [respectively, $\Lambda^2(\mathtt{M})$, $\Lambda^1(\mathtt{M})$, $\Lambda^0(\mathtt{M})$]. Let $\mathcal{H}(\Lambda^2(\mathtt{M}), G)$ be the Hilbert space describing all the physical degrees of freedom on $\mathtt{M}$. To classify generic excitations within $\mathtt{C}$, we need to analyze the subspace of $\mathcal{H}(\Lambda^2(\mathtt{M}), G)$ selected by the projector

$$P(\mathtt{M}) := \prod_{v \in \Lambda^0(\mathtt{M}^\circ)} P_v. \tag{263}$$

Let $\mathcal{H}_0(\mathtt{M})$ denote this subspace, i.e., the image of $P(\mathtt{M})$.

Let $\mathtt{M}^x_i$ with $i \in \{x'_0 + 1, x'_0 + 2, \ldots, x'_1\}$ (respectively, $\mathtt{M}^y_j$ with $j \in \{y'_0 + 1, y'_0 + 2, \ldots, y'_1\}$, $\mathtt{M}^z_k$ with $k \in \{z'_0 + 1, z'_0 + 2, \ldots, z'_1\}$) be the intersection of $\mathtt{M}$ with the plane $x = i - \frac{1}{2}$ (respectively, $y = j - \frac{1}{2}$, $z = k - \frac{1}{2}$), i.e., the region of Σ^x_i (respectively, Σ^y_j, Σ^z_k) inside $\mathtt{M}$. As in Fig. 7(b), we embed $\mathtt{M}^x_i$ (respectively, $\mathtt{M}^y_j$, $\mathtt{M}^z_k$) into a triangulated annulus $\overline{\mathtt{M}}^x_i$ (respectively, $\overline{\mathtt{M}}^y_j$, $\overline{\mathtt{M}}^z_k$). If the plane does not cut $\mathtt{C}$, then $\overline{\mathtt{M}}^x_i$ (respectively, $\overline{\mathtt{M}}^y_j$, $\overline{\mathtt{M}}^z_k$) reduces to a topological sphere. We pick the base point of the outer/inner boundary of $\overline{\mathtt{M}}^x_i$ (respectively, $\overline{\mathtt{M}}^y_j$, $\overline{\mathtt{M}}^z_k$) to be in the line $(y, z) = (y'_0, z'_0)/(y_0, z_0)$ (respectively, $(z, x) = (z'_0, x'_0)/(z_0, x_0)$, $(x, y) = (x'_0, y'_0)/(x_0, y_0)$).

For convenience, we write $\mathtt{C}^x := \{x_0 + 1, x_0 + 2, \ldots, x_1\}$, $\mathtt{C}^y := \{y_0 + 1, y_0 + 2, \ldots, y_1\}$ and $\mathtt{C}^z := \{z_0 + 1, z_0 + 2, \ldots, z_1\}$. Let g^x_i (respectively, g^y_j, g^z_k) be the group element associated with the inner boundary of $\overline{\mathtt{M}}^x_i$ (respectively, $\overline{\mathtt{M}}^y_j$, $\overline{\mathtt{M}}^z_k$). For $i \notin \mathtt{C}^x$ (respectively, $j \notin \mathtt{C}^y$, $k \notin \mathtt{C}^z$), we write $g^x_i = 0$ (respectively, $g^y_j = 0$, $g^z_k = 0$) because $\partial\overline{\mathtt{M}}^x_i = \emptyset$ (respectively, $\partial\overline{\mathtt{M}}^y_j = \emptyset$, $\partial\overline{\mathtt{M}}^z_k = \emptyset$). Hence, to describe the fluxes, we need

$$\boldsymbol{g} := (\boldsymbol{g}^x, \boldsymbol{g}^y, \boldsymbol{g}^z) \in G^{\mathtt{C}^x} \times G^{\mathtt{C}^y} \times G^{\mathtt{C}^z}, \tag{264}$$

$$\boldsymbol{g}^x := \left(g^x_{x_0+1}, g^x_{x_0+2}, \ldots, g^x_{x_1}\right) \in G^{\mathtt{C}^x}, \tag{265}$$

$$\boldsymbol{g}^y := \left(g^y_{y_0+1}, g^y_{y_0+2}, \ldots, g^y_{y_1}\right) \in G^{\mathtt{C}^y}, \tag{266}$$

$$\boldsymbol{g}^z := \left(g^z_{z_0+1}, g^z_{z_0+2}, \ldots, g^z_{z_1}\right) \in G^{\mathtt{C}^z}. \tag{267}$$

Often, $\boldsymbol{g}$ (respectively, $\boldsymbol{g}^x$) is also written as $(g_n^\mu)_{n\in\mathbb{C}^\mu}^{\mu=x,y,z}$ [respectively, $(g_i^x)_{i\in\mathbb{C}^x}$]. These data are subject to the constraint

$$\sum_{\mu=x,y,z}\sum_{n\in\mathbb{C}^\mu} g_n^\mu = 0. \tag{268}$$

We denote the set of all allowed values of $\boldsymbol{g}$ by $F(\mathbb{C})$. As a group, $F(\mathbb{C})$ is isomorphic to $G^{x_1-x_0+y_1-y_0+z_1-z_0-1}$.

Using the triangulations of $\overline{\mathbb{M}}_i^x$, $\overline{\mathbb{M}}_j^y$, and $\overline{\mathbb{M}}_k^z$, we define a set of vectors forming an orthonormal basis of $\mathcal{H}_0(\mathbb{M})$ by

$$\left|\chi,\overline{\chi};s,\mathbb{D}_{\boldsymbol{g}}^{\boldsymbol{s}}\right\rangle := \sum_{\vartheta\in G_B^{\Lambda^2(\mathbb{M})}(s,\chi,\overline{\chi})} \frac{Z\left(\vartheta;\mathbb{D}_{\boldsymbol{g}}^{\boldsymbol{s}}\right)}{|G|^{\frac{1}{2}|\Lambda^0(\mathbb{M}^\circ)|}}|\vartheta\rangle \tag{269}$$

with $\boldsymbol{g}\in F(\mathbb{C})$, $s\in G$, $\boldsymbol{s}\in G^{\mathbb{C}^x}\times G^{\mathbb{C}^y}\times G^{\mathbb{C}^z}$, and $\chi\in G^{\Lambda^2(\partial\mathbb{C}')}$ (respectively, $\overline{\chi}\in G^{\Lambda^2(\partial\mathbb{C})}$) being a spin configuration on $\partial\mathbb{C}'$ (respectively, $\partial\mathbb{C}$) compatible with $\boldsymbol{g}$. In detail, s specifies the sum of group elements on the faces in the lower left square region (orange online) and $G_B^{\Lambda^2(\mathbb{M})}(s,\chi,\overline{\chi})$ denotes the set of $\vartheta\in G_B^{\Lambda^2(\mathbb{M})}$ compatible with s and coinciding with $\overline{\chi}$, χ on $\partial\mathbb{C}$, $\partial\mathbb{C}'$. In addition,

$$Z\left(\vartheta;\mathbb{D}_{\boldsymbol{g}}^{\boldsymbol{s}}\right) := \prod_{i=x_0'+1}^{x_1'} Z_i^x\left(\vartheta;\mathbb{D}_{\boldsymbol{g}}^{\boldsymbol{s}}\right)\cdot\prod_{j=y_0'+1}^{y_1'} Z_j^y\left(\vartheta;\mathbb{D}_{\boldsymbol{g}}^{\boldsymbol{s}}\right)\cdot\prod_{k=z_0'+1}^{z_1'} Z_k^z\left(\vartheta;\mathbb{D}_{\boldsymbol{g}}^{\boldsymbol{s}}\right), \tag{270}$$

where $Z_n^\mu(\vartheta;\mathbb{D}_{\boldsymbol{g}}^{\boldsymbol{s}})$ is the Dijkgraaf-Witten partition function of a ball with surface $-\overline{\mathbb{M}}_n^\mu$ for $n\notin\mathbb{C}^\mu$ or a solid torus with surface $(-\overline{\mathbb{M}}_n^\mu)\cup_{\varpi\overline{\varpi}}\mathbb{D}_{g_n^\mu}^{s_n^\mu}$ [as in Fig. 8(b)] for $n\in\mathbb{C}^\mu$ in the coloring specified by ϑ. The minus sign before $\overline{\mathbb{M}}_n^\mu$ means that the orientation of $\overline{\mathbb{M}}_n^\mu$ is pointing toward the inside of the solid according to the right-hand rule.

To manipulate the states within $\mathcal{H}_0(\mathbb{M})$, we can define a collection of operators P_v^g for $v\in\Lambda^0(\partial\mathbb{C})$ [respectively, $v\in\Lambda^0(\partial\mathbb{C}')$], commuting with $P(\mathbb{M})$ and supported near $\partial\mathbb{C}$ (respectively, $\partial\mathbb{C}'$), by Eq. (129) with Λ replaced by $\mathbb{M}$ and using the triangulations of $\overline{\mathbb{M}}_i^x$, $\overline{\mathbb{M}}_j^y$, $\overline{\mathbb{M}}_k^z$. Clearly, $\overline{\chi}$ and χ can be manipulated by P_v^g for $v\in\Lambda^0(\partial\mathbb{C})$ and $v\in\Lambda^0(\partial\mathbb{C}')$, respectively. Thus they are local degrees of freedom and can be neglected in the discussion of particle types. The reduced Hilbert space, denoted by $\mathcal{H}_*(\overline{\mathbb{M}})$, is spanned by $|s,\mathbb{D}_{\boldsymbol{g}}^{\boldsymbol{s}}\rangle$ with $\boldsymbol{g}\in F(\mathbb{C})$, $s\in G$ and $\boldsymbol{s}\in G^{\mathbb{C}^x}\times G^{\mathbb{C}^y}\times G^{\mathbb{C}^z}$.

As in the twisted quantum double models, we can define states $|s,\mathbb{D}_{\boldsymbol{g}}^{\boldsymbol{s}}\mathbb{D}_{\boldsymbol{h}}^{\boldsymbol{t}}\rangle$ by replacing $\mathbb{D}_{\boldsymbol{g}}^{\boldsymbol{s}}$ by $\mathbb{D}_{\boldsymbol{g}}^{\boldsymbol{s}}\mathbb{D}_{\boldsymbol{h}}^{\boldsymbol{t}}$ in Eqs. (269) and (270). Analogously, we have

$$\left|s,\mathbb{D}_{\boldsymbol{g}}^{\boldsymbol{s}}\mathbb{D}_{\boldsymbol{h}}^{\boldsymbol{t}}\right\rangle = \delta_{\boldsymbol{g},\boldsymbol{h}}\prod_{\mu,n}\omega_{n,g_n^\mu}^\mu\left(s_n^\mu,t_n^\mu\right)\left|s,\mathbb{D}_{\boldsymbol{g}}^{\boldsymbol{s}+\boldsymbol{t}}\right\rangle. \tag{271}$$

This motivates us to consider the algebra

$$\mathcal{D}[\mathbb{C}] := \mathbb{C}G\otimes\mathcal{D}_x[\mathbb{C}]\otimes\mathcal{D}_y[\mathbb{C}]\otimes\mathcal{D}_z[\mathbb{C}] \tag{272}$$

with each factor $\mathcal{D}_\mu[\mathbb{C}]$ and its basis given by

$$\mathcal{D}_\mu[\mathbb{C}] := \bigotimes_{n\in\mathbb{C}^\mu}\mathcal{D}^{\omega_n^\mu}(G),\quad D_{\boldsymbol{g}^\mu}^{\boldsymbol{s}^\mu} := \bigotimes_{n\in\mathbb{C}^\mu} D_{g_n^\mu}^{s_n^\mu}, \tag{273}$$

$\forall\mu=x,y,z$. For short, we write $D_{\boldsymbol{g}}^{\boldsymbol{s}} := D_{\boldsymbol{g}^x}^{\boldsymbol{s}^x}\otimes D_{\boldsymbol{g}^y}^{\boldsymbol{s}^y}\otimes D_{\boldsymbol{g}^z}^{\boldsymbol{s}^z}$, where $\boldsymbol{g}=(\boldsymbol{g}^x,\boldsymbol{g}^y,\boldsymbol{g}^z)$, $\boldsymbol{s}=(\boldsymbol{s}^x,\boldsymbol{s}^y,\boldsymbol{s}^z)\in G^{\mathbb{C}^x}\times G^{\mathbb{C}^y}\times G^{\mathbb{C}^z}$.

In addition, $\forall t\in G$, we have operators

$$P_{z\geqslant k}^t := \prod_{v\in\Lambda^0(\partial\mathbb{C}',k\leqslant z\leqslant z_1)} P_v^t, \tag{274}$$

$$\overline{P}_{z\geqslant k}^t := \prod_{v\in\Lambda^0(\partial\mathbb{C},z\geqslant k)}\left(P_v^t\right)^\dagger, \tag{275}$$

with $\Lambda^0(\partial\mathbb{C},z\geqslant k) := \{(x,y,z)\in\Lambda^0(\partial\mathbb{C})|z\geqslant k\}$ and $\Lambda^0(\partial\mathbb{C}',k\leqslant z\leqslant z_1) := \{(x,y,z)\in\Lambda^0(\partial\mathbb{C}')|k\leqslant z\leqslant z_1\}$. which do not change χ, $\overline{\chi}$. They act on $\mathcal{H}_*(\overline{\mathbb{M}})$ as

$$P_{z\geqslant k}^t\left|s,\mathbb{D}_{\boldsymbol{g}}^{\boldsymbol{s}}\right\rangle = \begin{cases}\left|t+s,\mathbb{D}_{\boldsymbol{g}}^{\boldsymbol{s}}\right\rangle, & k\leqslant z_0,\\ \left|s,\mathbb{D}_{\boldsymbol{g}}^{t^{\delta_k^z}}\mathbb{D}_{\boldsymbol{g}}^{\boldsymbol{s}}\right\rangle, & z_0<k\leqslant z_1,\\ \left|s,\mathbb{D}_{\boldsymbol{g}}^{\boldsymbol{s}}\right\rangle, & k>z_1,\end{cases} \tag{276}$$

$$\overline{P}_{z\geqslant k}^t\left|s,\mathbb{D}_{\boldsymbol{g}}^{\boldsymbol{s}}\right\rangle = \begin{cases}\left|s+t,\mathbb{D}_{\boldsymbol{g}}^{\boldsymbol{s}}\right\rangle, & k\leqslant z_0,\\ \left|s,\mathbb{D}_{\boldsymbol{g}}^{\boldsymbol{s}}\mathbb{D}_{\boldsymbol{g}}^{t^{\delta_k^z}}\right\rangle, & z_0<k\leqslant z_1,\\ \left|s,\mathbb{D}_{\boldsymbol{g}}^{\boldsymbol{s}}\right\rangle, & k>z_1.\end{cases} \tag{277}$$

Similarly, replacing $z\geqslant k$ by $x\geqslant i$ and $y\geqslant j$, we have operators $P_{x\geqslant i}^h$, $P_{y\geqslant j}^h$ supported near $\partial\mathbb{C}'$ and $\overline{P}_{x\geqslant i}^h$, $\overline{P}_{y\geqslant j}^h$ supported near $\partial\mathbb{C}$. Moreover, there is clearly a projector $T_{\boldsymbol{h}}$ (respectively, $\overline{T}_{\boldsymbol{h}}$) supported on $\partial\mathbb{C}'$ (respectively, $\partial\mathbb{C}$) that acts as

$$\overline{T}_{\boldsymbol{h}}\left|s,\mathbb{D}_{\boldsymbol{g}}^{\boldsymbol{s}}\right\rangle = T_{\boldsymbol{h}}\left|s,\mathbb{D}_{\boldsymbol{g}}^{\boldsymbol{s}}\right\rangle = \delta_{\boldsymbol{h},\boldsymbol{g}}\left|s,\mathbb{D}_{\boldsymbol{g}}^{\boldsymbol{s}}\right\rangle. \tag{278}$$

In terms of these operators, we can define a left action π and a right action $\overline{\pi}$ of $\mathcal{D}(\mathbb{C})$ on $\mathcal{H}_0(\overline{\mathbb{M}})$ as

$$\pi\left(s\otimes D_{\boldsymbol{g}}^{\boldsymbol{s}}\right) := T_{\boldsymbol{g}}P_{z\geqslant z_0}^s\prod_{i\in\mathbb{C}^x}P_{x\geqslant i}^{s_i^x}\prod_{j\in\mathbb{C}^y}P_{y\geqslant j}^{s_j^y}\prod_{k\in\mathbb{C}^z}P_{z\geqslant k}^{s_k^z}, \tag{279}$$

$$\overline{\pi}\left(s\otimes D_{\boldsymbol{g}}^{\boldsymbol{s}}\right) := \overline{T}_{\boldsymbol{g}}\overline{P}_{z\geqslant z_0}^s\prod_{i\in\mathbb{C}^x}\overline{P}_{x\geqslant i}^{s_i^x}\prod_{j\in\mathbb{C}^y}\overline{P}_{y\geqslant j}^{s_j^y}\prod_{k\in\mathbb{C}^z}\overline{P}_{z\geqslant k}^{s_k^z}, \tag{280}$$

$\forall s\in G$, $\forall\boldsymbol{s},\boldsymbol{g}\in G^{\mathbb{C}^x}\times G^{\mathbb{C}^y}\times G^{\mathbb{C}^z}$. By construction,

$$\pi\left(s\otimes D_{\boldsymbol{g}}^{\boldsymbol{s}}\right)\left|t,\mathbb{D}_{\boldsymbol{h}}^{\boldsymbol{t}}\right\rangle = \left|s+t,\mathbb{D}_{\boldsymbol{g}}^{\boldsymbol{s}}\mathbb{D}_{\boldsymbol{h}}^{\boldsymbol{t}}\right\rangle, \tag{281}$$

$$\overline{\pi}\left(s\otimes D_{\boldsymbol{g}}^{\boldsymbol{s}}\right)\left|t,\mathbb{D}_{\boldsymbol{h}}^{\boldsymbol{t}}\right\rangle = \left|t+s,\mathbb{D}_{\boldsymbol{h}}^{\boldsymbol{t}}\mathbb{D}_{\boldsymbol{g}}^{\boldsymbol{s}}\right\rangle. \tag{282}$$

Thus $\mathcal{H}_*(\overline{\mathbb{M}})$ is equivalent to $\mathcal{A}[\mathbb{C}]$ as a $\mathcal{D}(\mathbb{C})$-$\mathcal{D}(\mathbb{C})$ bimodule by the obvious map

$$\mathcal{H}_*(\overline{\mathbb{M}})\xrightarrow{\sim}\mathcal{A}[\mathbb{C}]:\ \left|s,\mathbb{D}_{\boldsymbol{g}}^{\boldsymbol{s}}\right\rangle\mapsto s\otimes D_{\boldsymbol{g}}^{\boldsymbol{s}}, \tag{283}$$

where $\mathcal{A}[\mathbb{C}]$ is the subalgebra of $\mathcal{D}[\mathbb{C}]$ spanned by $s\otimes D_{\boldsymbol{g}}^{\boldsymbol{s}}$ with $\boldsymbol{g}$ constrained by Eq. (268), i.e., $\boldsymbol{g}\in F(\mathbb{C})$.

Since both $\mathbb{C}G$ and $\mathcal{D}^{\omega_n^\mu}(G)$ are semisimple,

$$\rho = \bigoplus_{(q,\mathfrak{a}_n^\mu)_{n\in\mathbb{C}^\mu}^{\mu=x,y,z}}\varrho_q\otimes\bigotimes_{\mu,n}\rho_{\mathfrak{a}_n^\mu} \tag{284}$$

gives an isomorphism of algebras

$$\mathcal{D}[\mathbb{C}]\simeq\bigoplus_{(q,\mathfrak{a}_n^\mu)_{n\in\mathbb{C}^\mu}^{\mu=x,y,z}}\mathcal{L}(\mathcal{V}_q)\otimes\bigotimes_{\mu,n}\mathcal{L}\left(\mathcal{V}_{\mathfrak{a}_n^\mu}\right). \tag{285}$$

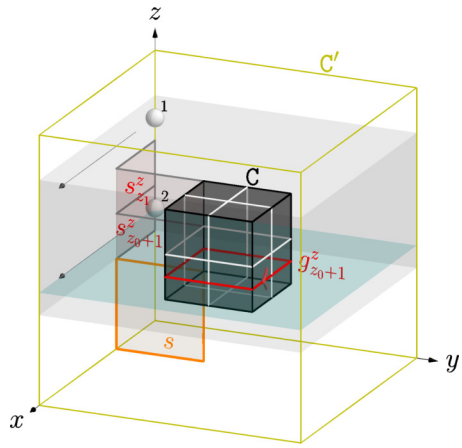

FIG. 19. A z topological charge $\mathfrak{a}^z_k$ of an excited cuboid $\mathtt{C} = [x_0, x_1] \times [y_0, y_1] \times [z_0, z_1]$ can be detected by braiding a pair of quasiparticles along $\partial\mathtt{C}'$ with operator supported near the grey region in $\partial\mathtt{C}'$. Quasiparticle 1 is kept above $z = z_1$ and quasiparticle 2 moves near the plane $z = k$ (cyan).

In detail, the character group $\widehat{G}$ of a group G collects all its one-dimensional representations and $\mathcal{V}_q = (\varrho_q, V_q)$ is a representation corresponding to $q \in \widehat{G}$ acting on Hilbert space V_q. Moreover, $\mathfrak{a}^\mu_n$ labels equivalent classes of irreducible representations of $\mathcal{D}^{\omega^\mu_n}(G)$ and $\mathcal{V}_{\mathfrak{a}^\mu_n} = (\rho_{\mathfrak{a}^\mu_n}, V_{\mathfrak{a}^\mu_n})$ is an explicit representation on a Hilbert space $V_{\mathfrak{a}^\mu_n}$ corresponding to $\mathfrak{a}^\mu_n$. Explicitly, $\mathfrak{a}^\mu_n$ is specified by a pair (g^μ_n, ϱ^μ_n) with $g^\mu_n \in G$ describing the flux and ϱ^μ_n an irreducible ω^μ_{n,g^μ_n} representation (up to isomorphism) of G. Refer to Appendix B 5 for details of these representations.

Denote the set of $\mathfrak{a} = (q, \mathfrak{a}^\mu_n)^{\mu=x,y,z}_{n\in\mathtt{C}^\mu} = (q, g^\mu_n, \varrho^\mu_n)^{\mu=x,y,z}_{n\in\mathtt{C}^\mu}$ with $(g^\mu_n)^{\mu=x,y,z}_{n\in\mathtt{C}^\mu} \in F(\mathtt{C})$ by $\mathfrak{Q}[\mathtt{C}]$. Then the composition

$$\mathcal{H}_*(\overline{\mathtt{M}}) \xrightarrow[\sim]{|s,\mathrm{D}^s_g\rangle \mapsto s\otimes D^s_g} \mathcal{A}[\mathtt{C}] \xrightarrow[\sim]{\tilde{\rho}} \bigoplus_{\mathfrak{a}\in\mathfrak{Q}[\mathtt{C}]} \mathcal{L}(\mathcal{V}_q) \otimes \bigotimes_{\mu,n} \mathcal{L}\big(\mathcal{V}_{\mathfrak{a}^\mu_n}\big)$$
$$= \bigoplus_{\mathfrak{a}\in\mathfrak{Q}[\mathtt{C}]} \mathcal{V}_{\mathfrak{a}} \otimes \mathcal{V}^*_{\mathfrak{a}} \tag{286}$$

is an isomorphism of Hilbert spaces respecting both left and right actions of $\mathcal{D}[\mathtt{C}]$, where

$$\tilde{\rho} := \bigoplus_{\mathfrak{a}\in\mathfrak{Q}[\mathtt{C}]} \frac{1}{\sqrt{|G|}} \varrho_q \otimes \bigotimes_{\mu,n} \sqrt{\frac{\dim_{\mathbb{C}} \mathcal{V}_{\mathfrak{a}^\mu_n}}{|G|}} \rho_{\mathfrak{a}^\mu_n}, \tag{287}$$

$$\mathcal{V}_{\mathfrak{a}} := \mathcal{V}_q \otimes \bigotimes_{\mu,n} \mathcal{V}_{\mathfrak{a}^\mu_n}. \tag{288}$$

The normalization for each sector in $\tilde{\rho}$ is picked such that the inner product structure is respected. Clearly, $\mathfrak{Q}[\mathtt{C}]$ labels particle types of the excited cuboid $\mathtt{C}$ and $\mathcal{V}_{\mathfrak{a}}$ (respectively, $\mathcal{V}^*_{\mathfrak{a}}$) describes the degrees of freedom near $\partial\mathtt{C}'$ (respectively, $\partial\mathtt{C}$). Physically, $\mathfrak{a}^z_k = (g^z_k, \varrho^z_k)$ can be detected by braiding a pair of quasiparticles in the x and y directions via operator supported near grey region in $\partial\mathtt{C}'$ as in Fig. 19. Thus $\mathfrak{a}^z_k$ is called a z topological charge. Actually, q can also be viewed as a z topological charge, since $\mathfrak{a}^z_k$ reduces to $(0, \varrho_q)$ when quasiparticle 2 is lowered below $z = z_0$. Similarly, $\mathfrak{a}^x_i$ (respectively, $\mathfrak{a}^y_j$) can be detected by braiding processes in the y, z (respectively, z, x) directions and is called a x (respectively, y) topological charge. Also, q can be viewed as an x and a y topological charge.

Distinct from conventional topological orders, the number of allowed particle types of a finite excited region $\mathtt{C}$ in a fracton model increases/decreases as the size of $\mathtt{C}$ grows/shrinks. If a quasiparticle can be localized in a smaller cuboid $\mathtt{C}_a = [a^x_0, a^x_1] \times [a^y_0, a^y_1] \times [a^z_0, a^z_1] \subset \mathtt{C}$, then its particle type $\mathfrak{a} = (q, \mathfrak{a}^\mu_n)^{\mu=x,y,z}_{n\in\mathtt{C}^\mu} \in \mathfrak{Q}[\mathtt{C}]$ satisfies

$$\mathfrak{a}^\mu_n = \begin{cases} (0, \varrho_q), & n \leqslant a^\mu_0, \\ \mathfrak{o}, & n > a^\mu_1, \end{cases} \tag{289}$$

$\forall \mu = x, y, z$, where $\mathfrak{o}$ denotes the trivial representation (i.e., the counit) of any $\mathcal{D}^{\omega^\mu_n}(G)$. In other words, $\mathfrak{Q}[\mathtt{C}_a]$ can be viewed as a subset of $\mathfrak{Q}[\mathtt{C}]$; each $\mathcal{V}_{\mathfrak{a}}$ for $\mathfrak{a} \in \mathfrak{Q}[\mathtt{C}_a]$ carries an irreducible representation of $\mathcal{D}[\mathtt{C}]$ for any cuboid $\mathtt{C}$ containing $\mathtt{C}_a$.

B. Fusion of quasiparticles

Suppose that there are two spatially separated excited cuboids $\mathtt{C}_a$ and $\mathtt{C}_b$ containing deep inside a much larger cuboid $\mathtt{C}'$. Let $\mathtt{M} := \mathtt{C}' - \mathtt{C}^\circ_a - \mathtt{C}^\circ_b$. The discussion in the above section can be repeated here for the two-hole manifold $\mathtt{M}$. With the spin configuration on $\partial\mathtt{C}'$ and the local degrees of freedom near $\mathtt{C}_a$ and $\mathtt{C}_b$ fixed, we are left with Hilbert spaces $\mathcal{V}[\mathfrak{a}, \mathfrak{b}]$ labeled by $\mathfrak{a} \in \mathfrak{Q}[\mathtt{C}_a]$ and $\mathfrak{b} \in \mathfrak{Q}[\mathtt{C}_b]$. Using two copies of Eq. (287), we have

$$\mathcal{V}[\mathfrak{a}, \mathfrak{b}] \simeq \mathcal{V}_{\mathfrak{a}} \otimes \mathcal{V}_{\mathfrak{b}}, \tag{290}$$

where $\mathcal{V}_{\mathfrak{a}}$ and $\mathcal{V}_{\mathfrak{b}}$ are defined by Eq. (288).

All these states can be viewed as an excited cuboid $\mathtt{C}$, where $\mathtt{C}$ is cuboid containing both $\mathtt{C}_a$ and $\mathtt{C}_b$ inside $\mathtt{C}'$. With operators supported on $\mathtt{C}$, the Hilbert space $\mathcal{V}_{\mathfrak{a}} \otimes \mathcal{V}_{\mathfrak{b}}$ may be further reduced. To determine the total charge of $\mathtt{C}$, we study the action of $\mathcal{D}[\mathtt{C}]$ on via π defined in Eq. (279). Analogous to Sec. II C 2, it is specified by the coproduct

$$\Delta := \Delta_o \otimes \bigotimes_{\mu=x,y,z} \bigotimes_{n\in\mathtt{C}^\mu} \Delta^\mu_n, \tag{291}$$

where $\Delta_o : \mathbb{C}G \to \mathbb{C}G \otimes \mathbb{C}G$, $g \mapsto g \otimes g$ is the default coproduct of $\mathbb{C}G$. The vector space of intertwiners between the representations $\mathcal{V}_{\mathfrak{c}}$ and $\mathcal{V}_{\mathfrak{a}} \otimes \mathcal{V}_{\mathfrak{b}}$ of $\mathcal{D}(\mathtt{C})$

$$V^{\mathfrak{a}\mathfrak{b}}_{\mathfrak{c}} := \mathrm{Hom}(\mathcal{V}_{\mathfrak{c}}, \mathcal{V}_{\mathfrak{a}} \otimes \mathcal{V}_{\mathfrak{b}}) \tag{292}$$

encodes the ways of fusing $\mathfrak{a}$ and $\mathfrak{b}$ into $\mathfrak{c} \in \mathfrak{Q}[\mathtt{C}]$. In particular, $N^{\mathfrak{c}}_{\mathfrak{a}\mathfrak{b}} := \dim_{\mathbb{C}} V^{\mathfrak{a}\mathfrak{b}}_{\mathfrak{c}}$ is the corresponding fusion rule. It is possible to fuse $\mathfrak{a}$ and $\mathfrak{b}$ into $\mathfrak{c}$ if and only if $N^{\mathfrak{c}}_{\mathfrak{a}\mathfrak{b}} \geqslant 1$. Moreover, $N^{\mathfrak{c}}_{\mathfrak{a}\mathfrak{b}} \geqslant 1$ implies $q_c = q_a + q_b$, where $\mathfrak{a} = (q_a, \mathfrak{a}^\mu_n)^\mu_{n\in\mathtt{C}^\mu_a}$, $\mathfrak{b} = (q_b, \mathfrak{b}^\mu_n)^\mu_{n\in\mathtt{C}^\mu_b}$ and $\mathfrak{c} = (q_c, \mathfrak{c}^\mu_n)^\mu_{n\in\mathtt{C}^\mu}$.

Similarly to the discussion in Sec. II C 2, in order to describe three or more excitations, we need to be careful with their associations.

C. Mobility of quasiparticles

Now let us think about moving a quasiparticle from one cuboid $\mathtt{C}_a = [a^x_0, a^x_1] \times [a^y_0, a^y_1] \times [a^z_0, a^z_1]$ to another $\mathtt{C}_b = [b^x_0, b^x_1] \times [b^y_0, b^y_1] \times [b^z_0, b^z_1]$. The movement can be made by a local operator if and only if the initial and final states have

the same particle type $(q, g_n^\mu, \varrho_n^\mu)_{n\in\mathbb{C}^\mu}^{\mu=x,y,z} \in \mathfrak{Q}(\mathtt{C})$ as an excited cuboid $\mathtt{C}$, where $\mathtt{C}$ is a larger cuboid containing both $\mathtt{C}_a$ and $\mathtt{C}_b$. Because $\mathtt{C}_a \cap \mathtt{C}_b = \emptyset$, we have $[a_0^\mu, a_1^\mu] \cap [b_0^\mu, b_1^\mu] = \emptyset$ for at least one of $\mu = x, y, z$, in which case we say that the quasiparticle is mobile in the μ direction.

For instance, suppose $a_0^z > b_1^z$. Then the position of $\mathtt{C}_a$ implies that $P^t_{z\geqslant a_0^z}$ acts as $\varrho_q(t)$, while the position of $\mathtt{C}_b$ implies that $P^t_{z\geqslant a_0^z}$ acts trivially. Hence $q \in \widehat{G}$ has to be trivial. Obviously, it follows that q is trivial if the excited cuboid $\mathtt{C}$ of type $(q, g_n^\mu, \varrho_n^\mu)_{n\in\mathbb{C}^\mu}^{\mu=x,y,z} \in \mathfrak{Q}[\mathtt{C}]$ is a fusion result of mobile quasiparticles. In fact, it is not hard to see that the converse is true as well. Therefore an excitation is a *fracton* (i.e., a finite excited region that is not a fusion result of mobile quasiparticles) if and only if q is not trivial.

In fact, the mobility of an excited cuboid $\mathtt{C}_a$ in the z direction implies that $\mathfrak{a}_k^z$ is trivial for all $k \in \mathbb{C}^z$ as well. To see this, we notice that the operators $\pi(\mathcal{D}_x[\mathtt{C}_a])$ in Eq. (279) are supported near $\partial\mathtt{C}' \cap \{(x, y, z)|z_0 \leqslant z \leqslant z_1\}$, the excitation can be moved away along the z direction without touching the support region of $\pi(\mathcal{D}_x[\mathtt{C}_a])$ and hence z topological charges $\mathfrak{a}_k^z$ are conserved. Thus if $\mathfrak{a}_k^\mu$ is nontrivial, then it is not possible to move the excitation away along the z direction. In general, all μ topological charges must be trivial in order for a quasiparticle to be mobile in the μ direction. In addition, if a quasiparticle is mobile in two directions, then only topological charges in the third direction can be nontrivial. This is an important result of our work, since it relates the *mobility* of quasiparticles to their *topological charges*.

D. Braiding of mobile quasiparticles

If an excited spot is mobile in the μ direction (respectively, in both the μ and ν directions), we call it a μ-particle (respectively, $\mu\nu$-particle).

1. Braiding of 2d mobile quasiparticles

For braiding of 2d mobile quasiparticles (i.e., excitations mobile in two dimensions), the discussion in Sec. II D can be repeated. For example, the result of the measurement described by Eq. (103) involving an exchange of two identical xy-particles with z topological charges $\{\mathfrak{a}_k^z\}_{k\in\mathbb{C}^z}$ is

$$\prod_{k\in\mathbb{C}^z} \frac{\theta_{\mathfrak{a}_k^z}}{\dim_{\mathbb{C}} \mathcal{V}_{\mathfrak{a}_k^z}} = \prod_{k\in\mathbb{C}^z} \frac{\mathrm{tr}\left(\wp R_k^z, \mathcal{V}_{\mathfrak{a}_k^z} \otimes \mathcal{V}_{\mathfrak{a}_k^z}\right)}{\left(\dim_{\mathbb{C}} \mathcal{V}_{\mathfrak{a}_k^z}\right)^2}, \tag{293}$$

where R_k^z is the universal R matrix for $\mathcal{D}^{\omega_k^z}(G)$ and $\theta_{\mathfrak{a}_k^z}$ is the topological spin associated with the representation $\mathcal{V}_{\mathfrak{a}_k^z}$ defined in Eq. (B64). The quantum dimension and topological spin of the xy-particle are

$$d_{\mathfrak{a}}^z = \prod_{k\in\mathbb{C}^z} \dim_{\mathbb{C}} \mathcal{V}_{\mathfrak{a}_k^z}, \tag{294}$$

$$\theta_{\mathfrak{a}}^z = \prod_{k\in\mathbb{C}^z} \theta_{\mathfrak{a}_k^z} = \prod_{k\in\mathbb{C}^z} \frac{\mathrm{tr}\left(\wp R_k^z, \mathcal{V}_{\mathfrak{a}_k^z} \otimes \mathcal{V}_{\mathfrak{a}_k^z}\right)}{\dim_{\mathbb{C}} \mathcal{V}_{\mathfrak{a}_k^z}}. \tag{295}$$

The results for yz-particles and zx-particles are analogous.

In general, the topological charges of a quasiparticle can be detected by braiding 2d particles around it. We may measure the quantum dimension $d_{\mathfrak{a}_n^\mu}$ associated with each μ topological charge $\mathfrak{a}_n^\mu$ through Eq. (89). Further, this leads to a notion of quantum dimension of any particle type $\mathfrak{a} = (q, \mathfrak{a}_n^\mu) = (q, g_n^\mu, \varrho_n^\mu)$, defined by

$$d_{\mathfrak{a}} := \prod_{\mu,n} d_{\mathfrak{a}_n^\mu}. \tag{296}$$

For twisted fracton models based on an Abelian group, the quantum dimension of $\mathfrak{a}_n^\mu = (g_n^\mu, \varrho_n^\mu)$ equals the degree (i.e., the dimension) of the representation ϱ_n^μ.

Crucially, the quantum dimension of fracton $(q, \mathfrak{o})$ (i.e., with $\mathfrak{a}_n^\mu = \mathfrak{o}, \forall n \in \mathbb{C}^\mu, \forall \mu = x, y, z$ but $q \neq 0$) is one, where $\mathfrak{o}$ denote trivial topological charge and 0 the identity element of the character group $\widehat{G} \simeq G$. Thus every fracton $(q, \mathfrak{a}_n^\mu)_{n\in\mathbb{C}^\mu}^\mu$ is a fusion result of a fracton with quantum dimension 1 and some mobile particles; explicitly, $(q, \mathfrak{a}_n^\mu)_{n\in\mathbb{C}^\mu}^\mu = (q, \mathfrak{o}) \times \prod_{\mu,n}(0, \mathfrak{a}_n^\mu)$. Therefore there is no inextricably non-Abelian fracton in any twisted X-cube model.

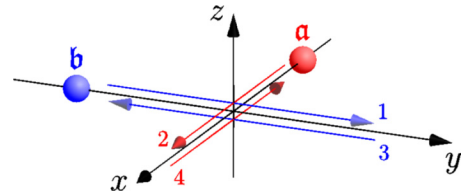

FIG. 20. Arrows 1,3 (respectively, 2,4) indicate that the movements of quasiparticle $\mathfrak{b}$ (respectively, $\mathfrak{a}$) made by operators $\mathcal{O}_y^\mathfrak{b}$, $(\mathcal{O}_y^\mathfrak{b})^\dagger$ [respectively, $\mathcal{O}_x^\mathfrak{a}$, $(\mathcal{O}_x^\mathfrak{a})^\dagger$] supported near the y (respectively, x) axis. A full braiding of the z topological charges can be realized by $(\mathcal{O}_x^\mathfrak{a})^\dagger(\mathcal{O}_y^\mathfrak{b})^\dagger\mathcal{O}_x^\mathfrak{a}\mathcal{O}_y^\mathfrak{b}$.

2. Full braiding of 1d mobile quasiparticles

Given two quasiparticles of types $\mathfrak{a}$ and $\mathfrak{b}$ mobile along two different directions (e.g., the x and y directions) respectively, a full braiding of them can be easily made, as depicted in Fig. 20. Let $\mathcal{O}_x^\mathfrak{a}$ be an operator supported near the x axis that moves the x-particle in the way indicated by arrow 1 pointing towards the positive x direction. This operator is normalized such that $(\mathcal{O}_x^\mathfrak{a})^\dagger\mathcal{O}_x^\mathfrak{a} = 1$ on the x-particle. Similarly, we have operators $\mathcal{O}_y^\mathfrak{b}$ and $(\mathcal{O}_y^\mathfrak{b})^\dagger$ supported near the y axis that move the y-particle forth and back as indicated by arrows 1,3 in Fig. 20; they are normalized by $(\mathcal{O}_y^\mathfrak{b})^\dagger\mathcal{O}_y^\mathfrak{b} = 1$ on the initial state of the y-particle. Then $(\mathcal{O}_x^\mathfrak{a})^\dagger(\mathcal{O}_y^\mathfrak{b})^\dagger\mathcal{O}_x^\mathfrak{a}\mathcal{O}_y^\mathfrak{b}$ describes a full braiding of the z topological charges of $\mathfrak{a}$ and $\mathfrak{b}$. If the two quasiparticles carry z topological charges $\mathfrak{a}_k^z$, $\mathfrak{b}_k^z$ separately and a definite total z topological charge $\mathfrak{c}_k^z$ together, then the full braiding acts as a scalar

$$\left(\mathcal{O}_x^\mathfrak{a}\right)^\dagger\left(\mathcal{O}_y^\mathfrak{b}\right)^\dagger\mathcal{O}_x^\mathfrak{a}\mathcal{O}_y^\mathfrak{b} = \prod_k \frac{\theta_{\mathfrak{c}_k^z}}{\theta_{\mathfrak{a}_k^z}\theta_{\mathfrak{b}_k^z}}, \tag{297}$$

where $\theta_{\mathfrak{a}_k^z}$, $\theta_{\mathfrak{b}_k^z}$, and $\theta_{\mathfrak{c}_k^z}$ are the topological spins associated with the representation $\mathcal{V}_{\mathfrak{a}_k^z}$, $\mathcal{V}_{\mathfrak{b}_k^z}$, and $\mathcal{V}_{\mathfrak{c}_k^z}$, respectively, defined in Eq. (B64).

Similarly, we can make the S-matrix measurements. For example, $\mathsf{S}_{\mathfrak{a}\mathfrak{b}}^z$ is the expectation value (on the vacuum) of the process shown in Fig. 21, in the normalization that $\mathcal{O}^\dagger\mathcal{O} = 1$

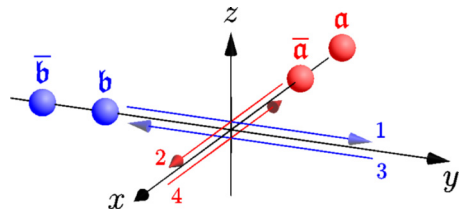

FIG. 21. An S-matrix measurement $\mathsf{S}^z_{\mathfrak{a}\mathfrak{b}}$ is associated with the process made of three steps: (1) creating a pair of x-particles $\mathfrak{a}, \bar{\mathfrak{a}}$ and a pair of y-particles $\mathfrak{b}, \bar{\mathfrak{b}}$ from vacuum; (2) a full braiding of $\bar{\mathfrak{a}}$ and $\mathfrak{b}$, i.e., moving them according to arrows 1,2,3,4 in order; (3) annihilating the pairs $\mathfrak{a}, \bar{\mathfrak{a}}$ and $\mathfrak{b}, \bar{\mathfrak{b}}$ back to vacuum.

for any step $\mathcal{O}$ on its initial state. The result is

$$\mathsf{S}^z_{\mathfrak{a}\mathfrak{b}} = \prod_k \mathsf{S}_{\mathfrak{a}^z_k \mathfrak{b}^z_k}, \tag{298}$$

where $\mathsf{S}_{\mathfrak{a}^z_k \mathfrak{b}^z_k}$ can be computed by Eq. (109) on representations $\mathcal{V}_{\mathfrak{a}^z_k}$ and $\mathcal{V}_{\mathfrak{b}^z_k}$ of $\mathcal{D}^{\omega^z_k}(G)$. Analogously, we have $\mathsf{S}^x_{\mathfrak{a}\mathfrak{b}}$ (respectively, $\mathsf{S}^y_{\mathfrak{a}\mathfrak{b}}$) for braidings in the yz directions (respectively, zx directions).

3. Half braiding of 1d mobile quasiparticles

It is also possible to make a half braiding in order to exchange two 1d mobile particles. For example, two y-particles, both of type $\mathfrak{a}$, can be braided by $\mathcal{U}^{\mathfrak{a}}_3 \mathcal{O}^{\mathfrak{a}}_2 \mathcal{U}^{\mathfrak{a}}_1$ as illustrated in Fig. 22. Naturally, we require $\mathcal{U}^{\mathfrak{a}}_3 \mathcal{U}^{\mathfrak{a}}_1 \mathcal{O}^{\mathfrak{a}}_2 = 1$ on a single y-particle of type $\mathfrak{a}$ on the left. All fracton models considered in this paper allow splitting a 1d mobile quasiparticle into two 1d mobile quasiparticles in the other two directions (e.g., a particle mobile along the x direction can split into one mobile along y and another mobile along z). Thus we can make a topological spin measurement described by the expression on the right-hand side of Eq. (103). The result for the situation shown in Fig. 22 is $\frac{\theta^x_{\mathfrak{a}}}{d^x_{\mathfrak{a}}} \cdot \frac{\theta^z_{\mathfrak{a}}}{d^z_{\mathfrak{a}}}$, where $d^z_{\mathfrak{a}}$, $\theta^z_{\mathfrak{a}}$, $d^x_{\mathfrak{a}}$, and $\theta^x_{\mathfrak{a}}$ are computed by Eqs. (294) and (295) and their analogues. In particular, the quantum dimension of a y-particle is $d^x_{\mathfrak{a}} d^z_{\mathfrak{a}}$, which can also be simply defined in the same way as in Eq. (89).

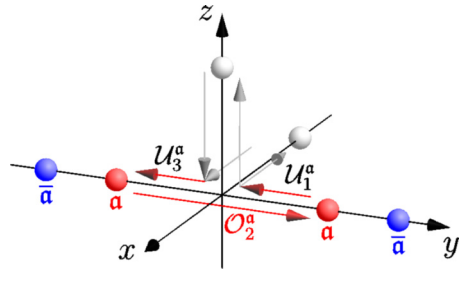

FIG. 22. Two y-particles both of type $\mathfrak{a}$ are braided by $\mathcal{U}^{\mathfrak{a}}_3 \mathcal{O}^{\mathfrak{a}}_2 \mathcal{U}^{\mathfrak{a}}_1$, where $\mathcal{U}^{\mathfrak{a}}_1$ splits the y-particle of type $\mathfrak{a}$ on the right into an x-particle and a z-particle, $\mathcal{U}^{\mathfrak{a}}_3$ fuses the x-particle and the z-particle into the y-particle of type $\mathfrak{a}$ on the left and $\mathcal{O}^{\mathfrak{a}}_2$ is hopping operator for the y-particle of type $\mathfrak{a}$. In addition, $\mathcal{U}^{\mathfrak{a}}_1$, $\mathcal{U}^{\mathfrak{a}}_3$ and $\mathcal{O}^{\mathfrak{a}}_2$ are supported near the corresponding arrows, respectively.

E. Examples

For concreteness, we now consider examples of twisted X-cube models which host quasiparticles exhibiting novel and interesting behaviors. In particular, we will study models wherein the one-dimensional particles carry either semionic or non-Abelian statistics. But there is no inextricably non-Abelian fracton in these models; each fracton can split into a fracton of quantum dimension one and several mobile particles.

1. $G = \mathbb{Z}_2$: 1d mobile semions

Let us start with the simplest nontrivial group $G = \mathbb{Z}_2 = \{0, 1\}$. It is well-known [20] that $H^3(\mathbb{Z}_2, \mathrm{U}(1)) = \mathbb{Z}_2$ and its nontrivial element is presented by the 3-cocyle

$$\omega(f, g, h) = \begin{cases} -1, & f = g = h = 1, \\ 1, & \text{otherwise.} \end{cases} \tag{299}$$

The group structure of $H^3(\mathbb{Z}_2, \mathrm{U}(1))$ is given by $[\omega] + [\omega] = [\omega^2] = 0$, where $[\omega]$ and $[\omega^2]$ denotes the elements of the cohomology group presented by ω and $\omega^2(f, g, h) := (\omega(f, g, h))^2$ respectively. Obviously, $\omega^2 \equiv 1$ presents the identity element 0 of $H^3(\mathbb{Z}_2, \mathrm{U}(1))$.

Along each cross section Σ^μ_n of the lattice Λ, the model can be either untwisted or twisted. The pure charges (i.e., the flux is trivial everywhere) behave in the same way, no matter whether the model is twisted or not. Thus we are more interested in excitations that violate $B_c = 1$ below.

To compare the untwisted case (i.e., the original X-cube model [61]) with the fully twisted case, we may consider the braiding of an x-particle of type $\mathfrak{a}$ and a y-particle of type $\mathfrak{b}$. In either case, we can identify their z topological charges by requiring that they fuse into a z-particle. In other words, $\mathfrak{a}^z_k \times \mathfrak{b}^z_k = \mathfrak{o}$ implies that $\mathfrak{a}^z_k = \mathfrak{b}^z_k$, where $\mathfrak{o}$ denote the trivial topological charge. Then we may braid them as in Fig. 21 and use this as a diagnostic of the effect of twisting on $\mathsf{S}^z_{\mathfrak{a}\mathfrak{b}}$. When $\mathfrak{a}^z_k \times \mathfrak{b}^z_k = \mathfrak{o}$,

$$\mathsf{S}_{\mathfrak{a}^z_k \mathfrak{b}^z_k} = \frac{\theta_{\mathfrak{o}}}{\theta_{\mathfrak{a}^z_k} \theta_{\mathfrak{b}^z_k}} = \theta^{-2}_{\mathfrak{a}^z_k}. \tag{300}$$

In the untwisted case, $\theta^{-2}_{\mathfrak{a}^z_k}$ is always 1 and hence $\mathsf{S}^z_{\mathfrak{a}\mathfrak{b}} = 1$ if $\mathfrak{a}^z_k \times \mathfrak{b}^z_k = \mathfrak{o}, \forall k$.

In the twisted case, $\theta_{\mathfrak{a}^z_k}$ may be $\pm i$. Explicitly, in the notation used in Appendix B 7 b, $\theta_{(1,0)} = i$ and $\theta_{(1,1)} = -i$. Further, we may imagine an x-particle of type $\mathfrak{a}$ centered at $(x + \frac{1}{2}, \frac{1}{2}, \frac{1}{2})$ whose only nontrivial topological charges are $\mathfrak{a}^z_1 = \mathfrak{a}^y_1 = (1, 0)$ and a y-particle of type $\mathfrak{b}$ at $(\frac{1}{2}, y + \frac{1}{2}, \frac{1}{2})$ whose only nontrivial topological charges are $\mathfrak{b}^z_1 = \mathfrak{b}^x_1 = (1, 0)$. The braiding is made on the plane $z = \frac{1}{2}$. Then we have $\mathsf{S}^z_{\mathfrak{a}\mathfrak{b}} = -1$ even when $\mathfrak{a}^z_k \times \mathfrak{b}^z_k = \mathfrak{o}$, $\forall k$. This behavior demonstrates the effect of twisting along the plane $z = \frac{1}{2}$, thereby revealing the existence of excitations with semionic mutual statistics, which are restricted to move along one-dimensional submanifolds.

We note that this twisted X-cube model, based on $G = \mathbb{Z}_2$, can also be realized by coupling interpenetrating layers of doubled semion string-net models [70].

2. $G = \mathbb{Z}_2 \times \mathbb{Z}_2 \times \mathbb{Z}_2$: non-Abelian 1d mobile quasiparticles

An example of a twisted X-cube model with non-Abelian one-dimensional particles can be constructed based on the group $G = \mathbb{Z}_2 \times \mathbb{Z}_2 \times \mathbb{Z}_2$ with the 3-cocycle

$$\omega(f, g, h) = e^{i\pi(f^{(1)}g^{(2)}h^{(3)})}, \tag{301}$$

where $f = (f^{(1)}, f^{(2)}, f^{(3)}), g = (g^{(1)}, g^{(2)}, g^{(3)}), h = (h^{(1)}, h^{(2)}, h^{(3)}) \in G$. We also write the elements of G simply as 000, 100, 110 and so on for short. As examples, we have $\omega(100, 010, 001) = -1$ and $\omega(100, 001, 010) = 1$ in these notations.

Clearly, we may have an x-particle whose nontrivial fluxes are $g_1^y = g_1^z = 100$. It cannot be a 2d mobile particle or a fusion result of 2d mobile particles, because the fluxes of any 2d mobile particle satisfy the constraint

$$\sum_i g_i^x = \sum_j g_j^y = \sum_k g_k^z = 0, \tag{302}$$

which easily follows from Eq. (268). Thus it is *intrinsically* 1d mobile in the terminology introduced in Sec. I A. Further, if either Σ_1^y or Σ_1^z is twisted by the 3-cocycle in Eq. (301), then either ϱ_1^y or ϱ_1^z has to be two-dimensional, as shown in Table I. Thus this x-particle has quantum dimension greater than 1, clearly reflecting its non-Abelian character. The braiding properties of such non-Abelian 1d particles can be computed following the methods described in Sec. VI D. Details of a similar calculation will be given later for the twisted checkerboard based on the same group and the same 3-cocycle.

However, this x-particle is still *not inextricably non-Abelian* if the model is only *partially* twisted. Suppose that the non-Abelian behavior comes from the twisting of Σ_1^z and that there is a nearby parallel plane, say Σ_2^z, which remains untwisted. Then the x-particle can be split into an Abelian x-particle with fluxes $g_1^y = g_2^z = 100$ and a non-Abelian xy-particle with fluxes $g_1^z = g_2^z = 100$, implying that it is not inextricably non-Abelian according to the definition in Sec. I A. Contrarily, if the model is fully twisted in at least one direction, then such a splitting is no longer possible and hence the x-particle becomes inextricably non-Abelian. In this case, we call the corresponding fracton phase *non-Abelian*; it is clearly distinct from an Abelian fracton phase with some layers of conventional non-Abelian topological states inserted. This dramatic change between the fully and partially twisted cases is also reflected in their GSD on $\mathtt{T}^3$, which is explicitly given by Eqs. (199), (209), and (210) for three fully twisted cases and Eq. (196) for any partially twisted case. In particular, Eq. (199) is larger than Eq. (196) with $|X| = |Y| = 0$ and $|Z| = L_z$; thus, fully twisted case looks more entangled than partially twisted cases, wherein twisted layers are less entangled due to the separation by untwisted layers. Therefore both the presence of inextricably non-Abelian 1d mobile quasiparticles and their exotic GSD establishes that these non-Abelian fracton phases are a completely new type of quantum states.

Moreover, we emphasize that *no* twisted X-cube model, defined in Sec. III A, hosts inextricably non-Abelian fractons. To see this, we notice that a quasiparticle $(q, \mathfrak{a}_n^\mu)$ is a fracton if and only if $q \neq 0$. However, such excitations can always be viewed as a fusion result of a fracton $(q, \mathfrak{o})$ of quantum dimension 1—thus, an Abelian fracton—and some mobile quasiparticles. In other words, there is no inextricably non-Abelian fracton in twisted X-cube models. Thus in order to find a model with inextricably non-Abelian fractons, we look to the twisted checkerboard models next.

VII. QUASIPARTICLES IN TWISTED CHECKERBOARD MODELS

We now study quasiparticles in the twisted checkerboard models, proceeding analogously to the previous section. Here, the particle types can also be labeled by their x, y, and z topological charges, subject to certain constraints. After systematically analyzing the mobility, fusion and braiding of quasiparticles in terms of their topological charges, we will then study specific examples to elucidate the plethora of novel phenomena which may occur in the twisted checkerboard models.

A. Particle type and topological charges

Any excited spot (i.e., quasiparticle) can be enclosed in a finite cuboid $\mathtt{C} = [x_0, x_1] \times [y_0, y_1] \times [z_0, z_1]$. Let $\mathtt{C}' = [x_0', x_1'] \times [y_0', y_1'] \times [z_0', z_1']$ be a much larger cuboid containing $\mathtt{C}$. Without loss of generality, $x_0, x_1, y_0, y_1, z_0, z_1, x_0', x_1', y_0', y_1', z_0', z_1'$ are picked to be even integers. In the following, we use Fig. 23(a) for illustration, where $\mathtt{C} = [4, 6] \times [4, 6] \times [4, 6]$, $\mathtt{C}' = [0, 10] \times [0, 10] \times [0, 10]$ and the coordinates are chosen such that the grey unit cubes are centered at $(x, y, z) + \frac{1}{2}(1, 1, 1)$ with $x, y, z \in \mathbb{Z}$ and $x + y + z$ even.

For convenience, we write $\mathtt{C}^x := \{x_0, x_0 + 1, \ldots, x_1\}$, $\mathtt{C}^y := \{y_0, y_0 + 1, \ldots, y_1\}$ and $\mathtt{C}^z := \{z_0, z_0 + 1, \ldots, z_1\}$. Let $\mathtt{M} = \mathtt{C}' - \mathtt{C}^\circ$, where $\mathtt{X}^\circ$ denotes the interior of any topological space $\mathtt{X}$. Then $\mathtt{M}$ is a three-dimensional manifold with boundary. Let $\mathcal{H}(\Lambda^0(\mathtt{M}), G)$ be the Hilbert space describing all the physical degrees of freedom on $\mathtt{M}$ and $G_B^{\Lambda^0(\mathtt{M})} := \{\vartheta \in G^{V(\mathtt{M})} | B_c|\vartheta\rangle = |\vartheta\rangle, \forall c \in \Lambda_\bullet^3(\mathtt{M})\}$. To classify excitations inside $\mathtt{C}$, we analyze the subspace $\mathcal{H}_0(\mathtt{M})$ selected out of $\mathcal{H}(\Lambda^0(\mathtt{M}), G)$ by the projector

$$P(\mathtt{M}) := \prod_{c \in \Lambda_\bullet^3(\mathtt{M}^\circ)} P_c, \tag{303}$$

where c labels grey cubes in the interior of $\mathtt{M}$.

The Hilbert space $\mathcal{H}(\Lambda^0(\mathtt{M}), G)$ has an orthonormal basis $\{|\vartheta\rangle | \vartheta \in G^{\Lambda^0(\mathtt{M})}\}$, where $\Lambda^0(\mathtt{M})$ is the set of vertices in $\mathtt{M}$ and $G^{\Lambda^0(\mathtt{M})}$ is the set of functions from $\Lambda^0(\mathtt{M})$ to G. Let $\mathtt{M}_i^x$, $\mathtt{M}_j^y$, and $\mathtt{M}_k^z$ be the intersection of $\mathtt{M}$ with the plane

$$x = i - \tfrac{1}{2}, \ \forall i = x_0' + 1, x_0' + 2, \ldots, x_1'; \tag{304}$$

$$y = j - \tfrac{1}{2}, \ \forall j = y_0' + 1, y_0' + 2, \ldots, y_1'; \tag{305}$$

$$z = k - \tfrac{1}{2}, \ \forall k = z_0' + 1, z_0' + 2, \ldots, z_1'; \tag{306}$$

(i.e., the region of Σ_i^x, Σ_j^y, and Σ_k^z inside $\mathtt{M}$), respectively. Each of them is either a disk or an annulus as a topological space and a region of two-dimensional checkerboard. Respectively, we can embed it into either a triangulated sphere or a

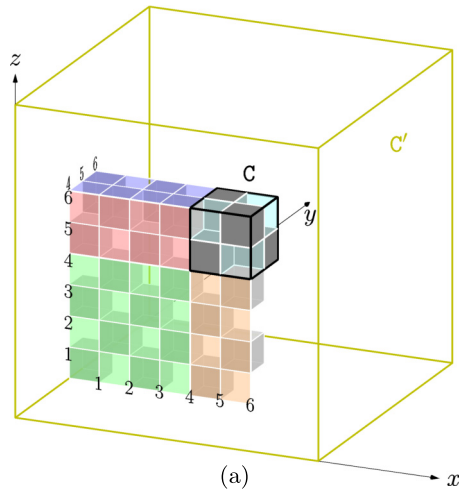

(a)

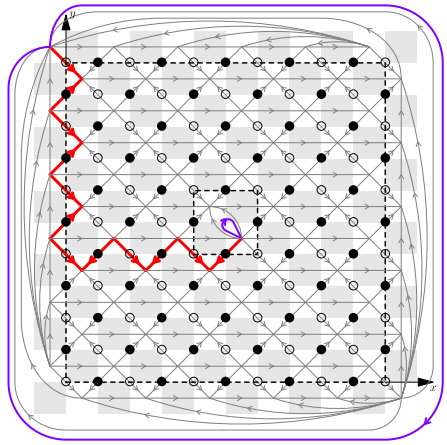

(b) $\overline{\mathtt{M}}_k^z$ with $k = 5$

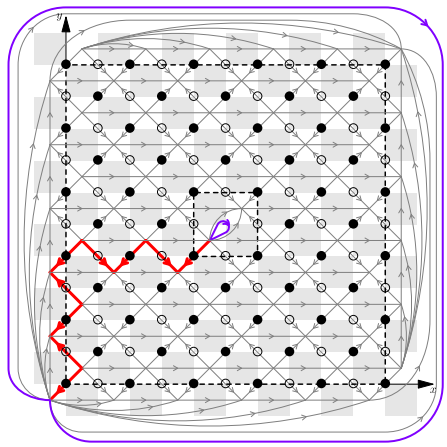

(c) $\overline{\mathtt{M}}_k^z$ with $k = 6$

FIG. 23. (a) An excited cuboid $\mathtt{C} = [4, 6] \times [4, 6] \times [4, 6]$ isolated from other excitations outside $\mathtt{C}'$ in a checkerboard model. The membranes (orange, blue, green and red) between $\partial\mathtt{C}$ and $\partial\mathtt{C}'$ indicates the bulk degrees of freedom used for defining s_i^x, s_j^y, and s_k^z in the main text. [(b) and (c)] A triangulation of cross section $\overline{\mathtt{M}}_k^z$. Some edges are thickened to highlight the outer and inner boundaries (purple) of $\overline{\mathtt{M}}_k^z$ and a path (red) in between.

triangulated annulus with two loops as boundary, denoted $\overline{\mathtt{M}}_n^\mu$ for $\mu = x,\ y,\ z$. Let $\Delta^m(\overline{\mathtt{M}}_n^\mu)$ be the set of m-simplices in this triangulation.

Examples of $\overline{\mathtt{M}}_k^z$ are given in Figs. 23(b) and 23(c). Marks • and ○ are added to show the positions of vertices of $\mathtt{M}$ on the plane $z = k$ and the value of $(-1)^v$ on these vertices. Let $E(\overline{\mathtt{M}}_k^z)$ be the subset of $\Delta^1(\overline{\mathtt{M}}_k^z)$ containing the edges with a • or ○ mark; it has a one-to-one correspondence with $\Lambda^1[\mathtt{M}_k^z]$ (i.e., the set of edges of $\mathtt{M}$ intersecting with the plane $z = k - \frac{1}{2}$). Given $\vartheta \in G_B^{\Lambda^0(\mathtt{M})}$, we color $\Lambda^1[\mathtt{M}_k^z]$ and hence $E(\mathtt{M}_k^z)$ by $\partial\vartheta$ as in Eq. (147), which extends uniquely to a coloring of $\overline{\mathtt{M}}_k^z$. The triangulation and coloring for $\overline{\mathtt{M}}_i^x$ and $\overline{\mathtt{M}}_j^y$ are obtained analogously. After picking $\overline{\mathtt{M}}_i^x$ (respectively, $\overline{\mathtt{M}}_j^y$, $\overline{\mathtt{M}}_k^z$) for each cross section $\mathtt{M}_i^x$ (respectively, $\mathtt{M}_j^y$, $\mathtt{M}_k^z$), we can define P_c^g for c touching $\partial\mathtt{M}$.

To give a basis of $\mathcal{H}_0(\mathtt{M})$, we pick paths (going inwards) connecting base points of the outer and inner boundaries of each annulus $\overline{\mathtt{M}}_i^x$, $\overline{\mathtt{M}}_j^y$, and $\overline{\mathtt{M}}_k^z$. Let s_i^x for $x_0 < i \leqslant x_1$, s_j^y for $y_0 < j \leqslant y_1$ and s_k^z for $z_0 < i \leqslant z_1$ be the group elements associated with these paths. Examples of such paths are shown by the zigzag sequences of thick (red online) edges in Figs. 23(b) and 23(c); correspondingly,

$$s_k^z = \sum_{(x,y)\in\text{path}} (-1)^{(x,y,k)} \vartheta_k^z(x, y) \tag{307}$$

$$= \sum_{(x,y)\in\text{path}} (-1)^{(x,y,k)} [\vartheta(x, y, k) - \vartheta(x, y, k-1)], \tag{308}$$

where $(x, y) \in \mathbb{Z} \times \mathbb{Z}$ labels vertices of $\mathtt{M}_k^z$.

In Fig. 23(a), a choice of such paths for all annuli $\overline{\mathtt{M}}_i^x$ (respectively, $\overline{\mathtt{M}}_j^y$, $\overline{\mathtt{M}}_k^z$) is illustrated as a rectangular ribbon, colored orange (respectively, blue, red) online, connecting $\partial\mathtt{C}$ and $\partial\mathtt{C}'$. The ribbon shows the positions of spins (inside $\mathtt{M}^\circ$) in terms of which s_i^x (respectively, s_j^y, s_k^z) can be expressed; for cleanness, we do not draw the part of these paths on $\partial\mathtt{M}$. In addition, we need

$$s_{x_0}^x = \sum_{x_0'<i\leqslant x_0} \sum_{z_0'<k<z_0} (-1)^{(i,y_0,k)} \vartheta(i, y_0, k), \tag{309}$$

$$s_{y_0}^y = -\sum_{x_0'<i<x_0} \sum_{z_0'<k<z_0} (-1)^{(i,y_0,k)} \vartheta(i, y_0, k), \tag{310}$$

$$s_{z_0}^z = \sum_{x_0'<i<x_0} \sum_{z_0'<k\leqslant z_0} (-1)^{(i,y_0,k)} \vartheta(i, y_0, k), \tag{311}$$

in terms of spins on the square (green online) sheet in Fig. 23(a). Collectively, we write

$$\boldsymbol{s} := (\boldsymbol{s}^x, \boldsymbol{s}^y, \boldsymbol{s}^z) \in G^{\mathtt{C}^x} \times G^{\mathtt{C}^y} \times G^{\mathtt{C}^z}, \tag{312}$$

$$\boldsymbol{s}^x := \left(s_{x_0}^x, s_{x_0+1}^x, \ldots, s_{x_1}^x\right) \in G^{\mathtt{C}^x}, \tag{313}$$

$$\boldsymbol{s}^y := \left(s_{y_0}^y, s_{y_0+1}^y, \ldots, s_{y_1}^y\right) \in G^{\mathtt{C}^y}, \tag{314}$$

$$\boldsymbol{s}^z := \left(s_{z_0}^z, s_{z_0+1}^z, \ldots, s_{z_1}^z\right) \in G^{\mathtt{C}^z}. \tag{315}$$

Moreover, we need to label fluxes as well. Let g_i^x (respectively, g_j^y, g_k^z) be the group element associated with either the inner or the outer boundary of $\overline{\mathtt{M}}_i^x$ (respectively, $\overline{\mathtt{M}}_j^y$, $\overline{\mathtt{M}}_k^z$). By assumption, $B_c = 1$ for c outside $\mathtt{C} = [x_0, x_1] \times [y_0, y_1] \times$

$[z_0, z_1]$, so we write $g_i^x = 0$ (respectively, $g_j^y = 0$, $g_k^z = 0$) unless $x_0 < i \leqslant x_1$ (respectively, $y_0 < j \leqslant y_1$, $z_0 < k \leqslant z_1$). The data needed for describing fluxes are collected as

$$\boldsymbol{g} := \left(\boldsymbol{g}^x, \boldsymbol{g}^y, \boldsymbol{g}^z\right) \in G^{\mathbb{C}^x} \times G^{\mathbb{C}^y} \times G^{\mathbb{C}^z}, \tag{316}$$

$$\boldsymbol{g}^x := \left(0, g^x_{x_0+1}, \ldots, g^x_{x_1}\right) \in G^{\mathbb{C}^x}, \tag{317}$$

$$\boldsymbol{g}^y := \left(0, g^y_{y_0+1}, \ldots, g^y_{y_1}\right) \in G^{\mathbb{C}^y}, \tag{318}$$

$$\boldsymbol{g}^z := \left(0, g^z_{z_0+1}, \ldots, g^z_{z_1}\right) \in G^{\mathbb{C}^z}. \tag{319}$$

Not all of them are independent; they are subject to the constraints

$$\sum_{k \text{ even}} g_k^z = \sum_{i \text{ odd}} g_i^x - \sum_{j \text{ odd}} g_j^y, \tag{320}$$

$$\sum_{i \text{ even}} g_i^x = \sum_{j \text{ odd}} g_j^y - \sum_{k \text{ odd}} g_k^z, \tag{321}$$

$$\sum_{j \text{ even}} g_j^y = \sum_{k \text{ odd}} g_k^z - \sum_{i \text{ odd}} g_i^x. \tag{322}$$

Let $F[\mathtt{C}]$ be the set of $\boldsymbol{g}$ in the form of Eqs. (316)–(319) satisfying Eqs. (320)–(322). As a group, $F(\mathtt{C})$ is isomorphic to $G^{x_1-x_0+y_1-y_0+z_1-z_0-3}$.

Let $G_B^{\Lambda^0(\mathtt{M})}(\boldsymbol{s}, \chi, \overline{\chi})$ be the set of $\vartheta \in G_B^{\Lambda^0(\mathtt{M})}$ compatible with $\boldsymbol{s}$ and coinciding with $\chi \in G^{\Lambda^0(\partial\mathtt{C}')}$ and $\overline{\chi} \in G^{\Lambda^0(\partial\mathtt{C})}$ on $\partial\mathtt{M} = \partial\mathtt{C} \cup \partial\mathtt{C}'$. Now we have enough notations to give the basis vectors of $\mathcal{H}_0(\mathtt{M})$; they are defined by

$$\left|\chi, \overline{\chi}; \mathtt{D}_{\boldsymbol{g}}^{\boldsymbol{s}}\right\rangle := \sum_{\vartheta \in G_B^{\Lambda^0(\mathtt{M})}(\boldsymbol{s}, \chi, \overline{\chi})} Z\left(\vartheta; \mathtt{D}_{\boldsymbol{g}}^{\boldsymbol{s}}\right)|\vartheta\rangle \tag{323}$$

with $\boldsymbol{s} \in G^{\mathbb{C}^x} \times G^{\mathbb{C}^y} \times G^{\mathbb{C}^z}$, $\boldsymbol{g} \in F(\mathtt{C})$, $\chi \in G^{\Lambda^0(\partial\mathtt{C}')}$, and $\overline{\chi} \in G^{\Lambda^0(\partial\mathtt{C})}$. To complete the definition, the phase factor $Z(\vartheta; \mathtt{D}_{\boldsymbol{g}}^{\boldsymbol{s}})$ is given by

$$Z\left(\vartheta; \mathtt{D}_{\boldsymbol{g}}^{\boldsymbol{s}}\right) := \prod_{i=x_0'+1}^{x_1'} Z_i^x\left(\vartheta; \mathtt{D}_{\boldsymbol{g}}^{\boldsymbol{s}}\right) \cdot \prod_{j=y_0'+1}^{y_1'} Z_j^y\left(\vartheta; \mathtt{D}_{\boldsymbol{g}}^{\boldsymbol{s}}\right) \cdot \prod_{k=z_0'+1}^{z_1'} Z_k^z\left(\vartheta; \mathtt{D}_{\boldsymbol{g}}^{\boldsymbol{s}}\right), \tag{324}$$

where $Z_i^x(\vartheta; \mathtt{D}_{\boldsymbol{g}}^{\boldsymbol{s}})$ is the Dijkgraaf-Witten partition function of a ball with surface colored by ϑ_i^x if $\overline{\mathtt{M}}_i^x$ is a sphere or a solid torus with surface colored by $(\vartheta_i^x; \mathtt{D}_{g_i^x}^{s_i^x})$ if $\overline{\mathtt{M}}_i^x$ is a annulus. Clearly, the vector $|\mathtt{D}_{\boldsymbol{g}}^{\boldsymbol{s}}; \chi, \overline{\chi}\rangle \neq 0$ if and only if $\chi \in G^{\Lambda^0(\partial\mathtt{C}')}$ and $\overline{\chi} \in G^{\Lambda^0(\partial\mathtt{C})}$ are compatible with $\boldsymbol{g} \in F(\mathtt{C})$. Analogously, $Z_j^y(\vartheta; \mathtt{D}_{\boldsymbol{g}}^{\boldsymbol{s}})$ and $Z_k^z(\vartheta; \mathtt{D}_{\boldsymbol{g}}^{\boldsymbol{s}})$ are defined.

For the purposes of finding all local operators, let

$$\left|\chi, \overline{\chi}; \mathtt{D}_{\boldsymbol{g}}^{\boldsymbol{s}}\mathtt{D}_{\boldsymbol{g}'}^{\boldsymbol{s}'}\right\rangle := \sum_{\vartheta \in G_B^{\Lambda^0(\mathtt{M})}(\boldsymbol{s}+\boldsymbol{s}', \chi, \overline{\chi})} Z\left(\vartheta; \mathtt{D}_{\boldsymbol{g}}^{\boldsymbol{s}}\mathtt{D}_{\boldsymbol{g}'}^{\boldsymbol{s}'}\right)|\vartheta\rangle, \tag{325}$$

where $Z(\vartheta; \mathtt{D}_{\boldsymbol{g}}^{\boldsymbol{s}}\mathtt{D}_{\boldsymbol{g}'}^{\boldsymbol{s}'})$ is given by Eq. (324) with $\mathtt{D}_{\boldsymbol{g}}^{\boldsymbol{s}}$ replaced by $\mathtt{D}_{\boldsymbol{g}}^{\boldsymbol{s}}\mathtt{D}_{\boldsymbol{g}'}^{\boldsymbol{s}'}$. Clearly, $|\chi, \overline{\chi}; \mathtt{D}_{\boldsymbol{g}}^{\boldsymbol{s}}\mathtt{D}_{\boldsymbol{g}'}^{\boldsymbol{s}'}\rangle = 0$ if $\boldsymbol{g} \neq \boldsymbol{g}'$. Moreover, χ (respectively, $\overline{\chi}$) can be changed by P_v^g on $\partial\mathtt{C}'$ (respectively, $\partial\mathtt{C}$) and hence describes degrees of freedom near $\partial\mathtt{C}'$ (respectively, $\partial\mathtt{C}$). To classify particles, we can keep $\chi, \overline{\chi}$ fixed and consider the subspace $\mathcal{H}_*(\overline{\mathtt{M}})$ spanned by $|\mathtt{D}_{\boldsymbol{g}}^{\boldsymbol{s}}; \chi, \overline{\chi}\rangle$ for $\boldsymbol{g} \in F(\mathtt{C})$ and $\boldsymbol{s} \in G^{\mathbb{C}^x} \times G^{\mathbb{C}^y} \times G^{\mathbb{C}^z}$. Since $\chi, \overline{\chi}$ are fixed, we omit them in notation and simply write $|\mathtt{D}_{\boldsymbol{g}}^{\boldsymbol{s}}\rangle$.

Next, let us construct a set of operators supported near either $\partial\mathtt{C}$ or $\partial\mathtt{C}'$ to distinguish states in $\mathcal{H}_*(\overline{\mathtt{M}})$. For $t \in G$, we have gauge transformation operators given by

$$Z_k^t := \prod_{c \sim (\partial\mathtt{C}', z = k+\frac{1}{2})} P_c^{(-1)^{c_y} t}, \tag{326}$$

$$\overline{Z}_k^t := \prod_{c \sim (\partial\mathtt{C}, z = k+\frac{1}{2})} \left(P_c^{(-1)^{c_y} t}\right)^\dagger, \tag{327}$$

where $c \sim (\partial\mathtt{C}', z = k + \frac{1}{2})$ [respectively, $c \sim (\partial\mathtt{C}, z = k + \frac{1}{2})$] means that the cube c is cut by plane $z = k + \frac{1}{2}$ and touches $\partial\mathtt{C}'$ (respectively, $\partial\mathtt{C}$). They act as the identity on $\mathcal{H}_*(\overline{\mathtt{M}})$ unless $z_0 - 1 \leqslant k \leqslant z_1$. In addition, for $h \in G$, let $T_h[\mathtt{M}_k^z]$ (respectively, $\overline{T}_h[\mathtt{M}_k^z]$) be the projector supported on $\partial\mathtt{C}'$ (respectively, $\partial\mathtt{C}$) requiring that the group element associated with the outer (respectively, inner) boundary of $\overline{\mathtt{M}}_k^z$ is h.

Then the two sets of operators

$$D_{k,h}^{z,t} := T_h\left[\mathtt{M}_k^z\right] \prod_{l \in k+2\mathbb{N}} Z_l^t, \tag{328}$$

$$\overline{D}_{k,h}^{z,t} := \overline{T}_h\left[\mathtt{M}_k^z\right] \prod_{l \in k+2\mathbb{N}} \overline{Z}_l^t \tag{329}$$

commute with $P(\mathtt{M})$, keep χ and $\overline{\chi}$ fixed and hence act on $\mathcal{H}_*(\overline{\mathtt{M}})$, where $\mathbb{N}$ denotes the set of non-negative integers. For $z_0 < k \leqslant z_1$,

$$D_{k,h}^{z,t}\left|\mathtt{D}_{\boldsymbol{g}}^{\boldsymbol{s}}\right\rangle = \delta_{h,g_k^z}\left|\mathtt{D}_{\boldsymbol{g}}^{t\delta_k^z}\mathtt{D}_{\boldsymbol{g}}^{\boldsymbol{s}}\right\rangle, \tag{330}$$

$$\overline{D}_{k,h}^{z,t}\left|\mathtt{D}_{\boldsymbol{g}}^{\boldsymbol{s}}\right\rangle = \delta_{h,g_k^z}\left|\mathtt{D}_{\boldsymbol{g}}^{\boldsymbol{s}}\mathtt{D}_{\boldsymbol{g}}^{t\delta_k^z}\right\rangle, \tag{331}$$

where the component of $h\delta_k^z \in G^{\mathbb{C}^x} \times G^{\mathbb{C}^y} \times G^{\mathbb{C}^z}$ corresponding to $k \in \mathbb{C}^z$ is h and the other components are zero. For $k > z_1$ or $k \leqslant z_0$, these operators act as

$$D_{k,h}^{z,t}\left|\mathtt{D}_{\boldsymbol{g}}^{\boldsymbol{s}}\right\rangle = \overline{D}_{k,h}^{z,t}\left|\mathtt{D}_{\boldsymbol{g}}^{\boldsymbol{s}}\right\rangle = \begin{cases} \delta_{h,0}\left|\mathtt{D}_{\boldsymbol{g}}^{\boldsymbol{s}}\right\rangle, & k > z_1, \\ \delta_{h,0}\left|\mathtt{D}_{\boldsymbol{g}}^{t\delta_{z_0}^z}\mathtt{D}_{\boldsymbol{g}}^{\boldsymbol{s}}\right\rangle, & k \leqslant z_0 \text{ even}, \\ \delta_{h,0}\left|\mathtt{D}_{\boldsymbol{g}}^{t\delta_{x_0}^x - t\delta_{y_0}^y}\mathtt{D}_{\boldsymbol{g}}^{\boldsymbol{s}}\right\rangle, & k \leqslant z_0 \text{ odd}. \end{cases} \tag{332}$$

Analogously, we can define operators $D_{i,n}^{x,h}$, $\overline{D}_{i,n}^{x,h}$, $D_{j,n}^{y,h}$, and $\overline{D}_{j,n}^{y,h}$. Their actions on $\mathcal{H}_*(\overline{\mathtt{M}})$ are obtained by permuting x, y, z cyclically in Eqs. (330)–(332). In particular, for $i > x_1$, $i \leqslant x_0$ and $j > y_1$, $j \leqslant y_0$, we have

$$D_{i,h}^{x,t}\left|\mathtt{D}_{\boldsymbol{g}}^{\boldsymbol{s}}\right\rangle = \overline{D}_{i,h}^{x,t}\left|\mathtt{D}_{\boldsymbol{g}}^{\boldsymbol{s}}\right\rangle = \begin{cases} \delta_{h,0}\left|\mathtt{D}_{\boldsymbol{g}}^{\boldsymbol{s}}\right\rangle, & i > x_1 \\ \delta_{h,0}\left|\mathtt{D}_{\boldsymbol{g}}^{t\delta_{x_0}^x}\mathtt{D}_{\boldsymbol{g}}^{\boldsymbol{s}}\right\rangle, & i \leqslant x_0 \text{ even}, \\ \delta_{h,0}\left|\mathtt{D}_{\boldsymbol{g}}^{t\delta_{y_0}^y - t\delta_{z_0}^z}\mathtt{D}_{\boldsymbol{g}}^{\boldsymbol{s}}\right\rangle, & i \leqslant x_0 \text{ odd}, \end{cases} \tag{333}$$

$$D^{y,t}_{j,h}\left|\mathtt{D}^s_{\boldsymbol{g}}\right\rangle = \overline{D}^{y,t}_{j,h}\left|\mathtt{D}^s_{\boldsymbol{g}}\right\rangle = \begin{cases} \delta_{h,0}\left|\mathtt{D}^s_{\boldsymbol{g}}\right\rangle, & j > y_1 \\ \delta_{h,0}\left|\mathtt{D}^{t\delta^y_{y_0}}_{\boldsymbol{g}}\mathtt{D}^s_{\boldsymbol{g}}\right\rangle, & j \leqslant y_0 \text{ even}, \\ \delta_{h,0}\left|\mathtt{D}^{t\delta^z_{z_0}-t\delta^x_{x_0}}_{\boldsymbol{g}}\mathtt{D}^s_{\boldsymbol{g}}\right\rangle, & j \leqslant y_0 \text{ odd}. \end{cases} \tag{334}$$

To get these operators organized, we consider the algebra $\mathcal{D}[\mathtt{C}] := \mathcal{D}_x[\mathtt{C}] \otimes \mathcal{D}_y[\mathtt{C}] \otimes \mathcal{D}_z[\mathtt{C}]$ with each factor $\mathcal{D}_\mu[\mathtt{C}]$ and its basis given by

$$\mathcal{D}_\mu[\mathtt{C}] := \bigotimes_{n\in\mathtt{C}^\mu} \mathcal{D}^{\omega^\mu_n}(G), \quad D^{\boldsymbol{t}^\mu}_{\boldsymbol{h}^\mu} := \bigotimes_{i\in\mathtt{C}^\mu} D^{t^\mu_n}_{h^\mu_n}, \tag{335}$$

$\forall \mu = x, y, z$. We write $D^{\boldsymbol{t}}_{\boldsymbol{h}} := D^{\boldsymbol{t}^x}_{\boldsymbol{h}^x} \otimes D^{\boldsymbol{t}^y}_{\boldsymbol{h}^y} \otimes D^{\boldsymbol{t}^z}_{\boldsymbol{h}^z}$ for short, where $\boldsymbol{h} = (\boldsymbol{h}^x, \boldsymbol{h}^y, \boldsymbol{h}^z), \boldsymbol{t} = (\boldsymbol{t}^x, \boldsymbol{t}^y, \boldsymbol{t}^z) \in G^{\mathtt{C}^x} \times G^{\mathtt{C}^y} \times G^{\mathtt{C}^z}$. The left and right actions of $\mathcal{D}(\mathtt{C})$ on $\mathcal{H}_*(\overline{\mathtt{M}})$ are

$$\pi\left(D^{\boldsymbol{t}}_{\boldsymbol{h}}\right) = \prod_{i=x_0}^{x_1} D^{x,t^x_i}_{i,h^x_i} \cdot \prod_{j=y_0}^{y_1} D^{y,t^y_j}_{j,h^y_j} \cdot \prod_{k=z_0}^{z_1} D^{z,t^z_k}_{k,h^z_k}, \tag{336}$$

$$\overline{\pi}\left(D^{\boldsymbol{t}}_{\boldsymbol{h}}\right) = \prod_{i=x_0}^{x_1} \overline{D}^{x,t^x_i}_{i,h^x_i} \cdot \prod_{j=y_0}^{y_1} \overline{D}^{y,t^y_j}_{j,h^y_j} \cdot \prod_{k=z_0}^{z_1} \overline{D}^{z,t^z_k}_{k,h^z_k}, \tag{337}$$

supported near $\partial\mathtt{C}'$ and $\partial\mathtt{C}$ respectively. More precisely, $\pi(D^{\boldsymbol{t}}_{\boldsymbol{h}})$ can be realized by operators near the region on $\partial\mathtt{C}'$ between planes $z = z_0$ and $z = z_1$, since Z^t_l in Eq. (328) acts trivially unless $z_0 - 1 \leqslant l \leqslant z_1$. By construction,

$$\pi\left(D^{\boldsymbol{t}}_{\boldsymbol{h}}\right)\left|\mathtt{D}^s_{\boldsymbol{g}}\right\rangle = \left|\mathtt{D}^{\boldsymbol{t}}_{\boldsymbol{h}}\mathtt{D}^s_{\boldsymbol{g}}\right\rangle, \tag{338}$$

$$\overline{\pi}\left(D^{\boldsymbol{t}}_{\boldsymbol{h}}\right)\left|\mathtt{D}^s_{\boldsymbol{g}}\right\rangle = \left|\mathtt{D}^s_{\boldsymbol{g}}\mathtt{D}^{\boldsymbol{t}}_{\boldsymbol{h}}\right\rangle. \tag{339}$$

In particular, they are zero if $\boldsymbol{h} \notin F(\mathtt{C})$.

Let $\mathcal{A}[\mathtt{C}]$ be the subalgebra of $\mathcal{D}[\mathtt{C}]$ spanned by $D^{\boldsymbol{t}}_{\boldsymbol{h}}$ with $\boldsymbol{h} \in F(\mathtt{C})$ and $\boldsymbol{t} \in G^{\mathtt{C}^x} \times G^{\mathtt{C}^y} \times G^{\mathtt{C}^z}$. Then

$$\mathcal{H}_*(\overline{\mathtt{M}}) \xrightarrow{\sim} \mathcal{A}[\mathtt{C}] : \left|\mathtt{D}^s_{\boldsymbol{g}}\right\rangle \mapsto D^s_{\boldsymbol{g}} \tag{340}$$

is an isomorphism between $\mathcal{H}_*(\mathtt{M})$ and $\mathcal{A}[\mathtt{C}]$ as a $\mathcal{D}[\mathtt{C}]$-$\mathcal{D}[\mathtt{C}]$-bimodule (i.e., a vector space carrying both left and right actions of $\mathcal{D}[\mathtt{C}]$).

Let $\mathfrak{Q}^\mu_n$ be the isomorphism classes of irreducible representations of $\mathcal{D}^{\omega^\mu_n}(G)$. We call each element of $\mathfrak{Q}^\mu_n$ a μ *topological charge*. Pick an irreducible representation $\mathcal{V}_{\mathfrak{a}^\mu_n} = (\rho_{\mathfrak{a}^\mu_n}, V_{\mathfrak{a}^\mu_n})$ on a Hilbert space with $\dagger$ respected for each $\mathfrak{a}^\mu_n \in \mathfrak{Q}^\mu_n$. Then

$$\rho = \bigoplus_{(\mathfrak{a}^\mu_n)^{\mu=x,y,z}_{n\in\mathtt{C}^\mu}} \bigotimes_{\mu,n} \rho_{\mathfrak{a}^\mu_n} \tag{341}$$

gives an isomorphism of algebras

$$\mathcal{D}[\mathtt{C}] \simeq \bigoplus_{(\mathfrak{a}^\mu_n)^{\mu=x,y,z}_{n\in\mathtt{C}^\mu}} \bigotimes_{\mu,n} \mathcal{L}\left(\mathcal{V}_{\mathfrak{a}^\mu_n}\right). \tag{342}$$

Explicitly, a μ topological charge $\mathfrak{a}^\mu_n \in \mathfrak{Q}^\mu_n$ is labeled by a pair (g^μ_n, ϱ^μ_n), where $g^\mu_n \in G$ describes the flux and ϱ^μ_n is an irreducible ω^μ_{n,g^μ_n} representation (up to isomorphism) of G. Refer to Appendix B 5 for the details of the labels.

Let $\mathfrak{Q}[\mathtt{C}]$ be the set of $\mathfrak{a} = (\mathfrak{a}^\mu_n)^{\mu=x,y,z}_{n\in\mathtt{C}^\mu} = (g^\mu_n, \varrho^\mu_n)^{\mu=x,y,z}_{n\in\mathtt{C}^\mu}$ with $(g^\mu_n)^{\mu=x,y,z}_{n\in\mathtt{C}^\mu} \in F(\mathtt{C})$. Then the composition

$$\mathcal{H}_*(\overline{\mathtt{M}}) \xrightarrow[\sim]{|\mathtt{D}^s_{\boldsymbol{g}}\rangle \mapsto D^s_{\boldsymbol{g}}} \mathcal{A}[\mathtt{C}] \xrightarrow[\sim]{\tilde{\rho}} \bigoplus_{\mathfrak{a}\in\mathfrak{Q}[\mathtt{C}]} \bigotimes_{\mu,n} \mathcal{L}\left(\mathcal{V}_{\mathfrak{a}^\mu_n}\right) = \bigoplus_{\mathfrak{a}\in\mathfrak{Q}[\mathtt{C}]} \mathcal{V}_{\mathfrak{a}} \otimes \mathcal{V}^*_{\mathfrak{a}} \tag{343}$$

is an isomorphism of Hilbert spaces respecting both the left and right actions of $\mathcal{D}[\mathtt{C}]$, where $\mathcal{V}_{\mathfrak{a}} := \bigotimes_{\mu,n} \mathcal{V}_{\mathfrak{a}^\mu_n}$ and

$$\tilde{\rho} := \bigoplus_{\mathfrak{a}\in\mathfrak{Q}[\mathtt{C}]} \bigotimes_{\mu,n} \sqrt{\frac{\dim_{\mathbb{C}} \mathcal{V}_{\mathfrak{a}^\mu_n}}{|G|}}\, \rho_{\mathfrak{a}^\mu_n}. \tag{344}$$

The normalization for each sector in $\tilde{\rho}$ is picked such that the inner product structure is respected. Clearly, $\mathfrak{Q}[\mathtt{C}]$ labels particle types of the excited cuboid $\mathtt{C}$ and $\mathcal{V}_{\mathfrak{a}}$ (respectively, $\mathcal{V}^*_{\mathfrak{a}}$) describes the degrees of freedom near $\partial\mathtt{C}'$ (respectively, $\partial\mathtt{C}$). Physically, $\mathfrak{a}^z_k = (g^z_k, \varrho^z_k)$ can be detected by braiding a pair of quasiparticles in the x and y directions via operator supported near grey region in $\partial\mathtt{C}'$ as in Fig. 19. Thus $\mathfrak{a}^z_k$ is called a z topological charge. Similarly, $\mathfrak{a}^x_i$ (respectively, $\mathfrak{a}^y_j$) is called a x (respectively, y) topological charge. Since $g^x_{x_0} = g^y_{y_0} = g^z_{z_0} = 0$, we have

$$\mathfrak{a}^x_{x_0} = (0, \varrho_{q^x}), \quad \mathfrak{a}^y_{y_0} = (0, \varrho_{q^y}), \quad \mathfrak{a}^z_{z_0} = (0, \varrho_{q^z}), \tag{345}$$

where $q^x,\ q^y,\ q^z \in G \simeq \widehat{G}$ with G identified with its character group $\widehat{G}$ and $\varrho_{q^x},\ \varrho_{q^y},\ \varrho_{q^z}$ denoting the corresponding representations.

Distinct from conventional topological orders, the number of allowed particle types of a finite excited region $\mathtt{C}$ in a fracton model increases/decreases as the size of $\mathtt{C}$ grows/shrinks. If a quasiparticle can be localized in a smaller cuboid $\mathtt{C}_a = [a^x_0, a^x_1] \times [a^y_0, a^y_1] \times [a^z_0, a^z_1] \subset \mathtt{C}$, then the analogues of Eqs. (332)–(334) for this smaller excitation imply that its particle type $\mathfrak{a} = (\mathfrak{a}^\mu_n)^{\mu=x,y,z}_{n\in\mathtt{C}^\mu} \in \mathfrak{Q}[\mathtt{C}]$ satisfies

$$\mathfrak{a}^z_k = \begin{cases} \mathfrak{o}, & k > a^z_1, \\ (0, \varrho_{q^z}), & k \leqslant a^z_0 \text{ even}, \\ (0, \varrho_{q^x - q^y}), & k \leqslant a^z_0 \text{ odd} \end{cases} \tag{346}$$

and the counterparts obtained by permuting x, y, z cyclically, where $\mathfrak{o}$ denotes the trivial representation (i.e., the counit) of any $\mathcal{D}^{\omega^\mu_n}(G)$. In other words, $\mathfrak{Q}[\mathtt{C}_a]$ can be viewed as a subset of $\mathfrak{Q}[\mathtt{C}]$; each $\mathcal{V}_{\mathfrak{a}}$ for $\mathfrak{a} \in \mathfrak{Q}[\mathtt{C}_a]$ carries an irreducible representation of $\mathcal{D}[\mathtt{C}]$ for any cuboid $\mathtt{C}$ containing $\mathtt{C}_a$.

B. Fusion of quasiparticles

Suppose that there are two spatially separated excited cuboids $\mathtt{C}_a$ and $\mathtt{C}_b$ contained deep inside a much larger cuboid $\mathtt{C}'$. Let $\mathtt{M} := \mathtt{C}' - \mathtt{C}^\circ_a - \mathtt{C}^\circ_b$. The discussion in the above section can be repeated here for the two-hole manifold $\mathtt{M}$. With the spin configuration on $\partial\mathtt{C}'$ and local degrees of freedom near $\mathtt{C}_a$ and $\mathtt{C}_b$ fixed separately, we are left with Hilbert spaces $\mathcal{V}[\mathfrak{a}, \mathfrak{b}]$ labeled by $\mathfrak{a} \in \mathfrak{Q}[\mathtt{C}_a]$ and $\mathfrak{b} \in \mathfrak{Q}[\mathtt{C}_b]$. Using two copies of Eq. (344), we have

$$\mathcal{V}[\mathfrak{a}, \mathfrak{b}] \simeq \mathcal{V}_{\mathfrak{a}} \otimes \mathcal{V}_{\mathfrak{b}}, \tag{347}$$

where $\mathcal{V}_{\mathfrak{a}} := \bigotimes_{\mu,n} \mathcal{V}_{\mathfrak{a}^\mu_n}$ and $\mathcal{V}_{\mathfrak{b}} := \bigotimes_{\mu,n} \mathcal{V}_{\mathfrak{b}^\mu_n}$.

The action of $\mathcal{D}[\mathbb{C}]$ on $\mathcal{V}_\mathfrak{a} \otimes \mathcal{V}_\mathfrak{b}$ via π defined in Eq. (279) is specified by the coproduct

$$\Delta := \bigotimes_{\mu=x,y,z} \bigotimes_{n\in\mathbb{C}^\mu} \Delta_n^\mu. \tag{348}$$

The linear space of intertwiners between the representations $\mathcal{V}_\mathfrak{c}$ and $\mathcal{V}_\mathfrak{a} \otimes \mathcal{V}_\mathfrak{b}$ of $\mathcal{D}[\mathbb{C}]$

$$V_\mathfrak{c}^{\mathfrak{a}\mathfrak{b}} := \mathrm{Hom}(\mathcal{V}_\mathfrak{c}, \mathcal{V}_\mathfrak{a} \otimes \mathcal{V}_\mathfrak{b}) \tag{349}$$

encodes the ways of fusing $\mathfrak{a}$ and $\mathfrak{b}$ into $\mathfrak{c} \in \mathfrak{Q}[\mathbb{C}]$. In particular, $N_{\mathfrak{a}\mathfrak{b}}^\mathfrak{c} := \dim_\mathbb{C} V_\mathfrak{c}^{\mathfrak{a}\mathfrak{b}}$ is the corresponding fusion rule. It is possible to fuse $\mathfrak{a}$ and $\mathfrak{b}$ into $\mathfrak{c}$ if and only if $N_{\mathfrak{a}\mathfrak{b}}^\mathfrak{c} \geqslant 1$. Moreover, $N_{\mathfrak{a}\mathfrak{b}}^\mathfrak{c} \geqslant 1$ implies $q_c^\mu = q_a^\mu + q_b^\mu, \forall \mu = x, y, z$, where $q_a^\mu, q_b^\mu, q_c^\mu \in G \simeq \widehat{G}$ are specified by $\mathfrak{a}_{\mu_0}^\mu$, $\mathfrak{b}_{\mu_0}^\mu$, $\mathfrak{c}_{\mu_0}^\mu$ as in Eq. (345).

C. Mobility of quasiparticles

Given an excitation of type $\mathfrak{a} \in \mathfrak{Q}[\mathbb{C}_a]$ inside a cuboid $\mathbb{C}_a = [a_0^x, a_1^x] \times [a_0^y, a_1^y] \times [a_0^z, a_1^z]$, it follows from the same argument in Sec. VI C that $\mathfrak{a}$ is mobile in the z direction if and only if all its z topological charges $\mathfrak{a}_k^z = (g_\mu^z, \varrho_k^z)$ are trivial. With Eqs. (320)–(322), $g_k^z = 0, \forall k$ implies that

$$\sum_{i \text{ odd}} g_i^x + \sum_{j \text{ odd}} g_j^y + \sum_{k \text{ odd}} g_k^z \in 2G, \tag{350}$$

where $2G := \{2g | g \in G\}$.

The form of $\mathfrak{a}_k^z$ for $k \leqslant a_0^z$ is given by Eq. (346). Then $\mathfrak{a}_k^z = \mathfrak{o}, \forall k \leqslant a_0^z$ implies that $q^z = 0$, $q^z = q^y$ and hence

$$q^x + q^y + q^z \in 2\widehat{G}, \tag{351}$$

where $q^\mu \in G \simeq \widehat{G}$ is specified by $\mathfrak{a}_{\mu_0}^\mu$ as in Eq. (345). Clearly, the conditions (350) and (351) hold as well if the excitation is movable in the x or y direction. In fact, both hold if and only if the excitation is a fusion result of movable quasiparticles. Thus an excitation is a fracton (i.e., *not* a fusion result of mobile quasiparticles) if and only if either $\sum_{i \text{ odd}} g_i^x + \sum_{j \text{ odd}} g_j^y + \sum_{k \text{ odd}} g_k^z \notin 2G$ or $q^x + q^y + q^z \notin 2\widehat{G}$. Similarly to the excitations in the twisted X-cube models, we thus see that the mobility of quasiparticles is determined by their topological charges, thereby allowing us to utilize familiar concepts from the study of topological order to reveal the intriguing phenomenology of fracton order.

D. Braiding of mobile quasiparticles

The general discussion of braidings in Sec. VI D applies here as well. What changes are the constraints on topological charges $\mathfrak{a} = (\mathfrak{a}_n^\mu)_{n\in\mathbb{C}^\mu}^{\mu=x,y,z}$. Rather than analyzing the implications of these modified constraints abstractly, we study the physical consequences directly through examples below.

E. Examples

We now illustrate through examples how fracton excitations in the twisted checkerboard models can exhibit semionic or non-Abelian braiding statistics. Importantly, distinct from the twisted X-cube models, it is possible to construct a twisted checkerboard model with inextricably non-Abelian fractons that is not a fusion result of immobile excitations of quantum dimension 1 and mobile quasiparticles.

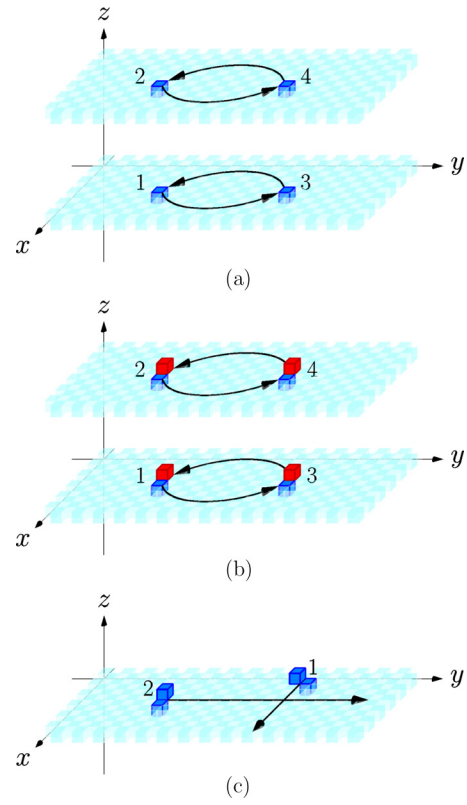

FIG. 24. Braidings of particles in twisted or untwisted checkerboard models with $G = \mathbb{Z}_2 = \{0, 1\}$. (a) Each labeled cube (blue online) in the illustrated checkerboard layers (cyan online) carries a nontrivial flux, i.e., the sum of group elements on its vertices equals $1 \neq 0$. In the untwisted model, $A_c = 1$ can be kept on all cubes. If a labeled cube is in a twisted layer Σ_k^z, it carries the projective representation $\varrho_k^z(s) = i^s$ and the trivial representation $\varrho_{k'}^z(s) = 1$ for $k' \neq k$, where $s \in G$. (b) Each cube (red online) on top of the drawn layers (cyan online) indicates a violation of $A_c = 1$ in the untwisted model. (c) Quasiparticle 1 (respectively, 2) is movable in the x direction (respectively, y direction).

1. $G = \mathbb{Z}_2$ (untwisted)

For $G = \mathbb{Z}_2 = \{0, 1\}$, it is known [20] that the third cohomology group $H^3(G, \mathrm{U}(1)) = \mathbb{Z}_2$, whose nontrivial element is presented by the 3-cocycle in Eq. (299). Each layer of cubes in the checkerboard model can be either untwisted or twisted. The pure charges (i.e., quasiparticles without nontrivial flux) behave in the same way, no matter whether the model is twisted or not. Thus we are more interested in excitations that violate $B_c = 1$ below.

First, we explain the braiding process of two xy-particles in the original (untwisted) checkerboard model in order to build familiarity with our notations and procedure. We consider the four fractons shown as the cubes (blue online) labeled as 1, 2, 3, and 4 in Fig. 24(a), where only $B_c = 1$ is violated. In the chosen coordinates, the four cubes are centered at $\frac{1}{2}(1, 1, 1) + \{(6, 8, 0), (6, 8, 10), (6, 20, 0), (6, 20, 10)\}$, respectively.

To study the braidings in the x and y directions, we group them into two pairs $\mathtt{C}_{12}$ (containing cubes 1,2) and $\mathtt{C}_{34}$ (containing cubes 3,4). Both $\mathtt{C}_{12}$ and $\mathtt{C}_{34}$ are xy-particles; they have trivial fluxes in both the x and y directions. Explicitly, the particle type of $\mathtt{C}_{12}$ is specified by its fluxes in each cross section $\mathtt{M}_k^z$

$$g_k^z = \begin{cases} 1, & k = 1 \text{ or } 11, \\ 0, & \text{otherwise.} \end{cases} \tag{352}$$

In fact, Eq. (352) also holds for $\mathtt{C}_{34}$ for the configuration shown in Fig. 24(a); it is easy to see that we can move $\mathtt{C}_{12}$ to $\mathtt{C}_{34}$ and that they are of the same particle type. Also, $\mathtt{C}_{12}$ and $\mathtt{C}_{34}$ can fuse into a completely trivial particle. Without violation of $A_c = 1$, these are pure fluxes. Hence the braiding operator $\mathcal{R}$, exchanging $\mathtt{C}_{12}$ and $\mathtt{C}_{34}$ illustrated by the arrows in Fig. 24(a), acts trivially (i.e., $\mathcal{R} = 1$).

If $A_c = 1$ is also violated on the extra cubes (red online) shown in Fig. 24(b), then both $\mathtt{C}_{12}$ and $\mathtt{C}_{34}$ have charges as well. Explicitly, the relevant representation of $G = \mathbb{Z}_2$, carried by both $\mathtt{C}_{12}$ and $\mathtt{C}_{34}$, is specified by

$$\varrho_k^z(1) = \begin{cases} -1, & 1 < k \leqslant 11 \text{ and } k \text{ odd}, \\ 1, & \text{otherwise.} \end{cases} \tag{353}$$

Therefore the braiding operator acts as

$$\mathcal{R} = \bigotimes_k \varrho_k^z\left(g_k^z\right) = -1. \tag{354}$$

Hence, $\mathtt{C}_{12}$ and $\mathtt{C}_{34}$ shown in Fig. 24(b) behave like fermions as for braiding in the x and y directions.

2. $G = \mathbb{Z}_2$ (Σ_k^z twisted for $k > z_0$)

Suppose $1 < z_0 < 11$. In particular, the upper layer Σ_{11}^z (respectively, the lower layer Σ_1^z) drawn in Fig. 24(a) is twisted (untwisted). Still, we can pair fractons 1,2 (respectively, 3,4) into an xy-particle $\mathtt{C}_{12}$ (respectively, $\mathtt{C}_{34}$). We also assume that $\mathtt{C}_{12}$ and $\mathtt{C}_{34}$ are of the same particle type with their flux configuration given by Eq. (352).

Since the relevant quantum double algebra is twisted on $\mathtt{M}_{11}^z$ satisfying

$$D_{11,1}^{z,s} D_{11,1}^{z,t} = \omega_1(s,t) D_{11,1}^{z,s+t}, \quad \forall s, t \in G, \tag{355}$$

an allowed collection of representations carried by both $\mathtt{C}_{12}$ and $\mathtt{C}_{34}$ can be specified by

$$\varrho_k^z(1) = \begin{cases} i, & k = 11, \\ 1, & \text{otherwise.} \end{cases} \tag{356}$$

The braiding operator that exchanges $\mathtt{C}_{12}$ and $\mathtt{C}_{34}$ as illustrated in Fig. 24(a) is

$$\mathcal{R} = \bigotimes_k \varrho_k^z\left(g_k^z\right) = \varrho_{11}^z(1) = i, \tag{357}$$

which shows a semionic behavior. However, the semionic behavior cannot appear in an untwisted model, where $\varrho_k^z(g_k^z)$ is always ± 1. This clearly shows that there is no continuous path of gapped local Hamiltonians connecting the untwisted model and a partially twisted model, in which $\mathtt{M}_k^z$ is twisted for $k \geqslant z_0$ and untwisted for $k < z_0$.

3. $G = \mathbb{Z}_2$ (Σ_k^z twisted for k odd)

There are many different ways of twisting the checkerboard model. Another simple case is to twist all $\mathtt{M}_k^z$ with k odd but to leave all Σ_k^z with k even untwisted, which we called the half twisted model for short. In this case, there are no semionic 2d mobile particles. However, we could instead consider 1d mobile particles, as shown in Fig. 24(c). The nontrivial fluxes and representations carried by quasiparticle 1 are

$$g_1^z = g_2^z = 1, \tag{358}$$

$$g_n^y = g_{n+1}^y = 1, \tag{359}$$

$$\varrho_1^z(s) = i^s, \forall s \in \mathbb{Z}_2, \tag{360}$$

while quasiparticle 2 carries

$$h_1^z = h_2^z = 1, \tag{361}$$

$$h_m^x = h_{m+1}^x = 1, \tag{362}$$

$$\varsigma_1^z(t) = i^t, \forall t \in \mathbb{Z}_2, \tag{363}$$

with some $m, n \in \mathbb{Z}$. Together, they fuse into a z-particle.

Let $\mathcal{O}_x$ (respectively, $\mathcal{O}_y$) be the operator moving quasiparticle 1 (respectively, 2) along the x (respectively, y) direction. They (i.e., $\mathcal{O}_x$ and $\mathcal{O}_y$) are supported near the corresponding arrows in Fig. 24(c). Then $\mathcal{O}_x\mathcal{O}_y$ and $\mathcal{O}_y\mathcal{O}_x$ differ by a full braiding of the identical z-topological charges of the two quasiparticles, which equals

$$\mathcal{R}^2 = \bigotimes_k \left[\varrho_k^z\left(h_k^z\right) \otimes \varsigma_k^z\left(g_k^z\right)\right] = -1. \tag{364}$$

On the other hand, if the model is untwisted, $\mathcal{R}^2 = 1$ as long as the two one-dimensional particles 1,2 fuse to a particle mobile in the third direction. This is because the fusion condition implies $g_k^z = h_k^z \in G$ and $\varrho_k^z = \varsigma_k^z$ as one-dimensional representations of $G, \forall k$. Thus $\varrho_k^z(h_k^z) \otimes \varsigma_k^z(g_k^z) = [\varrho_k^z(g_k^z)]^2 = 1$ in the untwisted model.

In summary, in the untwisted model, if an x-particle and a y-particle fuse into a z-particle, then the corresponding hopping operators always commute

$$\mathcal{O}_x\mathcal{O}_y = \mathcal{O}_y\mathcal{O}_x, \tag{365}$$

while in the model with $\mathtt{M}_k^z$ twisted alternately, we can have

$$\mathcal{O}_x\mathcal{O}_y = -\mathcal{O}_y\mathcal{O}_x. \tag{366}$$

This clearly distinguishes the half twisted model from the untwisted model.

4. $G = \mathbb{Z}_2$ (fully twisted)

Suppose that Σ_k^z is twisted for all $k \in \mathbb{Z}$. Here, we have not found a characteristic braiding process which distinguishes this model from the untwisted case.

However, we can still argue that there is no continuous path of gapped local Hamiltonians connecting the untwisted model and the fully twisted model. Let us give a proof by contradiction. Suppose there exists a continuous change of gapped local Hamiltonians $\mathcal{H}(\tau)$ parameterized by $\tau \in [0, 1]$ such that $\mathcal{H}(0)$ and $\mathcal{H}(1)$ are the untwisted and the

fully twisted checkerboard models respectively. Then there exists a local unitary transformation U^{loc}, which can be described as a finite-depth quantum circuit, such that $\mathcal{H}(1) = (U^{\mathrm{loc}})^\dagger \mathcal{H}(0) U^{\mathrm{loc}}$ [5]. Let $U^{\mathrm{loc}}_{z>0}$ be a local unitary operator obtained by keeping only operators in U^{loc} supported on the region $z > 0$. Then $(U^{\mathrm{loc}}_{z>0})^\dagger \mathcal{H}(0) U^{\mathrm{loc}}_{z>0}$ describes a model which is untwisted for $z \leqslant 0$ and twisted for $z \geqslant L$, where L is a finite positive number characterizing the correlation length.

Moreover, let us consider the braiding process shown in Fig. 24(a) with fractons 1,3 located in $z \leqslant 0$ and fractons 2,4 in $z \geqslant L$. If the braiding is made on the ground state of $\mathcal{H}(0)$ [respectively, $(U^{\mathrm{loc}}_{z>0})^\dagger \mathcal{H}(0) U^{\mathrm{loc}}_{z>0}$], then the exchange of $\mathtt{C}_{12}$ and $\mathtt{C}_{34}$ cannot be semionic (respectively, can be semionic). However, the *local* unitary transformation cannot change the braiding statistics, which are a nonlocal property of the topological charges. This leads to a contradiction, which proves the nonexistence of a continuous path of gapped local Hamiltonians connecting the untwisted model and the fully twisted model. It remains to be seen whether there exists a braiding process which clearly distinguishes these two cases.

5. $G = \mathbb{Z}_2 \times \mathbb{Z}_2 \times \mathbb{Z}_2$: Non-Abelian fractons

Finally, let us give an example of a model which provides an explicit realization of non-Abelian fractons, one of the central results of our work. It is constructed with the group $G = \mathbb{Z}_2 \times \mathbb{Z}_2 \times \mathbb{Z}_2$ and the 3-cocycle

$$\omega(f, g, h) = e^{i\pi (f^{(1)} g^{(2)} h^{(3)})}, \tag{367}$$

where $f = (f^{(1)}, f^{(2)}, f^{(3)})$, $g = (g^{(1)}, g^{(2)}, g^{(3)})$, $h = (h^{(1)}, h^{(2)}, h^{(3)}) \in G$. We will also interchangeably write the elements of G simply as 000, 100, 110 and so on for short. As examples, we have $\omega(100, 010, 001) = -1$ and $\omega(100, 001, 010) = 1$ in such notations. Now, to work out an explicit example, we twist Σ^z_k for all k.

Let us consider the eight fractons labeled as $1, 2, \ldots, 8$ in Fig. 25(a), divided into two groups. Each group is created by an operator supported near the corresponding grey sheet. In the left (respectively, right) group, each fracton carries a flux 100 (respectively, 011) and a projective representation ϱ_{100} (respectively, ϱ_{011}) satisfying

$$\varrho_{100}(s)\varrho_{100}(t) = \omega_{100}(s, t)\varrho_{100}(st), \tag{368}$$

$$\varrho_{011}(s)\varrho_{011}(t) = \omega_{011}(s, t)\varrho_{011}(st), \tag{369}$$

$\forall s, t \in G$ with $\omega_g(s, t)$ defined by Eq. (B26). A choice of ϱ_{100} and ϱ_{011} is given by

$$\varrho_{100}(100) = \sigma_0,\ \varrho_{100}(010) = \sigma_1,\ \varrho_{100}(001) = \sigma_3, \tag{370}$$

$$\varrho_{011}(100) = \sigma_3,\ \varrho_{011}(010) = \sigma_1,\ \varrho_{011}(001) = \sigma_1, \tag{371}$$

where $\sigma_0, \sigma_1, \sigma_2, \sigma_3$ denote the 2×2 identity matrix and the three Pauli matrices. Together with fluxes, they correspond to ρ^+_{100} and ρ^+_{011} in Table I of Appendix B 7.

In particular, each fracton with flux 100 (respectively, 011) carries a two-dimensional Hilbert space $\mathcal{V}_{100}$ (respectively, $\mathcal{V}_{011}$), whose basis is denoted as $\{|100;\uparrow\rangle, |100;\downarrow\rangle\}$ (respectively, $\{|011;\uparrow\rangle, |011;\downarrow\rangle\}$). When the flux is clear from context, we simply write $|\uparrow\rangle$, $|\downarrow\rangle$ for short. We pair fractons 1 and 5 into an xy-particle, denoted $\mathtt{C}_{15}$. Similarly, we have xy-particles $\mathtt{C}_{26}$, $\mathtt{C}_{37}$, $\mathtt{C}_{48}$.

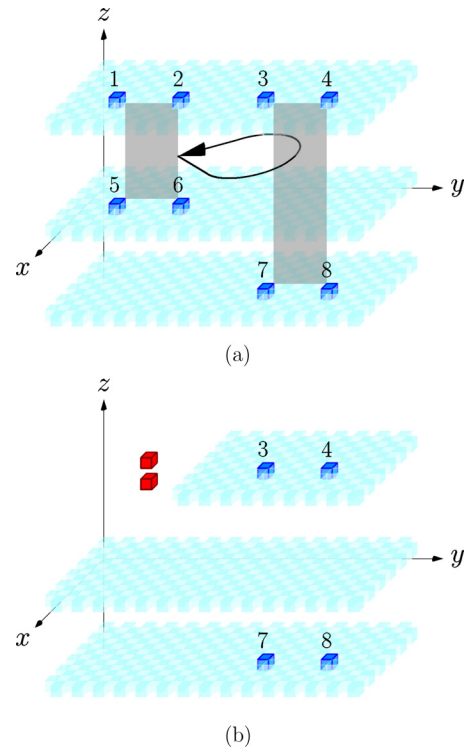

FIG. 25. (a) Two groups of fractons with nontrivial flux 1, 2, 5, 6 and 3, 4, 7, 8 are created from vacuum separately by an operator supported near the corresponding grey membrane. Fractons 2 and 6 are paired into a quasiparticle mobile in two dimensions and move around fracton 3 along the path indicated by the arrow. (b) After the braiding, fractons 1, 2, 5, and 6 cannot fuse back into vacuum any more but left with a pair of pure charges (red online) just above and below the checkerboard layer (cyan online) where fractons 1, 2, 3, and 4 violate $B_c = 1$, if the checkerboard model based on the group $G = \mathbb{Z}_2 \times \mathbb{Z}_2 \times \mathbb{Z}_2$ is twisted by $\omega(f, g, h) = e^{i\pi (f^{(1)} g^{(2)} h^{(3)})}$ along this layer. Clearly, the braiding process in (a) does not commute with any braiding that can distinguish the fusion channels of fractons 1 and 2; this explicitly demonstrates the non-Abelianness of fractons.

Since fractons 1, 2, 5, 6 are created together from the ground state, their total topological charge is trivial and hence they are in the state $|\uparrow\uparrow + \downarrow\downarrow\rangle_{12} \otimes |\uparrow\uparrow + \downarrow\downarrow\rangle_{56}$. For example, in the chosen coordinates, the fractons 1,2 carry flux 100 each in Σ^z_{11}; direct computation shows

$$\begin{aligned} &\Delta\big(D^{z,s}_{11,g}\big)|\uparrow\uparrow + \downarrow\downarrow\rangle_{12} \\ &\quad = \delta_{g,000}\omega^s(100, 100)\varrho_{100}(s) \otimes \varrho_{100}(s)|\uparrow\uparrow + \downarrow\downarrow\rangle_{12} \\ &\quad = \delta_{g,000}|\uparrow\uparrow + \downarrow\downarrow\rangle_{12} \end{aligned} \tag{372}$$

for $s = 100, 010, 001$ and hence the z topological charge of $|\uparrow\uparrow + \downarrow\downarrow\rangle_{12}$ is trivial, where $\omega^s(h, h')$ is defined by Eq. (B27). Similarly, the state of fractons 3, 4, 7, 8 with trivial topological charge is $|\uparrow\downarrow + \downarrow\uparrow\rangle_{34} \otimes |\uparrow\downarrow + \downarrow\uparrow\rangle_{78}$.

Next, let us consider the monodromy operator braiding $\mathtt{C}_{26}$ around $\mathtt{C}_{37}$ as shown in Fig. 25(a). It acts trivially on

5, 6, 7, 8 and nontrivially on 1, 2, 3, 4 as

$$\sigma_0 \otimes \varrho_{100}(011) \otimes \varrho_{011}(100) \otimes \sigma_0 |\uparrow\uparrow + \downarrow\downarrow\rangle_{12} |\uparrow\downarrow + \downarrow\uparrow\rangle_{34} = -|\uparrow\downarrow - \downarrow\uparrow\rangle_{12} |\uparrow\downarrow - \downarrow\uparrow\rangle_{34}, \tag{373}$$

where we have used

$$\varrho_{100}(011) = \omega_{100}(010, 001)\varrho_{100}(010)\varrho_{100}(001) = -\sigma_1\sigma_3 \tag{374}$$

and the associator between $(\mathcal{V}_{100} \otimes \mathcal{V}_{100}) \otimes (\mathcal{V}_{011} \otimes \mathcal{V}_{011})$ and $(\mathcal{V}_{100} \otimes (\mathcal{V}_{100} \otimes \mathcal{V}_{011})) \otimes \mathcal{V}_{011}$ equals the identity.

As in Eq. (372), direct computation shows that $D^{z,s}_{11,g}$ with $g, s \in G$ acts as

$$\begin{aligned} &\Delta\big(D^{z,s}_{11,g}\big)|\uparrow\downarrow - \downarrow\uparrow\rangle_{12} \\ &\quad = \delta_{g,000}\omega^s(100, 100)\varrho_{100}(s) \otimes \varrho_{100}(s)|\uparrow\downarrow - \downarrow\uparrow\rangle_{12} \\ &\quad = \delta_{g,000}(-1)^{s^{(2)}+s^{(3)}}|\uparrow\downarrow - \downarrow\uparrow\rangle_{12}, \end{aligned} \tag{375}$$

$$\begin{aligned} &\Delta\big(D^{z,s}_{11,g}\big)|\uparrow\downarrow - \downarrow\uparrow\rangle_{34} \\ &\quad = \delta_{g,000}\omega^s(011, 011)\varrho_{011}(s) \otimes \varrho_{011}(s)|\uparrow\downarrow - \downarrow\uparrow\rangle_{34} \\ &\quad = \delta_{g,000}(-1)^{s^{(2)}+s^{(3)}}|\uparrow\downarrow - \downarrow\uparrow\rangle_{34}. \end{aligned} \tag{376}$$

This implies that the group of fractons 1, 2, 5, 6 cannot fuse back into the vacuum any more after braiding. At best, we can annihilate all fluxes, resulting in a pair of pure charges, as depicted in Fig. 25(b). This analysis holds for the group of fractons 3, 4, 7, 8 as well. Thus the braiding process described here is a clear and unambiguous signature of fractons with a quantum dimension greater than 1. A similar braiding was discussed in the context of anyons in twisted gauge theory [116].

Clearly, if the model is twisted fully by Eq. (367) in at least one direction (e.g., Σ^z_k is twisted for all k), then the above fractons are all *inextricably* non-Abelian, i.e., their quantum dimension cannot be reduced to 1 by adding or removing some mobile quasiparticles. To see this, we note that fluxes have to be paired in order to be mobile; technically, Eqs. (320)–(322) implies that $\sum_i g^x_i = \sum_j g^y_j = \sum_k g^z_k = 0$ for each mobile quasiparticle. Thus the flux of each fracton shown in Fig. 25(a) cannot be canceled by adding or removing a mobile quasiparticle. In a fully twisted model, a nontrivial flux requires the fracton to remain non-Abelian.

However, if Σ^z_k is alternately twisted between even and odd layers, then the above fractons can be made Abelian by adding or removing 1d mobile quasiparticles [like those shown in Fig. 24(c)] and these are hence not inextricably non-Abelian fractons. But 1d mobile quasiparticles can be inextricably non-Abelian. For instance, suppose that the model is alternately twisted in the z direction. Then the fluxes of each 1d mobile quasiparticle in Fig. 24(c), which satisfies $\sum_{k\ \mathrm{odd}} g^k_z = \sum_{k\ \mathrm{even}} g^k_z \neq 0$ and implies non-Abelianness, cannot be canceled by adding or removing 2d mobile quasiparticles whose fluxes must satisfy $\sum_{i\ \mathrm{odd}} g^\mu_n = \sum_{i\ \mathrm{even}} g^\mu_n = 0, \forall \mu = x, y, z$ following from Eqs. (320)–(322). Thus such a model still displays a novel non-Abelian fracton phase.

Finally, if Σ^z_k is only partially twisted for both even and odd layers, then each fracton (respectively, 1d mobile quasiparticle) can be viewed as a fusion result of an Abelian fracton (respectively, 1d mobile quasiparticle) and non-Abelian (2d mobile) anyons; thus, the fracton phase is not strictly non-Abelian. This crucial distinction between these three cases is also reflected in their GSD on T^3, as given by Eqs. (260), (257), and (253).

VIII. CONCLUSIONS AND OUTLOOK

In this work, we have constructed a large class of novel three-dimensional quantum phases of matter exhibiting fracton order. Here, we shall summarize our main results and discuss some open questions which go beyond the scope of this paper but deserve further investigation.

The key result of our work is the construction of "twisted fracton models," which represent a general class of type-I fracton phases of matter, including those with inextricably non-Abelian fractons. In particular, we have constructed and studied the twisted versions of both the X-cube and checkerboard models, with spins—labeled by elements of a finite Abelian group G—on the faces (respectively, vertices) of a cubic (respectively, checkerboard) lattice for the X-cube (respectively, checkerboard) model. For either case, the untwisted Hamiltonian consists of local (generalized) gauge transformations and local flux projections. Their twisted versions are obtained by adding to the gauge transformations an extra phase factor specified by 3-cocycles $\omega \in H^3(G, \mathrm{U}(1))$ and locally flat spin configurations.

Both families of models are then carefully studied. We have made an exact computation of their ground-state degeneracy (GSD) on the 3-torus T^3, which depends subextensively on the system size. In particular, our computation discovers for the first time the exotic GSD [e.g., Eqs. (199), (209), (210), and (262)] of non-Abelian fracton phases (i.e., fracton phases hosting either inextricably non-Abelian fractons or inextricably non-Abelian 1d mobile quasiparticles) on T^3.

In addition, we have systematically analyzed the braiding and fusion properties of quasiparticles in twisted fracton phases and, in the process of doing so, defined necessary notions such as topological charge, quantum dimension, and inextricably non-Abelian fractons and 1d mobile quasiparticles. Thus our work also provides the first systematic route for describing the braiding and fusion of quasiparticles in type-I fracton phases, including those which are non-Abelian. As such, our work provides a general framework within which future studies of fracton order may be conducted. As an important intermediate step, we have also provided a detailed derivation of anyon properties of lattice models of twisted gauge theories in two spatial dimensions, which is then readily applicable to the twisted fracton models.

Concurrently with the development of the twisted fracton models, it has been realized that certain non-Abelian type-I fracton phases can also be constructed by coupling together $d = 2$ topological orders, a procedure carried out in Refs. [74,92]. In particular, Ref. [92] constructs so-called "cage-net" fracton models, a distinct non-Abelian generalisation of the X-cube model, by coupling together layers of string-net models through a process dubbed "flux-string" condensation. The resulting cage-net fracton model was shown to exhibit inextricably non-Abelian 1d mobile quasiparticles but not non-Abelian fractons; it remains an important open

question whether a similar coupled layer construction can lead to a phase with inextricable non-Abelian fractons (e.g., twisted checkerboard models). Indeed, even the correspondence between the twisted X-cube models and the cage-net fracton models remains unknown, as it is not thus far apparent whether all twisted fracton models can be accessed through some nontrivial coupling between $d = 2$ topological orders. In general, a major future direction in the study of fracton orders is to understand the generic possibilities which are allowed for type-I fracton phases and to study the relationships between their various existing constructions.

Further generalizing our results regarding the properties of twisted fracton models to generic type-I fracton phases constitutes another important open direction. A first step towards this goal would be to apply our systematic approach for describing quasiparticles to other fracton phases, which lie beyond our construction here, such as the cage-net models, in order to understand the generic features of excitations. In addition, it is desirable to understand the GSD of a non-Abelian twisted fracton model on T^3, which depends exotically on the system size, in terms of its quasiparticle properties. This will likely be crucial in determining the GSD of a generic non-Abelian fracton phase on T^3.

Moreover, generalizations of the X-cube model on more generic lattices [89] and on general three-dimensional manifolds [88] were proposed recently. Both these works found that the X-cube Hamiltonian may be defined on a lattice or manifold where the vertices locally resemble the vertex of a cubic lattice. In the language of Ref. [88], this construction involves the notion of a "singular compact total foliation" of the spatial manifold, wherein the lattice may be understood as being constructed with transversely intersecting stacks of parallel surfaces. In principle, there appears to be no obstruction to generalizing the twisted variants of the X-cube and checkerboard models to generic spatial manifolds; however, it will be an interesting challenge to understand the dependence of their GSD on both the global topology and the foliation.

With a rich landscape of type-I fracton systems uncovered by our construction, a better classification scheme for fracton phases is more needed than ever. While we have focused on the braiding-related differences amongst twisted fracton phases here, we can see, for instance, that twisted X-cube models based on a given group G share certain similarities, such as how the topological charges of a quasiparticle are constrained. Roughly speaking, these similarities reflect the 3d information inherent in these states while the differences treat the 2d features. Based on these ideas, we expect that an improved classification scheme would explicitly inform us how information at different levels is organized, which would allow for a more systematic study of fracton phases. Such investigations may lead to an instructive quantum field theoretical description capturing the universal properties of these phases.

As with most recent studies of fracton orders, we have focused here on type-I fracton phases, i.e., those where fractons are created at the corners of membrane operators and whose full spectrum contains additional quasiparticles with restricted mobility. It remains to be seen whether insights from this work can be extended to type-II fracton models, such as Haah's code [59], which host type-II fractons, i.e., those created by fractal operators. One possible route for realizing twisted versions of type-II fracton phases may be to study dual theories of the recently introduced "fractal SPT" states [118,119]. It will be especially interesting to see whether a multi-channel fusion rule is allowed for type-II fractons.

Besides searching for, and studying mechanisms of, new fracton phases, it is also important to explore possible realizations and potential applications of twisted fracton models. This line of investigation leads to several interesting questions worthy of future studies, such as the possibility of making quantum simulations of twisted fracton phases in cold atomic systems and of using non-Abelian fracton phases for quantum information storage or topological quantum computation to achieve better resilience to noise and decoherence.

ACKNOWLEDGMENTS

We are grateful to Danny Bulmash, Fiona Burnell, Meng Cheng, Guillaume Dauphinais, Trithep Devakul, Michael Hermele, Yuting Hu, Rahul Nandkishore, Wilbur Shirley, Kevin Slagle, Shivaji Sondhi, Oscar Viyuela, Juven Wang, and Yizhi You for stimulating conversations and correspondence. H.S. and M.A.M.-D. acknowledge financial support from the Spanish MINECO Grant FIS2015-67411, and the CAM research consortium Grants QUITEMAD+ S2013/ICE-2801 and S2018/TCS-4342 QUITEMAD-CM. The research of M.A.M.-D. has been supported in part by the U.S. Army Research Office through Grants No. W911N F-14-1-0103 and No. WN11NF-14-1-0103. A.P. acknowledges support from the University of Colorado at Boulder. S.-J. H. is supported by the U.S. Department of Energy, Office of Science, Basic Energy Sciences (BES) under Award No. DE-SC0014415.

APPENDIX A: GROUP COHOMOLOGY AND DIJKGRAAF-WITTEN WEIGHT

1. Definition of group cohomology

Let G be a finite group with its identity element denoted as e and $\mathrm{U}(1) := \{z \in \mathbb{C} \mid |z| = 1\}$ be the Abelian group of phase factors. For each nonnegative integer n, let $C^n(G, \mathrm{U}(1))$ be the set of functions from G^n (i.e., direct product of n copies of G) to U(1). Also, for each n, there is a so-called coboundary map

$$\delta : C^n(G, \mathrm{U}(1)) \to C^{n+1}(G, \mathrm{U}(1)), \qquad \omega \mapsto \delta\omega \tag{A1}$$

given by

$$\begin{aligned}\delta\omega(g_1, g_2, \ldots, g_{n+1}) &= \omega(g_2, g_3, \ldots, g_{n+1}) \cdot \prod_{j=1}^{n} \omega(g_1, \ldots, g_{j-1}, g_j g_{j+1}, \\ &\quad g_{j+2}, g_{j+3}, \ldots, g_{n+1})^{(-1)^j} \cdot \omega(g_1, g_2, \ldots, g_n)^{(-1)^{n+1}}.\end{aligned} \tag{A2}$$

In addition, let

$$Z^n(G, \mathrm{U}(1)) := \{\omega \in C^n(G, \mathrm{U}(1)) | \delta\omega = 1\}, \tag{A3}$$

whose elements are called n-cocycles, and $\delta\omega = 1$ is called the cocycle condition. We denote the image of $C^{n-1}(G, \mathrm{U}(1))$

under δ by

$$B^n(G, \mathrm{U}(1)) := \delta C^{n-1}(G, \mathrm{U}(1)), \tag{A4}$$

whose elements are called n-coboundaries. Induced by the Abelian group structure of U(1), all $C^n(G, \mathrm{U}(1))$, $Z^n(G, \mathrm{U}(1))$, and $B^n(G, \mathrm{U}(1))$ can be viewed as Abelian groups with coboundary maps viewed as homomorphisms of Abelian groups.

It can be checked that applying δ twice always gives a trivial map $\delta^2 : C^{n-1}(G, \mathrm{U}(1)) \to C^{n+1}(G, \mathrm{U}(1))$, i.e., $\delta^2 c = 1, \forall c \in C^{n-1}(G, \mathrm{U}(1))$. Hence $B^n(G, \mathrm{U}(1)) \subset Z^n(G, \mathrm{U}(1))$. The quotient of them

$$H^n(G, \mathrm{U}(1)) := \frac{Z^n(G, \mathrm{U}(1))}{B^n(G, \mathrm{U}(1))} \tag{A5}$$

is called nth cohomology group of G with coefficients in U(1), whose elements can be labeled by the coset of $\omega \in Z^n(G, \mathrm{U}(1))$, i.e.,

$$[\omega] := \omega \cdot B^n(G, \mathrm{U}(1)). \tag{A6}$$

Dijkgraaf-Witten topological quantum field theories constructed from $\omega, \omega' \in Z^3(G, \mathrm{U}(1))$ with $[\omega] = [\omega']$ are equivalent.

An n-cocycle $\omega \in Z^n(G, \mathrm{U}(1))$ is called normalized if $\omega(g_1, g_2, \ldots, g_n) = 1$ whenever any of $g_1, \ldots, g_n$ is the identity element e of G. It is a standard result that any element of an nth cohomology group can be presented by a normalized n-cocycle. For simplicity, we always work with normalized cocycles without loss of generality.

2. Triangulated manifold

Roughly, a triangulation of a topological space $\mathtt{X}$ is a decomposition of $\mathtt{X}$ into simplices. A *k-simplex* is the k-dimensional analogue of triangle; for lower dimensions, a 0-simplex (respectively, 1-simplex, 2-simplex, 3-simplex) is a point (respectively, segment, triangle, tetrahedron). In algebraic topology, such a decomposition is called a simplical structure. A topological space with a simplical structure is called a simplicial complex. Keeping only k-simplices with $k \leqslant m$ in a simplicial complex $\mathtt{X}$ results in a subcomplex called the m-skeleton of $\mathtt{X}$ and denoted $\mathtt{X}^m$. By definition, there is a sequence of inclusions $\mathtt{X}^0 \subset \mathtt{X}^1 \subset \mathtt{X}^2 \cdots$. Since $\mathtt{X}^1$ is a graph, terminology from graph theory is used; 0-simplices (respectively, 1-simplices) are usually called vertices (respectively, edges).

To work with topological quantum field theories of Dijkgraaf-Witten type, we want to decompose manifolds into *ordered simplices*, i.e., simplices whose vertices are ordered. Such a decomposition is called an *ordered simplicial structure*. It is equivalent to a simplicial structure together with a branching structure. A *branching structure* is a choice of orientation of each edge in the simplicial complex so that there is no triangle whose three edges form a closed walk [20]. A topological space with ordered simplicial structure is called an ordered simplicial complex.

Technically, the notion of a simplicial complex is too restrictive; no vertices of a simplex can coincide. A slight generalization of an ordered simplicial complex, dropping this restriction, leads to the notion of a Δ-complex. The definition of a Δ-complex structure can be found in Ref. [114]. To ensure everything is well-defined, we always work with finite Δ-complexes, i.e., those with finite number of simplices. To summarize, in this paper, the precise meaning of a *triangulation* of a topological space is a finite Δ-complex structure on it; vertices of each simplex are assumed ordered and allowed to coincide. In particular, triangles can be singular, whose vertices may coincide.

3. Dijkgraaf-Witten weight

Let us now consider a gauge field labeled by a finite group G on an n-dimensional triangulated oriented manifold $\mathtt{X}$ (probably with boundaries $\partial\mathtt{X} \neq \emptyset$). Let $\Delta^1(\mathtt{X})$ be the set of its 1-simplices (i.e., ordered edges). A gauge field configuration is specified by an assignment $\xi : \Delta^1(\mathtt{X}) \to G$. It will be called a *coloring* of $\mathtt{X}$, if it is *locally flat*, i.e., $\xi([v_0v_1])\xi([v_1v_2]) = \xi([v_0v_2])$ for any 2-simplex (i.e., ordered triangle) $[v_0v_1v_2]$ in $\mathtt{X}$. The sets of all colorings of $\mathtt{X}$ and its boundary $\partial\mathtt{X}$ are denoted $\mathrm{Col}(\mathtt{X}; G)$ and $\mathrm{Col}(\partial\mathtt{X}; G)$ (or simply $\mathrm{Col}(\mathtt{X})$ and $\mathrm{Col}(\partial\mathtt{X})$) respectively. Let $\zeta \in \mathrm{Col}(\partial\mathtt{X})$, then we write $\mathrm{Col}(\mathtt{X}, \zeta)$ for the set of colorings of $\mathtt{X}$, which coincide with ζ on $\partial\mathtt{X}$.

Given $\omega \in Z^n(G, \mathrm{U}(1))$, the *Dijkgraaf-Witten weight*

$$\omega[\mathtt{X}, \xi] \equiv \langle \omega, \xi_{\#}\mathtt{X} \rangle := \prod_{\sigma} \langle \omega, \xi\sigma \rangle^{\mathrm{sgn}(\sigma)} \tag{A7}$$

is assigned to each $\xi \in \mathrm{Col}(\mathtt{X})$, where the product is over all n-simplices σ in $\mathtt{X}$. The sign $\mathrm{sgn}(\sigma) = 1$ (respectively, -1) if the orientation of $\sigma = [\sigma_0\sigma_1\cdots\sigma_n]$ determined by the ordering of its vertices is the same as (respectively, opposite to) the orientation of $\mathtt{X}$. In addition,

$$\langle \omega, \xi\sigma \rangle := \omega(\xi([\sigma_0\sigma_1]), \xi([\sigma_1\sigma_2]), \ldots, \xi([\sigma_{n-1}\sigma_n])), \tag{A8}$$

which is often simply written as $[\sigma_0\sigma_1\cdots\sigma_n]$ to avoid heavy notations in concrete calculations, when ω and ξ are clear from context.

Before proceeding further, let us further elucidate the dependence of $\omega[\mathtt{X}, \xi]$ on $\xi \in \mathrm{Col}(\mathtt{X}, \zeta)$. To borrow terms from topology, $\xi \in \mathrm{Col}(\mathtt{X})$ can be viewed as a continuous map from $\mathtt{X}$ to the classifying space BG for the group and it maps $\mathtt{X}^0$ to a base point of BG. To be concrete, we always refer to the standard Δ-complex realization of BG. In general, if $\xi, \xi' \in \mathrm{Col}(\mathtt{X}, \zeta)$ are homotopic to each other relative to $\partial\mathtt{X}$, then $\omega[\mathtt{X}, \xi] = \omega[\mathtt{X}, \xi']$.

We notice that such a homotopy can be presented as a coloring on $\mathtt{X} \times \mathtt{I}$, where $\mathtt{I} = [0, 1]$. The Δ-complex structure of $\mathtt{X} \times \mathtt{I}$ is induced by that of $\mathtt{X}$ as follows: if $[v_0v_1\cdots v_k]$ is a k-simplex of $\mathtt{X}$, then $[v_0v_1\cdots v_kv'_k]$, $[v_0v_1\cdots v_{k-1}v'_{k-1}v'_k]$, ..., $[v_0v'_1\cdots v'_{k-1}v'_k]$ are $(k+1)$-simplices of $\mathtt{X} \times \mathtt{I}$. Here $\mathtt{X} \times \{0\}$ is identified with $\mathtt{X}$; we write v (respectively, v') for vertices in $\mathtt{X} \times \{0\}$ (respectively, $\mathtt{X} \times \{1\}$). A homotopy ϑ from ξ to ξ' relative to $\partial\mathtt{X}$ can be presented as a coloring of $\mathtt{X} \times \mathtt{I}$ such that $\mathtt{X} \times \{0\}$ (respectively, $\mathtt{X} \times \{1\}$) is colored as ξ (respectively, ξ') and such that each $[vv']$ in $(\partial\mathtt{X}) \times \mathtt{I}$ is colored by the identity element of G. If such a homotopy exists for $\xi, \xi' \in \mathrm{Col}(\mathtt{X})$, we say ξ, ξ' are homotopic to each other relative to $\partial\mathtt{X}$.

To see $\omega[\mathtt{X},\xi]=\omega[\mathtt{X},\xi']$, let $C_{n+1}(\mathtt{X}\times\mathtt{I})$ be the group of $(n+1)$-chains of $\mathtt{X}\times\mathtt{I}$, i.e., the free Abelian group generated by $\Delta^{n+1}(\mathtt{X}\times\mathtt{I})$. We also use $\mathtt{X}\times\mathtt{I}$ to denote the orientation-dependent sum of all $(n+1)$-simplices in $\mathtt{X}\times\mathtt{I}$; we write $\mathtt{X}\times\mathtt{I}=\sum_\sigma \mathrm{sgn}(\sigma)\sigma\in C_{n+1}(\mathtt{X}\times\mathtt{I})$. Using the Abelian group homormophism $\vartheta_\#: C_{n+1}(\mathtt{X}\times\mathtt{I})\to C_{n+1}(BG)$ induced by the homotopy $\vartheta:\mathtt{X}\times\mathtt{I}\to BG$, we have

$$\langle\omega,\vartheta_\#\partial(\mathtt{X}\times\mathtt{I})\rangle=\langle\delta\omega,\vartheta_\#(\mathtt{X}\times\mathtt{I})\rangle=1. \tag{A9}$$

We notice that $\partial(\mathtt{X}\times\mathtt{I})=\mathtt{X}\times\{1\}-\mathtt{X}\times\{0\}+(\partial\mathtt{X})\times\mathtt{I}$ and that $\vartheta_\#$ coincides with group homomorphism $\xi_\#$ (respectively, $\xi'_\#$) induced by ξ (respectively, ξ') on $\mathtt{X}\times\{0\}$ (respectively, $\mathtt{X}\times\{1\}$). In addition, ω gives the trivial phase factor 1 on all n-simplices in $(\partial\mathtt{X})\times\mathtt{I}$. Hence $\langle\omega,\vartheta_\#\partial(\mathtt{X}\times\mathtt{I})\rangle=\langle\omega,\xi_\#\mathtt{X}\rangle/\langle\omega,\xi'_\#\mathtt{X}\rangle$, so we get $\langle\omega,\xi_\#\mathtt{X}\rangle=\langle\omega,\xi'_\#\mathtt{X}\rangle$.

Suppose that $\mathtt{X}$ and $\mathtt{X}'$ are the same manifold with probably different Δ-complex structures that coincide on boundary. Let us consider an $(n+1)$-dimensional Δ-manifold $\mathtt{X}\times\mathtt{I}$ whose boundary is triangulated as $\mathtt{X}$ (respectively, $\mathtt{X}'$) on $\mathtt{X}\times\{0\}$ (respectively, $\mathtt{X}\times\{1\}$) and the induced Δ-complex structure of $(\partial\mathtt{X})\times\mathtt{I}$.[5] Then a homotopy ϑ from $\xi\in\mathrm{Col}(\mathtt{X})$ to $\xi'\in\mathrm{Col}(\mathtt{X}')$ relative to $\partial\mathtt{X}$ can be defined as a coloring of this Δ-manifold $\mathtt{X}\times\mathtt{I}$ that coincides with ξ (respectively, ξ') on $\mathtt{X}\times\{0\}$ (respectively, $\mathtt{X}\times\{1\}$) and colors each $[vv']\in(\partial\mathtt{X})\times\mathtt{I}$ by the identity element of G. Again, repeating the above argument using Eq. (A9), we get $\langle\omega,\xi_\#\mathtt{X}\rangle=\langle\omega,\xi'_\#\mathtt{X}\rangle$ if ξ and ξ' are homotopic to each other.

To determine when two colorings on $\mathtt{X}$ are homotopic, we pick a vertex $s\in\mathtt{X}$ as the base point and a path $\langle s,v\rangle$ from s to every vertex v other than s, where $\mathtt{X}$ is assumed to be connected. Let $\pi_1(\mathtt{X},s)$ be the fundamental group of $\mathtt{X}$ based at s. For any subset $W\subseteq\mathtt{X}^0\backslash\{s\}$, we write $\langle s,W\rangle:=\{\langle s,v\rangle|v\in W\}$. Then $\mathrm{Col}(\mathtt{X};G)$ is in one-to-one correspondence to $\mathrm{Hom}(\pi_1(\mathtt{X},s),G)\times G^{\langle s,\mathtt{X}^0\backslash\{s\}\rangle}$, where $\mathrm{Hom}(\pi_1(\mathtt{X},s),G)$ is the set of group homomorphisms from $\pi_1(\mathtt{X},s)$ to G.

Further, suppose that $\mathtt{X}$ and $\mathtt{X}'$ are the same manifold with probably different Δ-complex structures that coincide on boundary. If $\partial\mathtt{X}\neq\emptyset$, the base point s is picked in $\partial\mathtt{X}$. Then $\xi\in\mathrm{Col}(\mathtt{X};G)$ and $\xi'\in\mathrm{Col}(\mathtt{X}';G)$ are homotopic relative to $\partial\mathtt{X}$ if and only if they assign the same group element to each path in $\pi_1(\mathtt{X},s)$ and $\langle s,\partial\mathtt{X}^0\backslash s\rangle$, where $\partial\mathtt{X}^0$ is the set of vertices in $\partial\mathtt{X}$. If $\partial\mathtt{X}=\partial\mathtt{X}'=\emptyset$, then $\xi\in\mathrm{Col}(\mathtt{X};G)$ and $\xi'\in\mathrm{Col}(\mathtt{X}';G)$ are homotopic if and only if there exists $g\in G$ such that $\xi'(q)=g\xi(q)g^{-1}$ for any $q\in\pi_1(\mathtt{X},s)$.

The summation of $\langle\omega,\xi_\#\mathtt{X}\rangle$ over $\xi\in\mathrm{Col}(\mathtt{X},\zeta)$ gives the *Dijkgraaf-Witten partition function*

$$Z_\omega(\mathtt{X},\zeta):=\frac{1}{|G|^{|\mathtt{X}^0\backslash\partial\mathtt{X}^0|}}\sum_{\xi\in\mathrm{Col}(\mathtt{X},\zeta)}\langle\omega,\xi_\#\mathtt{X}\rangle, \tag{A10}$$

where $|\mathtt{X}^0\backslash\partial\mathtt{X}^0|$ is the number of vertices of $\mathtt{X}$ not in $\partial\mathtt{X}$. From the discussion above, it is clear that $Z_\omega(\mathtt{X},\zeta)$ does not depend on how $\mathtt{X}\backslash\partial\mathtt{X}$ is triangulated.

[5]It is known that the Δ-complex structure on the boundary of manifold can be extended to the whole of the manifold.

APPENDIX B: ALGEBRA PRELIMINARIES FOR $\mathcal{D}^\omega(G)$

1. Some definitions for quasibialgebras

A *quasibialgebra* $(\mathcal{A},\Delta,\varepsilon,\phi)$ is an algebra $\mathcal{A}$ over $\mathbb{C}$ equipped with algebra homomorphisms $\Delta:\mathcal{A}\to\mathcal{A}\otimes\mathcal{A}$, $\varepsilon:\mathcal{A}\to\mathbb{C}$ and an invertible element $\phi\in\mathcal{A}\otimes\mathcal{A}\otimes\mathcal{A}$ such that

$$(\mathrm{id}\otimes\Delta)(\Delta(a))=\phi(\Delta\otimes\mathrm{id})(\Delta(a))\phi^{-1},\quad\forall a\in\mathcal{A}, \tag{B1}$$

$$\begin{aligned}&(\mathrm{id}\otimes\mathrm{id}\otimes\Delta)(\phi)(\Delta\otimes\mathrm{id}\otimes\mathrm{id})(\phi)\\&\quad=(1\otimes\phi)(\mathrm{id}\otimes\Delta\otimes\mathrm{id})(\phi)(\phi\otimes1),\end{aligned} \tag{B2}$$

$$(\varepsilon\otimes\mathrm{id})\circ\Delta=\mathrm{id}=(\mathrm{id}\otimes\varepsilon)\circ\Delta, \tag{B3}$$

$$(\mathrm{id}\otimes\varepsilon\otimes\mathrm{id})(\phi)=1\otimes1, \tag{B4}$$

where 1 denotes the identity element of $\mathcal{A}$. Respectively, Δ, ε and ϕ are called the *copruduct*, the*counit*, and the *Drinfeld associator*. A quasibialgebra is a generalization of bialgebra; it relaxes the coassociativity condition.

An *antipode* on a quasibialgebra $(\mathcal{A},\Delta,\varepsilon,\phi)$ is a triple (S,α,β), where $S:\mathcal{A}\to\mathcal{A}$ is an algebra antihomomorphism and $\alpha,\beta\in\mathcal{A}$, satisfying

$$\sum_j S\big(a_j^{(1)}\big)\alpha a_j^{(2)}=\varepsilon(a)\alpha, \tag{B5}$$

$$\sum_j a_j^{(1)}\beta S\big(a_j^{(2)}\big)=\varepsilon(a)\beta, \tag{B6}$$

$$\sum_j \phi_j^{(1)}\beta S\big(\phi_j^{(2)}\big)\alpha\phi_j^{(3)}=1, \tag{B7}$$

$$\sum_j S\big(\bar\phi_j^{(1)}\big)\alpha\bar\phi_j^{(2)}\beta S\big(\bar\phi_j^{(3)}\big)=1, \tag{B8}$$

for any $a\in\mathcal{A}$, where $\sum_j a_j^{(1)}\otimes a_j^{(2)}=\Delta(a)$, $\sum_j\phi_j^{(1)}\otimes\phi_j^{(2)}\otimes\phi_j^{(3)}=\phi$, and $\sum_j\bar\phi_j^{(1)}\otimes\bar\phi_j^{(2)}\otimes\bar\phi_j^{(3)}=\phi^{-1}$. A *quasi-Hopf* algebra $(\mathcal{A},\Delta,\varepsilon,\phi,S,\alpha,\beta)$ is a quasibialgebra with an antipode (S,α,β) such that S is bijective.

A *quasitriangular* quasibialgebra $(\mathcal{A},\Delta,\varepsilon,\phi,R)$ is a quasibialgebra equipped with an invertible element $R\in\mathcal{A}\otimes\mathcal{A}$, called the*universal R matrix*, satisfying

$$\Delta^{\mathrm{op}}(a)=R\Delta(a)R^{-1}, \tag{B9}$$

$$(\Delta\otimes\mathrm{id})(R)=\phi_{312}R_{13}\phi_{132}^{-1}R_{23}\phi, \tag{B10}$$

$$(\mathrm{id}\otimes\Delta)(R)=\phi_{231}^{-1}R_{13}\phi_{213}R_{12}\phi^{-1}, \tag{B11}$$

where $\Delta^{\mathrm{op}}:=\wp\circ\Delta$ with $\wp(a_1\otimes a_2):=a_2\otimes a_1$ and R_{ij} stands for R acting nontrivially in the ith and jth slots of $\mathcal{A}\otimes\mathcal{A}\otimes\mathcal{A}$. In addition, if σ denotes a permutation of $\{1,2,3\}$ and $\phi=\sum_j\phi_j^{(1)}\otimes\phi_j^{(2)}\otimes\phi_j^{(3)}$, then $\phi_{\sigma(1)\sigma(2)\sigma(3)}:=\sum_j\phi_j^{(\sigma^{-1}(1))}\otimes\phi_j^{(\sigma^{-1}(2))}\otimes\phi_j^{(\sigma^{-1}(3))}$.

2. Tensor product of quasibialgebras

Given two quasibialgebras $(\mathcal{A}_1,\Delta_1,\varepsilon_1,\phi_1)$ and $(\mathcal{A}_2,\Delta_2,\varepsilon_2,\phi_2)$, their tensor product $\mathcal{A}:=\mathcal{A}_1\otimes\mathcal{A}_2$ is also a quasibialgebra equipped with the coproduct $\Delta:\mathcal{A}\to\mathcal{A}\otimes\mathcal{A}$

given by the composition of the following two maps:

$$\begin{aligned}\mathcal{A} &= \mathcal{A}_1 \otimes \mathcal{A}_2 \xrightarrow{\Delta_1\otimes\Delta_2} (\mathcal{A}_1 \otimes \mathcal{A}_1) \otimes (\mathcal{A}_2 \otimes \mathcal{A}_2) \\ &\to (\mathcal{A}_1 \otimes \mathcal{A}_2) \otimes (\mathcal{A}_1 \otimes \mathcal{A}_2) = \mathcal{A} \otimes \mathcal{A},\end{aligned} \tag{B12}$$

where the second map swaps the middle two tensor factors $(\mathcal{A}_1 \otimes \mathcal{A}_2) \otimes (\mathcal{A}_1 \otimes \mathcal{A}_2) = \mathcal{A}_1 \otimes \mathcal{A}_2 \otimes \mathcal{A}_1 \otimes \mathcal{A}_2$. The counit ε is

$$\mathcal{A}_1 \otimes \mathcal{A}_2 \xrightarrow{\varepsilon_1\otimes\varepsilon_2} \mathbb{C} \otimes \mathbb{C} \to \mathbb{C}, \tag{B13}$$

where the second map is the multiplication of $\mathbb{C}$. The Drinfeld associator ϕ is also given by the tensor product of ϕ_1 and ϕ_2; more precisely, ϕ is the image of $\phi_1 \otimes \phi_2$ under the map

$$\left(\mathcal{A}_1^{\otimes 3}\right) \otimes \left(\mathcal{A}_2^{\otimes 3}\right) \to (\mathcal{A}_1 \otimes \mathcal{A}_2)^{\otimes 3} = \mathcal{A} \otimes \mathcal{A} \otimes \mathcal{A} \tag{B14}$$

swapping corresponding factors.

For notational compactness, we do not express the identification maps $\mathcal{A}_1^{\otimes n} \otimes \mathcal{A}_2^{\otimes n} \cong \mathcal{A}^{\otimes n}$ and $\mathbb{C} \otimes \mathbb{C} \cong \mathbb{C}$ explicitly. Thus we can simply write $\Delta = \Delta_1 \otimes \Delta_2$, $\varepsilon = \varepsilon_1 \otimes \varepsilon_2$, and $\phi = \phi_1 \otimes \phi_2$. This convention of notation simplification will be used below.

If $(\mathcal{A}_1, \Delta_1, \varepsilon_1, \phi_1)$ and $(\mathcal{A}_2, \Delta_2, \varepsilon_2, \phi_2)$ have antipodes (S_1, α_1, β_1) and (S_2, α_2, β_2), respectively, then their tensor product $(\mathcal{A}, \Delta, \varepsilon, \phi)$ is also a quai-Hopf algebra with antipode $(S_1 \otimes S_2, \alpha_1 \otimes \alpha_2, \beta_1 \otimes \beta_2)$.

In addition, if $(\mathcal{A}_1, \Delta_1, \varepsilon_1, \phi_1)$ and $(\mathcal{A}_2, \Delta_2, \varepsilon_2, \phi_2)$ are quasitriangular with universal matrices $R_1 \in \mathcal{A}_1 \otimes \mathcal{A}_1$ and $R_2 \in \mathcal{A}_2 \otimes \mathcal{A}_2$, respectively, then their tensor product $(\mathcal{A}, \Delta, \varepsilon, \phi)$ is also quasitriangular with a universal matrix $R = R_1 \otimes R_2$. This discussion here generalizes to the tensor product of a finite number of quasibialgebras.

3. Representation category of quasibialgebra

Below, all vector spaces are assumed to be finite-dimensional for simplicity. A representation (ρ, V) of $\mathcal{A}$ is a vector space V over $\mathbb{C}$ equipped with an algebra homomorphism $\rho : \mathcal{A} \to \mathrm{End}(V) \equiv \mathcal{L}(V)$, where $\mathrm{End}(V) \equiv \mathcal{L}(V)$ is the algebra of all linear operators on V. A morphism $f : (\rho_1, V_1) \to (\rho_2, V_2)$ is a linear map that commutes with the action of $\mathcal{A}$, i.e.,

$$f \circ \rho_1(a) = \rho_2(a) \circ f, \forall a \in \mathcal{A}. \tag{B15}$$

Such a map is called an *intertwiner* in representation theory. By the representation category of $\mathcal{A}$, we mean the category whose objects are the representations of $\mathcal{A}$ and whose morphisms are the intertwiners between them. As it fits in a more general setting on the categories of modules, the representation category of $\mathcal{A}$ is denoted by $\mathcal{A}$-Mod. In practice, we often write $\mathcal{V}$ short for (ρ, V) and treat $\mathcal{V}$ as an $\mathcal{A}$-module; the action of $a \in \mathcal{A}$ on $v \in \mathcal{V}$ is then written as $a \cdot v := \rho(a)v$.

For a quasibialgebra $(\mathcal{A}, \Delta, \varepsilon)$, a tensor category structure can be defined for $\mathcal{A}$-Mod. Given any two representations $\mathcal{V}_1 = (\rho_1, V_1)$ and $\mathcal{V}_2 = (\rho_2, V_2)$, their tensor product is $\mathcal{V}_1 \otimes \mathcal{V}_2 = (\rho_{12}, V_1 \otimes V_2)$ with

$$\rho_{12} := (\rho_1 \otimes \rho_2) \circ \Delta, \tag{B16}$$

which is also a representation of $\mathcal{A}$. The tensor product of morphisms is the standard tensor product of linear maps.

The unit object is the trivial representation $(\varepsilon, \mathbb{C})$. The following intertwiners

$$\begin{aligned}\mathbb{C} \otimes V \;&\cong\; V \;\cong\; V \otimes \mathbb{C}, \\ 1 \otimes v \;&\mapsto\; v \;\leftarrow\!\shortmid\; v \otimes 1\end{aligned} \tag{B17}$$

are isomorphisms and are called the left and right unitors of $\mathcal{A}$-Mod.

Given three representations $\mathcal{V}_j = (\rho_j, V_j)$, $j = 1, 2, 3$, we can construct two representations $(\mathcal{V}_1 \otimes \mathcal{V}_2) \otimes \mathcal{V}_3$ and $\mathcal{V}_1 \otimes (\mathcal{V}_2 \otimes \mathcal{V}_3)$, which are the same vector space but not necessarily identical as an $\mathcal{A}$-module. They are isomorphic by the intertwiner

$$\rho_1 \otimes \rho_2 \otimes \rho_3(\phi) : (V_1 \otimes V_2) \otimes V_3 \to V_1 \otimes (V_2 \otimes V_3), \tag{B18}$$

which is called the associator of $\mathcal{A}$-Mod.

In case that $(\mathcal{A}, \Delta, \varepsilon)$ is a quasi-Hopf algebra with an antipode (S, α, β), given any representation $\mathcal{V} = (\rho, V)$ we can construct a *dual representation* $\mathcal{V}^* = (\rho^*, V^*)$, where $V^* := \mathrm{Hom}_{\mathbb{C}}(V, \mathbb{C})$ and $\rho^*(a) = \rho(S(a))^{\mathsf{T}}$ is the transpose of $\rho(S(a))$ for any $a \in \mathcal{A}$. Explicitly, the action of $\forall a \in A$ on $\forall f \in V^*$ is given by $(a \cdot f)(v) := f(S(a) \cdot v)$, $\forall v \in V$. Using the properties of the antipode, delineated in Eqs. (B5)–(B8), we construct two intertwiners

$$\alpha_{\mathcal{V}} : \mathcal{V}^* \otimes \mathcal{V} \to \mathbb{C}, \quad f \otimes v \mapsto f(\rho(\alpha)v), \tag{B19}$$

$$\beta_{\mathcal{V}} : \mathbb{C} \to \mathcal{V} \otimes \mathcal{V}^*, \quad 1 \mapsto \rho(\beta) \in \mathcal{L}(\mathcal{V}) = \mathcal{V} \otimes \mathcal{V}^* \tag{B20}$$

such that the compositions

$$\mathcal{V} \xrightarrow{\beta_{\mathcal{V}}\otimes \mathrm{id}_{\mathcal{V}}} (\mathcal{V} \otimes \mathcal{V}^*) \otimes \mathcal{V} \xrightarrow{\phi} \mathcal{V} \otimes (\mathcal{V}^* \otimes \mathcal{V}) \xrightarrow{\mathrm{id}_{\mathcal{V}}\otimes\alpha_{\mathcal{V}}} \mathcal{V}, \tag{B21}$$

$$\mathcal{V}^* \xrightarrow{\mathrm{id}_{\mathcal{V}^*}\otimes\beta_{\mathcal{V}}} \mathcal{V}^* \otimes (\mathcal{V} \otimes \mathcal{V}^*) \xrightarrow{\phi^{-1}} (\mathcal{V}^* \otimes \mathcal{V}) \otimes \mathcal{V}^* \xrightarrow{\alpha_{\mathcal{V}}\otimes\mathrm{id}_{\mathcal{V}^*}} \mathcal{V}^* \tag{B22}$$

equal the identity maps $\mathrm{id}_{\mathcal{V}}$ and $\mathrm{id}_{\mathcal{V}^*}$, respectively. Thus $\mathcal{V}^*$ is a *left dual* of $\mathcal{V}$ in the tensor category $\mathcal{A}$-Mod. Another representation can be constructed on V^* with ${}^*\rho = \rho(S^{-1}(a))^{\mathsf{T}}$ and ${}^*\mathcal{V} = ({}^*\rho, V^*)$ is a *right dual* of $\mathcal{V}$. The notions of left dual and right dual can be found in many references on tensor categories, such as Ref. [120].

In case that $(\mathcal{A}, \Delta, \varepsilon)$ is quasitriangular with $R = \sum_j r_j^{(1)} \otimes r_j^{(2)}$, for any two objects $\mathcal{V}_1 = (\rho_1, V_1)$ and $\mathcal{V}_2 = (\rho_2, V_2)$ in $\mathcal{A}$-Mod we can define a morphism $\mathcal{R}^{\mathcal{V}_1,\mathcal{V}_2} : \mathcal{V}_1 \otimes \mathcal{V}_2 \to \mathcal{V}_2 \otimes \mathcal{V}_1$ by

$$\mathcal{R}^{\mathcal{V}_1,\mathcal{V}_2}(v_1 \otimes v_2) := \sum_j \left(r_j^{(2)} \cdot v_2\right) \otimes \left(r_j^{(1)} \cdot v_1\right). \tag{B23}$$

The above works as a braiding for $\mathcal{A}$-Mod. For a quasitriangular quasi-Hopf algebra, it is guaranteed that ${}^*\mathcal{V}$ is equivalent to $\mathcal{V}^*$ and that the double dual $\mathcal{V}^{**}$ is equivalent to $\mathcal{V}$ [121].

4. Algebra structures of $\mathcal{D}^{\omega}(G)$

Given a finite group G, whose identity element is denoted by e, and a normalized 3-cocycle $\omega \in Z^3(G, \mathrm{U}(1))$,

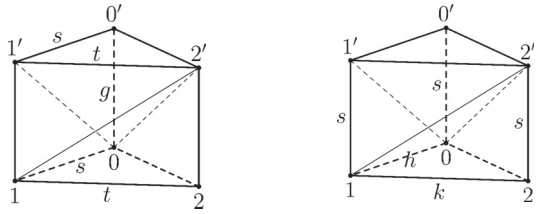

(a) $\omega_g(s,t)$ (b) $\omega^s(h,k)$

FIG. 26. Graphic representation of $\omega_g(s,t)$ and $\omega^s(h,k)$. The order of vertices is $0 < 0' < 1 < 1' < 2 < 2'$.

we can construct a quasitriangular quasi-Hopf algebra $(\mathcal{D}^\omega(G), \Delta, \varepsilon, \phi, S, \alpha, \beta, R)$. First of all, $\mathcal{D}^\omega(G)$ is a $|G|^2$-dimensional vector space over $\mathbb{C}$ with a basis denoted as $\{D_g^s\}_{g,s\in G}$. The multiplication and comultiplication laws are given by

$$D_g^s D_h^t = \delta_{g,shs^{-1}}\omega_g(s,t)D_g^{st}, \tag{B24}$$

$$\Delta\big(D_g^s\big) = \sum_{hk=g}\omega^s(h,k)D_h^s\otimes D_k^s. \tag{B25}$$

Here, $\omega_g(s,t)$ and $\omega^s(h,k)$ are phase factors defined as

$$\omega_g(s,t) := \frac{\omega(g,s,t)\omega(s,t,(st)^{-1}gst)}{\omega(s,s^{-1}gs,t)}, \tag{B26}$$

$$\omega^s(h,k) := \frac{\omega(h,k,s)\omega(s,s^{-1}hs,s^{-1}ks)}{\omega(h,s,s^{-1}ks)}. \tag{B27}$$

They correspond to the Dijkgraaf-Witten weights on the Δ-complexes with coloring shown in Fig. 26.

For convenience, we write

$$D^s := \sum_g D_g^s. \tag{B28}$$

It is evident that D^e is the unit of the algebra, where e is the identity element of G. In other words, $\mathbb{C}$ is included in $\mathcal{D}^\omega(G)$ as $\mathbb{C}D^e$; we often write 1 instead of D^e for the identity of $\mathcal{D}^\omega(G)$ for simplicity. Moreover, the counit is

$$\varepsilon : \mathcal{D}^\omega(G)\to\mathbb{C}$$
$$D_g^s \mapsto \varepsilon\big(D_g^s\big) = \delta_{g,e}. \tag{B29}$$

The Drinfeld associator is

$$\phi = \sum_{g,h,k\in G}\omega(g,h,k)^{-1}D_g^e\otimes D_h^e\otimes D_k^e. \tag{B30}$$

Further, $(\mathcal{D}^\omega(G), \Delta, \varepsilon, \phi)$ is a quasi-Hopf algebra with an antipode (S, α, β) given by

$$S\big(D_g^s\big) = \frac{1}{\omega_{g^{-1}}(s,s^{-1})\omega^s(g,g^{-1})}D^{s^{-1}}_{s^{-1}g^{-1}s}, \tag{B31}$$

$$\alpha = 1, \tag{B32}$$

$$\beta = \sum_{g\in G}\omega(g,g^{-1},g)D_g^e. \tag{B33}$$

It is also quasitriangular with

$$R = \sum_{g\in G} D_g^e\otimes D^g. \tag{B34}$$

In addition, $\mathcal{D}^\omega(G)$ is also a $*$-algebra. The Hermitian conjugate of D_g^s is given by

$$\big(D_g^s\big)^\dagger = \omega_g^*(s,s^{-1})D^{s^{-1}}_{s^{-1}gs}, \tag{B35}$$

where $\omega_g^*(s,s^{-1})$ is the complex conjugate of $\omega_g(s,s^{-1})$. Moreover, the Hermitian conjugate on $\mathcal{D}^\omega(G)\otimes\mathcal{D}^\omega(G)$ is given by

$$\big(D_g^s\otimes D_h^t\big)^\dagger = \big(D_g^s\big)^\dagger\otimes\big(D_h^t\big)^\dagger. \tag{B36}$$

It can be checked that $\forall A\in\mathcal{D}^\omega(G)$,

$$\Delta(A^\dagger) = (\Delta(A))^\dagger, \tag{B37}$$

$$\varepsilon(A^\dagger) = (\varepsilon(A))^*. \tag{B38}$$

In the main text, $\mathcal{D}^\omega(G)$ is faithfully represented, with the Hermitian conjugate respected, on a finite Hilbert space. So $\mathcal{D}^\omega(G)$ is in fact a C^*-algebra and is hence semisimple.

5. Representations of $\mathcal{D}^\omega(G)$

It is known [117] that $\mathcal{D}^\omega(G)$ is semisimple: all its representations can be decomposed into irreducible ones. Below, we construct all possible irreducible representations $\{\mathcal{V}_\mathfrak{a}\}_{\mathfrak{a}\in\mathfrak{Q}}$ of $\mathcal{D}^\omega(G)$. The index set can be $\mathfrak{Q} = \{(h,\varrho)|h\in J, \varrho\in(Z_G(h))^{\omega_h}_{\rm ir}\}$, where J is a subset of G selecting a representative for each conjugacy class and $(Z_G(h))^{\omega_h}_{\rm ir}$ selects a representative for each irreducible ω_h-representation isomorphism class of $Z_G(h) := \{g\in G|gh = hg\}$. Here $Z_G(h)$ is called the centralizer of h in G.

In detail, a ω_h representation of $Z_G(h)$ is a vector space V_ϱ equipped with a map $\varrho : Z_G(h)\to \mathrm{GL}(V_\varrho)$ satisfying $\varrho(s)\varrho(t) = \omega_h(s,t)\varrho(st)$, $\forall s,t\in G$, where $\mathrm{GL}(V_\varrho)$ is the group of all invertible linear transformations of V_ϱ. Then we can define a representation ϱ_h of $\mathcal{D}^\omega_h(G)$ on V_ϱ by

$$\varrho_h\big(D_g^s\big) = \delta_{g,h}\,\varrho(s), \tag{B39}$$

where $\mathcal{D}^\omega_h(G)$ is the subalgebra of $\mathcal{D}^\omega(G)$ spanned by $\{D_g^s|g\in G, s\in Z_G(h)\}$. Further, in short,

$$\mathcal{V}_{(h,\varrho)} = \mathcal{D}^\omega(G)\otimes_{\mathcal{D}^\omega_h(G)}V_\varrho. \tag{B40}$$

gives an explicit representation $\mathcal{V}_{(h,\varrho)}$ corresponding to $(h,\varrho)\in\mathfrak{Q}$. Moreover, an inner product can be added to $\mathcal{V}_{(h,\varrho)}$ such that $\rho_{(h,\varrho)}(A^\dagger) = (\rho_{(h,\varrho)}(A))^\dagger$, $\forall A\in\mathcal{D}^\omega(G)$.

Explicitly, we pick a representative q_j^h for each left coset of $G/Z_G(h)$. Since the conjugacy class containing h can be expressed as $[h] = \{q_j^h h(q_j^h)^{-1}\}$, the index j goes from 1 to $|[h]|$ (i.e., the cardinality of $[h]$). For convenience, we always take $q_1^h = e$. To proceed, if $\{\epsilon_i^\varrho\}_{i=1,2,\ldots,\deg\varrho}$ is a basis for V_ϱ, then so is $\{|q_j^h,\epsilon_i^\varrho\rangle := A^{q_j^h}\otimes|\epsilon_i^\varrho\rangle\}^{i=1,2,\ldots,\deg\varrho}_{j=1,2,\ldots,|[h]|}$ for $\mathcal{V}_{(h,\varrho)}$. Then the representation $\rho_{(h,\varrho)}$ on $\mathcal{V}_{(h,\varrho)}$ is given by

$$\rho_{(h,\varrho)}\big(D_g^t\big)\big|q_j^h,\epsilon_i^\varrho\big\rangle = \frac{\omega_g\big(t,q_j^h\big)}{\omega_g\big(q_k^h,s\big)}\delta_{g,tq_j^h h(tq_j^h)^{-1}}\big|q_k^h,\varrho(s)\epsilon_i^\varrho\big\rangle, \tag{B41}$$

where q_k^h and s are specified by $tq_j^h = q_k^h s$ and $s \in Z_G(h)$. Two representations $\mathcal{V}_{(h,\varrho)}$ and $\mathcal{V}_{(h',\varrho')}$ constructed this way are equivalent if h, h' are conjugate and ϱ, ϱ' are equivalent.

In addition, an inner product can be added on $\mathcal{V}_{(h,\varrho)}$ such that $\rho_{(h,\varrho)}(A^\dagger) = (\rho_{(h,\varrho)}(A))^\dagger, \forall A \in \mathcal{D}^\omega(G)$. To see this, we first apply Weyl' s unitarian trick to $(\varrho, V_\varrho) \in (Z_G(h))^{\omega_h}_{\text{ir}}$: starting with any inner product $(\cdot,\cdot) : V_\varrho \times V_\varrho \to \mathbb{C}$, we can construct a new inner product by

$$\langle v|w\rangle := \frac{\sum_{g\in Z_G(h)} (\varrho(g)v, \varrho(g)w)}{|Z_G(h)|}, \forall v, w \in V_\varrho. \tag{B42}$$

Since $\omega_h(f,g) \in \mathrm{U}(1)$, it is straightforward to see that ϱ is unitary under the new inner product $\langle\cdot|\cdot\rangle$, i.e., $\forall v, w \in V_\varrho, \forall g \in Z_G(h)$,

$$\langle\varrho(g)v|\varrho(g)w\rangle = \langle v|w\rangle. \tag{B43}$$

Further, if $\{\epsilon_i^\varrho\}_{i=1,2,\ldots,\deg\varrho}$ is an orthonormal basis for V_ϱ with respect to $\langle\cdot|\cdot\rangle$, then an inner product, also denoted $\langle\cdot|\cdot\rangle$, on $\mathcal{V}_{(h,\varrho)}$ is given by requiring that $\{|q_j^h, \epsilon_i^\varrho\rangle\}^{i=1,2,\ldots,\deg\varrho}_{j=1,2,\ldots,|[h]|}$ is orthonormal as well. It can be checked that

$$\rho_{(h,\varrho)}(A^\dagger) = (\rho_{(h,\varrho)}(A))^\dagger, \quad \forall A \in \mathcal{D}^\omega(G), \tag{B44}$$

where the two †'s denote the Hermitian conjugates for $\mathcal{D}^\omega(G)$ and operators on $(\mathcal{V}_d, \langle\cdot|\cdot\rangle)$ respectively.

Further, $\rho = \oplus_{\mathfrak{a}\in\mathfrak{Q}}\rho_\mathfrak{a}$ gives an isomorphism of algebras

$$\rho : \mathcal{D}^\omega(G) \simeq \bigoplus_{\mathfrak{a}\in\mathfrak{Q}} \mathcal{L}(\mathcal{V}_\mathfrak{a}), \tag{B45}$$

where $\mathcal{L}(\mathcal{V}_\mathfrak{a})$ is the algebra of all linear operators on $\mathcal{V}_\mathfrak{a}$ and is isomorphic to the algebra of all $\dim_\mathbb{C}\mathcal{V}_\mathfrak{a} \times \dim_\mathbb{C}\mathcal{V}_\mathfrak{a}$ matrices $M_{\dim_\mathbb{C}\mathcal{V}_\mathfrak{a}}(\mathbb{C})$. According to the Artin-Wedderburn theorem, a finite dimensional algebra over an algebraic closed field is semisimple if and only if such an isomorphism exist. The inverse of ρ, denoted γ, can be specified by its value on each basis vector $|q_j^h, \epsilon_i^\varrho\rangle\langle q_{j'}^h, \epsilon_{i'}^\varrho| \in \mathcal{L}(\mathcal{V}_{(h,\varrho)})$. To keep notations compact, we may not write γ explicitly as long as the representation is clearly carried by a vector space.

To work out the details step by step, we start with the subalgebra $\mathbb{C}[Z_G(h)]_{\omega_h}$ spanned by $\{D_h^s | s \in Z_G(h)\}$, which is a twisted group algebra and hence semisimple [122]. So we naturally write down

$$\gamma\left(|q_1^h, \epsilon_i^\varrho\rangle\langle q_1^h, \epsilon_{i'}^\varrho|\right) = \sum_{s\in Z_G(h)} \frac{\deg\varrho}{|Z_G(h)|}\langle\epsilon_{i'}^\varrho|\varrho(s)^{-1}|\epsilon_i^\varrho\rangle D_h^s. \tag{B46}$$

It can be checked that π respects the action of D_h^s for any $s \in Z_G(h)$ and that it sends $\sum_{\varrho,i}|q_1^h, \epsilon_i^\varrho\rangle\langle q_1^h, \epsilon_i^\varrho|$ to B_h. Hence $\pi \circ \rho(D_h^s) = D_h^s, \forall s \in Z_G(h)$. Also, $\rho \circ \pi$ equals the identity on $|q_1^h, \epsilon_i^\varrho\rangle\langle q_1^h, \epsilon_i^\varrho|$ by dimension counting.

In addition, we notice that

$$\langle q_{j'}^h, \epsilon_{i'}^\varrho| = \langle q_1^h, \epsilon_{i'}^\varrho|\left(D^{q_{j'}^h}\right)^\dagger = \frac{\langle q_1^h, \epsilon_i^\varrho| D_h^{(q_{j'}^h)^{-1}}}{\omega_h\left(\left(q_{j'}^h\right)^{-1}, q_{j'}^h\right)}. \tag{B47}$$

Therefore the inverse of ρ is given by

$$\begin{aligned}
&\gamma\left(|q_j^h, \epsilon_i^\varrho\rangle\langle q_{j'}^h, \epsilon_{i'}^\varrho|\right) \\
&= \gamma\left[D^{q_j^h}\frac{|q_1^h, \epsilon_i^\varrho\rangle\langle q_1^h, \epsilon_{i'}^\varrho|}{\omega_h\left((q_{j'}^h)^{-1}, q_{j'}^h\right)} D_h^{(q_{j'}^h)^{-1}}\right] \\
&= \sum_{s\in Z_G(h)} \frac{\deg\varrho}{|Z_G(h)|} D^{q_j^h} D_h^s \frac{\langle\epsilon_{i'}^\varrho|\varrho(s)^{-1}|\epsilon_i^\varrho\rangle}{\omega_h\left((q_{j'}^h)^{-1}, q_{j'}^h\right)} D_h^{(q_{j'}^h)^{-1}} \\
&= \sum_{s\in Z_G(h)} \frac{\deg\varrho}{|Z_G(h)|} \Gamma_\varrho^{i,j,i',j'}(s) D_{h_j,}^{q_j^h s (q_{j'}^h)^{-1}},
\end{aligned} \tag{B48}$$

where $h_j := q_j^h h (q_j^h)^{-1}$ and

$$\Gamma_\varrho^{i,j,i',j'}(s) := \frac{\langle\epsilon_{i'}^\varrho|\varrho(s)^{-1}|\epsilon_i^\varrho\rangle\omega_{h_j}\left(q_j^h, s\right)\omega_{h_j}\left(q_j^h s, \left(q_{j'}^h\right)^{-1}\right)}{\omega_h\left(\left(q_{j'}^h\right)^{-1}, q_{j'}^h\right)}. \tag{B49}$$

In case that G is Abelian, the basis vectors of $\mathcal{V}_{(h,\varrho)}$ can be written as $|h;\epsilon_i^\varrho\rangle := |q_1^h, \epsilon_i^\varrho\rangle$. The representation Eq. (B41) reduces to

$$\rho_{(h,\varrho)}\left(D_g^s\right)|h;\epsilon_i^\varrho\rangle = \delta_{g,h}\cdot\varrho(s)|h;\epsilon_i^\varrho\rangle, \tag{B50}$$

and the inverse of $\rho = \oplus\rho_{(h,\varrho)}$ reduces to

$$\gamma\left(|h;\epsilon_i^\varrho\rangle\langle h;\epsilon_{i'}^\varrho|\right) = \sum_{s\in G}\frac{\deg\varrho}{|G|}\langle\epsilon_{i'}^\varrho|\varrho(s)^{-1}|\epsilon_i^\varrho\rangle D_h^s. \tag{B51}$$

6. The braided tensor category $\mathcal{D}^\omega(G)$-Mod

Since $(\mathcal{D}^\omega(G), \Delta, \varepsilon, \phi, S, \alpha, \beta, R)$ is a quasitriangular quasi-Hopf algebra, its representation category $\mathcal{D}^\omega(G)$-Mod is a braided tensor category with duality. In addition, $\mathcal{D}^\omega(G)$-Mod is semisimple with finitely many isomorphism classes of simple objects. Let $\mathfrak{Q}$ label all the isomorphism classes of simple objects; irreducible representations are simple objects in a representation category. To be concrete, for each $\mathfrak{a} \in \mathfrak{Q}$, we pick an explicit representation $\mathcal{V}_a$, such as the one constructed in Appendix B 5. In particular, the trivial representation is denoted by $\mathcal{V}_\mathfrak{o}$ and the corresponding element of $\mathfrak{Q}$ is denoted by $\mathfrak{o}$. It can be checked that the dual representation $\mathcal{V}_\mathfrak{a}^*$ is also irreducible and works as both a right and left dual object of $\mathfrak{a}$. Let $\bar{\mathfrak{a}} \in \mathfrak{Q}$ label the isomorphism class of $\mathcal{V}_\mathfrak{a}^*$. By definition, $\mathcal{V}_{\bar{\mathfrak{a}}}$ is isomorphic to $\mathcal{V}_\mathfrak{a}^*$.

In the physics literature, a semisimple braided tensor category is often specified by the following data (1) fusion rule $N_{\mathfrak{a}\mathfrak{b}}^\mathfrak{c}$, (2) $6j$ symbols $F_{\mathfrak{d}\mathfrak{e}\mathfrak{f}}^{\mathfrak{a}\mathfrak{b}\mathfrak{c}}$ and (3) $\mathcal{R}$ symbols $\mathcal{R}_\mathfrak{c}^{\mathfrak{a}\mathfrak{b}}$, where $\mathfrak{a}, \mathfrak{b}, \mathfrak{c}, \mathfrak{d}, \mathfrak{e}, \mathfrak{f} \in \mathfrak{Q}$. Below, let us work out the definitions of these data for $\mathcal{D}^\omega(G)$-Mod. This can be done via the notion of a *splitting space* $V_\mathfrak{c}^{\mathfrak{a}\mathfrak{b}}$, defined as

$$V_\mathfrak{c}^{\mathfrak{a}\mathfrak{b}} := \mathrm{Hom}(\mathcal{V}_\mathfrak{c}, \mathcal{V}_\mathfrak{a}\otimes\mathcal{V}_\mathfrak{b}), \tag{B52}$$

where $\mathcal{V}_\mathfrak{a}$, $\mathcal{V}_\mathfrak{b}$, $\mathcal{V}_\mathfrak{c}$ are irreducible representations labeled by $\mathfrak{a}$, $\mathfrak{b}$, $\mathfrak{c} \in \mathfrak{Q}$. In other words, $V_\mathfrak{c}^{\mathfrak{a}\mathfrak{b}}$ is the vector space of intertwiners from $\mathcal{V}_\mathfrak{c}$ to $\mathcal{V}_\mathfrak{a}\otimes\mathcal{V}_\mathfrak{b}$.

The fusion rule $N_{\mathfrak{a}\mathfrak{b}}^\mathfrak{c}$ is just the dimension of $V_\mathfrak{c}^{\mathfrak{a}\mathfrak{b}}$, i.e.,

$$N_{\mathfrak{a}\mathfrak{b}}^\mathfrak{c} := \dim_\mathbb{C} V_\mathfrak{c}^{\mathfrak{a}\mathfrak{b}}, \tag{B53}$$

for any $\mathfrak{a},\ \mathfrak{b},\ \mathfrak{c} \in \mathfrak{Q}$. It satisfies

$$\sum_{\mathfrak{e}} N_{\mathfrak{a}\mathfrak{b}}^{\mathfrak{e}} N_{\mathfrak{e}\mathfrak{c}}^{\mathfrak{d}} = \sum_{\mathfrak{f}} N_{\mathfrak{a}\mathfrak{f}}^{\mathfrak{d}} N_{\mathfrak{b}\mathfrak{c}}^{\mathfrak{f}}, \tag{B54}$$

as a result of the isomorphism in Eq. (B60) below. The fusion rule can be viewed as the multiplication rule of the Grothendieck ring of $\mathcal{D}^{\omega}(G)$-Mod, and we write

$$\mathfrak{a} \times \mathfrak{b} = \sum_{\mathfrak{c}\in\mathfrak{Q}} N_{\mathfrak{a}\mathfrak{b}}^{\mathfrak{c}}\, \mathfrak{c}. \tag{B55}$$

Because of the isomorphism $\mathcal{R}^{\mathfrak{a}\mathfrak{b}} : \mathcal{V}_{\mathfrak{b}} \otimes \mathcal{V}_{\mathfrak{a}} \cong \mathcal{V}_{\mathfrak{a}} \otimes \mathcal{V}_{\mathfrak{b}}$, we have

$$N_{\mathfrak{a}\mathfrak{b}}^{\mathfrak{c}} = N_{\mathfrak{b}\mathfrak{a}}^{\mathfrak{c}}. \tag{B56}$$

In addition, for any semisimple braided tensor category with duality, we notice that

$$N_{\mathfrak{a}\mathfrak{b}}^{\mathfrak{o}} = \delta_{\bar{\mathfrak{a}}\mathfrak{b}}, \tag{B57}$$

which identifies $\bar{\mathfrak{a}}$ from the fusion rule.

To define $F_{\mathfrak{d}\mathfrak{e}\mathfrak{f}}^{\mathfrak{a}\mathfrak{b}\mathfrak{c}}$, we observe the isomorphisms of vector spaces

$$\bigoplus_{\mathfrak{e}\in\mathfrak{Q}} V_{\mathfrak{e}}^{\mathfrak{a}\mathfrak{b}} \otimes V_{\mathfrak{d}}^{\mathfrak{e}\mathfrak{c}} \cong \mathrm{Hom}(\mathcal{V}_{\mathfrak{d}}, (\mathcal{V}_{\mathfrak{a}} \otimes \mathcal{V}_{\mathfrak{b}}) \otimes \mathcal{V}_{\mathfrak{c}}),$$
$$\mu \otimes \nu \mapsto (\mu \otimes \mathrm{id}_{\mathfrak{c}}) \circ \nu, \tag{B58}$$
$$\bigoplus_{\mathfrak{f}\in\mathfrak{Q}} V_{\mathfrak{d}}^{\mathfrak{a}\mathfrak{f}} \otimes V_{\mathfrak{f}}^{\mathfrak{b}\mathfrak{c}} \cong \mathrm{Hom}(\mathcal{V}_{\mathfrak{d}}, \mathcal{V}_{\mathfrak{a}} \otimes (\mathcal{V}_{\mathfrak{b}} \otimes \mathcal{V}_{\mathfrak{c}})),$$
$$\kappa \otimes \lambda \mapsto (\mathrm{id}_{\mathfrak{a}} \otimes \lambda) \circ \kappa. \tag{B59}$$

Because of $\phi : (\mathcal{V}_{\mathfrak{a}} \otimes \mathcal{V}_{\mathfrak{b}}) \otimes \mathcal{V}_{\mathfrak{c}} \cong \mathcal{V}_{\mathfrak{a}} \otimes (\mathcal{V}_{\mathfrak{b}} \otimes \mathcal{V}_{\mathfrak{c}})$, we have $\mathrm{Hom}(\mathcal{V}_{\mathfrak{d}}, (\mathcal{V}_{\mathfrak{a}} \otimes \mathcal{V}_{\mathfrak{b}}) \otimes \mathcal{V}_{\mathfrak{c}}) \cong \mathrm{Hom}(\mathcal{V}_{\mathfrak{d}}, \mathcal{V}_{\mathfrak{a}} \otimes (\mathcal{V}_{\mathfrak{b}} \otimes \mathcal{V}_{\mathfrak{c}}))$. Thus there is an isomorphism of vector spaces

$$\bigoplus_{\mathfrak{e}\in\mathfrak{Q}} V_{\mathfrak{e}}^{\mathfrak{a}\mathfrak{b}} \otimes V_{\mathfrak{d}}^{\mathfrak{e}\mathfrak{c}} \cong \bigoplus_{\mathfrak{f}\in\mathfrak{Q}} V_{\mathfrak{d}}^{\mathfrak{a}\mathfrak{f}} \otimes V_{\mathfrak{f}}^{\mathfrak{b}\mathfrak{c}}. \tag{B60}$$

Restricting the isomorphism to the summand on the left-hand side corresponding to a given $\mathfrak{e} \in \mathfrak{Q}$ and projecting into the summand on the right-hand side corresponding to a given $\mathfrak{f} \in \mathfrak{Q}$, we get the homomorphism

$$F_{\mathfrak{d}\mathfrak{e}\mathfrak{f}}^{\mathfrak{a}\mathfrak{b}\mathfrak{c}} : V_{\mathfrak{e}}^{\mathfrak{a}\mathfrak{b}} \otimes V_{\mathfrak{d}}^{\mathfrak{e}\mathfrak{c}} \to V_{\mathfrak{d}}^{\mathfrak{a}\mathfrak{f}} \otimes V_{\mathfrak{f}}^{\mathfrak{b}\mathfrak{c}}, \tag{B61}$$

which is called the $6j$ symbol for $(\mathfrak{a}, \mathfrak{b}, \mathfrak{c}, \mathfrak{d}, \mathfrak{e}, \mathfrak{f}) \in \mathfrak{Q}^6$.

The R symbols $\mathcal{R}_{\mathfrak{c}}^{\mathfrak{a}\mathfrak{b}}$ are an isomorphism between $V_{\mathfrak{c}}^{\mathfrak{b}\mathfrak{a}}$ and $V_{\mathfrak{c}}^{\mathfrak{a}\mathfrak{b}}$; it is induced by the braiding $\mathcal{R}^{\mathfrak{a}\mathfrak{b}} : \mathcal{V}_{\mathfrak{b}} \otimes \mathcal{V}_{\mathfrak{a}} \to \mathcal{V}_{\mathfrak{a}} \otimes \mathcal{V}_{\mathfrak{b}}$ in the following way:

$$\mathcal{R}_{\mathfrak{c}}^{\mathfrak{a}\mathfrak{b}} : V_{\mathfrak{c}}^{\mathfrak{b}\mathfrak{a}} \to V_{\mathfrak{c}}^{\mathfrak{a}\mathfrak{b}},$$
$$\mu \mapsto \mathcal{R}^{\mathfrak{a}\mathfrak{b}} \circ \mu, \tag{B62}$$

for any $\mathfrak{a}, \mathfrak{b}, \mathfrak{c} \in \mathfrak{Q}$ and any $\mu \in V_{\mathfrak{c}}^{\mathfrak{a}\mathfrak{b}}$.

To give a matrix representation for the linear maps $F_{\mathfrak{d}\mathfrak{e}\mathfrak{f}}^{\mathfrak{a}\mathfrak{b}\mathfrak{c}}$ and $\mathcal{R}_{\mathfrak{c}}^{\mathfrak{a}\mathfrak{b}}$, we need to pick a basis for each splitting space. Thus one braided tensor category may have different matrix representations of $F_{\mathfrak{d}\mathfrak{e}\mathfrak{f}}^{\mathfrak{a}\mathfrak{b}\mathfrak{c}}$ and $\mathcal{R}_{\mathfrak{c}}^{\mathfrak{a}\mathfrak{b}}$; they are related by changes of basis, which are also referred to as *gauge transformations* sometimes in the physics literature. In order to distinguish inequivalent braided tensor categories, we want to find some useful quantities, invariant under changes of basis. The *topological spin* $\theta_{\mathfrak{a}}$ associated with each $\mathfrak{a} \in \mathfrak{Q}$ is an important one for this purpose; for $\mathcal{D}^{\omega}(G)$-Mod, it can be defined as

$$\theta_{\mathfrak{a}} := \sum_{\mathfrak{c}\in\mathfrak{Q}} \frac{\dim_{\mathbb{C}}(\mathcal{V}_{\mathfrak{c}})}{\dim_{\mathbb{C}}(\mathcal{V}_{\mathfrak{a}})} \mathrm{tr}\big(\mathcal{R}_{\mathfrak{c}}^{\mathfrak{a}\mathfrak{a}}\big), \tag{B63}$$

which is a root of unity and satisfies $\theta_{\bar{\mathfrak{a}}} = \theta_{\mathfrak{a}}$. More explicitly in terms of representations,

$$\theta_{\mathfrak{a}} = \frac{\mathrm{tr}(\mathcal{R}^{\mathfrak{a}\mathfrak{a}})}{\dim_{\mathbb{C}}(\mathcal{V}_{\mathfrak{a}})} = \frac{\mathrm{tr}(\wp R, \mathcal{V}_{\mathfrak{a}} \otimes \mathcal{V}_{\mathfrak{a}})}{\dim_{\mathbb{C}}(\mathcal{V}_{\mathfrak{a}})}, \tag{B64}$$

where $\wp$ is the operator permuting the two factors $\mathcal{V}_{\mathfrak{a}} \otimes \mathcal{V}_{\mathfrak{a}}$ and R is the universal R matrix of $\mathcal{D}^{\omega}(G)$. The topological spins are often collected into a matrix form $\mathcal{T}_{\mathfrak{a}\mathfrak{b}} = \theta_{\mathfrak{a}}\delta_{\mathfrak{a}\mathfrak{b}}, \forall \mathfrak{a}, \mathfrak{b} \in \mathfrak{Q}$, which is called the *topological T matrix*. It is well-known that the R symbols satisfy the "ribbon property"

$$\mathcal{R}_{\mathfrak{c}}^{\mathfrak{a}\mathfrak{b}} \mathcal{R}_{\mathfrak{c}}^{\mathfrak{b}\mathfrak{a}} = \frac{\theta_{\mathfrak{c}}}{\theta_{\mathfrak{a}}\theta_{\mathfrak{b}}} \mathrm{id}_{V_{\mathfrak{c}}^{\mathfrak{a}\mathfrak{b}}}. \tag{B65}$$

The *topological S matrix* $\mathcal{S} = (\mathcal{S}_{\mathfrak{a}\mathfrak{b}})_{\mathfrak{a},\mathfrak{b}\in\mathfrak{Q}}$ is another important quantity. For $\mathcal{D}^{\omega}(G)$-Mod, its matrix element $\mathcal{S}_{\mathfrak{a}\mathfrak{b}}, \forall \mathfrak{a}, \mathfrak{b} \in \mathfrak{Q}$ is defined as

$$\mathcal{S}_{\mathfrak{a}\mathfrak{b}} := \frac{1}{\mathcal{D}} \sum_{\mathfrak{c}\in\mathfrak{Q}} \dim_{\mathbb{C}}(\mathcal{V}_{\mathfrak{c}}) \mathrm{tr}\big(\mathcal{R}_{\mathfrak{c}}^{\bar{\mathfrak{a}}\mathfrak{b}} \mathcal{R}_{\mathfrak{c}}^{\mathfrak{b}\bar{\mathfrak{a}}}\big)$$
$$= \frac{1}{\mathcal{D}} \sum_{\mathfrak{c}\in\mathfrak{Q}} N_{\bar{\mathfrak{a}}\mathfrak{b}}^{\mathfrak{c}} \frac{\theta_{\mathfrak{c}}}{\theta_{\mathfrak{a}}\theta_{\mathfrak{b}}} \dim_{\mathbb{C}}(\mathcal{V}_{\mathfrak{c}}), \tag{B66}$$

$$\mathcal{D} := \sqrt{\sum_{\mathfrak{c}\in\mathfrak{Q}} [\dim_{\mathbb{C}}(\mathcal{V}_{\mathfrak{c}})]^2} = |G|. \tag{B67}$$

Given the topological S matrix, we can recover the fusion rule by the Verlinde formula [14,38,123]

$$N_{\mathfrak{a}\mathfrak{b}}^{\mathfrak{c}} = \sum_{\mathfrak{q}\in\mathfrak{Q}} \frac{\mathcal{S}_{\mathfrak{a}\mathfrak{q}} \mathcal{S}_{\mathfrak{b}\mathfrak{q}} \mathcal{S}_{\bar{\mathfrak{c}}\mathfrak{q}}}{\mathcal{S}_{\mathfrak{o}\mathfrak{q}}}. \tag{B68}$$

The topological T matrix and S matrix are also called the modular invariants, as they are closely related to the modular transformations [108,109].

7. Examples of $\mathcal{D}^{\omega}(G)$ and $\mathcal{D}^{\omega}(G)$-Mod

Below, let us study several concrete examples of $\mathcal{D}^{\omega}(G)$ and its representation category $\mathcal{D}^{\omega}(G)$-Mod.

a. $\mathcal{D}(\mathbb{Z}_2)$

Picking $G = \mathbb{Z}_2 = \{0, 1\}$ and ω trivial, we get the quantum double algebra $\mathcal{D}(\mathbb{Z}_2)$. Its four inequivalent irreducible representations, given by Eq. (B50), are

$$\rho_g^{\lambda}(D_h^s) = \delta_{g,h} \cdot e^{i\pi\lambda s}, \tag{B69}$$

labeled by $(g, \lambda) \in \mathbb{Z}_2 \times \mathbb{Z}_2 \equiv \mathfrak{Q}$, all of which are one-dimensional. For example,

$$\rho_0^1(D_0^1) = e^{i\pi(1\times 1)} = -1. \tag{B70}$$

In the notation widely used in the toric code model, the four simple objects $(0, 0), (0, 1), (1, 0), (1, 1)$ in $\mathcal{D}(\mathbb{Z}_2)$-Mod are denoted by $\mathfrak{1}$, $\mathfrak{e}$, $\mathfrak{m}$, $\boldsymbol{\varepsilon}$, respectively [15].

The fusion rule is given by

$$(g_1, \lambda_1) \times (g_2, \lambda_2) = (g_1 + g_2, \lambda_1 + \lambda_2). \tag{B71}$$

In other words,

$$\mathfrak{e} \times \mathfrak{e} = \mathfrak{m} \times \mathfrak{m} = \boldsymbol{\varepsilon} \times \boldsymbol{\varepsilon} = \mathfrak{1}, \tag{B72}$$

$$\mathfrak{e} \times \mathfrak{m} = \boldsymbol{\varepsilon}, \quad \mathfrak{e} \times \boldsymbol{\varepsilon} = \mathfrak{m}, \quad \mathfrak{m} \times \boldsymbol{\varepsilon} = \mathfrak{e}. \tag{B73}$$

The unit object is $\mathbf{1} \equiv (0, 0)$ and $\bar{\mathfrak{a}} = \mathfrak{a}, \forall \mathfrak{a} \in \mathfrak{Q}$.

All $6j$ symbols, allowed by fusion rules, equal 1. The R symbols are given by

$$\mathcal{R}^{(g_1,\lambda_1)(g_2,\lambda_2)} = e^{i\pi\lambda_1 g_2}, \tag{B74}$$

where we omit $\mathfrak{c}$ in $\mathcal{R}_{\mathfrak{c}}^{\mathfrak{a}\mathfrak{b}}$ since $\mathfrak{c}$ is uniquely determined by $\mathfrak{a}$ and $\mathfrak{b}$. Then Eq. (B63) gives the topological spins

$$(\theta_{\mathfrak{1}}, \theta_{\mathfrak{e}}, \theta_{\mathfrak{m}}, \theta_{\boldsymbol{\varepsilon}}) = (1, 1, 1, -1). \tag{B75}$$

By Eq. (B66), the topological S matrix is given by

$$\mathcal{S}_{\mathfrak{a}\mathfrak{b}} = \frac{1}{2}\frac{\theta_{\mathfrak{a}\times\mathfrak{b}}}{\theta_{\mathfrak{a}}\theta_{\mathfrak{b}}}. \tag{B76}$$

In general, $\mathcal{R}^{\mathfrak{a}\mathfrak{b}}\mathcal{R}^{\mathfrak{b}\mathfrak{a}}$ is a scalar multiplication by $\frac{\theta_{\mathfrak{a}\times\mathfrak{b}}}{\theta_{\mathfrak{a}}\theta_{\mathfrak{b}}}$. For $\mathcal{D}^{\omega}(\mathbb{Z}_2)$-Mod, we notice that $\mathcal{R}^{\mathfrak{a}\mathfrak{a}}$ is a scalar multiplication by $\theta_{\mathfrak{a}}$.

b. $\mathcal{D}^{\omega}(\mathbb{Z}_2)$ with $\omega(1, 1, 1) = -1$

The nontrivial element of $H^3(G, \mathrm{U}(1)) = \mathbb{Z}_2$ for $G = \mathbb{Z}_2 = \{0, 1\}$ is represented by the normalized 3-cocycle

$$\omega(g, h, k) = \begin{cases} -1, & g = h = k = 1, \\ 1, & \text{otherwise}. \end{cases} \tag{B77}$$

Different from $\mathcal{D}(\mathbb{Z}_2)$, in $\mathcal{D}^{\omega}(\mathbb{Z}_2)$, we have $D_1^1 D_1^1 = -D_1^0$ because $\omega_1(1, 1) = -1$ by the definition in Eq. (B26).

The irreducible representations of $\mathcal{D}^{\omega}(\mathbb{Z}_2)$ are

$$\rho_g^{\lambda}(D_h^s) = \delta_{g,h} \cdot i^g \cdot e^{i\pi\lambda s}, \tag{B78}$$

labeled by $(g, \lambda) \in \mathbb{Z}_2 \times \mathbb{Z}_2 \equiv \mathfrak{Q}$. For example, we have

$$\rho_1^0(D_h^s) = i\delta_{1,h}. \tag{B79}$$

The fusion rule is still

$$(g_1, \lambda_1) \times (g_2, \lambda_2) = (g_1 + g_2, \lambda_1 + \lambda_2). \tag{B80}$$

The unit object is $(0, 0)$ and $\overline{(g, \lambda)} = (g, \lambda)$.

Suppose that $\mathcal{V}_{(g,\lambda)}$ is spanned by e_g^{λ}. Then $e_{g_1+g_2}^{\lambda_1+\lambda_2} \mapsto e_{g_1}^{\lambda_1} \otimes e_{g_2}^{\lambda_2}$ spans $V_{(g_1+g_2,\lambda_1+\lambda_2)}^{(g_1,\lambda_1)(g_2,\lambda_2)}$. Using such a basis for each splitting space and noticing that

$$\rho_{g_1}^{\lambda_1} \otimes \rho_{g_2}^{\lambda_2} \otimes \rho_{g_3}^{\lambda_3}(\phi) = \begin{cases} -1, & g_1 = g_2 = g_3 = 1, \\ 1, & \text{otherwise}, \end{cases} \tag{B81}$$

we have

$$F^{(g_1,\lambda_1)(g_2,\lambda_2)(g_3,\lambda_3)} = \begin{cases} -1, & g_1 = g_2 = g_3 = 1, \\ 1, & \text{otherwise}, \end{cases} \tag{B82}$$

where $\mathfrak{e}$, $\mathfrak{d}$, $\mathfrak{f}$ are omitted in $F_{\mathfrak{e}df}^{\mathfrak{a}bc}$ as they are uniquely determined by $\mathfrak{a}$, $\mathfrak{b}$, $\mathfrak{c}$.

By Eq. (B23), we directly read the R matrix

$$\mathcal{R}^{(g_1,\lambda_1)(g_2,\lambda_2)} = \sum_g \rho_{g_2}^{\lambda_2}(D^g) \otimes \rho_{g_1}^{\lambda_1}(D_g^e) = i^{g_2} \cdot e^{i\pi\lambda_2 g_1} \tag{B83}$$

from the universal R matrix $R = \sum_g D_g^e \otimes D^g$ with $D^s := \sum_g D_g^s$. Then Eq. (B63) gives the topological spins

$$(\theta_{(0,0)}, \theta_{(0,1)}, \theta_{(1,0)}, \theta_{(1,1)}) = (1, 1, i, -i). \tag{B84}$$

Hence, the simple objects $(1, 0)$ and $(1, 1)$ are often called semions. In addition, Eq. (B66) gives the topological S matrix

$$\mathcal{S}_{\mathfrak{a}\mathfrak{b}} = \frac{1}{2}\frac{\theta_{\mathfrak{a}\times\mathfrak{b}}}{\theta_{\mathfrak{a}}\theta_{\mathfrak{b}}}. \tag{B85}$$

In general, $\mathcal{R}^{\mathfrak{a}\mathfrak{b}}\mathcal{R}^{\mathfrak{b}\mathfrak{a}}$ is a scalar multiplication by $\frac{\theta_{\mathfrak{a}\times\mathfrak{b}}}{\theta_{\mathfrak{a}}\theta_{\mathfrak{b}}}$. For $\mathcal{D}^{\omega}(\mathbb{Z}_2)$-Mod, we notice that $\mathcal{R}^{\mathfrak{a}\mathfrak{a}}$ is a scalar multiplication by $\theta_{\mathfrak{a}}$.

c. $\mathcal{D}^{\omega}(\mathbb{Z}_2^3)$ with $\omega(g, h, k) = e^{i\pi g^{(1)}h^{(2)}k^{(3)}}$

This gives an example in which not all irreducible representations are one-dimensional, even though G itself is Abelian. The three $\mathbb{Z}_2$ components of $g \in G = \mathbb{Z}_2^3 = \mathbb{Z}_2 \times \mathbb{Z}_2 \times \mathbb{Z}_2$ are denoted by $g^{(1)}, g^{(2)}, g^{(3)}$. To keep notations compact, we will use 100 short for $(1, 0, 0) \in G$; thus, the eight group elements are also denoted 000, 100, 010, 001, 110, 011, 101, 111. Moreover, we write 0 short for 000 when it is clear from context. As G is Abelian, Eqs. (B26) and (B27) define a normalized 2-cocycle $\omega_g = \omega^g \in Z^2(G, \mathrm{U}(1))$ for each fixed $g \in G$. Explicitly,

$$\omega_g(h, k) = e^{i\pi(g^{(1)}h^{(2)}k^{(3)} - h^{(1)}k^{(2)}g^{(3)} + k^{(1)}g^{(2)}h^{(3)})}. \tag{B86}$$

Whenever $g \neq 0$, we notice $[\omega_g]$ corresponds to a nontrivial element of $H^2(G, \mathrm{U}(1))$.

In total, $\mathcal{D}^{\omega}(G)$ has 22 inequivalent irreducible representations. Eight of them are one-dimensional, labeled as ρ_0^{λ} with $\lambda = (\lambda^{(1)}, \lambda^{(2)}, \lambda^{(3)}) \in \mathbb{Z}_2^3$; explicitly,

$$\rho_0^{\lambda}(D_h^s) = \delta_{0,h}\, e^{i\pi\lambda\cdot s}, \tag{B87}$$

where $\lambda \cdot s := \lambda^{(1)}s^{(1)} + \lambda^{(2)}s^{(2)} + \lambda^{(3)}s^{(3)} \pmod 2$. The other fourteen irreducible representations are two-dimensional, labeled as ρ_g^+ and ρ_g^- with $g \neq 0$ in $\mathbb{Z}_2^3$; they can be specified by the action of $D_h^{100}, D_h^{010}, D_h^{001}$ as shown in Table I.

TABLE I. Two-dimensional irreducible representations of $\mathcal{D}^{\omega}(\mathbb{Z}_2^3)$ with $\omega(g, h, k) = e^{i\pi g^{(1)}h^{(2)}k^{(3)}}$, specified by the action of a set of generators. The 2×2 identity matrix and the Pauli matrices are denoted by σ_0, σ_1, σ_2, σ_3, respectively. The topological spin θ of each irreducible representation is listed in the last column.

	D_h^{100}	D_h^{010}	D_h^{001}	θ
$\rho_{100}^{\pm}$	$\pm\delta_{100,h} \cdot \sigma_0$	$\delta_{100,h} \cdot \sigma_1$	$\delta_{100,h} \cdot \sigma_3$	± 1
$\rho_{010}^{\pm}$	$\delta_{010,h} \cdot \sigma_3$	$\pm\delta_{010,h} \cdot \sigma_0$	$\delta_{010,h} \cdot \sigma_1$	± 1
$\rho_{001}^{\pm}$	$\delta_{001,h} \cdot \sigma_1$	$\delta_{001,h} \cdot \sigma_3$	$\pm\delta_{001,h} \cdot \sigma_0$	± 1
$\rho_{011}^{\pm}$	$\delta_{011,h} \cdot \sigma_3$	$\delta_{011,h} \cdot \sigma_1$	$\pm\delta_{011,h} \cdot \sigma_1$	± 1
$\rho_{101}^{\pm}$	$\pm\delta_{101,h} \cdot \sigma_1$	$\delta_{101,h} \cdot \sigma_3$	$\delta_{101,h} \cdot \sigma_1$	± 1
$\rho_{110}^{\pm}$	$\delta_{110,h} \cdot \sigma_1$	$\pm\delta_{110,h} \cdot \sigma_1$	$\delta_{110,h} \cdot \sigma_3$	± 1
$\rho_{111}^{\pm}$	$\pm\delta_{111,h} \cdot \sigma_1$	$\pm\delta_{111,h} \cdot \sigma_2$	$\pm\delta_{111,h} \cdot \sigma_3$	$\mp i$

The corresponding representation isomorphism classes are denoted by $(0,\lambda)$ for $\lambda\in\mathbb{Z}_2^3$ and $(g,\pm)\equiv(g,\pm 1)$ for $g\in\mathbb{Z}_2^3$, $g\neq 0$.

The dual of each simple object is isomorphic to itself; in particular, each two dimensional irreducible representation fuses with itself as

$$(100,\pm)^2=\mathfrak{o}+(0,010)+(0,001)+(0,011), \tag{B88}$$

$$(010,\pm)^2=\mathfrak{o}+(0,001)+(0,100)+(0,101), \tag{B89}$$

$$(001,\pm)^2=\mathfrak{o}+(0,100)+(0,010)+(0,110), \tag{B90}$$

$$(011,\pm)^2=\mathfrak{o}+(0,100)+(0,011)+(0,111), \tag{B91}$$

$$(101,\pm)^2=\mathfrak{o}+(0,010)+(0,101)+(0,111), \tag{B92}$$

$$(110,\pm)^2=\mathfrak{o}+(0,001)+(0,110)+(0,111), \tag{B93}$$

$$(111,\pm)^2=\mathfrak{o}+(0,110)+(0,101)+(0,011), \tag{B94}$$

where $\mathfrak{o}=(0,0)$ denotes the unit object. We notice that Eqs. (B88)–(B90) and Eqs. (B91)–(B93) are related by permuting components of $g,\lambda\in\mathbb{Z}_2^3$. In addition, $(g,\pm)\times(g,\mp)$ equals the sum of one-dimensional representations that do not appear in $(g,\pm)\times(g,\pm)$. For example,

$$\begin{aligned}&(100,\pm)\times(100,\mp)\\&\quad=(0,100)+(0,110)+(0,101)+(0,111).\end{aligned} \tag{B95}$$

The rest of the fusion rules are

$$(0,\lambda)\times(0,\mu)=(0,\lambda+\mu), \tag{B96}$$

$$(0,\lambda)\times(g,\pm)=(g,\pm e^{i\pi\lambda\cdot g}), \tag{B97}$$

$$(g,\kappa)\times(h,\kappa')=(g+h,+)+(g+h,-) \tag{B98}$$

for $g,\ h\neq 0$, $g\neq h$ in G, and $\kappa,\ \kappa'=\pm$.

For $6j$ symbols, let us compute $F^{\mathfrak{a}\mathfrak{a}\mathfrak{a}\mathfrak{a}}_{\mathfrak{a}ef}$ with $\mathfrak{a}=(111,\pm)$ as an example. In the current category, all allowed splitting spaces are one-dimensional. We pick a basis for each splitting space relevant here as follows:

$$\mu_0:=\frac{1}{\sqrt{2}}(0,1,-1,0)^T\in V^{\mathfrak{a}\mathfrak{a}}_{(0,000)}, \tag{B99}$$

$$\mu_1:=\frac{1}{\sqrt{2}}(1,0,0,-1)^T\in V^{\mathfrak{a}\mathfrak{a}}_{(0,011)}, \tag{B100}$$

$$\mu_2:=\frac{1}{\sqrt{2}}(1,0,0,1)^T\in V^{\mathfrak{a}\mathfrak{a}}_{(0,101)}, \tag{B101}$$

$$\mu_3:=\frac{1}{\sqrt{2}}(0,1,1,0)^T\in V^{\mathfrak{a}\mathfrak{a}}_{(0,110)}, \tag{B102}$$

$$\sigma_0=\begin{pmatrix}1&0\\0&1\end{pmatrix}\in V_{\mathfrak{a}}^{(0,000)\mathfrak{a}},V_{\mathfrak{a}}^{\mathfrak{a}(0,000)}, \tag{B103}$$

$$\sigma_1=\begin{pmatrix}0&1\\1&0\end{pmatrix}\in V_{\mathfrak{a}}^{(0,011)\mathfrak{a}},V_{\mathfrak{a}}^{\mathfrak{a}(0,011)}, \tag{B104}$$

$$\sigma_2=\begin{pmatrix}0&-i\\i&0\end{pmatrix}\in V_{\mathfrak{a}}^{(0,101)\mathfrak{a}},V_{\mathfrak{a}}^{\mathfrak{a}(0,101)}, \tag{B105}$$

$$\sigma_3=\begin{pmatrix}1&0\\0&-1\end{pmatrix}\in V_{\mathfrak{a}}^{(0,110)\mathfrak{a}},V_{\mathfrak{a}}^{\mathfrak{a}(0,110)}, \tag{B106}$$

where the intertwiners are presented in matrix form. From Eq. (B58), we get that $\{(\mu_j\otimes\mathrm{id}_{\mathfrak{a}})\sigma_j\}_{j=0,1,2,3}$ forms a basis of $\mathrm{Hom}(\mathcal{V}_{\mathfrak{a}},(\mathcal{V}_{\mathfrak{a}}\otimes\mathcal{V}_{\mathfrak{a}})\otimes\mathcal{V}_{\mathfrak{a}})$. By the Drinfeld associator $(\rho^{\pm}_{111}\otimes\rho^{\pm}_{111}\otimes\rho^{\pm}_{111})(\phi)=-1$, the basis is converted into $\{\psi_j:=-(\mu_j\otimes\mathrm{id}_{\mathfrak{a}})\sigma_j\}_{j=0,1,2,3}$ as a basis of $\mathrm{Hom}(\mathcal{V}_{\mathfrak{a}},\mathcal{V}_{\mathfrak{a}}\otimes(\mathcal{V}_{\mathfrak{a}}\otimes\mathcal{V}_{\mathfrak{a}}))$. On the other hand, $\{\varphi_j:=(\mathrm{id}_{\mathfrak{a}}\otimes\mu_j)\sigma_j\}_{j=0,1,2,3}$ forms another basis of $\mathrm{Hom}(\mathcal{V}_{\mathfrak{a}},\mathcal{V}_{\mathfrak{a}}\otimes(\mathcal{V}_{\mathfrak{a}}\otimes\mathcal{V}_{\mathfrak{a}}))$ from Eq. (B59). It is straightforward to check

$$\psi_j^{\dagger}\psi_{j'}=\delta_{jj'}\mathrm{id}_{\mathfrak{a}},\ \forall j,\ j'=0,\ 1,\ 2,\ 3; \tag{B107}$$

$$\varphi_j^{\dagger}\varphi_{j'}=\delta_{jj'}\mathrm{id}_{\mathfrak{a}},\ \forall j,\ j'=0,\ 1,\ 2,\ 3. \tag{B108}$$

Then, the 4×4 matrix $(F^{\mathfrak{a}\mathfrak{a}\mathfrak{a}\mathfrak{a}}_{\mathfrak{a}})_{\mathfrak{e},\mathfrak{f}}:=F^{\mathfrak{a}\mathfrak{a}\mathfrak{a}\mathfrak{a}}_{\mathfrak{a}ef}$, for $\mathfrak{e},\ \mathfrak{f}=(0,000),(0,011),(0,101),(0,110)$, describes the basis transformation; thus,

$$\begin{aligned}\left(F^{\mathfrak{a}\mathfrak{a}\mathfrak{a}\mathfrak{a}}_{\mathfrak{a}}\right)_{\mathfrak{e},\mathfrak{f}}&=(\langle\varphi_j|\psi_{j'}\rangle)_{j,j'}\\&=\frac{1}{2}\begin{pmatrix}1&-1&-i&1\\1&-1&i&-1\\-i&-i&-1&i\\-1&-1&-i&-1\end{pmatrix},\end{aligned} \tag{B109}$$

where $\langle\varphi_j|\psi_{j'}\rangle$ is defined by $\varphi_j^{\dagger}\psi_{j'}=\langle\varphi_j|\psi_{j'}\rangle\mathrm{id}_{\mathfrak{a}}$. For example, $F^{\mathfrak{a}\mathfrak{a}\mathfrak{a}\mathfrak{a}}_{\mathfrak{a}(0,000)(0,011)}=-\frac{1}{2}$. All the other $6j$ symbols can be computed in this way.

The universal R matrix $R=\sum_g D^e_g\otimes D^g$ is elegant enough to describe braidings; we will not list all $\mathcal{R}^{\mathfrak{a}\mathfrak{b}}_{\mathfrak{c}}$, which can be obtained by a well-defined but tedious computation from R. To illustrate the computation, let us calculate $\mathcal{R}^{\mathfrak{a}\mathfrak{a}}_{\mathfrak{c}}$ with $\mathfrak{a}=(0,111)$ as an example. Given by Eq. (B23), the matrix form of $\mathcal{R}^{\mathfrak{a}\mathfrak{a}}:\mathcal{V}_{\mathfrak{a}}\otimes\mathcal{V}_{\mathfrak{a}}\to\mathcal{V}_{\mathfrak{a}}\otimes\mathcal{V}_{\mathfrak{a}}$ is

$$\begin{aligned}\mathcal{R}^{\mathfrak{a}\mathfrak{a}}&=(\rho^{\pm}_{111}(D^{111})\otimes\mathrm{id}_{\mathfrak{a}})\wp,\\&=\mp i\begin{pmatrix}1&0&0&0\\0&0&1&0\\0&1&0&0\\0&0&0&1\end{pmatrix},\end{aligned} \tag{B110}$$

where $\wp:\mathcal{V}_{\mathfrak{a}}\otimes\mathcal{V}_{\mathfrak{a}}\to\mathcal{V}_{\mathfrak{a}}\otimes\mathcal{V}_{\mathfrak{a}}$ is the exchange of the two factors and

$$\begin{aligned}\rho^{\pm}_{111}(D^{111})&=\rho^{\pm}_{111}(D^{111}_{111})=\rho^{\pm}_{111}(D^{100}_{111}D^{011}_{111})\\&=\rho^{\pm}_{111}(-D^{100}_{111}D^{010}_{111}D^{001}_{111})=\mp\sigma_1\sigma_2\sigma_3=\mp i.\end{aligned} \tag{B111}$$

Using Eqs. (B99)–(B102) and (B62), we get

$$\mathcal{R}^{\mathfrak{a}\mathfrak{a}}_{\mathfrak{o}}=\pm i\cdot\mathrm{id}_{V^{\mathfrak{a}\mathfrak{a}}_{\mathfrak{o}}},\quad \mathcal{R}^{\mathfrak{a}\mathfrak{a}}_{\mathfrak{c}}=\mp i\cdot\mathrm{id}_{V^{\mathfrak{a}\mathfrak{a}}_{\mathfrak{c}}}, \tag{B112}$$

where $\mathfrak{c}=(0,011)$, $(0,101)$, or $(0,110)$. Thus the topological spin of $\mathfrak{a}=(111,\pm)$, defined by Eq. (B63), is

$$\theta_{(111,\pm)}=\mp i. \tag{B113}$$

The topological spins of all two-dimensional irreducible representations are listed in Table I, while all the topological spins of one-dimensional representations are 1. Given the topological spins and the fusion rules, we can read off the topological S matrix from Eq. (B66).

[1] D. C. Tsui, H. L. Stormer, and A. C. Gossard, Two-Dimensional Magnetotransport in the Extreme Quantum Limit, Phys. Rev. Lett. **48**, 1559 (1982).

[2] R. B. Laughlin, Anomalous Quantum Hall Effect: An Incompressible Quantum Fluid with Fractionally Charged Excitations, Phys. Rev. Lett. **50**, 1395 (1983).

[3] M. Levin and X.-G. Wen, Detecting Topological Order in a Ground State Wave Function, Phys. Rev. Lett. **96**, 110405 (2006).

[4] A. Kitaev and J. Preskill, Topological Entanglement Entropy, Phys. Rev. Lett. **96**, 110404 (2006).

[5] X. Chen, Z.-C. Gu, and X.-G. Wen, Local unitary transformation, long-range quantum entanglement, wave function renormalization, and topological order, Phys. Rev. B **82**, 155138 (2010).

[6] G. Moore and N. Read, Nonabelions in the fractional quantum hall effect, Nucl. Phys. B **360**, 362 (1991).

[7] X.-G. Wen and Q. Niu, Ground-state degeneracy of the fractional quantum hall states in the presence of a random potential and on high-genus riemann surfaces, Phys. Rev. B **41**, 9377 (1990).

[8] X.-G. Wen, Quantum orders and symmetric spin liquids, Phys. Rev. B **65**, 165113 (2002).

[9] R. Moessner, S. L. Sondhi, and E. Fradkin, Short-ranged resonating valence bond physics, quantum dimer models, and ising gauge theories, Phys. Rev. B **65**, 024504 (2001).

[10] L. Balents, M. P. A. Fisher, and S. M. Girvin, Fractionalization in an easy-axis kagome antiferromagnet, Phys. Rev. B **65**, 224412 (2002).

[11] T. H. Hansson, V. Oganesyan, and S. L. Sondhi, Superconductors are topologically ordered, Ann. Phys. **313**, 497 (2004).

[12] N. Read and D. Green, Paired states of fermions in two dimensions with breaking of parity and time-reversal symmetries and the fractional quantum hall effect, Phys. Rev. B **61**, 10267 (2000).

[13] A. Y. Kitaev, Unpaired majorana fermions in quantum wires, Phys.- Usp. **44**, 131 (2001).

[14] A. Kitaev, Anyons in an exactly solved model and beyond, Ann. Phys. **321**, 2 (2006).

[15] A. Y. Kitaev, Fault-tolerant quantum computation by anyons, Ann. Phys. **303**, 2 (2003),

[16] H. Bombin and M. A. Martin-Delgado, Topological Quantum Distillation, Phys. Rev. Lett. **97**, 180501 (2006).

[17] H. Bombin and M. A. Martin-Delgado, Topological Computation without Braiding, Phys. Rev. Lett. **98**, 160502 (2007).

[18] C. Nayak, S. H. Simon, A. Stern, M. Freedman, and S. Das Sarma, Non-Abelian anyons and topological quantum computation, Rev. Mod. Phys. **80**, 1083 (2008).

[19] X. Chen, Z.-C. Gu, Z.-X. Liu, and X.-G. Wen, Symmetry-protected topological orders in interacting bosonic systems, Science **338**, 1604 (2012).

[20] X. Chen, Z.-C. Gu, Z.-X. Liu, and X.-G. Wen, Symmetry protected topological orders and the group cohomology of their symmetry group, Phys. Rev. B **87**, 155114 (2013).

[21] F. D. M. Haldane, Continuum dynamics of the 1-d heisenberg antiferromagnet: Identification with the o(3) nonlinear sigma model, Phys. Lett. A **93**, 464 (1983).

[22] I. Affleck, T. Kennedy, E. H. Lieb, and H. Tasaki, Valence bond ground states in isotropic quantum antiferromagnets, Comm. Math. Phys. **115**, 477 (1988).

[23] F. Verstraete, M. A. Martin-Delgado, and J. I. Cirac, Diverging Entanglement Length in Gapped Quantum Spin Systems, Phys. Rev. Lett. **92**, 087201 (2004).

[24] F. Pollmann, E. Berg, A. M. Turner, and M. Oshikawa, Symmetry protection of topological phases in one-dimensional quantum spin systems, Phys. Rev. B **85**, 075125 (2012).

[25] Z.-C. Gu and X.-G. Wen, Tensor-entanglement-filtering renormalization approach and symmetry-protected topological order, Phys. Rev. B **80**, 155131 (2009).

[26] C. L. Kane and E. J. Mele, Z_2 Topological Order and the Quantum Spin Hall Effect, Phys. Rev. Lett. **95**, 146802 (2005).

[27] B. A. Bernevig, T. L. Hughes, and S.-C. Zhang, Quantum spin hall effect and topological phase transition in hgte quantum wells, Science **314**, 1757 (2006).

[28] L. Fu, C. L. Kane, and E. J. Mele, Topological Insulators in Three Dimensions, Phys. Rev. Lett. **98**, 106803 (2007).

[29] R. Roy, Topological phases and the quantum spin hall effect in three dimensions, Phys. Rev. B **79**, 195322 (2009).

[30] J. E. Moore and L. Balents, Topological invariants of time-reversal-invariant band structures, Phys. Rev. B **75**, 121306 (2007).

[31] M. Z. Hasan and C. L. Kane, Colloquium: Topological insulators, Rev. Mod. Phys. **82**, 3045 (2010).

[32] X.-L. Qi and S.-C. Zhang, Topological insulators and superconductors, Rev. Mod. Phys. **83**, 1057 (2011).

[33] A. Vishwanath and T. Senthil, Physics of Three-Dimensional Bosonic Topological Insulators: Surface-Deconfined Criticality and Quantized Magnetoelectric Effect, Phys. Rev. X **3**, 011016 (2013).

[34] M. A. Metlitski, C. L. Kane, and M. P. A. Fisher, Bosonic topological insulator in three dimensions and the statistical witten effect, Phys. Rev. B **88**, 035131 (2013).

[35] S. Moroz, A. Prem, V. Gurarie, and L. Radzihovsky, Topological order, symmetry, and hall response of two-dimensional spin-singlet superconductors, Phys. Rev. B **95**, 014508 (2017).

[36] A. Mesaros and Y. Ran, Classification of symmetry enriched topological phases with exactly solvable models, Phys. Rev. B **87**, 155115 (2013).

[37] A. M. Essin and M. Hermele, Classifying fractionalization: Symmetry classification of gapped $\mathbb{z}_2$ spin liquids in two dimensions, Phys. Rev. B **87**, 104406 (2013).

[38] M. Barkeshli, P. Bonderson, M. Cheng, and Z. Wang, Symmetry, defects, and gauging of topological phases, arXiv:1410.4540.

[39] Y.-M. Lu and A. Vishwanath, Classification and properties of symmetry-enriched topological phases: Chern-simons approach with applications to Z_2 spin liquids, Phys. Rev. B **93**, 155121 (2016).

[40] H. Song and M. Hermele, Space-group symmetry fractionalization in a family of exactly solvable models with $\mathbb{z}_2$ topological order, Phys. Rev. B **91**, 014405 (2015).

[41] H. Song, Interplay between Symmetry and Topological Order in Quantum Spin Systems, Ph.D. thesis, University of Colorado Boulder, 2015.

[42] H. Song, S.-J. Huang, L. Fu, and M. Hermele, Topological Phases Protected by Point Group Symmetry, Phys. Rev. X **7**, 011020 (2017).

[43] E. Rowell, R. Stong, and Z. Wang, On classification of modular tensor categories, Commun. Math. Phys. **292**, 343 (2009).

[44] F. A. Bais, B. J. Schroers, and J. K. Slingerland, Broken Quantum Symmetry and Confinement Phases in Planar Physics, Phys. Rev. Lett. **89**, 181601 (2002).
[45] H. Bombin and M. A. Martin-Delgado, Family of non-abelian kitaev models on a lattice: Topological condensation and confinement, Phys. Rev. B **78**, 115421 (2008).
[46] H. Bombin and M. A. Martin-Delgado, Nested topological order, New J. Phys. **13**, 125001 (2011).
[47] A. Hamma, P. Zanardi, and X.-G. Wen, String and membrane condensation on three-dimensional lattices, Phys. Rev. B **72**, 035307 (2005).
[48] H. Bombin and M. A. Martin-Delgado, Exact topological quantum order in $d = 3$ and beyond: Branyons and brane-net condensates, Phys. Rev. B **75**, 075103 (2007).
[49] C. Wang and M. Levin, Braiding Statistics of Loop Excitations in Three Dimensions, Phys. Rev. Lett. **113**, 080403 (2014).
[50] S. Jiang, A. Mesaros, and Y. Ran, Generalized Modular Transformations in $(3 + 1)$D Topologically Ordered Phases and Triple Linking Invariant of Loop Braiding, Phys. Rev. X **4**, 031048 (2014).
[51] A. Kubica, M. E. Beverland, F. Brandão, J. Preskill, and K. M. Svore, Three-Dimensional Color Code Thresholds via Statistical-Mechanical Mapping, Phys. Rev. Lett. **120**, 180501 (2018).
[52] W. P. Thurston, *Three-Dimensional Geometry and Topology*, edited by Silvio Levy (Princeton University Press, Princeton, NJ, 1997), Vol. 1.
[53] G. Perelman, The entropy formula for the Ricci flow and its geometric applications, arXiv:math/0211159.
[54] G. Perelman, Ricci flow with surgery on three-manifolds, arXiv:math/0303109.
[55] G. Perelman, Finite extinction time for the solutions to the Ricci flow on certain three-manifolds, arXiv:math/0307245.
[56] Tian Lan, Liang Kong, and Xiao-Gang Wen, Classification of $(3 + 1)$D Bosonic Topological Orders: The Case when Pointlike Excitations are all Bosons, Phys. Rev. X **8**, 021074 (2018).
[57] T. Lan and X.-G. Wen, A classification of 3+1d bosonic topological orders (ii): the case when some point-like excitations are fermions, arXiv:1801.08530.
[58] C. Chamon, Quantum Glassiness in Strongly Correlated Clean Systems: An Example of Topological Overprotection, Phys. Rev. Lett. **94**, 040402 (2005).
[59] J. Haah, Local stabilizer codes in three dimensions without string logical operators, Phys. Rev. A **83**, 042330 (2011).
[60] S. Vijay, J. Haah, and L. Fu, A new kind of topological quantum order: A dimensional hierarchy of quasiparticles built from stationary excitations, Phys. Rev. B **92**, 235136 (2015).
[61] S. Vijay, J. Haah, and L. Fu, Fracton topological order, generalized lattice gauge theory, and duality, Phys. Rev. B **94**, 235157 (2016).
[62] S. Bravyi, B. Leemhuis, and B. M. Terhal, Topological order in an exactly solvable 3d spin model, Ann. Phys. **326**, 839 (2011).
[63] C. Castelnovo and C. Chamon, Topological quantum glassiness, Philos. Mag. **92**, 304 (2012).
[64] S. Bravyi and J. Haah, Quantum Self-Correction in the 3d Cubic Code Model, Phys. Rev. Lett. **111**, 200501 (2013).
[65] B. Yoshida, Exotic topological order in fractal spin liquids, Phys. Rev. B **88**, 125122 (2013).
[66] M. Pretko, Subdimensional particle structure of higher rank $u(1)$ spin liquids, Phys. Rev. B **95**, 115139 (2017).
[67] M. Pretko, Generalized electromagnetism of subdimensional particles: A spin liquid story, Phys. Rev. B **96**, 035119 (2017).
[68] D. J. Williamson, Fractal symmetries: Ungauging the cubic code, Phys. Rev. B **94**, 155128 (2016).
[69] A. Prem, J. Haah, and R. Nandkishore, Glassy quantum dynamics in translation invariant fracton models, Phys. Rev. B **95**, 155133 (2017).
[70] H. Ma, E. Lake, X. Chen, and M. Hermele, Fracton topological order via coupled layers, Phys. Rev. B **95**, 245126 (2017).
[71] S. Vijay, Isotropic layer construction and phase diagram for fracton topological phases, arXiv:1701.00762.
[72] T. H. Hsieh and G. B. Halász, Fractons from partons, Phys. Rev. B **96**, 165105 (2017).
[73] K. Slagle and Y. B. Kim, Fracton topological order from nearest-neighbor two-spin interactions and dualities, Phys. Rev. B **96**, 165106 (2017).
[74] S. Vijay and L. Fu, A generalization of non-Abelian anyons in three dimensions, arXiv:1706.07070.
[75] B. Shi and Y.-M. Lu, Deciphering the nonlocal entanglement entropy of fracton topological orders, Phys. Rev. B **97**, 144106 (2018).
[76] G. B. Halász, T. H. Hsieh, and L. Balents, Fracton Topological Phases from Strongly Coupled Spin Chains, Phys. Rev. Lett. **119**, 257202 (2017).
[77] K. Slagle and Y. B. Kim, Quantum field theory of x-cube fracton topological order and robust degeneracy from geometry, Phys. Rev. B **96**, 195139 (2017).
[78] M. Pretko, Higher-spin witten effect and two-dimensional fracton phases, Phys. Rev. B **96**, 125151 (2017).
[79] A. Prem, M. Pretko, and R. M. Nandkishore, Emergent phases of fractonic matter, Phys. Rev. B **97**, 085116 (2018).
[80] O. Petrova and N. Regnault, Simple anisotropic three-dimensional quantum spin liquid with fractonlike topological order, Phys. Rev. B **96**, 224429 (2017).
[81] V. V Albert, S. Pascazio, and M. H. Devoret, General phase spaces: from discrete variables to rotor and continuum limits, J. Phys. A: Math. Theor. **50**, 504002 (2017).
[82] T. Devakul, S. A. Parameswaran, and S. L. Sondhi, Correlation function diagnostics for type-i fracton phases, Phys. Rev. B **97**, 041110 (2018).
[83] H. He, Y. Zheng, B. A. Bernevig, and N. Regnault, Entanglement entropy from tensor network states for stabilizer codes, Phys. Rev. B **97**, 125102 (2018).
[84] H. Ma, A. T. Schmitz, S. A. Parameswaran, M. Hermele, and R. M. Nandkishore, Topological entanglement entropy of fracton stabilizer codes, Phys. Rev. B **97**, 125101 (2018).
[85] A. T. Schmitz, H. Ma, R. M. Nandkishore, and S. A. Parameswaran, Recoverable information and emergent conservation laws in fracton stabilizer codes, Phys. Rev. B **97**, 134426 (2018).
[86] M. Pretko and L. Radzihovsky, Fracton-Elasticity Duality, Phys. Rev. Lett. **120**, 195301 (2018).
[87] A. Gromov, Chiral Topological Elasticity and Fracton Order, Phys. Rev. Lett. **122**, 076403 (2019).
[88] W. Shirley, K. Slagle, Z. Wang, and X. Chen, Fracton Models on General Three-Dimensional Manifolds, Phys. Rev. X **8**, 031051 (2018).

[89] K. Slagle and Y. B. Kim, X-cube model on generic lattices: Fracton phases and geometric order, Phys. Rev. B **97**, 165106 (2018).

[90] S. Pai and M. Pretko, Fractonic line excitations: An inroad from 3d elasticity theory, Phys. Rev. B **97**, 235102 (2018).

[91] Y. You, T. Devakul, F. J. Burnell, and S. L. Sondhi, Subsystem symmetry protected topological order, Phys. Rev. B **98**, 035112 (2018).

[92] A. Prem, S.-J. Huang, H. Song, and M. Hermele, Cage-Net Fracton Models, arXiv:1806.04687 [cond-mat.str-el].

[93] A. Prem, S. Vijay, Y.-Z. Chou, M. Pretko, and R. M. Nandkishore, Pinch Point Singularities of Tensor Spin Liquids, Phys. Rev. B **98**, 165140 (2018).

[94] R. M. Nandkishore and M. Hermele, Fractons, arXiv:1803.11196 [cond-mat.str-el].

[95] M. A. Levin and X.-G. Wen, String-net condensation: A physical mechanism for topological phases, Phys. Rev. B **71**, 045110 (2005).

[96] Z.-C. Gu and X.-G. Wen, Symmetry-protected topological orders for interacting fermions: Fermionic topological nonlinear σ models and a special group supercohomology theory, Phys. Rev. B **90**, 115141 (2014).

[97] L.-Y. Hung and Y. Wan, String-net models with Z_N fusion algebra, Phys. Rev. B **86**, 235132 (2012).

[98] M. Levin and Z.-C. Gu, Braiding statistics approach to symmetry-protected topological phases, Phys. Rev. B **86**, 115109 (2012).

[99] S. Beigi, P. W. Shor, and D. Whalen, The quantum double model with boundary: Condensations and symmetries, Commun. Math. Phys. **306**, 663 (2011).

[100] I. Cong, M. Cheng, and Z. Wang, Hamiltonian and algebraic theories of gapped boundaries in topological phases of matter, Commun. Math. Phys. **355**, 645 (2017).

[101] A. Y. Kitaev and L. Kong, Models for gapped boundaries and domain walls, Commun. Math. Phys. **313**, 351 (2012).

[102] L. Kong, Some universal properties of Levin-Wen models, in *XVIIth International Congress on Mathematical Physics* (World Scientific, Singapore, 2014), pp. 444–455.

[103] C.-H. Lin and M. Levin, Generalizations and limitations of string-net models, Phys. Rev. B **89**, 195130 (2014).

[104] T. Lan and X.-G. Wen, Topological quasiparticles and the holographic bulk-edge relation in $(2+1)$-dimensional string-net models, Phys. Rev. B **90**, 115119 (2014).

[105] I. Cong and Z. Wang, Topological quantum computation with gapped boundaries and boundary defects, arXiv:1710.07197 [quant-ph].

[106] C.-H. Lin, Multiflavor string-net models, Phys. Rev. B **95**, 195110 (2017).

[107] Z. Wang and X. Chen, Twisted gauge theories in three-dimensional walker-wang models, Phys. Rev. B **95**, 115142 (2017).

[108] R. Dijkgraaf and E. Witten, Topological gauge theories and group cohomology, Comm. Math. Phys. **129**, 393 (1990).

[109] Y. Hu, Y. Wan, and Y.-S. Wu, Twisted quantum double model of topological phases in two dimensions, Phys. Rev. B **87**, 125114 (2013).

[110] J. C. Wang and X.-G. Wen, Non-abelian string and particle braiding in topological order: Modular SL$(3,\mathbb{Z})$ representation and $(3+1)$-dimensional twisted gauge theory, Phys. Rev. B **91**, 035134 (2015).

[111] Y. Wan, J. C. Wang, and H. He, Twisted gauge theory model of topological phases in three dimensions, Phys. Rev. B **92**, 045101 (2015).

[112] Z.-C. Gu, J. C. Wang, and X.-G. Wen, Multikink topological terms and charge-binding domain-wall condensation induced symmetry-protected topological states: Beyond chern-simons/bf field theories, Phys. Rev. B **93**, 115136 (2016).

[113] Y. You, T. Devakul, F. J. Burnell, and S. L. Sondhi, Symmetric fracton matter: Twisted and enriched, arXiv:1805.09800 [cond-mat.str-el].

[114] A. Hatcher, *Algebraic Topology* (Cambridge University Press, Cambridge, 2002).

[115] M. Freedman, C. Nayak, K. Shtengel, K. Walker, and Z. Wang, A class of p,t-invariant topological phases of interacting electrons, Ann. Phys. **310**, 428 (2004).

[116] M. d. W. Propitius, Topological interactions in broken gauge theories, arXiv:hep-th/9511195.

[117] R. Dijkgraaf, V. Pasquier, and P. Roche, Quasi hope algebras, group cohomology and orbifold models, Nucl. Phys. B **18**, 60 (1991).

[118] A. Kubica and B. Yoshida, Ungauging quantum error-correcting codes, arXiv:1805.01836 [quant-ph].

[119] T. Devakul, Y. You, F. J. Burnell, and S. L. Sondhi, Fractal symmetric phases of matter, SciPost Phys. **6**, 007 (2019).

[120] P. Etingof, S. Gelaki, D. Nikshych, and V. Ostrik, *Tensor Categories* (American Mathematical Society, Providence, Rhode Island, 2015).

[121] D. Altschuler and A. Coste, Quasi-quantum groups, knots, three-manifolds, and topological field theory, Commun. Math. Phys. **150**, 83 (1992).

[122] C. Cheng, A character theory for projective representations of finite groups, Linear Algebra Appl. **469**, 230 (2015).

[123] E. Verlinde, Fusion rules and modular transformations in 2d conformal field theory, Nucl. Phys. B **300**, 360 (1988).